frontiers | Research Topics

Rising stars in pediatric cardiology 2023

Edited by
Laura Muiño Mosquera and Liqun Sun

Published in
Frontiers in Cardiovascular Medicine
Frontiers in Pediatrics

ISSN 1664-8714
ISBN 978-2-8325-5199-8
DOI 10.3389/978-2-8325-5199-8

About Frontiers

Frontiers is more than just an open access publisher of scholarly articles: it is a pioneering approach to the world of academia, radically improving the way scholarly research is managed. The grand vision of Frontiers is a world where all people have an equal opportunity to seek, share and generate knowledge. Frontiers provides immediate and permanent online open access to all its publications, but this alone is not enough to realize our grand goals.

Frontiers journal series

The Frontiers journal series is a multi-tier and interdisciplinary set of open-access, online journals, promising a paradigm shift from the current review, selection and dissemination processes in academic publishing. All Frontiers journals are driven by researchers for researchers; therefore, they constitute a service to the scholarly community. At the same time, the *Frontiers journal series* operates on a revolutionary invention, the tiered publishing system, initially addressing specific communities of scholars, and gradually climbing up to broader public understanding, thus serving the interests of the lay society, too.

Dedication to quality

Each Frontiers article is a landmark of the highest quality, thanks to genuinely collaborative interactions between authors and review editors, who include some of the world's best academicians. Research must be certified by peers before entering a stream of knowledge that may eventually reach the public - and shape society; therefore, Frontiers only applies the most rigorous and unbiased reviews. Frontiers revolutionizes research publishing by freely delivering the most outstanding research, evaluated with no bias from both the academic and social point of view. By applying the most advanced information technologies, Frontiers is catapulting scholarly publishing into a new generation.

What are Frontiers Research Topics?

Frontiers Research Topics are very popular trademarks of the *Frontiers journals series*: they are collections of at least ten articles, all centered on a particular subject. With their unique mix of varied contributions from Original Research to Review Articles, Frontiers Research Topics unify the most influential researchers, the latest key findings and historical advances in a hot research area.

Find out more on how to host your own Frontiers Research Topic or contribute to one as an author by contacting the Frontiers editorial office: frontiersin.org/about/contact

Rising stars in pediatric cardiology 2023

Topic editors
Laura Muiño Mosquera — Ghent University Hospital, Belgium
Liqun Sun — University of Toronto, Canada

Citation
Muiño Mosquera, L., Sun, L., eds. (2024). *Rising stars in pediatric cardiology 2023*. Lausanne: Frontiers Media SA. doi: 10.3389/978-2-8325-5199-8

Table of contents

frontiers | Frontiers in Pediatrics

TYPE Editorial
PUBLISHED 10 July 2024
DOI 10.3389/fped.2024.1452884

OPEN ACCESS

EDITED AND REVIEWED BY
Ruth Heying,
University Hospital Leuven, Belgium

*CORRESPONDENCE
Liqun Sun
liqun.sun@sickkids.ca;
liqun.sun@mail.utoronto.ca

RECEIVED 21 June 2024
ACCEPTED 02 July 2024
PUBLISHED 10 July 2024

CITATION
Sun L and Muiño-Mosquera L (2024) Editorial: Rising stars in pediatric cardiology 2023. Front. Pediatr. 12:1452884. doi: 10.3389/fped.2024.1452884

Editorial: Rising stars in pediatric cardiology 2023

Liqun Sun[1,2]* and Laura Muiño-Mosquera[3,4]

[1]Division of Cardiology, Department of Pediatrics, The Hospital for Sick Children, University of Toronto, Toronto, ON, Canada, [2]Translational Medicine Program, The Hospital for Sick Children, University of Toronto, Toronto, ON, Canada, [3]Division of Pediatric Cardiology, Department of Pediatrics, Ghent University Hospital, Ghent, Belgium, [4]Center for Medical Genetics, Ghent University Hospital, Ghent, Belgium

KEYWORDS

pediatric cardiology, cardiovascular health, echocardiography, early stages, future innovations

Editorial on the Research Topic
Rising stars in pediatric cardiology 2023

Introduction

In this collection several researchers in the early stages of their careers present some of their latest works. This collection includes contributions across different aspects of pediatric cardiology.

Fetal cardiovascular remodeling and post-natal cardiac function

Recent studies have demonstrated that different mechanisms leading to subclinical cardiac remodeling in fetal life, may predispose to clinical cardiac disease in childhood and adulthood after a second hit (1). Several of this mechanism have been postulated and include fetal growth restriction, preeclampsia, preterm birth, assist reproductive technology (ART), exposure to toxic drugs, twin-to-twin transfusion syndrome (TTTS) and maternal diabetes and obesity. Evidence suggests that ART induces alterations in cardiac and vascular morphology and physiology (2–5). In this collection, Li et al., conducted a comprehensive review of epigenetic mechanisms associated with an increased risk of cardiovascular disease (CVD) in offspring conceived via ART. Potential contributing factors include hormonal treatments, *in vitro* culture conditions, and epigenetic modifications. The findings underscore the significance of prenatal and postnatal monitoring of children conceived through ART, aiming to detect and address cardiovascular issues proactively associated with ART. The differences in DNA methylation might be due to aspects of ART procedures such as hormonal treatments, *in vitro* culture conditions, or other yet unknown factors. Reactive Oxygen Species (ROS) contribute to elevated oxidative stress in ART, potentially mitigated by antioxidants. Altered methylation patterns of genes, like AGTR1 and eNOS, are implicated in blood pressure abnormalities, with the ROS inhibitor melatonin preventing hypermethylation of eNOS (Li et al.).

Congenital heart disease in the context of non-cardiovascular conditions

Congenital heart disease (CHD) encompasses a range of cardiac malformations present from birth, significantly impacting heart function. The prognostic outcomes in CHD are heterogeneous; certain malformations can be surgically corrected, resulting in near-normal life expectancy and quality of life. Individuals living with CHD frequently confront an elevated risk of subsequent cardiac complications, necessitating lifestyle adjustments and vigilant monitoring to prevent further cardiac deterioration. In this collection, Aly et al. studied the incidence of severe CHD in premature children and the impact of prematurity on outcome of children with severe CHD. The authors retrospectively examined a National multicenter database. They found a higher risk of severe CHD in premature infants from less affluent backgrounds. The study also examined the mortality rates in severe CHD cases vs. gestational age- matched controls and show increased major neonatal morbidity including higher rates of necrotizing enterocolitis, bronchopulmonary dysplasia, interventricular hemorrhage and periventricular leukomalacia adjusted for relevant factors such as birth weight and gender (Aly et al.). In another manuscript, Huang et al., conducts a study focusing on the importance of considering non-cardiac anomalies (NCAs) in children with CHD, as these can significantly impact the overall prognosis and management of the condition. Recognizing the varied probabilities and types of NCAs across different CHD subtypes is crucial for early detection, comprehensive evaluation, and tailored therapeutic approaches. The findings underscore the need for multidisciplinary teamwork involving cardiologists, geneticists, and other specialists to optimize care for these patients (Huang et al.). From the same group, Zhao et al., presented their comprehension of the complex interplay between primary ciliary dyskinesia (PCD), heterotaxy, and CHD, but it also highlights the necessity for preoperative screening of ciliary dysfunction in patients with heterotaxy and CHD. This proactive strategy can substantially improve postoperative respiratory care and ultimately enhance the overall health and well-being of these patients (Zhao et al.). Another example of the importance of considering NCAs in children with CHD is the study of Peng et al., which emphasizes importance of considering Tuberous Sclerosis Complex (TSC) in fetus and children with ardiac rhabdomyomas, regardless of size or location. Concurrent TSC leads to a generally less favorable prognosis due to epilepsy and neurological abnormalities, also granting a specialized and multidisciplinary approach (Peng et al.).

Cardiovascular outcome in children with acquired cardiovascular diseases

Mu et al., devised a nomogram model specifically for patients diagnosed with Diffuse Large B-Cell Lymphoma (DLBCL). This model demonstrated admirable predictive efficacy and exceptional discriminative capability. Such a tool may substantially assist clinicians in formulating refined therapeutic strategies at the time of the initial diagnosis. The predictors identified for cardiovascular mortality (CVM) encompassed age at diagnosis, gender, ethnicity, tumor grade, Ann Arbor staging, receipt of radiotherapy, and specific chemotherapy regimens. Clinical variables ascertained at the diagnostic juncture can discern DLBCL patients who are at a heightened risk of CVM, thereby suggesting that preventative interventions should be contemplated for this subpopulation (Mu et al.).

In a multicenter prospective observational study, De Wolf et al., report on the late cardiac outcomes of 36 children who were recruited during the acute phase of multisystem inflammatory syndrome. In the late-term follow-up visit, the evaluation of late cardiac outcomes CMR does not show any myocardial scarring in children with a normal echocardiographic LVEF. Subclinical myocardial damage can persist in the late term, and further follow-up seems appropriate in these patients (De Wolf et al.).

Illustrative case reports

This collection includes three interesting case reports illustrating different aspect of pediatric cardiology care. In the first case Luo et al., present a fetus with prenatal diagnosis of severe pulmonary stenosis with intact ventricular septum. In this case report, while the right ventricular volume did not reach significant values to support prenatal intervention, the authors observed a significant decrease in tricuspid valve gradient and annular z-score. Postnatally, a 1.5 ventricular circulation seemed the only feasible option. The authors concluded that besides right ventricular volume, which is the most accepted parameter for biventricular repair (PMID: 30238627), tricuspid valve regurgitation and z-score could be useful additional parameters.

In the second case report, Xu et al., present a child with excessive vagal tone manifesting as sinus pauzes of up to 7,4 s, multiple episodes of sinus bradycardia, and junctional escape rhythms. The authors apply for the first time in a child cardioneuroablation (CNA) therapy for this indication and demonstrate improved clinical outcomes, including symptom alleviation and resolution of rhythm disorders (Luo et al.). This innovative approach seemed therefor safe and effective.

Finally, in the last case report, Zhou et al., show a singular case of an infant diagnosed with Williams-Beuren syndrome (WS) who manifested an accelerated progression of arterial stenosis and exhibited left ventricular endocardial calcification. This case was associated with a novel heterozygous deletion not previously described in the literature. While arterial stenosis represents the most frequently encountered cardiovascular complication in patients with WS, the occurrence of endocardial calcification during infancy is exceptionally uncommon. To our knowledge, this is the first documented instance of endocardial calcification in an infant with WS, suggesting a unique phenotype that expands the known cardiovascular manifestations associated with this genetic condition (Zhou et al.).

Conclusions

This collection gathers some interesting aspect of pediatric cardiology: (1) The study of cardiovascular remodeling during

fetal life and its sequelae demands a multidisciplinary effort, encompassing developmental biology, genetics, epidemiology, and clinical cardiology. (2) A broad understanding of the molecular and environmental determinants of cardiovascular health and of disease associated with congenital and acquired heart diseases, will facilitate the development of innovative preventive, diagnostic, and therapeutic strategies. As research progresses, it is imperative that findings are translated into clinical practices that can mitigate the onset and progression of cardiovascular diseases, ultimately enhancing the quality of life and longevity for those affected.

Author contributions

LS: Conceptualization, Writing – original draft, Writing – review & editing. LM-M: Writing – review & editing.

Funding

The author(s) declare that financial support was received for the research, authorship, and/or publication of this article.

LS holds a grant from the National Natural Science Foundation of China (Grant No. 81601291; 2018YFC1004604). LM-M holds a grant from the Fund of Innovative Research of the Ghent University Hospital (Grant No. KW2296 PED 002 001).

Conflict of interest

MM-M is co-author of one of the included manuscripts.

The remaining author declares that the research was conducted in the absence of any commercial or financial relationships that could be construed as a potential conflict of interest.

Publisher's note

References

1. Youssef L, Castellani R, Valenzuela-Alcaraz B, Sepulveda-Martinez Á, Crovetto F, Crispi F Cardiac remodeling from the fetus to adulthood. *J Clin Ultrasound*. (2023) 51:249–64. doi: 10.1002/jcu.23336

2. Kulkarni A, Garcia-Cañadilla P, Khan A, Lorenzo JM, Beckerman K, Valenzuela-Alcaraz B, et al. Remodeling of the cardiovascular circulation in fetuses of mothers with diabetes: a fetal computational model analysis. *Placenta*. (2018) 63:1–6. doi: 10.1016/j.placenta.2017.12.020

3. Meister TA, Rimoldi SF, Soria R, von Arx R, Messerli FH, Sartori C, et al. Association of assisted reproductive technologies with arterial hypertension during adolescence. *J Am Coll Cardiol*. (2018) 72:1267–74. doi: 10.1016/j.jacc.2018.06.060

4. Scherrer U, Rimoldi SF, Sartori C, Messerli FH, Rexhaj E. Fetal programming and epigenetic mechanisms in arterial hypertension. *Curr Opin Cardiol*. (2015) 30:393–7. doi: 10.1097/HCO.0000000000000192

5. Valenzuela-Alcaraz B, Crispi F, Bijnens B, Cruz-Lemini M, Creus M, Sitges M, et al. Assisted reproductive technologies are associated with cardiovascular remodeling in utero that persists postnatally. *Circulation*. (2013) 128:1442–50. doi: 10.1161/CIRCULATIONAHA.113.002428

frontiers | Frontiers in Pediatrics

TYPE Original Research
PUBLISHED 24 August 2023
DOI 10.3389/fped.2023.1253608

OPEN ACCESS

EDITED BY
Nazmi Narin,
Izmir Katip Celebi University, Türkiye

REVIEWED BY
Mehmet Burhan Oflaz,
Necmettin Erbakan University, Türkiye
Tülay Demircan,
Dokuz Eylul University, Türkiye

*CORRESPONDENCE
Rik De Wolf
r.de_wolf@lumc.nl

RECEIVED 05 July 2023
ACCEPTED 01 August 2023
PUBLISHED 24 August 2023

CITATION
De Wolf R, Zaqout M, Tanaka K, Muiño-Mosquera L, van Berlaer G, Vandekerckhove K, Dewals W and De Wolf D (2023) Evaluation of late cardiac effects after multisystem inflammatory syndrome in children. Front. Pediatr. 11:1253608. doi: 10.3389/fped.2023.1253608

Evaluation of late cardiac effects after multisystem inflammatory syndrome in children

Rik De Wolf[1]*, Mahmoud Zaqout[2,3], Kaoru Tanaka[4], Laura Muiño-Mosquera[5], Gerlant van Berlaer[6], Kristof Vandekerckhove[5], Wendy Dewals[2] and Daniël De Wolf[1,5]

[1]Department of Pediatric Cardiology, University Hospital Brussels, Brussels, Belgium, [2]Department of Pediatric Cardiology, Antwerp University Hospital, Antwerp, Belgium, [3]Department of Pediatric Cardiology, ZNA Queen Paola Children's Hospital, Antwerp, Belgium, [4]Department of Radiology, University Hospital Brussels, Brussels, Belgium, [5]Department of Pediatric Cardiology, Ghent University Hospital, Ghent, Belgium, [6]Department of Pediatric Intensive Care, University Hospital Brussels, Brussels, Belgium

Introduction: Multisystem inflammatory syndrome in children (MIS-C) is associated with important cardiovascular morbidity during the acute phase. Follow-up shows a swift recovery of cardiac abnormalities in most patients. However, a small portion of patients has persistent cardiac sequelae at mid-term. The goal of our study was to assess late cardiac outcomes of MIS-C.

Methods: A prospective observational multicenter study was performed in children admitted with MIS-C and cardiac involvement between April 2020 and March 2022. A follow-up by NT-proBNP measurement, echocardiography, 24-h Holter monitoring, and cardiac MRI (CMR) was performed at least 6 months after MIS-C diagnosis.

Results: We included 36 children with a median age of 10 (8.0–11.0) years, and among them, 21 (58%) were girls. At diagnosis, all patients had an elevated NT-proBNP, and 39% had a decreased left ventricular ejection fraction (LVEF) (<55%). ECG abnormalities were present in 13 (36%) patients, but none presented with arrhythmia. Almost two-thirds of patients (58%) had echocardiographic abnormalities such as coronary artery dilation (20%), pericardial effusion (17%), and mitral valve insufficiency (14%). A decreased echocardiographic systolic left ventricular (LV) function was detected in 14 (39%) patients. A follow-up visit was done at a mean time of 12.1 ($\pm$5.8) months (range 6–28 months). The ECG normalized in all except one, and no arrhythmias were detected on 24-h Holter monitoring. None had persistent coronary artery dilation or pericardial effusion. The NT-proBNP level and echocardiographic systolic LV function normalized in all patients, except for one, who had a severely reduced EF. The LV global longitudinal strain (GLS), as a marker of subclinical myocardial dysfunction, decreased ($z < -2$) in 35%. CMR identified one patient with severely reduced EF and extensive myocardial fibrosis requiring heart transplantation. None of the other patients had signs of myocardial scarring on CMR.

Conclusion: Late cardiac outcomes after MIS-C, if treated according to the current guidelines, are excellent. CMR does not show any myocardial scarring in children with normal systolic LV function. However, a subgroup had a decreased GLS at follow-up, possibly as a reflection of persistent subclinical myocardial dysfunction.

KEYWORDS

MIS-C, CMR, pediatric, SARS-CoV-2, children, outcome, cardiac

Introduction

Children affected with a SARS-CoV-2 infection usually have a mild clinical disease course (1). However, in April 2020, a hyperinflammatory multisystem syndrome was described, which occurred 2–6 weeks after SARS-CoV-2 exposure. It was referred to as multisystem inflammatory syndrome in children (MIS-C). Up to 80% of MIS-C patients have cardiovascular involvement, including signs of myocarditis with an elevated N-terminal prohormone of brain natriuretic peptide (NT-proBNP) and a decreased systolic left ventricular (LV) function, coronary artery dilation, pericardial effusion, arrhythmias, and conduction abnormalities (2–6). Although the follow-up demonstrated a swift recovery of cardiac abnormalities and left ventricular function in most patients, a small number had persistent cardiac sequelae at mid-term, including a decreased left ventricular ejection fraction (LVEF) (7–9), subclinical myocardial damage illustrated by reduced LV strain (10), and myocardial fibrosis on CMR (11). The goal of our study was to assess late cardiac outcomes after hospitalization for MIS-C using NT-proBNP, echocardiography, 24-h Holter monitoring, and CMR.

Materials and methods

We performed a prospective observational multicenter study in patients aged <18 years diagnosed with MIS-C according to WHO criteria (12) between May 2020 and August 2022 in one of the following Belgian centers: Brussels University Hospital, ZNA Queen Paola Children's Hospital, Ghent University Hospital, and Antwerp University Hospital. The exclusion criteria were the presence of pre-existing myocardial dysfunction and the need for general anesthesia to perform cardiac MRI, as the risk would outweigh the benefit. The follow-up visit was organized at least 6 months after hospitalization for MIS-C. From a total of 62 patients who met the inclusion criteria, 36 were included, 18 declined to participate, and 8 could not give informed consent because of a language barrier. Written informed consent was given by the parents of the participating patients. The study protocol was approved by the Ethics Committees of all participating centers (EC 2021-115/B.U.N. 1432021000463).

Patient data

All demographical, clinical, biochemical, and echocardiographic data were collected in a standardized form. Demographic (sex, ethnicity, and age at admission), history (recent infection with SARS-CoV-2 or close contact in the weeks before presentation), anthropometric [height, weight, and body mass index (BMI)], and clinical (need for ICU admission, inotropic support, and treatment regime) data were collected at baseline (admission for MIS-C).

Laboratory investigations

All patients underwent SARS-CoV-2 testing at admission by polymerase chain reaction on nasopharyngeal swabs. Previous SARS-CoV-2 exposure was detected through IgG serological assessment. Biochemical data included cardiovascular disease biomarkers (NT-proBNP and troponin) and D-dimers. NT-proBNP measurement was repeated at the follow-up visit, simultaneously with the peripheral intravenous cannulation necessary to perform the CMR with gadolinium administration.

Echocardiographic and electrocardiogram data

Echocardiography was performed by a single pediatric cardiologist in each participating center at baseline and at follow-up. The echocardiographic parameters recorded included the presence of pulmonary hypertension (PH), pericardial effusion, coronary dilation, and valvular insufficiency as well as cardiac dimensions and function. Coronary dilation was defined as a z-score of ≥ 2.0 (13). Cardiac function was evaluated by left ventricular fractional shortening (FS) (M-mode) and left ventricular ejection fraction (Simpson biplane method). A decreased cardiac function was defined as an FS of $< 28\%$ or EF of $< 55\%$. Left ventricular end-diastolic diameter (LVEDD) and left ventricular end-systolic diameter (LVEDs) and their respective z-scores were recorded. An evaluation of LV regional wall abnormalities and subclinical LV dysfunction by global longitudinal strain (GLS) measurement through speckle tracking echocardiography (STE) was performed at follow-up. It was added to the study at a later stage; thus, results are only partially available for the cohort. Three apical views (four-chamber, two-chamber, and three-chamber) were used. GLS calculation was performed offline using a semiautomatic method (GE EchoPac Software, GE Healthcare, USA). The borders of the studied LV myocardial segments were adjusted manually. The peak longitudinal strain values for each view were averaged to calculate LV GLS. An adjustment for body surface area was performed and represented by the z-score as described by Dallaire et al. (14). A decreased GLS was defined as a z-score of <-2.

A standard 12-lead electrocardiogram (ECG) was performed during admission for MIS-C and was repeated, combined with a 24-h Holter monitoring at follow-up, to detect arrhythmia as a possible late complication of MIS-C.

CMR-imaging

A standard CMR protocol was performed using a Philips Achieva dStream 1.5T or Ingenia 3.0T scanner (Philips Medical Systems, Best, Netherlands). SSFP-cine sequences were performed for LV and RV measurements. Tissue characterization before contrast was performed with T1 and T2 mapping to visualize myocardial injury and edema, respectively. A T2-weighted short tau inversion recovery sequence was used to visualize edema.

10.3389/fped.2023.1253608

Late gadolinium enhancement (LGE) imaging was performed 10 min after an intravenous administration of 0.1 mmol/kg gadoterate meglumine (Dotarem, Guerbet, Villepinte, France). Cardiac volumes and mass of the left and right ventricles were analyzed using Circle Cardiovascular Imaging Inc. (Calgary, Canada). An increased left ventricular end-diastolic volume adjusted for body surface area (ml/m^2) was defined as an LVEDD of >p97 using pediatric CMR reference values (15).

Statistical analysis

Statistical analysis was done with IBM SPSS Statistics 28.0 (IBM Corp., Armonk, NY, USA). Shapiro–Wilk test and histogram were used to test the normality for each variable. Continuous variables are expressed as mean ± standard deviation or median and interquartile range (25th–75th percentile) as appropriate. Discrete variables are expressed as numbers and percentages. A comparison of characteristics between the different patient groups was done by using the Mann–Whitney *U* test for continuous variables and Fisher's exact test for dichotomous variables.

Results

Patients

We included 36 children with MIS-C. Patient characteristics at baseline are outlined in **Table 1**. The median age at admission was 10.0 (8.0–11.0) years, and among them, 21 (58%) were girls. Most patients had Caucasian descent (69%). A body mass index (BMI) of >25 was observed in three (8%) patients. Comorbidity was limited to one patient with familial Mediterranean fever and one with pre-existing renal failure. All except one received immunoglobulins and/or corticosteroids as MIS-C treatment. Treatment with low-dose aspirin was started in all patients. ICU admission was warranted in 29 patients (81%), with almost half of them (48%) needing inotropic support for a mean duration of 3.6 ± 0.6 days.

Cardiac assessment at MIS-C admission

The cardiac assessment was performed routinely during MIS-C admission, and the results are presented in **Table 2**. Cardiac biomarkers measurement showed significantly elevated NT-proBNP and D-dimers in all patients and an elevated troponin level in 28 (78%).

A total of 13 patients (36%) had ECG abnormalities during admission. More than half of those had repolarization abnormalities (ST segment elevation, flattened or inverted T waves), three (8%) had QTc prolongation, two (6%) had left ventricular hypertrophy, one (3%) had sinus bradycardia despite inotropes, and one (3%) had a first-degree AV block. None demonstrated supraventricular or ventricular arrhythmias.

All patients underwent an echocardiographic evaluation, and abnormalities were present in almost two-thirds of patients (58%). A total of 20 patients (56%) had dilated coronary arteries, but

TABLE 1 Clinical patient characteristics.

	n = 36
Age at admission (years)	10.0 (8.0–11.0)
Sex (Female)	21 (58)
Height (cm)	141.5 ± 2.4
Weight (kg)	34.5 (25.0–49.3)
BMI (kg/m^2)	17.8 (14.6–19.9)
Ethnicity	
Caucasian	25 (69)
African	9 (25)
Asian	2 (6)
COVID status	
IgG+	25 (69)
PCR+	4 (11)
Contact	4 (11)
IgG and PCR+	3 (8)
Treatment regime	
Immunoglobulins	13 (36)
Immunoglobulins + corticosteroids	21 (58)
Corticosteroids	1 (3)
None	1 (3)
ICU admission	29 (81)
Inotropic support	14 (39)
Duration of inotropic support (days)	3.6 ± 0.6

Values are presented as *n* (%), means ± SD, or median (Q1–Q3). BMI, body mass index; ICU, intensive care unit; IgG, immunoglobulin G; PCR, polymerase chain reaction.

TABLE 2 Cardiac findings at baseline.

	n = 36
Biomarkers	
D-dimer (ng/ml)	3,368.5 (1,565.0–4,781.8)
Troponin (ng/L)	48.5 (15.5–146.0)
NT-proBNP (pg/ml)	5,125.0 (1,505.0–20,153.0)
Echocardiographic findings	
Decreased LV function	21 (58)
LVEF (%)	57.0 ± 1.9
FS <28%	13 (37)
FS (%)	29.0 ± 1.2
LVEF <55%	14 (39)
LVEDD *z*-score >2 (%)	1 (3)
Echocardiographic abnormality at diagnosis	21 (58)
Coronary artery dilation	20 (56)
Pericardial effusion	6 (17)
Mitral valve insufficiency	5 (13)
Pulmonary hypertension	3 (8)
Left ventricular hypertrophy	
ECG abnormalities	13 (36)
Repolarization abnormalities	7 (19)
QTc prolongation	3 (8)
Left ventricular hypertrophy	2 (6)
First-degree AV block	1 (3)
Sinus bradycardia	1 (3)

Values are presented as *n* (%), means ± SD, or median (Q1–Q3). NT-proBNP, N-terminal prohormone of brain natriuretic peptide; LVEF, left ventricular ejection fraction; FS, fractional shortening; LVEDD, left ventricular end-diastolic diameter; AV block, atrioventricular block.

none had more than small coronary artery aneurysms (*z*-score <5). Pericardial effusion was observed in a small portion of patients (17%), none of which was hemodynamically relevant. A total of five patients (14%) had mitral valve insufficiency (MI), three (8%) had pulmonary hypertension, and three (8%) had septal hypertrophy.

An evaluation of left ventricular function was performed by calculating FS, LVEF, and LVEDD. A total of 13 patients (36%) had both a diminished LVEF and FS in combination with an LVEDD *z*-score of >2 in 1 (3%) patient. One had a decreased LVEF and a borderline FS of 29%. The LV dysfunction was mostly mild (71%), but some had moderate (21%) or severe (8%) impaired systolic LV function. An LVEDD *z*-score of >2 was present in one patient (3%) only.

Cardiac assessment at the follow-up visit

The mean time interval to the follow-up visit was 12.1 ± 5.8 months (range 6–28 months). The follow-up data are outlined in Table 3. The ECG was normal in all except one patient with persistent repolarization abnormalities. A 24-h Holter monitoring showed no pathological supraventricular or ventricular arrhythmias. An echocardiographic evaluation of persistent cardiac abnormalities or decreased LV function was performed in all patients. None had persistent coronary artery dilation or pericardial effusion. Mitral valve insufficiency and PH normalized in patients with a normal systolic LV function. One patient showed persistent septal hypertrophy. The echocardiographic LV systolic function was still impaired in only one patient with an extremely elevated NT-proBNP. In this patient, echocardiographic parameters showed an increased LVEDD (*z*-score +5), a diminished LVEF of 10%, and an FS of 8% with consequent mitral valve insufficiency and PH.

TABLE 3 Cardiac findings at follow-up.

	N = 36
Follow-up time (months)	12.1 ± 5.8
NT-proBNP (pg/ml)	35.0 (24.8–51.0)
Echocardiographic findings	
Echocardiographic evaluation of LV function	
LVEF (%)	64.9 ± 1.8
LVEF <55%	1 (3)
FS (%)	35.6 ± 1.1
FS <28%	1 (3)
LVEDD *z*-score >2	1 (3)
GLS (%, *n* = 14)	−18.2 ± 0.7
Echocardiographic abnormality at follow-up	2 (6)
Coronary artery dilation	0
Pericardial effusion	0
Mitral valve insufficiency	1
Pulmonary hypertension	1
Left ventricular hypertrophy	1
Abnormal Holter findings	0
ECG abnormalities	1 (3)
Repolarization abnormalities	1 (3)
CMR findings	
LVEF	60.7 ± 10.2
LVEF <55%	3 (9)
LVEDD (ml/m^2)	78.3 ± 24.1
LVEDD >p97	3 (9)
Fibrosis	1 (3)

Values are presented as *n* (%), means ± SD, or median (Q1–Q3). NT-proBNP, N-terminal prohormone of brain natriuretic peptide; LVEF, left ventricular ejection fraction; FS, fractional shortening; ECG, electrocardiogram; LVEDD, left ventricular end-diastolic diameter.

A measurement of the global LV strain was added to detect subclinical LV dysfunction later during follow-up. The GLS was calculated in 14 patients, and 5 (35%) had a decreased GLS percentage adjusted for BSA (*z*-score <−2; range −3.4/−2.5). The distribution of the affected LV myocardial regions in patients with a decreased GLS was variable and different. All children with a decreased GLS were admitted to the ICU during the acute phase, and two had a decreased echocardiographic LV function. However, only one needed inotropic support. Three patients had an increased troponin level, and coronary arteries were dilated in four children. None had an abnormal baseline ECG. We found no correlation between children with either normal or decreased GLS regarding the need for inotropic support, PICU admission, increased cardiac biomarkers, decreased cardiac function, or any other cardiac abnormalities at baseline. All of these patients had normal biochemical, echocardiographic (except for a decreased GLS), and Holter results at follow-up.

A CMR was performed in 35 patients at follow-up. In one patient with claustrophobia, the CMR could not be obtained. The CMR LVEF decreased (LVEF <55%) in three patients, of which one had a severely reduced LVEF of 10%. This was the only patient with LGE as a sign of myocardial fibrosis. This 16-year-old patient was admitted to our hospital with heart failure when the pandemic was first reported (April 2020), 6 weeks after a SARS-CoV2 infection needing respiratory support. He was our first MIS-C patient and did not receive immunoglobulins or corticosteroids. Heart transplantation was necessary due to the severity of the heart failure, despite maximal medical treatment. The patient is now doing well. The two other patients had a mild reduced LVEF on CMR (45%–55%) and no signs of fibrosis, and the echocardiographic evaluation of systolic LV function was normal. LVEDD was >p97 in three children of which one is the patient described above. The CMR LVEF and echocardiographic LV function and dimensions were normal in the remaining two. All patients with a decreased echocardiographic GLS had a normal CMR.

Discussion

In this Belgian multicenter prospective observational study, we report on the late cardiac outcomes of 36 children who were recruited during the acute phase of an MIS-C episode. In the late-term follow-up visit, with the evaluation of late cardiac outcomes through NT-proBNP measurement, ECG and 24-h Holter monitoring, echocardiography, and CMR performed after a mean period of 1 year with a maximal interval of 28 months after MIS-C admission. To the best of our knowledge, this includes the longest follow-up interval of a multimodal cardiac evaluation, including CMR, after MIS-C.

Echocardiographic abnormalities

As in Kawasaki disease, coronary dilatation is a common finding in the acute phase of MIS-C with a prevalence rate ranging from 7% to 35%. Most patients have coronary dilatation or small coronary artery aneurysms. Giant coronary aneurysms are rare. The follow-up demonstrates a regression of the coronary artery dilatation to 79% after 30 days and up to 100% after 90 days, although there are reports of persistent giant coronary artery aneurysms (4, 6, 11, 16, 17). In our cohort, a relatively large number (56%) had coronary artery dilation, but none had more than small coronary aneurysms, defined as a *z*-score of <5. It is suggested that fever and tachycardia caused by the hyperinflammatory state are responsible for the frequent mild coronary artery dilation and not the inflammatory damage to the arterial wall itself, as seen in Kawasaki disease (18). This could also explain the rapid normalization of the coronary artery dimension in our cohort. As there is a significant overlap between the symptomatology of MIS-C and Kawasaki disease, it is possible that some of the children with persistent important coronary aneurysms reported in the literature had incomplete Kawasaki disease rather than MIS-C.

Pericardial effusion occurs in up to 28% of patients in the acute phase of MIS-C and resolves quickly (19). Severe effusion with tamponade necessitating pericardiocentesis is very rare (11). In our cohort, 17% had a pericardial effusion, but none needed percutaneous drainage nor showed pericardial effusion at follow-up echocardiography or CMR.

Mitral valve incompetence is associated with MIS-C, possibly secondary to a decreased LV function with LV dilation or as a sign of valvulitis. Valverde et al. (6) describe a prevalence of MI in 42% of patients at diagnosis. In our population, MI was present in five patients (13%). Four had a decreased LV function and one had a concomitant increased LVEDD. An isolated MI, representing valvulitis, was observed only in one patient and did not persist at follow-up. MI was present at follow-up in the patient with persistent LV dysfunction and dilation.

PH was seen in three patients of whom one had a decreased systolic LV function, one had mitral valve insufficiency, and one had isolated PH. None had interference of any pulmonary involvement (pneumonia, atelectasis, and pleural effusion). Isolated PH is not known to be an expected condition in MIS-C. In our patients, it can be hypothesized that both pulmonary vascular reactivity, caused by systemic inflammation, and LV dysfunction could be the cause for this increased pulmonary arterial pressure. Only the patient with a severely impaired LV systolic function had a postcapillary PH at follow-up.

ECG abnormalities

ECG abnormalities are associated with MIS-C and are observed in up to two-thirds of patients (3, 11). This study showed ECG abnormalities in 36% of children, mainly during repolarization. Myopericarditis with consequent myocardial inflammation and edema seems to be responsible for these conduction abnormalities, a hypothesis supported by the normalization of the ECG in most cases after MIS-C recovery (20). Tachyarrhythmias are rare in MIS-C. Dionne et al. (2) reported a 1.7% prevalence in 2,343 patients <21 years of supraventricular tachycardia, accelerated junctional rhythm, or ventricular tachycardia. In our patient group, we did not observe any tachyarrhythmias during admission nor at the 24-h Holter monitoring during follow-up.

Echocardiographic evaluation of cardiac function

An impaired echocardiographic systolic LV function is observed in 31%–63% of MIS-C patients at diagnosis. An ICU admission and the need for inotropic support are not uncommon, and a small number even need extracorporeal membrane oxygenation (21, 22). However, recovery of LV systolic function on echocardiography is observed in most patients already at short-term follow-up. Persistence of LV dysfunction at mid-term follow-up is rare (7). In our cohort, 39% of patients had a decreased LVEF during MIS-C, all needing inotropic support. None required ECMO. Our follow-up data confirm the lasting recovery of systolic LV function at late-term. Severely impaired systolic LV function was observed in one patient at follow-up.

As LVEF is a marker of clinical myocardial function, LV GLS represents both clinical and subclinical myocardial performance. In MIS-C, LV GLS is significantly reduced, and mainly the basal LV segments seem to be affected. The decreased GLS seems to persist longer than a diminished LVEF. The latter is usually recovered at the 2-month follow-up, while GLS improves especially between 2 and 6 months after disease onset (10, 23, 24). It is suggested that a diminished GLS could reflect persistent subclinical myocardial damage. In our study, 5 out of 14 patients (35%) had a GLS *z*-score of <−2 at follow-up. The FS, LVEF, and CMR were normal in all patients. We could not identify any differences in characteristics at baseline in these groups. Thus, it remains uncertain which patients are at greater risk for a decreased GLS during long-term follow-up, as even children with normal LVEF are at risk (25). Although GLS has proved its value in the detection of subclinical myocardial dysfunction, further investigation is necessary to assess the clinical significance and predictive value of a decreased LV GLS during MIS-C follow-up. We believe that follow-up needs to be continued in these patients with diminished GLS until normalization.

CMR

CMR data in the acute phase of MIS-C are scarce. Myocardial edema and LGE as signs of myocardial fibrosis are present in 14%–35% (6, 26). In a multicenter study by Aeschlimann et al. (27), 18% of patients met the Lake Louise criteria for myocarditis at a median time of 28 days after the onset of symptoms. It seems clear that myocarditis can be present during the hyperinflammatory state in MIS-C and can persist for a short term in some patients. Emerging mid-term follow-up CMR data after MIS-C have

become available, but conflicting results are being published. Bartoszek et al. (28) could not identify any CMR abnormalities at the 3-month follow-up in 19 children with cardiac involvement during the acute phase of MIS-C, and neither could Barris et al. (3) at the 9-month follow-up. These results contrast with other data that show the presence of LGE, without LV dysfunction or any other clinically significant cardiac abnormalities, in up to 50% after a mean follow-up of 9 months (11, 29). We performed a CMR after a mean period of 12 months with a range of 6–28 months and observed normalization of the cardiac function in almost all patients. The patient described above, who did not receive adequate MIS-C treatment because of a late recognition in the early stages of the pandemic, had a severely reduced EF (10%) and an increased LVEDD (197 ml/m^2) and LGE on CMR 6 months after MIS-C. Interestingly, two other patients had mildly reduced EF on CMR and normal echocardiographic LVEF and FS. The discrepancy between the evaluation of cardiac function on echocardiography and CMR is not clearly understood. Possibly, CMR, as the gold standard for LV function evaluation, is more sensitive for detecting a subtle decreased LV function. CMR LVEDD was >p97 in two patients with normal echocardiographic LVEDD and LV function.

It can be hypothesized that CMR at mid-term follow-up still shows persistent anomalies that may recover over time. Sirico et al. (10) described 6 patients with LGE on initial CMR 18 days after the disease onset, who underwent repeat CMR 6 months later. Although LGE was still present in 5 out of 6 patients, reduced extension was observed. Benvenuto et al. (30) describe a similar patient with LGE on CMR 2 months after MIS-C, with an improvement on repeat CMR at the 9-month follow-up. CMR can be a useful tool during MIS-C follow-up; however, the timing is still open for discussion. Timing CMR 3–6 months after MIS-C diagnosis can be performed to assess whether participating in competitive sports is safe, in addition to an exercise stress test and/or 24-h Holter monitoring. However, if echocardiography is normal, it could be considered to evaluate for myocardial fibrosis at a later stage during follow-up, as the degree of LGE seems to improve over time. CMR even seems unnecessary in most children, as no relevant cardiac abnormalities were found in patients with LGE on CMR and with normal echocardiographic cardiac function. Our findings seem to support this idea as no LGE was observed after a long mean follow-up period of 12 months in patients who received adequate MIS-C treatment.

Limitations

There are some limitations in our study. First, although the mean follow-up duration is one of the longest reported, it occurred not at a fixed time interval after MIS-C admission because of various factors such as the availability of CMR during the pandemic. Second, our LV GLS results could be biased as we added evaluation for subclinical myocardial damage through LV GLS at a later stage of the study course. Finally, we could include only 36 out of 62 MIS-C patients; however, this has not significantly changed our results because the standard follow-up in those children who did not participate in the study did not show cardiac abnormalities.

Conclusion

Late cardiac outcomes after MIS-C, if treated according to current guidelines, are excellent. CMR does not show any myocardial scarring in children with a normal echocardiographic LVEF. Subclinical myocardial damage can persist in the late term, and further follow-up seems appropriate in these patients. However, the clinical significance of these findings has yet to be determined.

Data availability statement

The raw data supporting the conclusions of this article will be made available by the authors without undue reservation.

Ethics statement

The studies involving humans were approved by the Brussels University Hospital ethics committee. The studies were conducted in accordance with local legislation and institutional requirements. Written informed consent for participation in this study was provided by the participants' legal guardians/next of kin.

Author contributions

RW was involved in the following activities: conceptualization, data curation, formal analysis, investigation, methodology preparation, project administration, validation, visualization, writing—original draft, and writing—review and editing; DW was involved in conceptualization, data curation, methodology preparation, resource collection, supervision, and writing—review and editing; MZ, WD, LM-M, and KV were involved in investigation and writing—review and editing; KT was involved in investigation and writing—original draft and writing—review and editing; GB was involved in writing—review and editing. All authors contributed to the article and approved the submitted version.

Acknowledgments

The authors would like to thank all participating children and parents.

Conflict of interest

The authors declare that the research was conducted in the absence of any commercial or financial relationships that could be construed as a potential conflict of interest.

Publisher's note

References

1. Howard-Jones AR, Burgner DP, Crawford NW, Goeman E, Gray PE, Hsu P, et al. COVID-19 in children. II: pathogenesis, disease spectrum and management. *J Paediatr Child Health*. (2022) 58:46–53. doi: 10.1111/jpc.15811

2. Dionne A, Friedman KG, Young CC, Newhams MM, Kucukak S, Jackson AM, et al. Tachyarrhythmias during hospitalization for COVID-19 or multisystem inflammatory syndrome in children and adolescents. *J Am Heart Assoc*. (2022) 11: e025915. doi: 10.1161/jaha.122.025915

3. Barris DM, Keelan J, Ahluwalia N, Jhaveri S, Cohen J, Stern K, et al. Midterm outcomes and cardiac magnetic resonance imaging following multisystem inflammatory syndrome in children. *J Pediatr*. (2022) 241:237–41.e1. doi: 10.1016/j.jpeds.2021.10.009

4. Feldstein LR, Rose EB, Horwitz SM, Collins JP, Newhams MM, Son MBF, et al. Multisystem inflammatory syndrome in U.S. children and adolescents. *N Engl J Med*. (2020) 383:334–46. doi: 10.1056/NEJMoa2021680

5. Kwak JH, Lee SY, Choi JW. Clinical features, diagnosis, and outcomes of multisystem inflammatory syndrome in children associated with coronavirus disease 2019. *Clin Exp Pediatr*. (2021) 64:68–75. doi: 10.3345/cep.2020.01900

6. Valverde I, Singh Y, Sanchez-de-Toledo J, Theocharis P, Chikermane A, Di Filippo S, et al. Acute cardiovascular manifestations in 286 children with multisystem inflammatory syndrome associated with COVID-19 infection in Europe. *Circulation*. (2021) 143:21–32. doi: 10.1161/circulationaha.120.050065

7. Farooqi KM, Chan A, Weller RJ, Mi J, Jiang P, Abrahams E, et al. Longitudinal outcomes for multisystem inflammatory syndrome in children. *Pediatrics*. (2021) 148. doi: 10.1542/peds.2021-051155

8. Capone CA, Misra N, Ganigara M, Epstein S, Rajan S, Acharya SS, et al. Six month follow-up of patients with multi-system inflammatory syndrome in children. *Pediatrics*. (2021) 148. doi: 10.1542/peds.2021-050973

9. Davies P, du Pré P, Lillie J, Kanthimathinathan HK. One-year outcomes of critical care patients post-COVID-19 multisystem inflammatory syndrome in children. *JAMA Pediatr*. (2021) 175:1281–3. doi: 10.1001/jamapediatrics.2021.2993

10. Sirico D, Basso A, Sabatino J, Reffo E, Cavaliere A, Biffanti R, et al. Evolution of echocardiographic and cardiac magnetic resonance imaging abnormalities during follow-up in patients with multisystem inflammatory syndrome in children. *Eur Heart J Cardiovasc Imaging*. (2022) 23:1066–74. doi: 10.1093/ehjci/jeac096

11. Cantarutti N, Battista V, Stagnaro N, Labate ME, Cicenia M, Campisi M, Vitali V, Secinaro A, Campana A, Trocchio G, et al. Long-term cardiovascular outcome in children with MIS-C linked to SARS-CoV-2 infection-an Italian multicenter experience. *Biology (Basel)* (2022) 11. doi: 10.3390/biology11101474

12. Organization WH. Multisystem inflammatory syndrome in children and adolescents with COVID-19: Scientific brief. Geneva, Switzerland: World Health Organization (2020). Available at: https://apps.who.int/iris/handle/10665/332095 (Accessed May 15, 2020).

13. McCrindle BW, Rowley AH, Newburger JW, Burns JC, Bolger AF, Gewitz M, et al. Diagnosis, treatment, and long-term management of Kawasaki disease: a scientific statement for health professionals from the American Heart Association. *Circulation*. (2017) 135:e927–99. doi: 10.1161/cir.0000000000000484

14. Dallaire F, Slorach C, Bradley T, Hui W, Sarkola T, Friedberg MK, et al. Pediatric reference values and Z score equations for left ventricular systolic strain measured by two-dimensional speckle-tracking echocardiography. *J Am Soc Echocardiogr*. (2016) 29:786–93.e8. doi: 10.1016/j.echo.2016.03.018

15. van der Ven JPG, Sadighy Z, Valsangiacomo Buechel ER, Sarikouch S, Robbers-Visser D, Kellenberger CJ, et al. Multicentre reference values for cardiac magnetic resonance imaging derived ventricular size and function for children aged 0–18 years. *Eur Heart J Cardiovasc Imaging*. (2020) 21:102–13. doi: 10.1093/ehjci/jez164

16. Whittaker E, Bamford A, Kenny J, Kaforou M, Jones CE, Shah P, et al. Clinical characteristics of 58 children with a pediatric inflammatory multisystem syndrome temporally associated with SARS-CoV-2. *JAMA*. (2020) 324:259–69. doi: 10.1001/jama.2020.10369

17. Alsaied T, Tremoulet AH, Burns JC, Saidi A, Dionne A, Lang SM, et al. Review of cardiac involvement in multisystem inflammatory syndrome in children. *Circulation*. (2021) 143:78–88. doi: 10.1161/circulationaha.120.049836

18. Shulman ST, Rowley AH. Kawasaki disease: insights into pathogenesis and approaches to treatment. *Nat Rev Rheumatol*. (2015) 11:475–82. doi: 10.1038/nrrheum.2015.54

19. Hejazi OI, Loke YH, Harahsheh AS. Short-term cardiovascular complications of multi-system inflammatory syndrome in children (MIS-C) in adolescents and children. *Curr Pediatr Rep*. (2021) 9:93–103. doi: 10.1007/s40124-021-00258-5

20. Regan W, O'Byrne L, Stewart K, Miller O, Pushparajah K, Theocharis P, et al. Electrocardiographic changes in children with multisystem inflammation associated with COVID-19: associated with coronavirus disease 2019. *J Pediatr*. (2021) 234:27–32.e2. doi: 10.1016/j.jpeds.2020.12.033

21. Wong J, Theocharis P, Regan W, Pushparajah K, Stephenson N, Pascall E, et al. Medium-term cardiac outcomes in young people with multi-system inflammatory syndrome: the era of COVID-19. *Pediatr Cardiol*. (2022) 43:1728–36. doi: 10.1007/s00246-022-02907-y

22. Penner J, Abdel-Mannan O, Grant K, Maillard S, Kucera F, Hassell J, et al. 6-month multidisciplinary follow-up and outcomes of patients with paediatric inflammatory multisystem syndrome (PIMS-TS) at a UK tertiary paediatric hospital: a retrospective cohort study. *Lancet Child Adolesc Health*. (2021) 5:473–82. doi: 10.1016/s2352-4642(21)00138-3

23. Matsubara D, Kauffman HL, Wang Y, Calderon-Anyosa R, Nadaraj S, Elias MD, et al. Echocardiographic findings in pediatric multisystem inflammatory syndrome associated with COVID-19 in the United States. *J Am Coll Cardiol*. (2020) 76:1947–61. doi: 10.1016/j.jacc.2020.08.056

24. Başar EZ, Usta E, Akgün G, Güngör HS, Sönmez HE, Babaoğlu K. Is strain echocardiography a more sensitive indicator of myocardial involvement in patients with multisystem inflammatory syndrome in children (MIS-C) associated with SARS-CoV-2? *Cardiol Young*. (2022) 32:1657–67. doi: 10.1017/s1047951122000646

25. Das N, Hill R, Trivedi M, Kenkre TS, Alsaied T, Feingold B, et al. Longitudinal assessment of cardiac function following multisystem inflammatory syndrome in children associated with COVID-19. *Pediatr Cardiol*. (2023) 44:607–17. doi: 10.1007/s00246-022-02972-3

26. Theocharis P, Wong J, Pushparajah K, Mathur SK, Simpson JM, Pascall E, et al. Multimodality cardiac evaluation in children and young adults with multisystem inflammation associated with COVID-19. *Eur Heart J Cardiovasc Imaging*. (2021) 22:896–903. doi: 10.1093/ehjci/jeaa212

27. Aeschlimann FA, Misra N, Hussein T, Panaioli E, Soslow JH, Crum K, et al. Myocardial involvement in children with post-COVID multisystem inflammatory syndrome: a cardiovascular magnetic resonance based multicenter international study-the CARDOVID registry. *J Cardiovasc Magn Reson*. (2021) 23:140. doi: 10.1186/s12968-021-00841-1

28. Bartoszek M, Małek ŁA, Barczuk-Falęcka M, Brzewski M. Cardiac magnetic resonance follow-up of children after pediatric inflammatory multisystem syndrome temporally associated with SARS-CoV-2 with initial cardiac involvement. *J Magn Reson Imaging*. (2022) 55:883–91. doi: 10.1002/jmri.27870

29. DiLorenzo MP, Farooqi KM, Shah AM, Channing A, Harrington JK, Connors TJ, et al. Ventricular function and tissue characterization by cardiac magnetic resonance imaging following hospitalization for multisystem inflammatory syndrome in children: a prospective study. *Pediatr Radiol*. (2023) 53(3):394–403. doi: 10.1007/s00247-022-05521-5

30. Benvenuto S, Simonini G, Della Paolera S, Abu Rumeileh S, Mastrolia MV, Manerba A, et al. Cardiac MRI in midterm follow-up of MISC: a multicenter study. *Eur J Pediatr*. (2023) 182:845–54. doi: 10.1007/s00431-022-04748-6

frontiers | Frontiers in Cardiovascular Medicine

TYPE Original Research
PUBLISHED 20 November 2023
DOI 10.3389/fcvm.2023.1293210

OPEN ACCESS

EDITED BY
Liqun Sun,
University of Toronto, Canada

REVIEWED BY
Mingfu Wu,
University of Houston, United States
Zhang Cheng,
Chongqing Medical University, China
Kui Hu,
Guizhou Provincial People's Hospital, China

*CORRESPONDENCE
Weicheng Chen
✉ weicheng.chern@gmail.com
Wei Sheng
✉ sheng_wei@fudan.edu.cn
Guoying Huang
✉ gyhuang@shmu.edu.cn

†These authors have contributed equally to this work and share first authorship

RECEIVED 12 September 2023
ACCEPTED 27 October 2023
PUBLISHED 20 November 2023

CITATION
Huang X, Gao Y, Chen W, Sheng W and Huang G (2023) Noncardiac anomalies in children with congenital heart disease. Front. Cardiovasc. Med. 10:1293210. doi: 10.3389/fcvm.2023.1293210

Noncardiac anomalies in children with congenital heart disease

Xianghui Huang[1,2†], Yuan Gao[1,3†], Weicheng Chen[1,3*], Wei Sheng[1,3,4*] and Guoying Huang[1,3,4*]

[1]Cardiovascular Center, Children's Hospital of Fudan University, Shanghai, China, [2]Fujian Key Laboratory of Neonatal Diseases, Xiamen Children's Hospital, Fujian, China, [3]Shanghai Key Laboratory of Birth Defects, Shanghai, China, [4]Unit of Early Intervention of Genetically Related Childhood Cardiovascular Diseases, Shanghai, China

Introduction: Noncardiac anomalies (NCAs) in patients with congenital heart defects (CHDs) are crucial for perioperative management and etiology studies. This study aimed to investigate NCAs in Chinese children with CHDs.
Methods: Medical records for CHD-diagnosed children hospitalized from 1 January 2015 to 31 December 2019 were collected and subjected to retrospective analyses to excavate potential association rules between CHDs and noncardiac malformations.
Results: A total of 3,788 CHD patients were included in this study. The main phenotypes of CHD were Ventricular Septal Defect (VSD, 33.69%), Atrial Septal Defect (ASD, 12.72%), and Tetralogy of Fallot (TOF, 5.54%). A total of 887 (23.42%) cases showed noncardiac anomalies, which were mainly associated with the central nervous system (34.61%), nose/ear/mandibular/face (19.39%), genitourinary system (15.78%), and musculoskeletal system (15.56%). Compared to other CHD subtypes, septal defects had a lower percentage of associated NCAs ($P = 3.7 \times 10^{-9}$) while AVSD had a higher percentage ($P = 0.0018$).
Disscussion: NCAs are prevalent among CHD-diagnosed children in China, and the spectrums of NCAs in different CHD subcategories were different.

KEYWORDS

congenital heart defects, noncardiac anomalies, Chinese children, retrospective analyses, phenotype

1. Introduction

Congenital heart defects (CHDs) are a leading cause of infant mortality and the most commonly diagnosed major congenital anomaly worldwide (1, 2) with a prevalence of 8.98 per 1,000 live births in China (3). Although diagnostic capabilities and surgical strategies have significantly advanced, CHD remains a costly and onerous disease burden in many countries (4, 5). CHDs manifest as diverse structural abnormalities of the heart and great vessels that arise during embryonic development. The complexity of structural anomalies, defect severity, and the presence of comorbidities are essential determinants of CHD outcomes (6).

It is important to identify whether a CHD presents as an isolated condition or has developed in combination with noncardiac anomalies, as is frequently the case. Multiple organs originate from a common germ layer and can be regulated by shared signaling pathways (7). Moreover, chromosomal aberrations, which represent a leading cause of CHDs, alter the activities of multiple genes that may have different functions in embryogenesis. CHD comorbidities affecting other systems have a significant impact on clinical course. Despite advances in cardiac surgery and perioperative management, Eskedal et al. (8) reported that survival has not improved for CHD-diagnosed children

with extracardiac anomalies. A 15-year follow-up study showed that noncardiac anomalies (NCAs) had a more significant effect on mortality in patients with CHDs than potential heart disease (9). Indeed, some have recommended that prediction modeling of thoracic surgery mortality risk for CHD patients could be augmented by adding a covariate that represents noncardiac congenital anatomic abnormalities (10). NCAs can increase the risk of postoperative complications, such as respiratory complications with heterotaxy (11), and children with CHD undergoing noncardiac surgery can have an increased mortality risk (12). Consequently, to identify optimal perioperative and long-term management of patients with CHDs and to elucidate the etiology of congenital defects, a detailed description of coexisting NCAs in children with CHD is necessary.

Reported frequencies of NCAs in CHD-diagnosed patients range widely from 4.53% to 50% (13–15). Different types of CHD are associated with distinct incidences of extracardiac comorbidities. For example, the NCA risk has been reported to be elevated among CHD patients with a cardiac looping defect, conotunal defect (CTD), or atrial septal defect (ASD) and reduced among CHD patients with a ventricular septal defect (VSD) or Ebstein anomaly (16, 17). Moreover, specific associations have been identified between common truncus and limb reduction defects and between great vessel-transposition and situs inversus (18). Piran found a trend toward a higher prevalence of major congenital extracardiac anomalies involving the musculoskeletal and genitourinary systems in adults with tetralogy of Fallot (TOF) (19). Thus far, there are limited data in the literature regarding the occurrence of NCAs in CHD-diagnosed children in China, and this study aimed to describe the proportions and distributions of NCAs in Chinese children of Han ethnicity who have been diagnosed with a CHD.

2. Materials and methods

2.1. Study population

Children diagnosed with a CHD and hospitalized in the Department of Cardiac Surgery, Children's Hospital of Fudan University from 1 January 2015 to 31 December 2019 were eligible for inclusion. Data collection and analysis processes were conducted with the permission of and under the guidance of the ethics committee. Written informed consent to participate was obtained from the guardians. Medical histories, surgical records, imaging data, outpatient medical records, and genetic test results of enrolled patients were collected and examined retrospectively. CHD diagnoses were confirmed by clinical assessment, echocardiography, cardiac catheterization, and, if necessary, surgical observations. Patent foramen ovale, patent ductus arteriosus (PDA) in premature infants, and a PDA that resolved within 3 months after birth were excluded. The analyses did not include patients with cardiomyopathies, cardiac arrhythmias, or primary pulmonary hypertension.

2.2. Phenotype classification

Individual patients' CHDs were classified based on anatomy and etiology (20–23) into the level 1 and 2 categories (**Table 1**), where the latter are subcategories of the former. Level 1 categories included the following: septal defects, atrioventricular canal defect (AVSD), conotruncal cardiac defect (CTD), left ventricular outflow tract obstruction (LVOTO), right ventricular outflow tract obstruction (RVOTO), abnormal cell growth, heterotaxy (HTX), others, and associations.

Diagnosed NCAs were summarized and aggregated according to affected systems. All developmental delays, including growth retardation, intellectual disability, mental delays, learning difficulties, and language/motor deficits, were classified as central nervous system (CNS) anomalies (24). We ignored syndrome diagnoses to focus on phenotypes. Syndrome-associated noncardiac phenotypes were disassociated and classified according to their respective affected systems. Anomalies within the same affected system were counted as one. CHD cases with and without NCAs are referred to as associated CHD cases and isolated CHD cases, respectively.

2.3. Statistical analysis

R (version 4.1.2), R Studio (version 1.4.1717), and SPSS (IBM version 20) were used for statistical analysis. Analysis of description was used to provide the whole picture of CHD and NCAs; Pearson's χ^2 test or Fisher's exact test was applied to compare the proportions of isolated CHD between different genders and different CHD subtypes. The apriori principle (25) was used to analyze CHD diagnosis-to-NCA association, setting thresholds for support and confidence at 0.01 and 0.1, respectively. Rules with a lift ≥ 3 were considered of value.

3. Results

3.1. Proportions of congenital heart defects

A total of 3,788 CHD-diagnosed children were identified retrospectively, of which 2,065 (54.51%) were male and 1,723 were female (45.49%) with a median age of 3.96 years (IQR, 2.56–5.39). The proportions of level 1 and level 2 diagnostic classifications are reported in **Table 1** with sex ratios and the number of co-occurring anomalies. The most common level 1 diagnoses were septal defect (56.89%), CTD (13.83%), and RVOTO (6.39%); besides different septal defects TOF (5.54%), pulmonary artery/valve atresia or other malformations of the pulmonary artery/valve (3.85%), DORV (2.03%), valvular/supravalvular aortic stenosis or other malformation of the aorta

TABLE 1 Distribution of CHD subtypes and corresponding number of NCAs.

CHD phenotypes[a]	*n* (%)[b]	Sex ratio (M/F)	Number of noncardiac malformation, *n* (%)[c]			
			0	1	2	≥3
Septal defect	2,155 (56.89)	1.11	1,727 (80.14)	277 (12.85)	115 (5.34)	36 (1.67)
VSD	1,276 (33.69)	1.34	1,056 (82.76)	146 (11.44)	54 (4.23)	20 (1.57)
ASD	482 (12.72)	0.88	361 (74.90)	76 (15.77)	37 (7.68)	8 (1.66)
VSD + ASD	397 (10.48)	0.83	310 (78.09)	55 (13.85)	24 (6.05)	8 (2.02)
AVSD	124 (3.27)	0.8	80 (64.52)	22 (17.74)	17 (13.71)	5 (4.03)
AVSD	108 (2.85)	0.83	70 (64.81)	18 (16.67)	17 (15.74)	3 (2.78)
AVSD + OTO	16 (0.42)	0.60	10 (62.50)	4 (25.00)	0 (0.00)	2 (12.50)
CTD	524 (13.83)	1.94	400 (76.34)	80 (15.27)	37 (7.06)	7 (1.34)
PTA	9 (0.24)	0.50	6 (66.67)	2 (22.22)	0 (0.00)	1 (11.11)
DTGA-IVS	48 (1.27)	3.36	43 (89.58)	4 (8.33)	1 (2.08)	0 (0.00)
DTGA-IVS + OTO	11 (0.29)	$F = 0$	5 (45.45)	4 (36.36)	2 (18.18)	0 (0.00)
DTGA + VSD	65 (1.72)	2.61	56 (86.15)	8 (12.31)	1 (1.54)	0 (0.00)
TOF	210 (5.54)	1.76	163 (77.62)	28 (13.33)	14 (6.67)	5 (2.38)
PA-VSD	43 (1.14)	1.05	32 (74.42)	6 (13.95)	5 (11.63)	0 (0.00)
DORV	77 (2.03)	1.85	58 (75.32)	13 (16.88)	6 (7.79)	0 (0.00)
APW	7 (0.18)	1.33	3 (42.86)	2 (28.57)	2 (28.57)	0 (0.00)
IAA	26 (0.69)	1.89	19 (73.08)	5 (19.23)	2 (7.69)	0 (0.00)
Vasc ring malformations	28 (0.74)	3.00	15 (53.57)	8 (28.57)	4 (14.29)	1 (3.57)
LVOTO	66 (1.74)	1.64	46 (69.7)	16 (24.24)	1 (1.52)	3 (4.55)
HLH	3 (0.08)	2.00	2 (66.67)	1 (33.33)	0 (0.00)	0 (0.00)
Valvular/supravalvular aortic stenosis or other malformation of aorta or the aortic valve	63 (1.66)	1.63	44 (69.84)	15 (23.81)	1 (1.59)	3 (4.76)
RVOTO	242 (6.39)	1.00	192 (79.34)	37 (15.29)	11 (4.55)	2 (0.83)
Pulmonary artery/valve atresia or other malformations of pulmonary artery/valve	146 (3.85)	0.85	119 (81.51)	19 (13.01)	6 (4.11)	2 (1.37)
Eebstein	12 (0.32)	2.00	8 (66.67)	3 (25)	1 (8.33)	0 (0.00)
TA-VSD/TA + PA-IVS	6 (0.16)	1.00	3 (50.00)	2 (33.33)	1 (16.67)	0 (0.00)
DCRV	59 (1.56)	1.19	45 (76.27)	12 (20.34)	2 (3.39)	0 (0.00)
HRH	19 (0.50)	1.38	17 (89.47)	1 (5.26)	1 (5.26)	0 (0.00)
Abnormal cell growth	75 (1.98)	1.78	59 (78.67)	11 (14.67)	4 (5.33)	1 (1.33)
APVD	56 (1.48)	2.73	46 (82.14)	6 (10.71)	3 (5.36)	1 (1.79)
Cor triatriatum	19 (0.50)	0.58	13 (68.42)	5 (26.32)	1 (5.26)	0 (0.00)
Others	151 (3.99)	0.61	108 (71.52)	30 (19.87)	10 (6.62)	3 (1.99)
CCTGA	6 (0.16)	2.00	4 (66.67)	2 (33.33)	0 (0.00)	0 (0.00)
SV	7 (0.18)	2.50	6 (85.71)	1 (14.29)	0 (0.00)	0 (0.00)
Isolated malformations of great arteries	3 (0.08)	2.00	1 (33.33)	2 (66.67)	0 (0.00)	0 (0.00)
Isolated malformation of the coronary arteries	15 (0.40)	0.36	12 (80.00)	2 (13.33)	0 (0.00)	1 (6.67)
Isolated malformations of heart valve	38 (1.00)	0.46	28 (73.68)	7 (18.42)	3 (7.89)	0 (0.00)
Isolated PDA	82 (2.16)	0.58	57 (69.51)	16 (19.51)	7 (8.54)	2 (2.44)
HTX	87 (2.30)	1.35	8 (9.2)	62 (71.26)	13 (14.94)	4 (4.6)
HTX + no CVM	5 (0.13)	$F = 0$	4 (80.00)	0 (0.00)	0 (0.00)	1 (20.00)
HTX + simple CVM	37 (0.98)	0.76	2 (5.41)	26 (70.27)	7 (18.92)	2 (5.41)
HTX + complex CVM	45 (1.19)	1.81	2 (4.44)	36 (80.00)	6 (13.33)	1 (2.22)
Associations	364 (9.61)	1.38	281 (77.2)	52 (14.29)	20 (5.49)	11 (3.02)
AVSD + CTD	10 (0.26)	1.00	2 (20.00)	5 (50.00)	1 (10.00)	2 (20.00)
Septal defects + APVD	104 (2.75)	1.48	87 (83.65)	10 (9.62)	6 (5.77)	1 (0.96)
Septal defects + RVOTO	95 (2.51)	1.07	73 (76.84)	14 (14.74)	7 (7.37)	1 (1.05)
Septal defects + LVOTO	123 (3.25)	1.51	95 (77.24)	19 (15.45)	5 (4.07)	4 (3.25)
RVOTO + LVOTO	9 (0.24)	2.00	6 (66.67)	1 (11.11)	1 (11.11)	1 (11.11)
CTD + LVOTO	17 (0.45)	2.40	15 (88.24)	1 (5.88)	0 (0.00)	1 (5.88)

(*Continued*)

TABLE 1 Continued

CHD phenotypes[a]	*n* (%)[b]	Sex ratio (M/F)	Number of noncardiac malformation, *n* (%)[c]			
			0	1	2	≥3
CTD + APVD	6 (0.16)	1.00	3 (50.00)	2 (33.33)	0 (0.00)	1 (16.67)
TOTAL	3,788 (100)	1.20	2,901 (76.58)	587 (15.50)	228 (6.02)	72 (1.90)

VSD, ventricular septal defect; ASD, atrial septa defect; AVSD, atrioventricular septal defect; OTO, outflow tract obstruction, including LVOTO (left ventricular outflow tract obstruction) and RVOTO (right ventricular outflow tract obstruction); CTD: conotruncal defect; PTA, persistent truncus arteriosus; D-TGA, dextro-transposition of the great arteries; IVS, intact ventricular septum; TOF, tetralogy of fallot; PA, pulmonary atresia; DORV, double outlet right ventricle; APW, aortopulmonary window; IAA, interruption of aortic arch, including type A/B/C; vasc ring malformations, including right arch and sling; HLH, hypoplastic left ventricle; TA, tricuspid atresia; DCRV, double-chambered right ventricle; HRH, hypoplastic right ventricle; APVD, anomalous pulmonary venous drainage; CCTGA, congenitally corrected transposition of the great arteries; SV, single ventricle; PDA, patent ductus arteriosus; HTX, heterotaxy or situs inversus totalis; CVM, refer to above structural cardiovascular malformations, and complex CVM refers to more than one above cardiovascular malformations.

[a]CHD level 1 subcategories are represented in bold font centered on the center, and the level 2 subcategories included in each level 1 subcategories are aligned to the left below each other.

[b]Percentage denominator was total *N* of 3,788.

[c]Percentage denominator was total number of each CHD subcategories.

or the aortic valve (1.66%), and dextro-transposition of the great arteries (D-TGA, 1.27%) were common level 2 diagnoses. Furthermore, 3.25% children had both septal defects and LVOTO and 2.75% children had septal defects and RVOTO.

3.2. Noncardiac malformations in children with CHDs

A total of 887 (23.42%) cases of CHD were associated with noncardiac malformations, comprising 587 (15.50%) with one malformation, 228 (6.02%) with two malformations, and 72 (1.90%) with three or more malformations (Table 1).There were 1,284 noncardiac malformations among the 887 children, including 307 (34.61%) in the nervous system, 172 (19.39%) in the nose/ear/mandibular/face, and 140 (15.78%) in the musculoskeletal system (Table 2). The most common discrete NCA phenotype by far was developmental delay ($n = 262$, 29.54%), inguinal hernia ($n = 83$, 9.36%), and cryptorchidism and hydrocele ($n = 77$, 8.68%).

3.3. NCA spectra for CHD subcategories

The level 1 diagnoses with the highest percentages of isolated CHDs were septal defects, wherein about four fifths of each were isolated (Table 1). Conversely, besides heterotaxy, the diagnosis with the greatest percentage of associated CHDs was AVSD, wherein almost two fifths of the patients have associated CHDs (Table 1). Statistical analysis proved that septal defects, especially VSD ($P = 3.7 \times 10^{-9}$) and D-TGA with an intact ventricular septum (D-TGA + IVS, $P = 0.038$), are less likely to associated with NCAs. Furthermore, there were a higher probability of combined NCAs in children with AVSD ($P = 0.002$) and vasc ring malformations ($P = 0.007$).

Although NCAs involving the CNS, nose/ear/mandibular/face, genitourinary system, and musculoskeletal system were common for most CHD subtypes, the distribution of NCAs differed slightly (Table 3). NCAs affecting the CNS were most frequently observed in AVSD and RVOTO cases, wherein approximately one third of patients were affected. Nose/ear/mandibular/face anomalies were observed in more than one fifth of AVSD cases. Children in groups of septal defects or groups of associations showed relatively larger proportions of combined musculoskeletal anomalies (12.16% and 12.00%) and abdominal wall deficiency (9.48% and 8.80%). Genitourinary malformations were less prevalent in LVOTO-diagnosed children whereas respiratory system NCAs and digestive system NCAs were apparently common in children with CTD and LVOTO, respectively. Laterality defects were notably common in heterotaxy cases and, albeit to a lesser extent, CTD cases (Table 3). Furthermore, taking gender into account, among children with septal defects, especially those with VSD, PA-VSD, pulmonary artery/valve atresia, or other malformation of the pulmonary artery/valve and double-chambered right ventricule (DCRV), males were more likely to have associated CHD than females ($P < 0.05$), whereas the situation is opposite in LVOTO and RVOTO diagnostic groups.

3.4. Co-occurrence of CHDs and NCAs

With support and confidence levels set to 0.01 and 0.1, respectively, we attained 213 rules between CHD subtypes and NCAs. After filtering out low-value rules (lift < 3), 11 rules were retained (Table 4), showing the reliability or value of the rule which indicated the following potential CHD–NCA co-occurrence relationships: CCTGA-SV–laterality defect (lift = 13.02); CTD, RVOTO–laterality defect NCA (lift = 9.01); heterotaxy–laterality defect NCA (lift = 6.93); vasc ring malformations–respiratory system NCA (lift = 5.19); VSD, PDA, and CNS anomalies-LVOTO (lift = 3.66).

4. Discussion

In the present study sample, 23.42% of CHD diagnosed children had coexisting NCAs, a value about midway between

TABLE 2 Distribution of NCAs in 887 children with associated CHD.

Noncardiac anomaly	i (%)[a]
Central nervous system anomalies	307 (34.61)
Archinencephaly	69 (7.78)
Spina bifida	5 (0.56)
Hydrocephaly	9 (1.01)
Development delay, intellectual disability, mental delay, learning difficulties, language and motor deficit	262 (29.54)
Nose, ear, mandibular, and face anomalies	172 (19.39)
Genitourinary system anomalies	140 (15.78)
Renal or bladder dysplasia and hydronephrosis	20 (2.25)
Hypospadias and urethral valve	35 (3.95)
Abnormal genitalia	23 (2.59)
Cryptorchidism and hydrocele	77 (8.68)
Musculoskeletal anomalies	138 (15.56)
Polydactyly, syndactyly, and trigger finger	52 (5.86)
Developmental dysplasia of hip and other malformations of limbs	30 (3.38)
Spine anomalies	21 (2.37)
Skull deformity	4 (0.45)
Chest wall deformity and rib dysplasia	21 (2.37)
Torticollis and hypotonia	20 (2.25)
Heterotaxy	108 (12.18)
Abdominal wall deformity	98 (11.05)
Inguinal hernia	83 (9.36)
Umbilical hernia and omphalocele	15 (1.69)
Digestive system anomalies	56 (6.31)
Esophageal stricture/atresia and tracheoesopahgeal fistula	9 (1.01)
Biliary atresia and cholestasis	21 (2.37)
Hirschsprung's disease, stenosis/atresia of digestive tract, malrotation, and fistula	13 (1.47)
Annular pancreas and ectopic pancreas	5 (0.56)
Anal atresia and cloacal malformations	16 (1.80)
Respiratory system anomalies	55 (6.20)
Upper/lower airway stenosis or dysplasia	46 (5.19)
Pulmonary sequestration and other lung aplasia	9 (1.01)
Congenital hypothyroidism and other endocrine and metabolic disease	47 (5.30)
Hemangioma and lymphangioma	47 (5.30)
Cleft lip and/or palate	25 (2.82)
Absence of thymus and other immunodeficiency	19 (2.14)
Eye anomalies	19 (2.14)
Cataract, glaucoma and other abnormal structure of cornea, sclera, iris, and retina	13 (1.47)
Visual impairment	6 (0.68)
Hearing impairment	15 (1.69)
Miscellaneous/Others[b]	38 (4.28)
Total[c]	1,284

[a]Percentage denominator was 887 patients with associated CHD.
[b]Includes aplastic anemia, idiopathic thrombocytopenic purpura, thalassemia, vitiligo, alopecia areata, lipoma, skin growth, etc
[c]"TOTAL" represents the sum of noncardiac anomalies in 887 children with associated CHD, and anomalies within the same affected system were counted as one.

the wide range of percentages reported in the literature (4.53%–50%) (13–15) and somewhat similar to percentages obtained in extensive studies conducted in the city of Atlanta, GA in the USA (28.7%), the province of Alberta in Canada (25%), and Croatia (14.5%) (16, 26, 27). The wide range of findings reported in this regard may be attributed to different classifications, inclusion/exclusion criteria, and screening strategies. Stoll and colleagues reported that the incidence of NCAs co-occurring with CHDs was 24.2% in live births, 66.3% in stillbirths, and 69.4% in abnormal pregnancy terminations (21). The subjects in our study were all live births. The definition of associated CHD differs between studies as well. Some defined an associated CHD as an extracardiac or genetic abnormality (16, 21). In our study, we included anomalies affecting other organs but not genetic abnormalities. Consequently, the data are not fully comparable across different studies due to different methodologies. Nevertheless, the proportion of congenital defects was dramatically more significant than the prevalence of congenital defects for China's population as a whole (191.84/10,000) (28), which suggests that CHDs may be a risk factor for other defects and that a considerable number of children with CHDs have NCAs.

Our findings indicating that the most common NCAs observed were CNS anomalies, nose/ear/mandibular/face anomalies, genitourinary system anomalies, and musculoskeletal system anomalies are largely in agreement with previous reports (14, 21, 29–31). However, we observed relatively low percentages of gastrointestinal anomalies (6.31%) and respiratory system anomalies (6.20%), the ranges for which in the literature are 8%–35% and 2%–14%, respectively, but a relatively high percentage of nose/ear/mandibular/face anomalies (19.39%) (8, 14, 15, 18, 32–39). Divergences from prior reports may have several underlying causes. Firstly, we excluded stillbirths, fetal deaths, and pregnancy terminations, which are more likely to involve lethal and major anomalies than live births. Secondly, we included several minor NCAs that are often excluded in other literature (e.g., low set ears, atypical facial appearance, and high arched palate) because how little of an effect they have on prognoses. Lastly, we deconstructed phenotypes of known syndromes as discrete NCAs. Most syndromes that commonly present with CHDs—including Down syndrome, DiGeorge syndrome, and Turner syndrome—have clinically significant NCAs, such as development delays, atypical facial features, skeletal deformities, and genitourinary system anomalies (40); these syndromes explain in part the top four NCAs in our results. CNS anomalies, including development delays, account for a large portion of the NCAs observed in our study (**Table 2**). Because neurodevelopment is highly sensitive to oxygen, any cardiac defect that disturbs hemodynamics and oxygen transport has the potential to cause CNS anomalies. In addition, development delays continue to manifest with increasing child age; our study sample has a median age of 3.96 years (IQR, 2.56–5.39), providing recognition of NCAs with progressive symptoms that are not yet apparent in the fetal and infant stages. Furthermore, adverse neurodevelopmental outcomes after surgical repair of CHDs represent a clinically significant cause of morbidity. Indeed, neuropsychological deficits may occur in as many as 50% of children who undergo CHD repairs by the time they reach school age (41). Early diagnosis of CNS anomalies in

TABLE 3 Distribution of NCAs associated with each CHD subcategory[a].

NCAs \ CHDs	Septal defect	AVSD	CTD	LVOTO	RVOTO	Abnormal cell growth	Others	HTX	Associations
Central nervous system anomalies	160 (25.28)	22 (30.56)	36 (20.57)	9 (31.03)	21 (31.82)	9 (40.91)	9 (15.25)	9 (8.74)	32 (25.60)
Nose, ear, mandibular, face anomaly	88 (13.90)	16 (22.22)	27 (15.43)	3 (10.34)	9 (13.64)	3 (13.64)	8 (13.56)	4 (3.88)	14 (11.20)
Genitourinary	72 (11.37)	7 (9.72)	21 (12.00)	2 (6.90)	10 (15.15)	4 (18.18)	10 (16.95)	1 (0.97)	13 (10.40)
Musculoskeletal	77 (12.16)	7 (9.72)	16 (9.14)	3 (10.34)	6 (9.09)	0 (0.00)	8 (13.56)	6 (5.83)	15 (12.00)
Laterality defects	8 (1.26)	3 (4.17)	12 (6.86)	0 (0.00)	3 (4.55)	0 (0.00)	3 (5.08)	72 (69.9)	7 (5.60)
Respiratory system	23 (3.63)	1 (1.39)	15 (8.57)	1 (3.45)	0 (0.00)	1 (4.55)	4 (6.78)	3 (2.91)	7 (5.60)
Digestive system	31 (4.90)	3 (4.17)	8 (4.57)	4 (13.79)	1 (1.52)	0 (0.00)	0 (0.00)	3 (2.91)	6 (4.80)
Abdominal wall	60 (9.48)	3 (4.17)	8 (4.57)	2 (6.90)	5 (7.58)	2 (9.09)	5 (8.47)	2 (1.94)	11 (8.80)
Endocrine and metabolic	25 (3.95)	3 (4.17)	4 (2.29)	3 (10.34)	3 (4.55)	0 (0.00)	3 (5.08)	0 (0.00)	6 (4.80)
Hemangioma, lymphangioma	25 (3.95)	1 (1.39)	10 (5.71)	1 (3.45)	1 (1.52)	2 (9.09)	2 (3.39)	0 (0.00)	5 (4.00)
Cleft lip and/or palate	18 (2.84)	1 (1.39)	0 (0.00)	0 (0.00)	2 (3.03)	0 (0.00)	0 (0.00)	2 (1.94)	2 (1.60)
Immunodeficiency	7 (1.11)	2 (2.78)	8 (4.57)	0 (0.00)	1 (1.52)	0 (0.00)	0 (0.00)	0 (0.00)	1 (0.80)
Eye	5 (0.79)	2 (2.78)	4 (2.29)	0 (0.00)	1 (1.52)	0 (0.00)	5 (8.47)	0 (0.00)	2 (1.60)
Hearing impairment	8 (1.26)	1 (1.39)	2 (1.14)	0 (0.00)	1 (1.52)	0 (0.00)	1 (1.69)	0 (0.00)	2 (1.60)
Others	26 (4.11)	0 (0.00)	4 (2.29)	1 (3.45)	2 (3.03)	1(4.55)	1(1.69)	1(0.97)	2(1.60)
Total: NCAs/associated CHDs[b]	633/428	70/44	175/124	29/20	66/50	22/16	59/43	103/79	125/83

[a]Number of subjects with the certain CHD subcategories and NCAs are indicated; percentages in parentheses indicate the portion of specified NCA among all NCAs of children with each CHD phenotype in the header.
[b]NCAs refers to the total number of NCAs within the population with specific CHD subcategories while associated CHDs refers to the total number of patients with combined NCAs.

TABLE 4 Valuable rules with association analysis[a].

Type[b]	lhs[c]	rhs[c]	Count	Support[d]	Confidence[d]	Lift[d]	Coverage[d]	Lift[d]	Conviction[d]	FishersExactTest[V]
NCA	CNS, Miscellaneous	Face	13	0.0156	0.6842	3.3370	0.0228	3.3370	2.5174	6.4871×10^{-6}
NCA	Face, CNS	Miscellaneous	13	0.0156	0.1512	3.3176	0.1031	3.3176	1.1244	3.8934×10^{-5}
CHD_NCA	laterality defect (*N*)[f]	CCTGA, SV	13	0.0156	0.2653	13.0156	0.0588	13.0156	1.3334	3.8326×10^{-14}
CHD_NCA	CCTGA, SV	Laterality defect (*N*)	13	0.0156	0.7647	13.0156	0.0204	13.0156	4.0003	3.8326×10^{-14}
CHD_NCA	CTD, RVOTO	Laterality defect (*N*)	9	0.0108	0.5294	9.0108	0.0204	9.0108	2.0001	6.7795×10^{-8}
CHD_NCA	HTX	Laterality defect (*N*)	11	0.0132	0.4074	6.9342	0.0324	6.9342	1.5884	5.9480×10^{-8}
CHD_NCA	Laterality defect (*N*)	HTX	11	0.0132	0.2245	6.9342	0.0588	6.9342	1.2477	5.9480×10^{-8}
CHD_NCA	Vasc ring	Respiratory (*N*)	13	0.0156	0.3421	5.1876	0.0456	5.1876	1.4198	1.6641×10^{-7}
CHD_NCA	Respiratory (*N*)	Vasc ring	13	0.0156	0.2364	5.1876	0.0659	5.1876	1.2499	1.6641×10^{-7}
CHD_NCA	RVOTO, laterality defect (*N*)	CTD	9	0.0108	0.6923	4.8115	0.0156	4.8115	2.7824	8.6630×10^{-6}
CHD_NCA	CTD, laterality defect (*N*)	RVOTO	9	0.0108	0.4286	4.1084	0.0252	4.1084	1.5674	1.0061×10^{-4}
CHD_NCA	VSD, PDA, CNS (*N*)	LVOTO	10	0.0120	0.2326	3.6595	0.0516	3.6595	1.2202	1.7389×10^{-4}
CHD_NCA	VSD, LVOTO, CNS (*N*)	PDA	10	0.0120	0.8333	3.4236	0.0144	3.4236	4.5396	2.5161×10^{-5}

[a]Association analysis performed with the apriori principle to find rules; rules with a lift >3 were considered valuable.
[b]Association analyses for CHDs and NCAs involved 887 subjects with associated CHDs.
[c]lhs, left-hand side; rhs, right-hand side. A rule can be written as lhsrhs, "lhs" and "rhs" are collections of phenotypes that lie at the end of the arrow.
[d]Support = count (number of specific rule)/total subjects observed, represents rule frequency, and the numerator of the formula can be "lhs" or "rhs" as well; confidence = support(lhsurhs)/support(lhs), represents the probability "rhs" coexistence in subjects with "lhs"; lift = support(lhsurhs)/(support(lhs)*support(rhs)), measure of independence of "lhs" and "rhs".
[e]Quality measurement: Fisher's Exact Test inspects rule authenticity (rule valid at $P < 0.05$).
[f]When inspecting "CHD-NCA" rules, phenotypes with "(*N*)" refer to NCAs, and others represent CHDs.

10.3389/fcvm.2023.1293210

this patient population would be of great benefit to perioperative management.

Regarding NCA risk among different CHD phenotypes, we found that AVSD, PTA, vasc ring malformations, LVOTO, and heterotaxy had relatively high incidences of associated NCAs, whereas VSD and APVD had relatively low incidences. It could be that CHDs that emerge in earlier stages of morphogenesis are more likely to be associated with multiple and complex defects (42). Boundaries between tissues are blurred in early development, and regulatory molecular signaling pathways affect the development of many organs simultaneously.

Our finding of a specific link between VSD/LVOTO/PDA presence and CNS anomalies should be explored. Interestingly, the impact of AVSDs on CNS anomalies and nose/ear/mandibular/face anomalies could potentially relate to the well-known correlation between AVSDs and Down syndrome (32, 43, 44). The finding that vasc ring anomalies (including right arch and sling) often co-occurred with malformations of the respiratory system was unsurprising given the oppression of the malformed arteries on the trachea. Theoretically, most CHD-associated NCAs should have an etiological explanation, such as a mesoderm differentiation event that causes CHD and musculoskeletal defects simultaneously (16). The detailed mechanisms underlying the breadth of co-occurring anomalies have yet to be delineated.

5. Limitation

It was difficult to conduct a stratified analysis to correct for confounding factors as we did not obtain data related to risk factors for birth defects. We also did not capture associated CHD patterns in rural China, where there is a high prevalence of unrecognized CHDs (32). Thirdly, our sample included relatively few rare CHDs and NCAs, which may weaken the analyses.

6. Conclusion

Han Chinese children with CHDs were found to have a high prevalence of NCAs, including CNS, nose/ear/mandibular/face, and musculoskeletal anomalies. Different CHD subtypes had different NCA probabilities and spectrums. Compared to other CHD subtypes, septal defects had a lower percentage of associated NCAs while AVSD had a higher percentage. Clinicians treating patients with CHDs should be attentive to the risk of NCAs, particularly for perioperative management but also for long-term prognosis determination.

Data availability statement

The original contributions presented in the study are included in the article/Supplementary Materials, further inquiries can be directed to the corresponding authors.

Ethics statement

The studies involving humans were approved by Fudan University Children's Hospita. The studies were conducted in accordance with the local legislation and institutional requirements. Written informed consent for participation in this study was provided by the participants' legal guardians/next of kin.

Author contributions

XH: Data curation, Formal Analysis, Investigation, Writing – original draft. YG: Formal Analysis, Investigation, Methodology, Writing – original draft. WC: Project administration, Resources, Supervision, Writing – review & editing. WS: Formal Analysis, Project administration, Resources, Supervision, Writing – review & editing. GH: Conceptualization, Project administration, Resources, Supervision, Writing – review & editing.

Funding

The author(s) declare financial support was received for the research, authorship, and/or publication of this article.

This research was supported by the National Key Research and Development Program of China (grant no. 2021YFC2701000, 2016YFC1000500), the National Natural Science Foundation of China (grant no. 82270321, 81873482, 81873483), the Shanghai Natural Science Foundation of Science and Technology Innovation Action Plan (grant no. 20JC1418300), and the CAMS Innovation Fund for Medical Sciences (grant no. 2019-I2M-5-002).

Acknowledgments

The authors thank for the support from National Key Research and Development Program of China and National Natural Science Foundation of China. We also thank all the patients and families for their understanding and support.

Conflict of interest

The authors declare that the research was conducted in the absence of any commercial or financial relationships that could be construed as a potential conflict of interest.

Publisher's note

References

1. Nees SN, Chung WK. Genetic basis of human congenital heart disease. *Cold Spring Harb Perspect Biol.* (2020) 12(9):a036749. doi: 10.1101/cshperspect.a036749

2. Szot JO, Cuny H, Blue GM, Humphreys DT, Ip E, Harrison K, et al. A screening approach to identify clinically actionable variants causing congenital heart disease in exome data. *Circ Genom Precis Med.* (2018) 11(3):e001978. doi: 10.1161/CIRCGEN.117.001978

3. Zhao QM, Liu F, Wu L, Ma XJ, Niu C, Huang GY. Prevalence of congenital heart disease at live birth in China. *J Pediatr.* (2019) 204:53–8. doi: 10.1016/j.jpeds.2018.08.040

4. GBD 2017 Congenital Heart Disease Collaborators. Global, regional, and national burden of congenital heart disease, 1990-2017: a systematic analysis for the global burden of disease study 2017. *Lancet Child Adolesc Health.* (2020) 4(3):185–200. doi: 10.1016/s2352-4642(19)30402-x

5. Sun M, Wang T, Huang P, Diao J, Zhang S, Li J, et al. Association analysis of maternal MTHFR gene polymorphisms and the occurrence of congenital heart disease in offspring. *BMC Cardiovasc Disord.* (2021) 21(1):298. doi: 10.1186/s12872-021-02117-z

6. Chang CS, Hong SY, Kim SY, Kim YM, Sung JH, Choi SJ, et al. Prevalence of associated extracardiac anomalies in prenatally diagnosed congenital heart diseases. *PLoS One.* (2021) 16(3):e0248894. doi: 10.1371/journal.pone.0248894

7. Morton SU, Quiat D, Seidman JG, Seidman CE. Genomic frontiers in congenital heart disease. *Nat Rev Cardiol.* (2022) 19(1):26–42. doi: 10.1038/s41569-021-00587-4

8. Eskedal L, Hagemo P, Eskild A, Aamodt G, Seiler KS, Thaulow E. A population-based study of extra-cardiac anomalies in children with congenital cardiac malformations. *Cardiol Young.* (2004) 14(6):600–7. doi: 10.1017/S1047951104006043

9. Afilalo J, Therrien J, Pilote L, Ionescu-Ittu R, Martucci G, Marelli AJ. Geriatric congenital heart disease: burden of disease and predictors of mortality. *J Am Coll Cardiol.* (2011) 58(14):1509–15. doi: 10.1016/j.jacc.2011.06.041

10. Jacobs JP, O'Brien SM, Hill KD, Kumar SR, Austin EH 3rd, Gaynor JW, et al. Refining the society of thoracic surgeons congenital heart surgery database mortality risk model with enhanced risk adjustment for chromosomal abnormalities, syndromes, and noncardiac congenital anatomic abnormalities. *Ann Thorac Surg.* (2019) 108(2):558–66. doi: 10.1016/j.athoracsur.2019.01.069

11. Swisher M, Jonas R, Tian X, Lee ES, Lo CW, Leatherbury L. Increased postoperative and respiratory complications in patients with congenital heart disease associated with heterotaxy. *J Thorac Cardiovasc Surg.* (2011) 141(3):637–44. 44 e1-3. doi: 10.1016/j.jtcvs.2010.07.082

12. Faraoni D, Zurakowski D, Vo D, Goobie SM, Yuki K, Brown ML, et al. Post-operative outcomes in children with and without congenital heart disease undergoing noncardiac surgery. *J Am Coll Cardiol.* (2016) 67(7):793–801. doi: 10.1016/j.jacc.2015.11.057

13. Gonzalez JH, Shirali GS, Atz AM, Taylor SN, Forbus GA, Zyblewski SC, et al. Universal screening for extracardiac abnormalities in neonates with congenital heart disease. *Pediatr Cardiol.* (2009) 30(3):269–73. doi: 10.1007/s00246-008-9331-z

14. Wojtalik M, Mrowczynski W, Henschke J, Wronecki K, Siwinska A, Piaszczynski M, et al. Congenital heart defect with associated malformations in children. *J Pediatr Surg.* (2005) 40(11):1675–80. doi: 10.1016/j.jpedsurg.2005.06.004

15. Pastor-Garcia M, Gimeno-Martos S, Zurriaga O, Sorli JV, Cavero-Carbonell C. Congenital heart defects in the valencian community 2007–2014: the population-based registry of congenital anomalies. *An Pediatr.* (2020) 92(1):13–20. doi: 10.1016/j.anpedi.2018.12.019

16. Miller A, Riehle-Colarusso T, Alverson CJ, Frias JL, Correa A. Congenital heart defects and major structural noncardiac anomalies, Atlanta, Georgia, 1968–2005. *J Pediatr.* (2011) 159(1):70–8e2. doi: 10.1016/j.jpeds.2010.12.051

17. Pradat P, Francannet C, Harris JA, Robert E. The epidemiology of cardiovascular defects, part I: a study based on data from three large registries of congenital malformations. *Pediatr Cardiol.* (2003) 24(3):195–221. doi: 10.1007/s00246-002-9401-6

18. Pradat P. Noncardiac malformations at major congenital heart defects. *Pediatr Cardiol.* (1997) 18(1):11–8. doi: 10.1007/s002469900101

19. Piran S, Bassett AS, Grewal J, Swaby JA, Morel C, Oechslin EN, et al. Patterns of cardiac and extracardiac anomalies in adults with tetralogy of fallot. *Am Heart J.* (2011) 161(1):131–7. doi: 10.1016/j.ahj.2010.09.015

20. Riehle-Colarusso T, Strickland MJ, Reller MD, Mahle WT, Botto LD, Siffel C, et al. Improving the quality of surveillance data on congenital heart defects in the metropolitan Atlanta congenital defects program. *Birth Defects Res A.* (2007) 79(11):743–53. doi: 10.1002/bdra.20412

21. Stoll C, Dott B, Alembik Y, Roth MP. Associated noncardiac congenital anomalies among cases with congenital heart defects. *Eur J Med Genet.* (2015) 58(2):75–85. doi: 10.1016/j.ejmg.2014.12.002

22. Brodwall K, Greve G, Leirgul E, Tell GS, Vollset SE, Øyen N. Recurrence of congenital heart defects among siblings-a nationwide study. *Am J Med Genet A.* (2017) 173(6):1575–85. doi: 10.1002/ajmg.a.38237

23. Botto LD, Lin AE, Riehle-Colarusso T, Malik S, Correa A. National birth defects prevention study. Seeking causes: classifying and evaluating congenital heart defects in etiologic studies. *Birth Defects Res A Clin Mol Teratol.* (2007 Oct) 79(10):714–27. doi: 10.1002/bdra.20403

24. Savory K, Manivannan S, Zaben M, Uzun O, Syed YA. Impact of copy number variation on human neurocognitive deficits and congenital heart defects: a systematic review. *Neurosci Biobehav Rev.* (2020) 108:83–93. doi: 10.1016/j.neubiorev.2019.10.020

25. Kotu V, Deshpande B. Chapter 6 - association analysis. In: Kotu V, Deshpande B, editors. *Predictive analytics and data mining.* Boston: Morgan Kaufmann (2015). p. 195–216.

26. Lowry RB, Bedard T, Sibbald B, Harder JR, Trevenen C, Horobec V, et al. Congenital heart defects and major structural noncardiac anomalies in Alberta, Canada, 1995–2002. *Birth Defects Res A Clin Mol Teratol.* (2013) 97(2):79–86. doi: 10.1002/bdra.23104

27. Dilber D, Malcic I. Spectrum of congenital heart defects in Croatia. *Eur J Pediatr.* (2010) 169(5):543–50. doi: 10.1007/s00431-009-1064-3

28. Xie D, Yang T, Liu Z, Wang H. Epidemiology of birth defects based on a birth defect surveillance system from 2005 to 2014 in Hunan province, China. *PLoS One.* (2016) 11(1):e0147280. doi: 10.1371/journal.pone.0147280

29. Sørensen KM, El-Segaier M, Fernlund E, Errami A, Bouvagnet P, Nehme N, et al. Screening of congenital heart disease patients using multiplex ligation-dependent probe amplification: early diagnosis of syndromic patients. *Am J Med Genet A.* (2012) 158a(4):720–5. doi: 10.1002/ajmg.a.35214

30. Simons JS, Glidden R, Sheslow D, Pizarro C. Intermediate neurodevelopmental outcome after repair of ventricular septal defect. *Ann Thorac Surg.* (2010) 90(5):1586–91. doi: 10.1016/j.athoracsur.2010.06.082

31. Wallgren EI, Landtman B, Rapola J. Extracardiac malformations associated with congenital heart disease. *Eur J Cardiol.* (1978) 7(1):15–24.

32. Meberg A, Hals J, Thaulow E. Congenital heart defects–chromosomal anomalies, syndromes and extracardiac malformations. *Acta Paediatr.* (2007) 96(8):1142–5. doi: 10.1111/j.1651-2227.2007.00381.x

33. Ferencz C, Rubin JD, McCarter RJ, Boughman JA, Wilson PD, Brenner JI, et al. Cardiac and noncardiac malformations: observations in a population-based study. *Teratology.* (1987) 35(3):367–78. doi: 10.1002/tera.1420350311

34. Fung A, Manlhiot C, Naik S, Rosenberg H, Smythe J, Lougheed J, et al. Impact of prenatal risk factors on congenital heart disease in the current era. *J Am Heart Assoc.* (2013) 2(3):e000064. doi: 10.1161/JAHA.113.000064

35. Gallo P, Nardi F, Marinozzi V. Congenital extracardial malformations accompanying congenital heart disease. *G Ital Cardiol.* (1976) 6(3):450–9.

36. Greenwood RD, Rosenthal A, Parisi L, Fyler DC, Nadas AS. Extracardiac abnormalities in infants with congenital heart disease. *Pediatrics.* (1975) 55(4):485–92.

37. Kenna AP, Smithells RW, Fielding DW. Congenital heart disease in liverpool: 1960–69. *Q J Med.* (1975) 44(173):17–44.

38. Stephensen SS, Sigfusson G, Eiriksson H, Sverrisson JT, Torfason B, Haraldsson A, et al. Congenital cardiac malformations in Iceland from 1990 through 1999. *Cardiol Young.* (2004) 14(4):396–401. doi: 10.1017/S1047951104004081

39. Baker K, Sanchez-de-Toledo J, Munoz R, Orr R, Kiray S, Shiderly D, et al. Critical congenital heart disease–utility of routine screening for chromosomal and other extracardiac malformations. *Congenit Heart Dis.* (2012) 7(2):145–50. doi: 10.1111/j.1747-0803.2011.00585.x

40. Pierpont ME, Brueckner M, Chung WK, Garg V, Lacro RV, McGuire AL, et al. Genetic basis for congenital heart disease: revisited: a scientific statement from the American heart association. *Circulation.* (2018) 138(21):e653–711. doi: 10.1161/CIR.0000000000000606

41. Albers EL, Bichell DP, McLaughlin B. New approaches to neuroprotection in infant heart surgery. *Pediatr Res.* (2010) 68(1):1–9. doi: 10.1203/PDR.0b013e3181df5402

42. Opitz JM, Zanni G, Reynolds JF Jr, Gilbert-Barness E. Defects of blastogenesis. *Am J Med Genet.* (2002) 115(4):269–86. doi: 10.1002/ajmg.10983

43. Bosi G, Garani G, Scorrano M, Calzolari E, Party IW. Temporal variability in birth prevalence of congenital heart defects as recorded by a general birth defects registry. *J Pediatr.* (2003) 142(6):690–8. doi: 10.1067/mpd.2003.243

44. Calzolari E, Garani G, Cocchi G, Magnani C, Rivieri F, Neville A, et al. Congenital heart defects: 15 years of experience of the Emilia-Romagna registry (Italy). *Eur J Epidemiol.* (2003) 18(8):773–80. doi: 10.1023/A:1025312603880

frontiers | Frontiers in Cardiovascular Medicine

TYPE Original Research
PUBLISHED 29 November 2023
DOI 10.3389/fcvm.2023.1290482

OPEN ACCESS

EDITED BY
Liqun Sun,
University of Toronto, Canada

REVIEWED BY
Dan Wichterle,
Institute for Clinical and Experimental Medicine (IKEM), Czechia
Piotr Futyma,
University of Rzeszow, Poland

*CORRESPONDENCE
Tiewei Lu
✉ ltw200145@163.com

RECEIVED 07 September 2023
ACCEPTED 07 November 2023
PUBLISHED 29 November 2023

CITATION
Xu X, He S, Liu Q, Liu R, Zhang L, Chen W, Yin Y and Lu T (2023) Cardioneuroablation for successful treatment of symptomatic bradycardia in a 12-year-old child after a 6-month follow-up.
Front. Cardiovasc. Med. 10:1290482.
doi: 10.3389/fcvm.2023.1290482

Cardioneuroablation for successful treatment of symptomatic bradycardia in a 12-year-old child after a 6-month follow-up

Xin Xu[1], Shuang He[1], Qian Liu[1], Ruixi Liu[1], Lei Zhang[1], Weijie Chen[2], Yuehui Yin[2] and Tiewei Lu[1]*

[1]Department of Cardiology, Children's Hospital of Chongqing Medical University, National Clinical Research Center for Child Health and Disorders, Ministry of Education Key Laboratory of Child Development and Disorders, Chongqing Key Laboratory of Pediatrics, Chongqing, China, [2]Department of Cardiology, The Second Affiliated Hospital of Chongqing Medical University, Chongqing, China

Background: Cardioneuroablation (CNA) is recognized as a promising therapeutic option for adults with severe symptomatic bradycardia caused by excessive vagal tone. However, no pediatric cases have been reported to date. Therefore, the aim of this study is to evaluate the feasibility and efficacy of CNA in children.
Methods: A 12-year-old male patient was hospitalized with symptoms of fatigue, palpitations, and syncope for more than 2 months, and was definitively diagnosed with functional sinoatrial node dysfunction by using a 12-lead electrocardiogram, 24-h Holter monitoring, loading dose of atropine test (0.04 mg/kg), and treadmill exercise test. Simultaneously, whole-exome sequencing was performed on the child and his core family members. After completing the preoperative examination and signing the informed consent form, the child underwent CNA therapy.
Results: First, the electroanatomic structures of both atria were mapped out by using the Carto 3 system, according to the protocol of purely anatomy-guided and local fractionated intracardiac electrogram–guided CNA methods. Then, the local fractionated intracardiac electrograms of each cardiac ganglionated plexus (GP), including the GP between the aortic root and the medial wall of the superior vena cava, the GP between the posterior wall of the coronary sinus ostium and the left atrium, the GP between the anterior antrum of the right superior pulmonary vein and the superior vena cava, the GP in the superolateral area around the root of the left superior pulmonary vein, the GP around the root of the right inferior pulmonary vein, and the GP around the root of the left inferior pulmonary vein, were used as targets for ablation at a power of 30 W with an ablation index of 350–400. At a 6-month follow-up, the child's heart rhythm saw a complete restoration to sinus rhythm and clinical symptoms disappeared.
Conclusion: The first application of CNA in a child with symptomatic sinus bradycardia was achieved with better clinical outcomes. CNA can be carried out cautiously in children under suitable indications.

KEYWORDS

cardioneuroablation (CNA), sinus bradycardia, sinus arrest, ganglionated plexus, vagal tone, children

Abbreviations
Ao-SVC GP, the GP between the aortic root and the medial wall of the superior vena cava; PMLGP, the GP between the posterior wall of the coronary sinus ostium and the left atrium; RAGP, the GP between the anterior antrum of the right superior pulmonary vein and the superior vena cava; LSGP, the GP in the superolateral area around the root of the left superior pulmonary vein; RIGP, the GP around the root of the right inferior pulmonary vein; LIGP, the GP around the root of the left inferior pulmonary vein.

Introduction

Severe bradycardia with different etiologies can lead to serious clinical manifestations such as fatigue, palpitations, syncope, and even sudden death. The traditional therapy for patients with severe bradycardia is cardiac pacemaker implantation. However, when these patients are adolescents, or much younger, the children or their guardians refuse pacemaker implantations because of concerns about long-term complications (1–3). In recent years, studies have reported that cardioneuroablation (CNA) has become a promising therapeutic strategy for bradycardia caused by excessive vagal tone, and has achieved good clinical outcomes in adults (4–6). However, so far no case of a pediatric patient receiving CNA therapy has been reported. This study aims to fill this gap by presenting the case of a child with sinus arrest, sinus bradycardia, and junctional escape rhythms and showing improvement in clinical outcomes with the relieving of symptoms and rhythm disorders using CNA therapy.

Methods and materials

Study population

A 12-year-old male patient was hospitalized with symptoms of fatigue, palpitations, and syncope for more than 2 months. The 12-lead electrocardiogram (ECG) showed sinus bradycardia and junctional escape rhythm (**Figure 1A**). A 24 h Holter monitoring displayed a total of 62,108 heartbeats in 24 h, with 5,094 sinus arrests greater than 2 s and 971 sinus arrests greater than 3 s, with the longest cardiac arrest time being 7.424 s (**Figure 1B**). The child had no history of myocarditis prior to the onset of the disease, no structural cardiac abnormalities, no similar family history, and no positive findings on laboratory examinations. Normal sinus rhythm appeared after a loading dose of atropine test (0.04 mg/kg) and treadmill exercise test (**Figure 1C**). The child was diagnosed as having functional sinoatrial node dysfunction possibly due to excessive vagal tone based on the above results. Meanwhile, to exclude inherited heart disease, blood samples from the child, his elder sister, and his parents were collected, and whole-exome sequencing (WES) was performed by MyGenostics (Beijing, China) using the Illumina HiSeq X ten system. After strongly rejecting pacemaker implantation, the child's parents agreed to CNA therapy, for which they signed an informed consent form.

CNA procedure

After a satisfactory administration of anesthesia, the bilateral femoral veins were punctured successfully and a quadripolar electrode catheter was inserted into the right ventricle for an intracardiac electrophysiological study and right ventricle pacing. When severe bradycardia occurred in the patient during the procedure, a decapolar steerable electrode catheter was inserted into the coronary sinus for the intracardiac electrophysiological study. Surface ECG and intracardiac electrograms were continually monitored by using a multichannel recording system during the whole procedure (LEAD-7000; JJET, Chengdu, China). The three-dimensional (3D) electroanatomic structures of both atria were mapped out by using the Carto 3 system (Biosense Webster, Diamond Bar, CA, USA). The sinus atrial node, phrenic nerve, coronary sinus, and His bundle were labeled. A Thermocool® ST (Biosense Webster, Diamond Bar, CA, USA) irrigated catheter was inserted in the right/left atrium for the ablation therapy. According

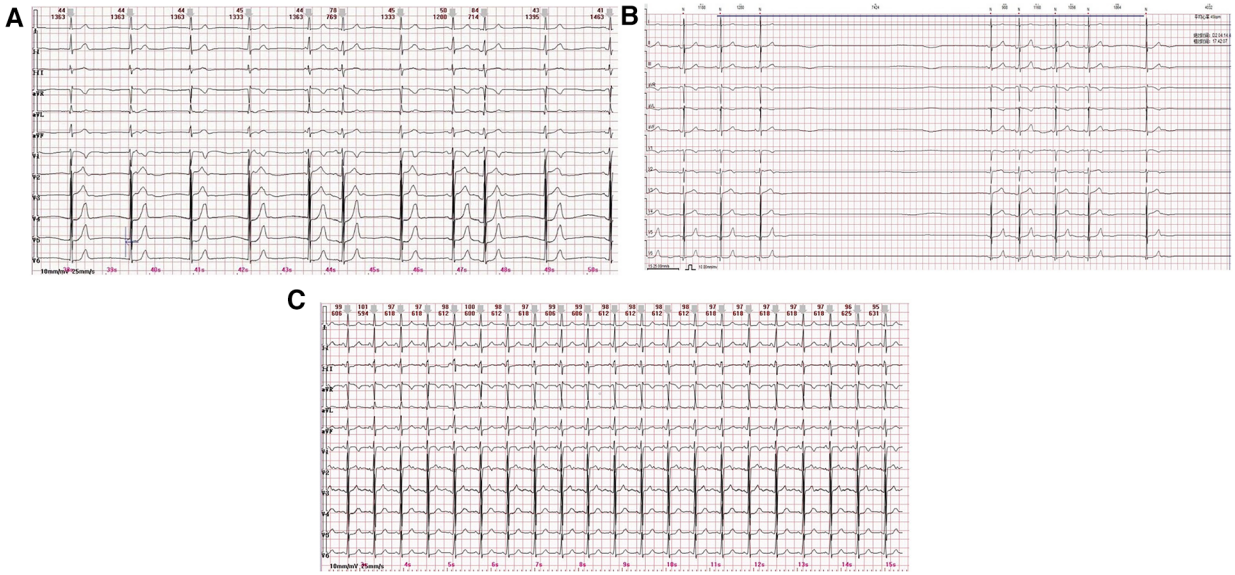

FIGURE 1
(A) 12-lead ECG displays a sinus bradycardia and junctional escape rhythm. (B) The 24 h Holter monitoring displays a sinus arrest of 7.424 s. (C) Normal sinus rhythm appears by a loading dose of atropine test (only the ECG graph after 1 min of atropine administration is displayed).

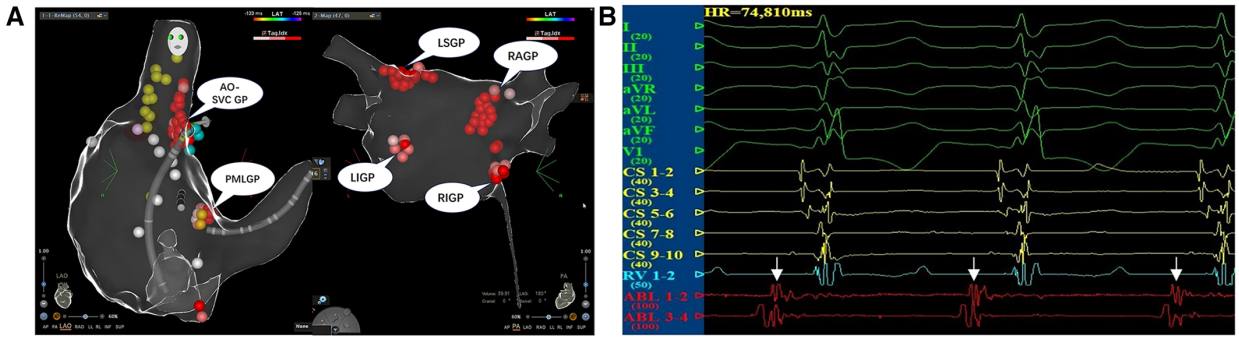

FIGURE 2
(A) The CNA procedure. The local fractionated intracardiac electrograms of each cardiac ganglionated plexus, including Ao-SVC GP, PMLGP, RAGP, LSGP, RIGP, and LIGP, were used as targets for ablation using a power of 30 W for 30 s with an ablation index of 350–400. (B) The local fractionated intracardiac electrograms of the ablation catheter from AO-SVC GP were used as the target potential during the CNA procedure.

to the protocol reported by Pachon et al. and Aksu et al. (3, 7), we administered the CNA therapy by sequentially targeting the ganglionated plexus (GP) between the aortic root and the medial wall of the superior vena cava (Ao-SVC GP), the GP between the posterior wall of the coronary sinus ostium and the left atrium (PMLGP), the GP between the anterior antrum of the right superior pulmonary vein and the superior vena cava (RAGP), the GP in the superolateral area around the root of the left superior pulmonary vein (LSGP), the GP around the root of the right inferior pulmonary vein (RIGP), and the GP around the root of the left inferior pulmonary vein (LIGP) (**Figure 2A**). The local fractionated intracardiac electrograms (**Figure 2B**) of each cardiac GP, including Ao-SVC GP, PMLGP, RAGP, LSGP, RIGP, and LIGP, were used as ablation targets, and the radio frequency of the GPs was performed in the power-controlled mode in a point-by-point fashion through the irrigated ST catheter. Energy was delivered at a power of 30 W for 30 s with an ablation index of 350–400. The ablation endpoint was the complete elimination of local fractionated intracardiac electrograms in each GP. Low-molecular heparin was administrated intravenously at 100 IU/kg during the CNA procedure with an additional half-dose of over 2 h of operating time. The duration of radiofrequency ablation in the child was 3 h with a fluoroscopy time of 11 m and dose of 5.4 mGy. Aspirin antiplatelet aggregation was routinely administered for 6 months after the CNA procedure.

Results

Change in electrical characteristics after CNA

After the completion of the purely anatomy-guided and local fractionated intracardiac electrogram–guided CNA procedure in the locations of the GPs, the child's surface ECG and intracardiac electrograms instantly shifted to sinus rhythm (**Figure 3A**). One week after the CNA procedure, the 12-lead ECG still presented sinus bradycardia and junctional escape rhythm, but the 24-h Holter monitoring displayed a total of 78,434 heartbeats in 24 h, with 143 sinus arrests greater than 2 s and one sinus arrest greater than 3 s, with the longest cardiac arrest time being 3.780 s (**Figure 3B**). Meanwhile, the child's palpitations were relieved significantly. At the 3-month follow-up, the child's 12-lead ECG completely restored to normal sinus rhythm, and 24 h Holter monitoring displayed a total of 120,457 heartbeats in 24 h without sinus arrest. At the 6-month follow-up, the child's 12-lead ECG still remained in normal sinus rhythm, and the 24 h Holter monitoring displayed a total of 102,912 heartbeats in 24 h without sinus arrest. Interestingly, the child's palpitations and syncope disappeared completely. A comparison of Holter features before and after the CNA procedure revealed a gradual increase in the total number of heartbeats, a marked improvement in cardiac rhythm, and a gradual disappearance of sinus arrests (**Table 1**).

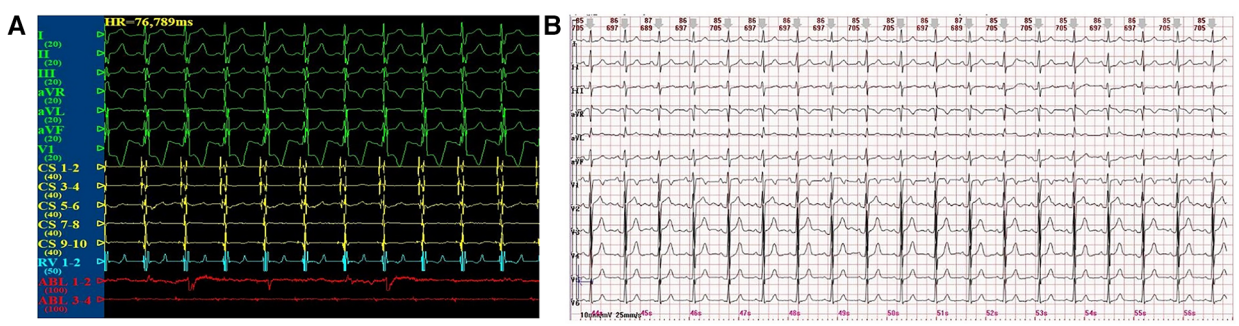

FIGURE 3
(A) Sinus rhythm after the CNA procedure. (B) 12-lead ECG at the 6-month follow-up after the CNA procedure.

TABLE 1 Change of Holter feature before and after the CNA procedure.

	Total number of heartbeats in 24 h	Cardiac rhythm (sinus/junctional)	Number of cardiac arrests >2 s	Number of cardiac arrests >3 s
Before CNA	62,108	Less sinus/more junctional	5,094	971
1 week after CNA	78,434	Less sinus/more junctional	143	1
3 months after CNA	120,457	Sinus	0	0
6 months after CNA	102,912	Sinus	0	0

The deceleration capacity (DC) of the heart rate, a new technique for assessing autonomic tone, is used to quantitatively assess vagal tone by analyzing the overall trend of sinus rhythm over a 24 h period. Normally, DC is positively correlated with vagal tone, but in our patient, the DC was 14.4 before CNA treatment and only 8.3 after CNA treatment, which confirmed that the child's symptoms and rhythm disturbances were closely related to high vagal tone.

WES outcome

The child's parents and sister had no previous history of similar illnesses. WES was performed on the child and his core family members. It showed the child had a novel c.611 + 1G>T heterozygous mutation in the *SCN5A* gene (**Figure 4**), which resulted in a splicing mutation of amino acids. No abnormalities were found in the other family members.

Complication

No intraoperative or postoperative puncture/ablation-related complications occurred in the child, such as vascular injury, arrhythmia, laryngeal reentrant nerve injury, and pericardial tamponade. Heart structure and function remained normal during follow-up.

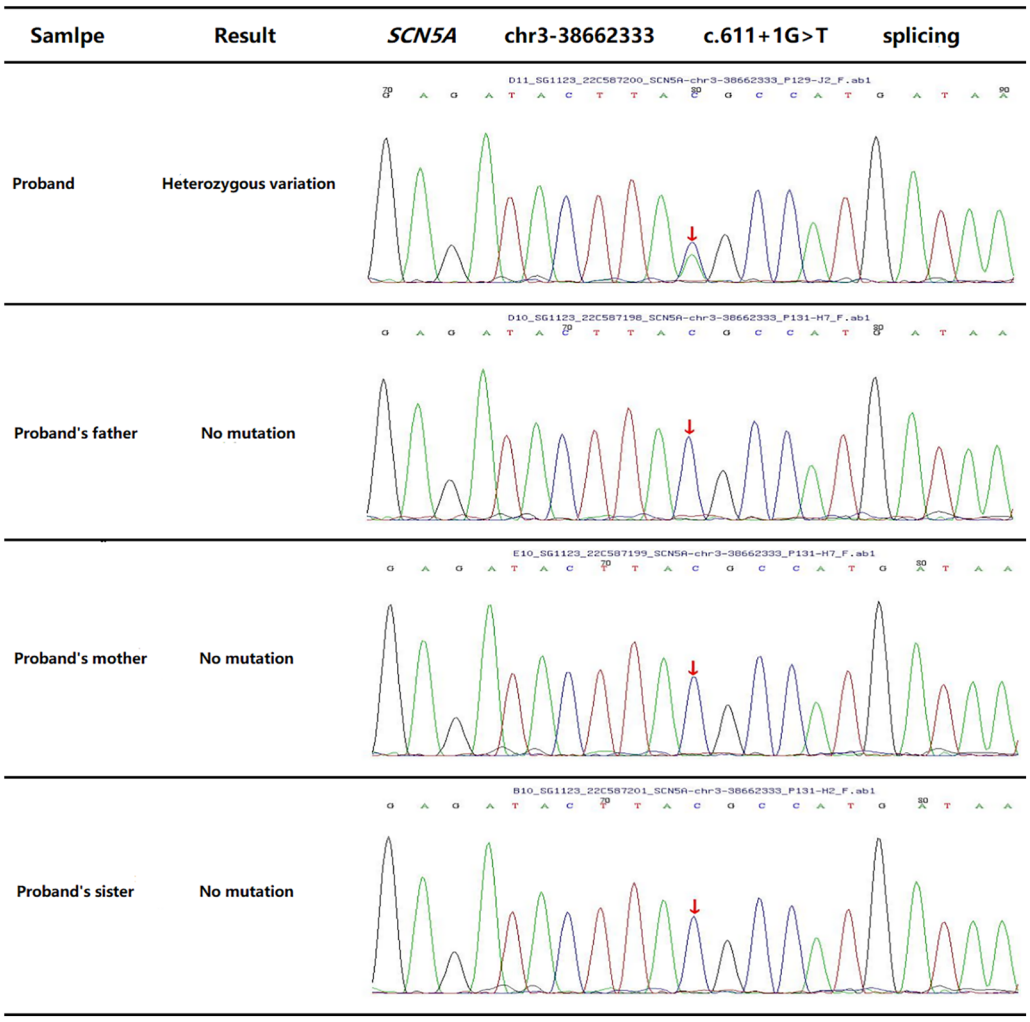

FIGURE 4
WES outcome of proband (the child) and his family members displays a novel c.611 + 1G>T heterozygous mutation in the *SCN5A* gene.

Discussion

This study displayed the first application of CNA in a child with symptomatic bradycardia. The child's heart rhythm was completely restored to sinus rhythm and clinical symptoms disappeared without any perioperative and long-term complications during the 6-month follow-up. Overall, this preliminary result was inspiring, showing that CNA may be safe and feasible for children with symptomatic bradycardia.

Principle of the CNA procedure for treating bradycardia

It is well-known that the autonomic nervous system plays an important role in cardiac functions. An imbalance in autonomic tone, mainly excessive vagal tone, is the common cause of functional sinoatrial node dysfunction (SND), functional atrioventricular block (AVB), and vasovagal syncope (VVS), except organic cardiac lesions (7–9). Traditionally, bradycardic patients who are at a high risk for clinically serious cardiovascular events if they developed hemodynamic disturbances may require pacemaker implantation to prevent sudden fatal events (1, 2). The cell bodies of cardiac efferent vagal postganglionic neurons have been shown to be contained in the intrinsic cardiac GP, which is embedded in the atrial wall and in epicardial fat pads (10, 11). Common GPs include Ao-SVC GP, PMLGP, RAGP, RIGP, LSGP, and LIGP with different physiological functions, and they interact with one another (6, 9, 10). Therefore, a disruption of nerve fibers by radiofrequency ablation can inhibit excessive activation of the vagal nerve, thereby eliminating or improving clinical symptoms. That is why CNA has proven to be a reliable therapeutic target for patients with excessive vagal tone.

In our study, our child patient presented with abnormal rhythm (sinus bradycardia, sinus arrest, and junctional escape rhythm) and symptoms of fatigue, palpitations, and syncope, while organic cardiac disorders and family history were excluded. Moreover, the resting heart rate of the child was approximately 58 bpm with sinus bradycardia and junctional escape rhythm, which rose to 97 bpm with sinus rhythm after atropine intravenous administration, which proved that the result of the atropine test was negative. Therefore, symptomatic bradycardia was considered to have been caused by excessive vagal tone. All these show that CNA is able to achieve better clinical outcomes.

Suitable indications for CNA

Currently, there is a lack of guidelines for the selection of suitable candidates for CNA. Some authors have reported that indications for CNA in adults include the following: (1) patients with severe symptomatic bradycardia of functional SND or AVB [bradycardia was documented by performing ECG and 24 h Holter monitoring and was associated with excessive vagal tone with evidence of correcting the bradycardia by a loading dose of atropine], or patients with a symptomatic vasovagal syncope (cardioinhibitory type or mixed type), which was documented by performing a head-up tilt table test (HUT); (2) patients aged between 14 and 65 years; (3) those with no structural heart diseases; and (4) those who rejected the option of implanting a cardiac pacemaker on them (6). However, no indications were noted for CNA in children.

The child patient in our study had no structural heart diseases, except for a novel c.611 + 1G>T heterozygous mutation in the *SCN5A* gene. Many studies have reported that *SCN5A*, encoding the pore-forming ion-conducting α-subunit of the cardiac sodium channel (Nav1.5), was the causative gene for ion channel disease, including sick sinus syndrome, long Q-T syndrome, and Brugada syndrome (12–14). It is worth considering that the child had a heterozygous mutation in the *SCN5A* gene but a negative atropine test, along with a satisfactory clinical outcome and DC value reduction after CNA. However, further basic research is needed to clarify the relationship between the novel c.611 + 1G>T heterozygous mutation and disease development. Meanwhile, this study provides probable clinical evidence for the development of CNA indications in pediatric patients in the future.

Therapeutic strategy of the CNA procedure

There is no guideline for the therapeutic strategy, including labeling methods, ablation strategies, and ablation endpoints, during the CNA procedure. Purely anatomy-guided CNA (15, 16) and intracardiac high-frequency stimulation (HFS)-guided CNA (17) were clinically performed in patients with symptomatic bradycardia caused by excessive vagal tone. The former procedure tends to enlarge the ablation area first and the latter procedure perhaps causes myocardial scarring, leading to other types of arrhythmias. The latter easily causes severe discomfort to the patient during HFS. With regard to the target GPs and chamber during the performance of the CNA procedure, the team of Dr. Pachon and Dr. Aksu tended to ablate all of the atrial GP groups in both atria (4, 8, 16, 17), while Dr. Yao's team (5) mainly focused on the GP groups in the left atrium, and Dr. Debruyne (18, 19) ablated the GP groups only in the right atrium. The determination of ablation endpoints has not been standardized to date. The techniques of inhibition of the vagal response, elimination of the intracardiac fractionated electrograms, and effecting improvements in electrophysiological parameters, such as increasing the heart rate and shortening the PR interval, have all been used by clinical investigators as ablation endpoints during the performance of the CNA procedure.

In our study, purely anatomy-guided CNA rather than intracardiac HFS–guided CNA was applied because most of the child's rhythms displayed junctional escape rhythms at the onset of the CNA procedure, all of the atrial GP locations in both atria were ablated, and the intracardiac fractionated electrograms in each GP location were used as ideal target intracardiac electrograms. Each ablation target employed 30 W of energy for 30 s with an ablation index of 350–400. Partial return to sinus rhythm and increased heart rate were used as ablation endpoints. The above ablation strategy helped achieve satisfactory clinical outcomes with no perioperative complications.

Limitations

Despite our obtaining satisfactory clinical results at a 6-month follow-up in our study, the CNA technique is not without its problems and limitations. GPs located in the atrial epicardium, and the medium- and long-term effects (20, 21) of ablation at the endocardial surface, need to be observed before conclusions can be drawn. Meanwhile, a partial reinnervation of the cardiac ganglion after GP ablation in dogs has been reported in the literature (22). It has also been found that the regenerative capacity of nerve fibers is higher in children than in adults, which may be a high-risk factor for producing poor long-term results or recurrence. Hence, multi-center, large-sample clinical studies are needed for the application of CNA in pediatrics.

Conclusions

In our study, CNA was successfully performed in a child whose rhythm returned to sinus rhythm and clinical symptoms disappeared after 6 months of follow-up. CNA may be an ideal therapeutic strategy for severely symptomatic bradycardic children with appropriate indications. However, the long-term safety and efficacy of CNA in children need to be further evaluated.

Data availability statement

The original contributions presented in the study are included in the article/Supplementary Material, further inquiries can be directed to the corresponding author.

Ethics statement

Written informed consent was obtained from the individual(s) for the publication of any potentially identifiable images or data included in this article.

Author contributions

XX: Writing – original draft. SH: Writing – original draft. QL: Writing – original draft. RL: Writing – original draft. LZ: Writing – original draft. WC: Writing – review & editing. YY: Writing – review & editing. TL: Writing – original draft, Writing – review & editing.

Funding

The authors declare that financial support was received for the research, authorship, and/or publication of this article.

This study was supported by the National Natural Science Foundation of China (81570218), the Program for Youth Innovation in Future Medicine, Chongqing Medical University (w0176), and the National Clinical Key Specialty Construction Project (010140).

Acknowledgments

The authors would like to thank all those who participated in this study.

Conflict of interest

The authors declare that the research was conducted in the absence of any commercial or financial relationships that could be construed as a potential conflict of interest.

The reviewer PF declared a past co-authorship with the author YY to the handling editor.

Publisher's note

References

1. Kusumoto FM, Schoenfeld MH, Barrett C, Edgerton JR, Ellenbogen KA, Varosy PD, et al. 2018 ACC/AHA/HRS guideline on the evaluation and management of patients with bradycardia and cardiac conduction delay: a report of the American College of Cardiology/American Heart Association task force on clinical practice guidelines and the Heart Rhythm Society [published correction appears in Circulation 2019 Aug 20;140 (8):e506-e508]. *Circulation*. (2019) 140(8):e382–482. doi: 10.1161/CIR.0000000000000628

2. Brignole M, Moya A, de Lange FJ, Deharo JC, Elliott PM, van Dijk JG, et al. 2018 ESC guidelines for the diagnosis and management of syncope. *Eur Heart J*. (2018) 39 (21):1883–948. doi: 10.1093/eurheartj/ehy037

3. Sandhu RK, Raj SR, Thiruganasambandamoorthy V, Kaul P, Morillo CA, Sivilotti M, et al. Canadian cardiovascular society clinical practice update on the assessment and management of syncope. *Can J Cardiol*. (2020) 36(8):1167–77. doi: 10.1016/j.cjca.2019.12.023

4. Pachon JC, Pachon EI, Pachon JC, Lobo TJ, Pachon MZ, Jatene AD, et al. "Cardioneuroablation"–new treatment for neurocardiogenic syncope, functional AV block and sinus dysfunction using catheter RF-ablation. *Europace*. (2005) 7 (1):1–13. doi: 10.1016/j.eupc.2004.10.003

5. Yao Y, Shi R, Wong T, Zheng L, Chen W, Zhang S, et al. Endocardial autonomic denervation of the left atrium to treat vasovagal syncope: an early experience in humans. *Circ Arrhythm Electrophysiol*. (2012) 5(2):279–86. doi: 10.1161/CIRCEP.111.966465

6. Chen W, Liu Z, Xiao P, Du H, Yin Y, Ling Z, et al. Extracardiac vagal stimulation-assisted cardioneuroablation: dynamically evaluating the impact of sequential

ganglionated plexus ablation on vagal control of SAN and AVN in patients with sinoatrial node dysfunction. *J Cardiovasc Dev Dis*. (2022) 9(6):188. doi: 10.3390/jcdd9060188

7. Aksu T, Golcuk E, Yalin K, Guler TE, Erden I. Simplified cardioneuroablation in the treatment of reflex syncope, functional AV block, and sinus node dysfunction. *Pacing Clin Electrophysiol*. (2016) 39(1):42–53. doi: 10.1111/pace.12756

8. Aksu T, Guler TE, Yalin K, Mutluer FO, Ozcan KS, Calò L. Catheter ablation of bradyarrhythmia: from the beginning to the future. *Am J Med Sci*. (2018) 355 (3):252–65. doi: 10.1016/j.amjms.2017.11.016

9. Alboni P, Holz A, Brignole M. Vagally mediated atrioventricular block: pathophysiology and diagnosis. *Heart*. (2013) 99(13):904–8. doi: 10.1136/heartjnl-2012-303220

10. Hanna P, Dacey MJ, Brennan J, Robbins S, Ardell JL, Shivkumar K, et al. Innervation and neuronal control of the mammalian sinoatrial node a comprehensive atlas. *Circ Res*. (2021) 128(9):1279–96. doi: 10.1161/CIRCRESAHA.120.318458

11. Pauza DH, Skripka V, Pauziene N, Stropus R. Morphology, distribution, and variability of the epicardiac neural ganglionated subplexuses in the human heart. *Anat Rec*. (2000) 259(4):353–82. doi: 10.1002/1097-0185(20000801)259:4<353::AID-AR10>3.0.CO;2-R

12. Wilde AAM, Amin AS. Clinical spectrum of SCN5A mutations: long QT syndrome, Brugada syndrome, and cardiomyopathy. *JACC Clin Electrophysiol*. (2018) 4(5):569–79. doi: 10.1016/j.jacep.2018.03.006

13. Benson DW, Wang DW, Dyment M, Knilans TK, Rhodes TH, George AL Jr, et al. Congenital sick sinus syndrome caused by recessive mutations in the cardiac sodium channel gene (SCN5A). *J Clin Invest*. (2003) 112(7):1019–28. doi: 10.1172/JCI18062

14. Wallace MJ, El Refaey M, Mesirca P, Hund TJ, Mangoni ME, Mohler PJ. Genetic complexity of sinoatrial node dysfunction. *Front Genet*. (2021) 12:654925. doi: 10.3389/fgene.2021.654925

15. Aksu T, De Potter T, John L, Osorio J, Gupta D, Davila A, et al. Procedural and short-term results of electroanatomic-mapping-guided ganglionated plexus ablation by first-time operators: a multicenter study. *J Cardiovasc Electrophysiol*. (2022) 33 (1):117–22. doi: 10.1111/jce.15278

16. Aksu T, Gopinathannair R, Bozyel S, Yalin K, Gupta D. Cardioneuroablation for treatment of atrioventricular block. *Circ Arrhythm Electrophysiol*. (2021) 14(9): e010018. doi: 10.1161/CIRCEP.121.010018

17. Aksu T, Padmanabhan D, Shenthar J, Yalin K, Olshansky RB, Gopinathannair R, et al. The benefit of cardioneuroablation to reduce syncope recurrence in vasovagal syncope patients: a case-control study. *J Interv Card Electrophysiol*. (2022) 63(1):77–86. doi: 10.1007/s10840-020-00938-0

18. Debruyne P, Wijns W. Cardio-neuromodulation: the right-sided approach. *JACC Clin Electrophysiol*. (2017) 3(9):1056–7. doi: 10.1016/j.jacep.2016.12.027

19. Debruyne P, Rossenbacker T, Collienne C, Roosen J, Dewilde W, Wijns W, et al. Unifocal right-sided ablation treatment for neurally mediated syncope and functional sinus node dysfunction under computed tomographic guidance. *Circ Arrhythm Electrophysiol*. (2018) 11(9):e006604. doi: 10.1161/CIRCEP.118.006604

20. Aksu T, Guler TE, Bozyel S, Golcuk SE, Yalin K, Lakkireddy D, et al. Medium-term results of cardioneuroablation for clinical bradyarrhythmias and vasovagal syncope: effects on QT interval and heart rate. *J Interv Card Electrophysiol*. (2021) 60(1):57–68. doi: 10.1007/s10840-020-00704-2

21. Pachon-M JC, Pachon-M EI, Pachon CTC, Santillana-P TG, Lobo TJ, Pachon-M JC, et al. Long-term evaluation of the vagal denervation by cardioneuroablation using Holter and heart rate variability. *Circ Arrhythm Electrophysiol*. (2020) 13(12):e008703. doi: 10.1161/CIRCEP.120.008703

22. Sakamoto S, Schuessler RB, Lee AM, Aziz A, Lall SC, Damiano RJ Jr. Vagal denervation and reinnervation after ablation of ganglionated plexi. *J Thorac Cardiovasc Surg*. (2010) 139(2):444–52. doi: 10.1016/j.jtcvs.2009.04.056

frontiers | Frontiers in Cardiovascular Medicine

TYPE Original Research
PUBLISHED 15 January 2024
DOI 10.3389/fcvm.2023.1333277

OPEN ACCESS

EDITED BY
Liqun Sun,
University of Toronto, Canada

REVIEWED BY
Maruti Haranal,
U N Mehta Institute of Cardiology and Research, India
Zongjie Weng,
Fujian Medical University, China

*CORRESPONDENCE
Wei Sheng
✉ sheng4616@126.com
Guoying Huang
✉ gyhuang@shmu.edu.cn

†These authors have contributed equally to this work

RECEIVED 04 November 2023
ACCEPTED 29 December 2023
PUBLISHED 15 January 2024

CITATION
Zhao T, Huang X, Chen W, Gao H, Feng Z, Tan C, Sun J, Ma X, Yan W, Sheng W and Huang G (2024) Clinical implications of respiratory ciliary dysfunction in heterotaxy patients with congenital heart disease: elevated risk of postoperative airway complications.
Front. Cardiovasc. Med. 10:1333277.
doi: 10.3389/fcvm.2023.1333277

Clinical implications of respiratory ciliary dysfunction in heterotaxy patients with congenital heart disease: elevated risk of postoperative airway complications

Tingting Zhao[1,2†], Xianghui Huang[3†], Weicheng Chen[1†], Han Gao[1,2], Zhiyu Feng[1,2], Chaozhong Tan[1,2], Jingwei Sun[4], Xiaojing Ma[1], Weili Yan[1,2,5], Wei Sheng[1,2,5*] and Guoying Huang[1,2,5*]

[1]Children's Hospital Affiliated to Fudan University, Shanghai, China, [2]Shanghai Key Laboratory of Birth Defects, Shanghai, China, [3]Fujian Provincial Key Laboratory of Neonatal Diseases, Xiamen Children's Hospital Affiliated to Children's Hospital of Fudan University, Shanghai, Xiamen, China, [4]Bengbu First People's Hospital Affiliated to Bengbu Medical University, Hefei, Anhui, China, [5]Research Unit of Early Intervention of Genetically Related Childhood Cardiovascular Diseases, Chinese Academy of Medical Sciences, Shanghai, China

Objective: Cardiac surgery in Congenital Heart Disease-Heterotaxy (CHD-HTX) patients often leads to increased postoperative airway complications. Abnormal respiratory ciliary function, resembling primary ciliary dyskinesia, has been observed. We expanded the sample size by retrospectively reviewing Ciliary Dysfunction (CD) in CHD-HTX patients to verify the increased risk of post-surgical respiratory complications.

Methods: We conducted a retrospective review of 69 CHD-HTX patients undergoing cardiac surgery, assessing abnormal respiratory function using nasal nitric oxide (nNO) levels and nasal ciliary motion observed in video microscopy. Data collected included demographics, surgical details, postoperative complications, length of stay, ICU hours, salvage procedures, intubation duration, and mortality.

Results: The CD and no-CD cohorts exhibited notable similarities in risk adjustment in Congenital Heart Surgery-1 (RACHS-1) risk categories, age at the time of surgery, and the duration of follow-up evaluations. We observed a trend toward an increased length of post-operative stay in the CD group (15.0 vs. 14.0; $P = 0.0017$). CHD-HTX patients with CD showed significantly higher rates of respiratory complications (70% vs. 44.4%; $P = 0.008$). There were no notable variances observed in postoperative hospitalization duration, mechanical ventilation period, or surgical mortality.

Conclusion: Our findings suggest that CHD-HTX patients with CD may face an elevated risk of respiratory complications. These results offer guidance for perioperative management and serve as a reference for further pathological studies.

KEYWORDS

postoperative airway complications, heterotaxy, congenital heart disease patients, respiratory ciliary dysfunction, primary ciliary dyskinesia

Introduction

Heterotaxy is defined as any discordant arrangement of visceral organ due to the randomization of left-right axis during embryogenesis. Complex congenital heart disease is often associated with heterotaxy patients. Some studies have observed that approximately 3% of CHD patients present with heterotaxy (1) and 67% of heterotaxy patients have complex congenital heart disease (2). The connection between cardiovascular morphogenesis and heterotaxy relies on motile cilia for normal heart looping and left-right pattern determination. Motile cilia is also essential for patients with primary ciliary dyskinesia (PCD), which leads to recurrent respiratory symptoms due to abnormal airway ciliary motion (3). 50% PCD patients have situs inversus totalis (SIT), while 6.3%–12.1% exhibit heterotaxy (2, 4). Ciliary dysfunction (CD) is characterized by testing and observing nasal epithelial ciliary motion (CM) in video microscopy by scraping the nasal tissue.

Compliance with clinical findings and incidence, previous study has also shown that known genes, such as *Dnah5* and *Dnail, in* mutant mouse with primary ciliary disease, displayed a high incidence of situs ambiguous with complex congenital heart disease (CHD) (5, 6). Furthermore, in our recent publication, we demonstrated that WES results in heterotaxy patients revealed a high presence of the PCD-causing gene DNAH11 (7). This observation reflects the known requirement for the left and right pattern of the motor cilia function of the embryonic node, as well as the important role of cilia function in airway clearance in the respiratory epithelium.

To investigate the association between cilia dysfunction and CHD with heterotaxy, Nader Nakhleh et al. conducted a retrospective analysis of 43 HTX-CHD patients. Among them, 18 patients exhibited CD, as evidenced by abnormal ciliary motion and nasal nitric oxide (nNO) level below or borderline of PCD cutoff value, resulting in increased airway symptoms. Sequencing results also revealed that known PCD-causing genes were more frequently found in heterotaxy patients with CD compared to controls without CD (8). Additionally, CHD patients with heterotaxy experienced higher postoperative events, postsurgical mortality rates, and increased respiratory complications when compared to CHD patients without laterality defects with similar RACHS-1 complexity scores (9).

Building on the previous retrospective analysis, it was initially underestimated whether respiratory complications were correlated with ciliary dyskinesia. The question of whether the ciliary dysfunction in CHD patients with heterotaxy leads to worse postoperative events remains controversial. Brandon Harden et al. conducted a small sample study in a limited regional population, which was insufficient to explain and support the issue (10). In our study, we divided our CHD-HTX patients into CD or no-CD groups based on video microscopical observation. We tested the assumption that HTX-CHD patients with abnormal ciliary motion have increased postsurgical events and respiratory complications compared to HTX-CHD without CD in the Chinese population. Our study includes a total of 110 operative events, consisting of 36 CHD-HTX-CD patients in 56 surgeries and 33 CHD-HTX-no-CD in 54 surgeries. The study provides a theoretical basis for perioperative management.

Materials and methods

Patient population

This study was conducted with the approval of the Children's hospital of Fudan university Institutional Review Board. We retrospectively enrolled patients with heterotaxy with CHD who had undergone cardiac surgery at the Children's Hospital of Fudan University Cardiac Surgery Center between 2012 and 2020. We collected relevant information from electronic medical records (EMR). Detailed cardiac anatomical data were obtained from cardiac catheterization reports, echocardiographic reports, enhanced cardiographs, and CT scans, as well as operative reports. Thoracic and abdominal situs were determined based on chest radiography and abdominal ultrasonography. Preoperative evaluation included nasal nitric oxide measurements and video microscopy of respiratory epithelia ciliary cells. The medical staff involved in the study were blinded to ciliary function throughout the research.

Definitions and inclusion criteria

In this study, heterotaxy was broadly defined as any thoracoabdominal organ discriminate from situs solitus. Our case-cohort consisted of patients with congenital heart defects undergoing cardiovascular surgery who also had laterality disorders. These laterality disorders included bronchial/pulmonary isomerism or inversus, midline or left-sided liver, midline or right-sided stomach, right-sided spleen, polysplenia or asplenia. Cardiovascular situs in CHD patients is classified as abnormal when they display dextrocardia/mesocardia, interrupted inferior vena cava, atrial isomerism/ambiguity/inversus, atrioventricular discordance, and superior/inferior ventricles (11). Cases with isolated CHD that didn't involve any of the cardiovascular situs anomalies mentioned above or other thoracoabdominal organ situs malformation were excluded.

Nasal nitric oxide measurements

PCD assessment included measure of nasal nitric oxide (nNO) when abnormal nNO value has high sensitivity and specificity for PCD. We measured nasal NO (nNO) using a chemiluminescence nitric oxide analyzer (CLD88 SP, ECOPHYSICS AG) following established protocols (12, 13). Due to age-related variations in nNo levels, we divided participants into three age groups: <1 year old, 1- to 6-year-old, and >6 year old. For those over 6 years of age, we followed the velum-closure technique according to American Thoracic Society/European Respiratory Society

guidelines. Normal nNO values are typically above 200 nl/min (12), whereas PCD patients exhibit values below 100 nl/min (14, 15). Values between 100 nl/min and 200 nl/min were considered borderline. For patients aged 1–6 years, nNO measurements were taken using tidal breath sampling (16). Healthy nNO value are generally >100 nl/min, while PCD patients often have values <50 nl/min (12). We categorized nNO levels as borderline low if they fell between 50 and 100 nl/min. In patients under 1 year old, specific nNO recommendations are limited due to measurement challenges. Phillip S. Adams et al. have developed a regression model to best estimate normative nNO values for infants less than 1 year old (17). We classified nNO values below the cutoff for each age group as abnormal, indicating CD.

Nasal tissue sampling and ciliary motion analysis

In our study, we divided our patients into CD or non-CD groups based on nasal tissue and ciliary motion analysis. Nasal epithelial tissue samples were obtained by curettage of the inferior nasal turbinate before the operation, suspended in L-15 medium (Invitrogen, CA) for video microscopy was conducted using a Leica inverted microscope (Leica DMI300B) equipped with a 67× oil objective under differential interference contrast optics. Recordings were captured at a frame rate of 200 frames/s at room temperature, employing a 680 PROSILICA GE camera (Allied Vision, PA). Digital recordings were evaluated by an expert panel of co-investigators (Weicheng Chen and Tingting Zhao), ensuring they remained blinded to the subjects' phenotype, heterotaxy status, and nNO level. In order to avoid the effect of secondary ciliary dyskinesia, nasal tissue was cultured for re-assessment of ciliary motion after reciliation. The reciliated tissue was observed by video microscopy to assess whether CM was normal (CD) or abnormal (no-CD). We closely examined the ciliary beat pattern to assess potential abnormalities in ciliary motion. The process involved the use of slow-motion video playback to create tracings of the ciliary beat, with a minimum of 10 tracings analyzed for each subject. The classification of ciliary beat patterns encompassed normal, immotile, minimal residual movements, stiff, restricted, and circular (18). The quantification of ciliary beat frequency (CBF) was performed using ImageJ and Photoshop software.

Data collection

Comprehensive demographic and preoperative data, encompassing visceral arrangement and medical history, were meticulously extracted from the medical records. Data regarding surgical procedures, including operation duration, Aortic Crossclamp Time, SVC Crossclamp Time, IVC Crossclamp Time, Cardiopulmonary Bypass, and Anesthetic duration, were documented. Additionally, we collected basic demographic information, such as age at the time of nNO and CM assessment, gender, race, gestational age, and diagnosis. RACHS-1 risk categories, known for their strong correlation with in-hospital mortality and postoperative hospital stay length, were used to facilitate relevant comparisons among different groups undergoing surgery for CHD/HTX.

Length of stay (LOS) parameters were also meticulously recorded, including total hospital stay duration, postoperative length of stay (PLOS), hours spent in the Cardiac Intensive Care Unit (CICU), and occurrences of in-hospital mortality. Postoperative mortality was characterized as any fatality within 30 days following the surgical procedure or during the patient's hospitalization after surgery. Measures related to postoperative respiratory outcomes encompassed the duration of mechanical ventilation in hours, the number of failed extubations, instances of prolonged ventilatory support, cases requiring salvage procedures, and the occurrence of fever. A patient's reintubation is characterized by failed extubation within 24 h. Viral infection was defined as positive nasal viral panel and clinical symptoms. Bacterial infection was defined as positive blood culture and clinical symptoms. The presence of fever combing with positive blood culture or nasal viral panel and clinical symptoms served as an indicator of postsurgical infection.

Statistical analysis

We used summary statistics, including proportions and medians with interquartile ranges, to describe patient characteristics and postoperative outcomes. For comparisons, we employed χ^2 tests, Fisher exact tests and Wilcoxon rank-sum tests for categorical and continuous variables. To address intrasubject correlations among surgical events, mixed-effects models were applied. For skewed continuous outcomes, we used linear mixed models on log-transformed data. Categorical outcomes were assessed with generalized linear mixed models. Multivariate analysis was conducted, controlling for baseline surgical characteristics. All tests were two-sided, and we set a significance level of $P < 0.05$. A more conservative threshold was used to adjust for multiple comparisons. SPSS was used for statistical analyses.

Results

We enrolled 69 patients with HTX-CHD, which included 36 patients with heterotaxy with ciliary dysfunction (CD group) and 33 patients with heterotaxy congenital heart disease without ciliary function (no-CD group). Supplementary Tables E1, E2 present the structural heart position and laterality defects based on Van Praagh classification. Laterality abnormalities included variations in heart position (62%), stomach (61%), liver (77%), spleen (96%) and lung (100%). In the CD group, 22 patients (61%) had dextrocardia, while 12 (33%) had levocardia. Additionally, 7 patients (19%) had bilateral superior vena cava. Atrial and ventricular abnormalities included atrial septal defects (ASD) in 15 patients (42%) in the CD group and 15 patients (45%) in the no-CD group. Regarding conotruncal defects, there were various cases: 1 (3%) with Tetralogy of Fallot (TOF) in the

CD group and 3 (9%) in the no-CD group, 1 (3%) with Pulmonary Atresia with Ventricular Septal Defect (PA/VSD) in the CD group and 3 (9%) in the no-CD group, 13 (36%) with D-transposition of the great arteries (D-TGA) in the CD group and 11 (33%) in the no-CD group, and 12 (33%) with Double Outlet Right Ventricle (DORV) in the CD group and 9 (27%) in the no-CD group (Table 1). For cases with a lack of or no record of imagological examination, findings showed 33% in stomach, 11% in liver, 27% in spleen, and 62% in lung. Specifically concerning the liver, in the CD group, 15 cases (42%) exhibited abnormalities compared to 14 cases (42%) in the no-CD group. The midline liver position was observed in 10 cases (28%) in the CD group and 8 cases (24%) in the no-CD group (Table 1).

Baseline demographics stratified by ciliary motion and nNO Status

Nasal scrapes were obtained from all 69 participants for CM analysis, and nNO measurements were conducted in 41 (59%) participants. Abnormal CM was observed in 28 (41%) of the participants, with 14 (34%) showing borderline nNo values and 12 (29%) exhibiting low nNo values. Among the 41 who underwent both CM and nNO measurement, 12 showed abnormalities in both CM and low nNO (Figure 1). The nNO level in the patients with CD (86.1 nl/min) was significantly lower than in the patients without CD (119.16 nl/min).

Clinical and surgical characteristics

Clinical and surgical outcomes are observed in Tables 2, 3. The patient age ranged from 6 days to 12 years at the time of surgery, with median age of 637.67 days for the CD group and 772.25 days for the no-CD group. Of the recruited patients, 65% were female, and 35% were male. All patients were of Asian descent and diagnosed at the Children's Hospital of Fudan university. The CD group underwent 56 cardiac surgical procedures, while the no-CD group underwent 54 surgeries. The median RACHS-1

TABLE 1 Cardiovascular anatomy and organ situs.

	CD, *n* (%) 36	No-CD, *n* (%) 33	Organ situs	CD, *n* (%) 36	No-CD, *n* (%) 33
Cardiac position			Stomach		
Dextrocardia	22 (61%)	19 (58%)	Normal	9 (25%)	9 (27%)
Mesocardia	2 (5.6%)	–	Opposite	14 (38%)	14 (42%)
Levocardia	12 (33%)	14 (42%)	No record	13 (36%)	10 (30%)
Venous anomalies			Liver		
Bilateral superior vena cava	7 (19%)	6 (18%)	Normal	8 (22%)	6 (18%)
Anomalous pulmonary venous return	3 (8.3%)	5 (15%)	Opposite	15 (42%)	14 (42%)
Atria and ventricles			Midline	10 (28%)	8 (24%)
Atrioventricular septal defect	9 (25%)	7 (21%)	No record	3 (8%)	5 (15%)
Atrial septal defect	15 (42%)	15 (45%)	Spleen		
Ventricular septal defect	17 (47%)	12 (36%)	Normal	2 (6%)	–
Atrioventricular valve atresia/stenosis	5 (14%)	5 (15%)	Right	16 (44%)	14 (42%)
Common atrium	2 (6%)	4 (12%)	Asplenia	7 (19%)	9 (27%)
Single ventricle morphology	13 (36%)	14 (42%)	Polysplenia	2 (6%)	–
Ventricular outflow and great vessels			No record	9 (25%)	10 (30%)
Double-out right ventricle	12 (33%)	9 (27%)	Lungs		
Pulmonary stenosis/atresia	22 (61%)	14 (42%)	Normal	–	–
Aortic stenosis/atresia	1 (3%)	4 (12%)	Inverted	10 (28%)	3 (9%)
Right aortic arch	10 (28%)	10 (30%)	Left isomerism	2 (6%)	-
Double-out left ventricle	1 (3%)	5 (15%)	Right isomerism	4 (11%)	7 (21%)
Conotruncal defect			No record	20 (56%)	22 (70%)
Tetralogy of Fallot, TOF	1 (3%)	3 (9%)	Van Praagh classification		
PA/VSD	1 (3%)	1 (3%)	{S,D,S}	1 (3%)	5 (15%)
D-TGA	13 (36%)	11 (33%)	{S,D,D}	–	4 (12%)
Double outlet right ventricle	12 (33%)	9 (27%)	{S,L,L}	5 (14%)	4 (12%)
L-TGA	4 (11%)	6 (18%)	{S,D,X}	2 (6%)	2 (6%)
			{S,D,L}	–	1 (3%)
			{I,L,L}	–	2 (6%)
			{I,D,D}	5 (14%)	1 (3%)
			{I,D,X}	2 (6%)	1 (3%)
			{A,D,D}	–	1 (3%)
			{A,D,S}	2 (6%)	2 (6%)
			{A,D,L}	1 (3%)	–
			{A,D,X}	2 (6%)	1 (3%)
			{A,L,D}	1 (3%)	–

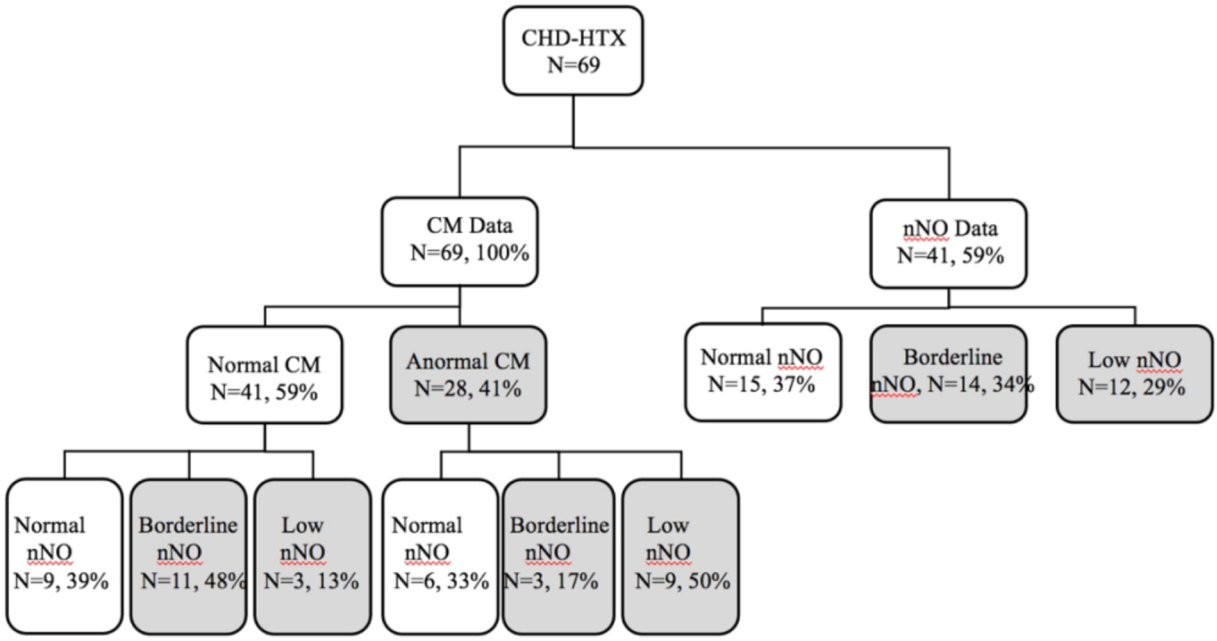

FIGURE 1
Enrollment data. Total congenital heart disease with HTX, $n = 69$. Results are presented as a flow chart. Shaded areas represent abnormal findings. CHD, congenital heart disease; nNO, nasal nitric oxide.

TABLE 2 Characteristics by surgical encounter.

	CD ($n = 56$)	No-CD ($n = 54$)	*P*-value
Age at surgery (d), median (IQR)	637.67 (286.00–1,487.50)	772.25 (240.25–1,491.00)	0.5601
Preoperative weight (kg), median (IQR)	9.8 (7.00–13.00)	11.43 (7.18–15.55)	0.2741
RACHS-1 risk category, median (IQR)	3.0 (2.0–3.0)	3.0 (2.0–3.0)	0.714
Length of hospitalization (d), median (IQR)	28.0 (19.5–34.7)	24.0 (20.0–33.5)	0.1141
Length of post-operative stay (d), median (IQR)	15.0 (10.0–21.0)	14.0 (11.0–18.8)	0.0017
Hours in ICU (h), median (IQR)	83.5 (44.5–170.5)	96 (48.0–164.25)	0.6803
No. of Salvage, *n* (%)	2 (3.6%)	5 (9.1%)	0.266*

P-values obtained by Wilcoxon rank-sum test for continuous variables or Pearson c2 test for categorical variables. nNO, nasal nitric oxide.
**P*-value determined by the Fisher exact test.

scores for these operations, under both single and biventricular repair tracks, were 3.0 (range: 2.0–3.0) in the CD cohort and 3.0 (range: 2.0–3.0) in the no-CD cohort.

TABLE 3 Comparison of RACHS-1 scores in CD and Non-CD.

RACHS-1 category	CD *N*	%	No-CD *N*	%	*P*-value
1	1	1.8%	0	0.0	0.714
2	24	42.9%	27	50.0%	
3	31	55.4%	26	48.1%	
4	0	0.0	1	1.9%	
5	0	0.0	0	0.0	
6	0	0.0	0	0.0	
Total	56		54		

The Wilcoxon rank-sum test was used to compare the distribution of the RACHS-1.

Comparison of surgical and postsurgical outcomes

Table 4 demonstrates that there were no statistically significant differences in age at the time of surgery, preoperative weight, or sex between the CD group and the no-CD group. However, there was a trend toward younger age at surgery in CD patients than no-CD patients, with median age of 637.67 vs. 772.25 respectively. The median length of hospitalization for the CD group was 28 days (IQR, 19.5–34.7 days), which was not statistically distinguished from the 54 surgical encounters of the no-CD group, while the no-CD group with median of 24 days (IQR, 20.0–33.5 days), which was not significantly different. The median length of post-operative stays in the CD cohort (15.0 days, IQR, 10.0–21.0) was longer than in the no-CD cohort (14.0 days, IQR, 11.0–18.8), and this difference was statistically significant ($P = 0.0017$). However, there were no statistically significant differences in the hours spent in the ICU between the CD cohort (median, 83.5 h)

TABLE 4 Comparison of surgery in CD and Non-CD.

	CD ($n = 56$)	No-CD ($n = 54$)	*P*-value
Length of surgery, median (IQR)	175.0 (150.00–220)	180.0 (144.15–207.63)	0.4032
Aortic Crossclamp Time, median (IQR)	8.6 (0.0–33.0)	15.0 (0.0–41.75)	0.6921
SVC Crossclamp Time, median (IQR)	28.0 (8.3–49.0)	41.75 (18.37–55.0)	0.1918
IVC Crossclamp Time, median (IQR)	0.0 (0.0–40.0)	27.25 (0.0–48.0)	0.0969
Cardiopulmonary bypass, median (IQR)	86.0 (67.0–115.0)	78.75 (53.5–100.5)	0.2234
Anesthetic duration, median (IQR)	205 (180.0–278.0)	210.0 (178.75–243.38)	0.1738

Data are median (interquartile range) or *n* (%). *P*-values obtained from Mann–Whitney and χ^2 for continuous and categorical variables.

and the no-CD cohort (median, 96 h). The number of postsurgical salvage cases in the CD group was 2 patients (3.6%) less than that of no-CD group ($n = 5$, 1%), with no statistically significant difference seen ($P = 0.438$) (Table 3). There was no difference in the length of surgery, Aortic Crossclamp time, SVC Crossclamp time, IVC Crossclamp time, Cardiopulmonary Bypass, or Anesthetic Duration between patients stratified by the CD group or no-CD group (Table 4).

Comparison of morbidity and mortality

A follow-up analysis was conducted on postsurgical patients who survived their last surgery. Death within 30 days post-hospitalization was considered a case. Two death cases were observed in the CD cohort, and six cases in the no-CD group. Notably, parents of patient #5,119, #5,876, and #51,372 in the no-CD group proactively discontinued treatment (Supplementary Table E2). Statistical analysis showed no statistical difference in postoperative mortality (≤30 days) between the CD group and no-CD group (Table 5).

Comparison of respiratory outcomes

In the case of the 56 CHD surgical procedures, the median duration of postoperative mechanical ventilation was 22.5 h (IQR, 10.25–93). Among these surgical encounter, one patient required a prolonged ventilator course (≥10 days) (Table 5).

TABLE 5 Comparison of morbidity and mortality between CD and No-CD.

	CD ($n = 36$)	No-CD ($n = 33$)	*P*-value
Death ≤30days, *n* (%)	2 (5.6%)	6 (18.2%)	0.14
Neonatal respiratory distress, *n* (%)	0 (0)	0 (0)	–

P-value determined by the Fisher exact test.

In contrast, the no-CD group, with 54 surgical outcomes, had a median length of intubation of 21.5 h (IQR, 10.82–69.25), with no significant difference in the duration of mechanical ventilation between the CD and no-CD group ($P = 0.37$). Only The patient in the CD cohort required reintubation. The number of postoperative fever (≥38.5°C) showed no statistical difference between the two groups, with the 18 instances of postoperative fever in the 56 surgical encounters compared to 12 instances in the no-CD group (Table 6).

The frequency of respiratory complications was compared between the 2 groups. Respiratory complications were identified through postoperative chest x-rays, encompassing pleural effusion, atelectasis, pneumothorax, pleural exudation, pneumonia, and delayed sternal closure. Notably, respiratory complications occurred 39 (70%) of the 56 cardiac surgeries in the CD cohort, whereas the no-CD group experienced these complications in only 24 (44.4%) of their surgeries, signifying a significantly lower frequency in the latter group ($P = 0.008$) (Table 6). In-depth subgroup analysis of respiratory complications, excluding those not solely attributed to cilia dysfunction (such as pleural effusions and pulmonary edema), consistently demonstrated a significantly higher prevalence of respiratory problems within the congenital heart disease (CD) cohort ($P < 0.02$).

Discussion

The mucociliary clearance system serves as a pivotal physiological mechanism responsible for the removal of inhaled foreign substances and endogenously generated secretions from the respiratory airways. Ciliary dysfunction, a critical component of this system, manifests in two primary forms: PCD, which is a congenital disorder characterized by impaired mucociliary transport, and secondary ciliary dyskinesia, which may develop subsequent to injuries such as respiratory infections. It is

TABLE 6 Respiratory outcome measures by surgical encounter.

	CD ($n = 56$)	No-CD ($n = 54$)	*P*-value
Length of mechanical ventilation (hr), median (IQR)	22.5 (10.25–93)	21.5 (10.82–69.25)	0.3700
Prolonged ventilator course (≥10days), *n* (%)	1 (2.7%)	0 (0)	>0.99
No. failed extubations, *n* (%)	1 (1.8%)	0 (0)	>0.99
Fever (≥38.5°C), *n* (%)	18 (32.1%)	12 (22.2%)	0.243
Respiratory complication, *n* (%)	39 (70%)	24 (44.4%)	0.008

Data are median (interquartile range) or *n* (%). *P*-values obtained from Mann Whitney and χ^2 for continuous and categorical variables.

noteworthy that secondary ciliary dyskinesia presents distinct ultrastructural abnormalities in contrast to the primary form of the disorder, PCD.

In our research investigation, patients were categorized into groups based on the presence or absence of ciliary dysfunction, which encompassed primary ciliary dyskinesia and secondary ciliary dysfunction. Ciliary motion can be induced by secondary ciliary dyskinesia, such as from respiratory infection and allergy to environmental insults, but in our study, this can be eliminated by observing the ciliary motion after culturing and reciliation of nasal tissue (19–21). Although some individuals, particularly those with heterotaxy and CHD, may not exhibit overt structural deficiencies in their cilia ultrastructure, the observation of abnormal ciliary motion through microscopic analysis suggests that their ciliary response to environmental stimuli is fragile. Significantly, our findings indicate that this ciliary dysfunction is potentially reversible when the affected tissue is removed from the infected or inflamed environment. Neonatal respiratory distress and bronchiectasis, as well as respiratory symptom, are frequently observed in individuals with PCD. Early research has provided insights indicating that an escalation in sinopulmonary symptoms does not appear to be contingent on the presence of heterotaxy. This implies that patients with CHD face an elevated risk for respiratory ailments linked to reduced nNO levels or abnormal ciliary motion, rather than the condition of heterotaxy itself (8). In an endeavor to gain a more comprehensive understanding of whether abnormal ciliary motion is linked to CHD-HTX, we conducted an observational study. Our findings revealed that 28 out of 69 (41%) of CHD-HTX patients presented CD. The ciliary motion anomalies identified in these CHD-HTX patients closely resembled those classically seen in PCD, characterized by the presence of stiff, dyskinetic or wavy ciliary beat. Remarkably, among patients with CD, approximately 50% exhibited low nNO levels, while 17% exhibited nNO values in proximity to the PCD diagnostic threshold. Notably, the mean nNO values of the CHD-HTX patients with CD exceeded those of their counterparts without CD. This collection of observations strongly suggests that individuals with CHD and heterotaxy may harbor CD, which exhibits characteristics overlapping with PCD, including both abnormal ciliary motion and reduced nNO levels.

In a previous study, researchers analyzed the postoperative outcomes of 13 patients with heterotaxy and CHD who displayed CD, comparing them to 14 patients with heterotaxy and CHD but without CD. This earlier investigation revealed an increased risk of respiratory complications in those with CD (10). Nevertheless, it is essential to acknowledge that the limited sample size of this study could have introduced potential errors and inaccuracies. To rectify this limitation, we expanded the sample size and conducted a prospective assessment involving 36 heterotaxy patients with CHD and confirmed CD who underwent cardiac surgery. These individuals were juxtaposed with a control group comprising 33 CHD-heterotaxy patients without CD. Importantly, it is noteworthy that both the CD and no-CD groups were equivalent in terms of their Risk Adjustment for Congenital Heart Surgery (RACHS-1) scores, signifying that they underwent cardiac surgeries of comparable complexity. In contrast, the CD group exhibited increased incidences of respiratory complications following surgery and required extended post-operative hospital stays when compared to the no-CD group. This observation implies that patients with heterotaxy and CHD may be prone to experiencing respiratory complications due to underlying ciliary dysfunction. This hypothesis finds support in the notable occurrence of heterotaxy in a murine model of PCD, as documented in a previous study (5). Furthermore, our understanding is bolstered by research that has validated the significant roles played by DNAH11, DNAH5, and DNAI genes in encoding key components of respiratory and nodal ciliary outer dynein arm proteins (22, 23). These genetic factors have been established as contributors to the development of heterotaxy syndrome and CHD.

In light of our meticulous clinical observations and comprehensive research findings, our study contributes significantly to the nuanced understanding of the intricate associations between PCD, heterotaxy, and CHD. Postoperative evaluation of 36 CHD-HTX with CD undergoing cardiac surgery showed that high risks related to respiratory deficiency comparing to 33 CHD-HTX without CD. CHD-HTX with CD showed a greater need for mechanical ventilation, prolonged ventilator course and more failed extubation. We noted that no difference in number of death and neonatal respiratory distress between 2 groups. By raising awareness among healthcare practitioners regarding the potential risk of ciliary CD in patients with CHD, we aim to expedite the diagnostic process, ultimately leading to enhanced healthcare outcomes. Our investigation unearthed a noteworthy increase in the incidence of postoperative respiratory complications in the CD group, which was substantiated by a thorough analysis of chest x-rays conducted during the hospitalization period. These complications encompassed a range of conditions, including pleural effusion, atelectasis, pneumothorax, pleural exudation, pneumonia, and delayed sternal closure. It is essential to emphasize that ciliary dyskinesia, when considered in isolation, is not directly causative of conditions such as pleural effusion, stridor, and pulmonary edema. However, CD solely cannot account for pleural effusions, most likely to occur respiratory complication in the study to be further studied.

In our study, there was no difference in the length of surgery, Aortic Crossclamp time, SVC Crossclamp time, IVC Crossclamp time, Cardiopulmonary Bypass, or Anesthetic Durhuaation between patients stratified by the CD group or no-CD group, which keep consistency with RACHS-1 between CD and no-CD groups in case of surgery influence. With comparison to no-CD group, there were trends that CD groups took more time in the length of hospitalization, hours spent in the ICU, or the occurrence of prolonged ventilatory courses, though not statistically significant. In the case of the 56 CHD surgical procedures, the median duration of postoperative mechanical ventilation was 22.5 h more than 21.5 h in the no-CD group. Among these surgical encounter, one patient required a prolonged ventilator course (≥10 days) in CD group. Only the patient in the CD cohort required reintubation. The number of postoperative fevers showed 18 instances in the 56 surgical

encounters compared to 12 instances in the no-CD group, though no significant difference, which implied that HTX with CD were more susceptible to external factor. Given single center of the present study, further analysis of clinical treatment of patients is needed to further assess the impact of CD on these outcome parameters.

To provide a more precise analysis, a subgroup assessment was meticulously conducted, systematically excluding complications that could not be solely attributed to ciliary dysfunction (specifically, pleural effusions and pulmonary edema). Remarkably, this rigorous subgroup analysis demonstrated significantly higher rates of adverse respiratory outcomes within the CD cohort ($P < 0.02$). The observed increase in the median duration of postoperative hospital stays for the CD cohort aligns with our expectations, reflecting the extended period required for the recovery and recuperation of these patients. This underscores the intricate interplay between ciliary dysfunction, heterotaxy, and CHD, and the profound impact it has on clinical outcomes.

Limitation

In our study, no statistically significant increases were observed in the length of hospitalization, hours spent in the ICU, duration of postoperative mechanical ventilation, or the occurrence of prolonged ventilatory courses. These results diverge from earlier research that reported a rising trend in the duration of postoperative mechanical ventilation and prolonged ventilatory courses (10). This inconsistency might be linked to differences in the racial backgrounds and sample sizes of the populations studied.

Conclusion

In summary, our study not only advances our understanding of the intricate interplay between PCD, heterotaxy, and CHD but also underscores the need for preoperative screening of ciliary dysfunction in heterotaxy patients with CHD. This proactive approach can significantly enhance postsurgical respiratory therapy and ultimately improve the overall well-being of these patients (6).

Data availability statement

The original contributions presented in the study are included in the article/**Supplementary Material**, further inquiries can be directed to the corresponding authors.

Ethics statement

The studies involving humans were approved by Children's hospital of Fudan university. The studies were conducted in accordance with the local legislation and institutional requirements. Written informed consent for participation in this study was provided by the participants' legal guardians/next of kin.

Author contributions

TZ: Investigation, Methodology, Resources, Writing – original draft. XH: Resources, Writing – review & editing. WC: Supervision, Writing – review & editing. HG: Validation, Writing – review & editing. ZF: Formal Analysis, Writing – review & editing. CT: Resources, Writing – review & editing. JS: Data curation, Writing – review & editing. XM: Project administration, Writing – review & editing. WY: Project administration, Writing – review & editing. WS: Conceptualization, Writing – review & editing. GH: Conceptualization, Writing – review & editing.

Funding

The author(s) declare financial support was received for the research, authorship, and/or publication of this article.

This work was supported by the National Key Research and Development Program of China (2021YFC2701000 and 2016YFC1000500); National Natural Science Foundation of China (82270312, 81873482, 81873483, and 81800282); Shanghai Basic Research Project of Science and Technology Innovation Action Plan (20JC1418300); and CAMS (Chinese Academy of Medical Sciences) Innovation Fund for Medical Sciences (2019-I2M-5-002).

Acknowledgments

The authors thank the patients and their families for participating in the study.

Conflict of interest

The authors declare that the research was conducted in the absence of any commercial or financial relationships that could be construed as a potential conflict of interest.

Publisher's note

Supplementary material

The Supplementary Material for this article can be found online at: https://www.frontiersin.org/articles/10.3389/fcvm.2023.1333277/full#supplementary-material

References

1. Sutherland MJ, Ware SM. Disorders of left-right asymmetry: heterotaxy and situs inversus. *Am J Med Genet C Semin Med Genet*. (2009) 151C(4):307–17. doi: 10.1002/ajmg.c.30228

2. Kennedy MP, Omran H, Leigh MW, Dell S, Morgan L, Molina PL, et al. Congenital heart disease and other heterotaxic defects in a large cohort of patients with primary ciliary dyskinesia. *Circulation*. (2007) 115(22):2814–21. doi: 10.1161/CIRCULATIONAHA.106.649038

3. Sagel SD, Davis SD, Campisi P, Dell SD. Update of respiratory tract disease in children with primary ciliary dyskinesia. *Proc Am Thorac Soc*. (2011) 8(5):438–43. doi: 10.1513/pats.201103-024SD

4. Shapiro AJ, Davis SD, Ferkol T, Dell SD, Rosenfeld M, Olivier KN, et al. Leigh MW; genetic disorders of mucociliary clearance consortium. Laterality defects other than situs inversus totalis in primary ciliary dyskinesia: insights into situs ambiguus and heterotaxy. *Chest*. (2014) 146(5):1176–86. doi: 10.1378/chest.13-1704

5. Tan SY, Rosenthal J, Zhao XQ, Francis RJ, Chatterjee B, Sabol SL, et al. Heterotaxy and complex structural heart defects in a mutant mouse model of primary ciliary dyskinesia. *J Clin Invest*. (2007) 117(12):3742–52. doi: 10.1172/jci33284

6. Francis RJ, Christopher A, Devine WA, Ostrowski L, Lo C. Congenital heart disease and the specification of left-right asymmetry. *Am J Physiol Heart Circ Physiol*. (2012) 302(10):H2102–11. doi: 10.1152/ajpheart.01118.2011

7. Liu S, Chen W, Zhan Y, Li S, Ma X, Ma D, et al. DNAH11 variants and its association with congenital heart disease and heterotaxy syndrome. *Sci Rep*. (2019) 9(1):6683. doi: 10.1038/s41598-019-43109-6

8. Nakhleh N, Francis R, Giese RA, Tian X, Li Y, Zariwala MA, et al. High prevalence of respiratory ciliary dysfunction in congenital heart disease patients with heterotaxy. *Circulation*. (2012) 125(18):2232–42. doi: 10.1161/CIRCULATIONAHA.111.079780

9. Swisher M, Jonas R, Tian X, Lee ES, Lo CW, Leatherbury L. Increased postoperative and respiratory complications in patients with congenital heart disease associated with heterotaxy. *J Thorac Cardiovasc Surg*. (2011) 141(3):637–44.644.e1-3. doi: 10.1016/j.jtcvs.2010.07.082

10. Harden B, Tian X, Giese R, Nakhleh N, Kureshi S, Francis R, et al. Increased postoperative respiratory complications in heterotaxy congenital heart disease patients with respiratory ciliary dysfunction. *J Thorac Cardiovasc Surg*. (2014) 147(4):1291–8.e2. doi: 10.1016/j.jtcvs.2013.06.018

11. Stewart E, Adams PS, Tian X, Khalifa O, Wearden P, Zahid M, et al. Airway ciliary dysfunction: association with adverse postoperative outcomes in nonheterotaxy congenital heart disease patients. *J Thorac Cardiovasc Surg*. (2018) 155(2):755–63.e7. doi: 10.1016/j.jtcvs.2017.09.050

12. American Thoracic Society; European Respiratory Society. ATS/ERS recommendations for standardized procedures for the online and offline measurement of exhaled lower respiratory nitric oxide and nasal nitric oxide, 2005. *Am J Respir Crit Care Med*. (2005) 171(8):912–30. doi: 10.1164/rccm.200406-710ST

13. Beydon N, Chambellan A, Alberti C, de Blic J, Clément A, Escudier E, et al. Technical and practical issues for tidal breathing measurements of nasal nitric oxide in children. *Pediatr Pulmonol*. (2015) 50(12):1374–82. doi: 10.1002/ppul.23167

14. Leigh MW, Zariwala MA, Knowles MR. Primary ciliary dyskinesia: improving the diagnostic approach. *Curr Opin Pediatr*. (2009) 21(3):320–5. doi: 10.1097/MOP.0b013e328329cddb

15. Papon JF, Bassinet L, Cariou-Patron G, Zerah-Lancner F, Vojtek AM, Blanchon S, et al. Quantitative analysis of ciliary beating in primary ciliary dyskinesia: a pilot study. *Orphanet J Rare Dis*. (2012) 7:78. doi: 10.1186/1750-1172-7-78

16. Chawla KK, Shapiro A, Hazucha MJ, Brown DE, Leigh MW. Nasal nitric oxide during tidal breathing in children under 6 years of age. *[C]//American thoracic society international conference* (2009).

17. Adams PS, Tian X, Zahid M, Khalifa O, Leatherbury L, Lo CW. Establishing normative nasal nitric oxide values in infants. *Respir Med*. (2015) 109(9):1126–30. doi: 10.1016/j.rmed.2015.07.010

18. Guo Z, Chen W, Wang L, Qian L. Clinical and genetic spectrum of children with primary ciliary dyskinesia in China. *J Pediatr*. (2020) 225:157–65.e5. doi: 10.1016/j.jpeds.2020.05.052

19. Hirst RA, Jackson CL, Coles JL, Williams G, Rutman A, Goggin PM, et al. Culture of primary ciliary dyskinesia epithelial cells at air-liquid interface can alter ciliary phenotype but remains a robust and informative diagnostic aid. *PLoS One*. (2014) 9(2):e89675. doi: 10.1371/journal.pone.0089675

20. Hirst RA, Rutman A, Williams G, O'Callaghan C. Ciliated air-liquid cultures as an aid to diagnostic testing of primary ciliary dyskinesia. *Chest*. (2010) 138(6):1441–7. doi: 10.1378/chest.10-0175

21. Jorissen M, Willems T, Van der Schueren B. Ciliary function analysis for the diagnosis of primary ciliary dyskinesia: advantages of ciliogenesis in culture. *Acta Otolaryngol*. (2000) 120(2):291–5. doi: 10.1080/000164800750001116

22. Ostrowski LE, Yin W, Rogers TD, Busalacchi KB, Chua M, O'Neal WK, et al. Conditional deletion of dnaic1 in a murine model of primary ciliary dyskinesia causes chronic rhinosinusitis. *Am J Respir Cell Mol Biol*. (2010) 43(1):55–63. doi: 10.1165/rcmb.2009-0118OC

23. Seo JW, Brown NA, Ho SY, Anderson RH. Abnormal laterality and congenital cardiac anomalies. Relations of visceral and cardiac morphologies in the iv/iv mouse. *Circulation*. (1992) 86(2):642–50. doi: 10.1161/01.CIR.86.2.642

frontiers | Frontiers in Cardiovascular Medicine

TYPE Review
PUBLISHED 16 January 2024
DOI 10.3389/fcvm.2024.1287060

OPEN ACCESS

EDITED BY
Olivier M. Vanakker,
Ghent University, Belgium

REVIEWED BY
Stefan Pinter,
University of Connecticut Health Center, United States
Liqun Sun,
University of Toronto, Canada
Felix Sebastian Oberhoffer,
LMU Munich University Hospital, Germany

*CORRESPONDENCE
Hefeng Huang
✉ huanghefg@fudan.edu.cn
Li Jin
✉ jinl@fudan.edu.cn

†These authors have contributed equally to this work

RECEIVED 01 September 2023
ACCEPTED 08 January 2024
PUBLISHED 16 January 2024

CITATION
Li J, Liu Y, Huang H and Jin L (2024) Cardiovascular health of offspring conceived by assisted reproduction technology: a comprehensive review.
Front. Cardiovasc. Med. 11:1287060.
doi: 10.3389/fcvm.2024.1287060

Cardiovascular health of offspring conceived by assisted reproduction technology: a comprehensive review

Jie Li†, Yang Liu†, Hefeng Huang* and Li Jin*

Obstetrics and Gynecology Hospital, Institute of Reproduction and Development, Fudan University, Shanghai, China

Recently, the use of assisted reproductive technology (ART) has rapidly increased. As a result, an increasing number of people are concerned about the safety of offspring produced through ART. Moreover, emerging evidence suggests an increased risk of cardiovascular disease (CVD) in offspring conceived using ART. In this review, we discuss the epigenetic mechanisms involved in altered DNA methylation, histone modification, and microRNA expression, as well as imprinting disorders. We also summarize studies on cardiovascular changes and other risk factors for cardiovascular disease, such as adverse intrauterine environments, perinatal complications, and altered metabolism following assisted reproductive technology (ART). Finally, we emphasize the epigenetic mechanisms underlying the increased risk of CVD in offspring conceived through ART, which could contribute to the early diagnosis and prevention of CVD in the ART population.

KEYWORDS

cardiovascular diseases, assisted reproductive technology (ART), epigenetics, embryo development, DNA methylation

1 Introduction

Assisted reproductive technology (ART) encompasses a range of procedures, including *in vitro* fertilization (IVF), intracytoplasmic sperm injection (ICSI), oocyte donation (OD), superovulation, freeze-thawing, and other related techniques. The use of ART has increased in recent years owing to the increasing incidence of infertility in the population. In the United States, approximately 1.9% children are conceived through ART (1); similarly, over 1.0% of all births result from ART in mainland China (2). Moreover, it is predicted that over 150 million children, or 1.4% of the global population, will be conceived with ART by the end of the century (3).

It is widely accepted that the risk of developing diseases is linked to critical developmental periods such as the periconceptional, prenatal, and early postnatal stages (4). Barker's Developmental Origins of Health and Disease (DOHaD) theory suggests that changes in the conception microenvironment during both the intrauterine and postnatal periods can result in long-term damage, particularly in the form of cardiovascular and metabolic diseases (5, 6). Recently, adverse environmental exposure of oocytes during the pre-gestational period has shown to have lasting effects on offspring (7). Thus, concerns have been raised that ART techniques may interfere with early development and lead to long-term disorders in offspring.

The primary reason for premature death in China is due to cardiovascular disease (CVD) (8, 9). Additionally, in the Western, there has been a gradual rise in the frequency and prevalence of cardiovascular diseases, whether they are congenital or acquired, which has contributed to changes in risk factor profiles among children and young adults (10). Thus, CVD in offspring conceived via ART has received considerable attention, and emerging evidence suggests congenital heart defects (CHD) and an increased cardiovascular risk in offspring conceived using ART (11–21). In this comprehensive review, we collected evidence from humans and animals to explore the epigenetic alterations induced by ART and their subtle consequences on offspring cardiovascular health.

2 Epigenetic modification and ART-induced cardiovascular dysfunction

To ensure the quality of embryos and pregnancy outcomes, gametes are protected from environmental stress in the female reproductive tract by the tubal fluid during the pre-fertilization period *in vivo*. Despite efforts to minimize *in vivo* environmental stimuli during ART procedures, they still differ from those in the female reproductive tract. IVF and ICSI are two common ART used to help couples conceive. The process of IVF involves stimulating the ovaries to produce multiple eggs, retrieving the eggs, fertilizing them with sperm in a laboratory dish, and then transferring the resulting embryos into the uterus. ICSI is a type of IVF that involves injecting a single sperm directly into an egg to facilitate fertilization. Both procedures offer hope to couples struggling with infertility. More specifically, the ART setting involves exposure to a range of stimuli, including superovulation (22), cryopreservation (23, 24), exposure to various types of lights (25), fluctuations in pH and temperature (26, 27), changes in oxygen tension (28), culture media that contain specific substances such as Fe2+ and Cu2+ (29), and gamete or embryo manipulation. All these ART interventions act during gamete-imprinted gene reprogramming and embryonic gene demethylation (30). Thus, with exquisite sensitivity to environmental insults, the trajectories of gametic and embryonic development can be easily affected.

Epigenetics is the study of changes in gene expression that occur without alterations to the underlying DNA sequence. Epigenetic modifications can influence gene expression by modifying chromatin structure and DNA accessibility. These modifications can be influenced by environmental factors and can have long-lasting effects on an organism's phenotype (31). The relationship between epigenetics, cardiac development, and disease has been supported by a growing body of evidence (32). Epigenetic markers, such as DNA methylation and histone modification, are established in germ cells and maintained throughout embryonic development and postnatal life (33). Controlled ovarian stimulation acts during the period when the imprinted genes of oocytes are reprogrammed, while *in vitro* embryo culture acts during the sensitive period of gene demethylation (30). Consequently, ART can cause epigenetic dysregulation in embryos and adult offspring, ultimately affecting cardiovascular health.

2.1 DNA methylation

DNA methylation is a type of epigenetic modification that involves the addition of methyl groups to cytosine or adenine bases in DNA. This process primarily occurs in CpG (5′-C-phosphate-G-3′) dinucleotides (34). Non-CpG methylation is found in embryonic stem cells and non-dividing cells, such as neurons, and plays a role in regulating cell type-specific functions (35). CpG sites are highly concentrated in genomic regions called CpG islands, which are mainly located in promoter regions and are typically unmethylated. CpG sites outside of these islands are often methylated in mammals (36). DNMT3A and DNMT3B (DNA methyltransferase 3A and 3B) are responsible for *de novo* DNA methylation (37).

2.1.1 ROS and its role in the DNA methylation process

Oxidative stress (OS) is associated with excess reactive oxygen species (ROS) and a decrease in antioxidant enzymes (38). To ensure the quality of embryos and the outcome of pregnancy, gametes in the female reproductive tract are protected from environmental stress by tubal fluid during the pre-fertilization period. After shedding cumulus cells, the embryo depends on tubal fluid and internal antioxidant activities to gain protection against ROS-induced stress. All the external stimuli mentioned above may induce high ROS production in the ART setup (Figure 1). Excess ROS has been proposed to cause severe damage during embryonic development, and increasing evidence shows that the production of ROS is important for the development of the heart and the pathogenesis of cardiovascular disease (39, 40).

A theory of ROS induction has recently been proposed to explain the mechanisms underlying the establishment of DNA hypermethylation or hypomethylation (41–43). Elevated levels of ROS and DNA methylation have been observed in various types of cancer cells (43). ROS attack-induced hydroxylation of methylcytidine generates 5hmC, which disrupts the accurate transmission of genomic methylation patterns (44). ROS facilitate the hypermethylation of NDRG2 promoters in a manner that is dependent on DNMTs, key enzymes in DNA methylation (45). Moreover, ROS can induce site-specific hypermethylation by upregulating DNMTs or forming new DNMT-containing complexes (43). However, as ROS can affect numerous cellular processes, alternative mechanisms may contribute to DNA methylome alterations (46).

2.1.2 The relationship between imprinting abnormalities in ART offspring and CHD

Genomic imprinting is an epigenetic process that affects a specific set of mammalian genes, resulting in a monoallelic expression pattern that is inherited from one parent. To distinguish between parental alleles, imprinted genes are marked epigenetically in gametes at imprinting control elements using DNA methylation at the very least (47).

According to a recent study, ART causes abnormal expression of 1,060 genes in the mouse heart. The genes identified are mainly

10.3389/fcvm.2024.1287060

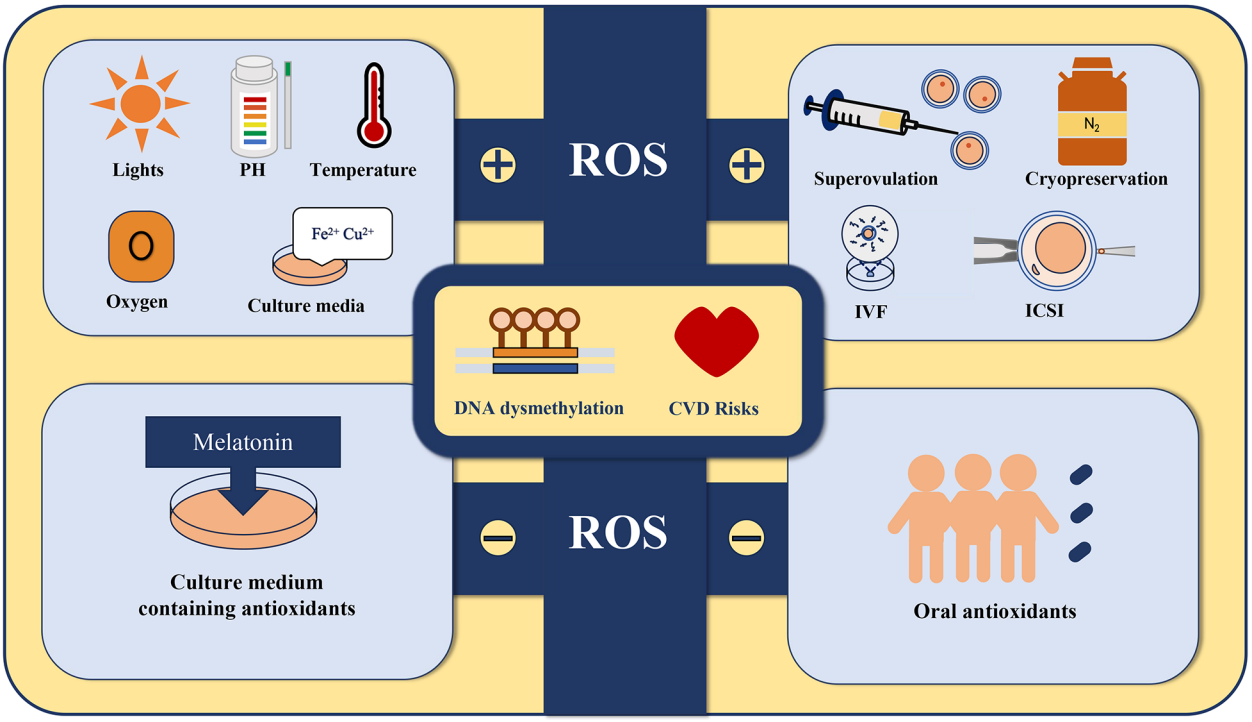

FIGURE 1
All the external stimuli including superovulation, cryopreservation (23, 24), exposure to various types of lights, fluctuations in pH and temperature, changes in oxygen tension, culture media that contain specific substances such as Fe2+ and Cu2+, and gamete or embryo manipulation may induce high ROS production in the ART setup. Adding antioxidants such as melatonin to the culture medium and administering antioxidant supplements to the offspring may protect their cardiovascular health by suppressing ROS production.

associated with RNA synthesis, processing, and the development of the cardiovascular system. The core interacting factors include Ccl2, Ptgs2, Rock1, Mapk14, Agt, and Wnt5a. Further investigation revealed that 42 epigenetic modifiers were abnormally expressed in the heart. In addition, in the hearts of ART offspring, the expression of imprinted genes Dhcr7, Igf2, Mest, and Smoc1 was found to be reduced, whereas the DNA methylation levels of the Igf2- and Mest-imprinting control regions (ICRs) were abnormally increased (19). Superovulation in adult mice has also been linked to alterations in Sgce and Zfp777 imprinted genes, whereas *in vitro* culture of follicles from the early pre-antral stage resulted in globally reduced methylation and heightened variability at imprinted loci in blastocysts (48).

Additionally, non-stimulated oocytes had lower methylation percentages in the imprinted genes APEG3, MEG3, and MEG9 and were higher in TSSC4 compared to stimulated oocytes in a bovine model. In terms of the CGI of imprinted genes, non-stimulated oocytes had higher methylation percentages of MEST (PEG1), IGF2R, GNAS (SCG6), KvDMR1, ICR, UMD, and IGF2. In another region around IGF2, non-stimulated oocytes had lower methylation percentages than stimulated oocytes (22).

Imprinting aberrations in SNRPN are involved in the pathogenesis of CHD (49). A study that followed children over time found who were conceived through ICSI had a higher incidence of SNRPN DMR hypermethylation. This occurrence remained stable even after the children reached seven years of age, indicating that these changes may persist over time (50). In addition to humans, oocyte vitrification can also result in the loss of Snrpn DNA methylation in mouse blastocysts. This loss of methylation is primarily caused by a reduction in DNMTs after oocyte vitrification (51).

It was reported that the skewed sex ratio is a result of developmental defects during the peri-implantation stage, which predominantly affect females. An imbalanced sex ratio, which serves as an indicator of reproductive hazards, has been reported in mouse (52), bovine (53), porcine (54) embryos as well as in newborns from human IVF procedures (55, 56). Male bias has been observed in both mammals and humans (52, 56). Given that women have a more favorable cardiovascular risk profile than men, particularly at younger ages (57), this sex bias may contribute to the increasing CVD risk following ART. Furthermore, these defects were reported to be caused by impaired imprinted X chromosome inactivation (iXCI) due to reduced expression of Rnf12/Xist in mice (52). Although humans do not undergo imprinted XCI like mice, they still exhibit a male bias in IVF. This suggests that impaired X chromosome inactivation may occur due to reasons other than imprinting in humans.

Although there is evidence of an increase in imprinting disorders in children conceived through IVF and ICSI, there is currently insufficient evidence to establish a link between ART

and the methylation of other imprinted genes. Further controlled studies using standardized methodologies in larger and more clinically defined populations are required to better understand the relationship between ART and the methylation of imprinted genes.

2.1.3 eNOS and Ang II: potential therapeutic targets

Vasculature from ART mice displayed endothelial dysfunction and increased stiffness, which could lead to arterial hypertension *in vivo*. The underlying mechanism was shown to be the decreased expression and function of endothelial eNOS, which is an isoform of nitric oxide synthase that is specific to endothelial cells (14). eNOS in endothelial cells (ECs) produces nitric oxide (NO), which contribute to the maintenance of proper vascular tone and systemic hemodynamics (58). Hypermethylation of the eNOS promoter can lead to decreased expression and function of endothelial eNOS, which can cause endothelial dysfunction and increased vascular stiffness in ART mice. This could lead to arterial hypertension *in vivo* (14). Moreover, addition of melatonin to culture media prevents the ART-induced eNOS dysmethylation and normalizes vascular dysfunction (59). Melatonin is known for its strong antioxidant activity, which helps scavenge free radicals, such as ROS (60). Using a culture medium containing antioxidants or vitrification and warming solutions supplemented with antioxidants has been shown to have a significant positive impact on the *in vitro* development of mouse preimplantation embryos, as well as on subsequent fetal development post-transfer (59, 61–63). In children with ART, the short-term use of oral antioxidants has also been found to have beneficial effects on vascular function (64).

The renin-angiotensin system (RAS) is a crucial physiological system that is responsible for regulating blood pressure and ensuring proper fluid and electrolyte balance within the body. In this system, angiotensin II (Ang II) is the primary effector hormone that acts as a systemic hormone and locally produced factor (65). Recent research discovered that ART-conceived mice showed an increased expression of myocardial AT1R, which encodes the type 1 receptor of Ang II, beginning at three weeks after birth. This increase was confirmed at 10 weeks and 1.5 years of age compared to the non-IVF group (66). Another study found that the vasoconstrictor response to ANG II was significantly higher in ART mice than that in non-ART mice. This increased response was associated with increased AT1R expression. The study also found that hypomethylation of two CpG sites located in the At1bR promoter led to increased gene transcription, further contributing to exaggerated vasoconstrictor responsiveness in ART mice (67). In human, a previous study reported that the IVF-ET group showed decreased mRNA expression of DNMT3A in the umbilical vein and hypomethylation of the AGTR1 gene, which codes for AT1R. These results indicate that IVF-ET treatments can alter Ang II-mediated vasoconstriction in umbilical veins, possibly due to increased expression of AT1R caused by dysmethylation (68).

2.2 Other epigenetic alternations in ART offspring

2.2.1 Histone modification

In addition to DNA methylation, histone modification is another crucial epigenetic mechanism. Trimethylation of lysine 4 (K4) and 27 (K27) of histone H3 (H3K4me3 and H3K27me3, respectively) is associated with gene activation and repression, respectively (69). Research studies have shown that histone lysine methylation plays a crucial role as an epigenetic regulator of heart development. Abnormalities during this process can lead to cardiac anomalies (32). According to the study by Maldonado et al. (70), the levels of H3K4me3 were approximately 20% lower, while the levels of H3K27me3 were higher in frozen-thawed bovine blastocysts compared to fresh embryos. Based on this hypothesis, the observed phenomenon was thought to be caused by cellular stress, particularly oxidative stress. To test this hypothesis, the blastocysts were placed under either normoxic (5%) or hyperoxic (20%) conditions and it was demonstrated that the levels of H3K4me2 and H3K9me2 were altered. Another study showed that the histone and chromatin status of mouse embryos was altered by *in vitro* culture rather than by prior vitrification and warming (71).

2.2.2 Micro RNA

Micro RNA (miRNA) are small non-coding RNA molecules approximately 22 bp in length. It can bind to the three prime untranslated region (3'UTR) of target mRNAs, causing cleavage or translational repression (72). They play a significant role in cardiac muscle proliferation and differentiation (73).

Dysregulated miRNA expression profiles have been observed in IVF-TE human placental tissues (74) and mouse embryos (75). Elevated levels of miR-100, miR-297, and miR-758 have been observed in the myocardial tissue of mice conceived through IVF compared to naturally bred mice of the same age (66), which might contribute to cardiovascular malformations by RAS. In addition, miR-1 (76), miR-206 (76) and miR-421 (77) might contribute to the pathology of tetralogy of Fallot (TOF), the most common type of cyanotic CHD. However, owing to limited research, the association between altered miRNAs in IVF offspring and CVD risk remains unclear.

3 Cardiovascular alterations induced by assisted reproductive technology

3.1 Alterations in cardiac structure and function

Cardiac remodelling and dysfunction have been reported in ART compared to spontaneously conceived fetuses (17, 78), which could persist in infants, children, and adolescents (15, 79, 80). A recent study found lower LV systolic function in ART subjects compared to spontaneously conceived peers. However, after adjusting for birth weight percentiles and gestational age,

M-mode-assessed LV systolic function showed no significant differences between the groups (21). Similarly, lower diastolic function in ART subjects was found in another study after adjusting for age, birth weight percentile, and gestational age (81), and there were no significant differences in LV diastolic function between the two groups.

CHD is the most prevalent type of birth defect and is characterized by congenital malformations of the heart walls, valves, and blood vessels (82). A large retrospective cohort study consisting of 507,390 patients reported a significant association between ART and CHD in general, without specifying the subtype. However, after assessing the mediation of twin pregnancies (which accounted for 87% of the total), the same correlation was found to be statistically insignificant (83). In a 2018 cohort study, an increased incidence of CHD (1.8% vs. 1%) was reported without specifying the subtype. Upon further analysis, it was found that the incidence of nonsevere CHD was higher in children conceived through ART (2.2%) compared to those conceived naturally (1%). However, when considering severe CHD, the incidence was comparable between ART and NC (1.4% and 1.2%, respectively) (84). Recently, a systematic review extracted twenty-four studies on the incidence of CHD in ART was conducted between January 2011 and May 2022 (20). It concluded that the incidence of CHDs among offspring conceived by IVF was 3% and decreased to 1% for major CHDs only. Compared to non-ART pregnancies, there appears to be an increased risk of CHDs in ART pregnancies, particularly minor cases that do not require surgical correction. However, evidence is insufficient to determine the actual risk of developing major CHDs. Additionally, certain confounding factors such as maternal age and male infertility may play a critical role in determining the increased risk of CHDs (85–87).

Owing to the conflicting results among studies, further research is needed to validate the evidence and accurately determine the risk of alterations in cardiac structure and function following ART pregnancies. More extensive research with larger sample sizes and extended follow-up periods is warranted.

3.2 Abnormal blood pressure

Increased arterial blood pressure was found in ART-conceived offspring (11, 88) compared to the control group. As mentioned previously, this could be a consequence of vascular dysfunction (88). Pulmonary hypertension in ART-conceived children has been reported under hypoxic and normoxic stress (13, 79, 89, 90), which may be attributed to decreased pulmonary vascular distensibility (89). A meta-analysis of over 35,000 mostly child offspring found that ART (compared to natural conception) resulted in similar blood pressure, heart rate, and glucose levels but higher cholesterol levels. Additionally, a long-term follow-up of 17,244 births (244 of which were ART) showed that children conceived through ART tended to have lower predicted systolic (SBP) and diastolic blood pressure (DBP) during childhood. However, as they entered young adulthood, there were slight indications of higher SBP and triglyceride levels. It's worth noting that most of these differences were not statistically significant (91).

Ovarian hyperstimulation syndrome (OHSS) is a significant and potentially dangerous complication of IVF. It is characterized by increased levels of estradiol in the bloodstream, enlargement of the ovaries with cysts, and a shift of fluid from the blood vessels to other areas of the body (92). According to a prior investigation, controlled ovarian hyperstimulation during IVF results in offspring with significantly higher SBP than those born through modified natural cycles (93). Accordingly, another study revealed that the systolic blood pressure SBP and DBP in children aged 3–6 years, who were conceived naturally, were significantly lower compared to the OHSS-ET group (94).

According to a meta-analysis conducted in 2017, a total of 19 studies were reviewed to better understand the health outcomes of children born through IVF-ICSI compared to those conceived naturally. These studies included 2,112 IVF-ICSI offspring and 4,096 naturally conceived offspring across various age groups from childhood to early adulthood. This study revealed that IVF-ICSI offspring had notably higher blood pressure levels than naturally conceived offspring. The weighted mean differences and confidence intervals were 1.88 mmHg [95% CI: 0.27, 3.49] for SBP and 1.51 mmHg [95% CI: 0.33, 2.70] for DBP, indicating a significant difference between the two groups (95).

Five animal studies reported varied results on the SBP/DBP and the mean blood pressures of the children at a specific time point between 9 and 52 weeks of age (14, 59, 67, 96, 97). Three studies conducted on 12–14-week-old male mice using telemetry (14, 59, 67) found that the mice conceived via IVF exhibited significantly higher mean fixed and continuous arterial pressures. Additionally, a study reported that female mice conceived through IVM had increased SBP levels at 1.5 years of age, but no significant increase was observed in male mice or those conceived through IVF or ICSI (97). More importantly, long-term exposure to high blood pressure can lead to structural abnormalities (98). Thus, differences in blood pressure are clinically important for early intervention of cardiac structure alterations in ART offspring.

3.3 Vascular dysfunction

A research team from Switzerland. paid significant attention to cardiovascular risks among ART offspring, both in humans (13, 88) and mice (14, 59). After assessing markers of early atherosclerosis in children (mean age, 11 years) who were conceived naturally and by ART (13), they found that carotid-femoral pulse-wave velocity (PWV), a proxy for elastic artery stiffness, was significantly faster in children who were conceived by ART than in control children. Defective flow-mediated dilation (FMD) of the brachial artery, which is related to endothelial dysfunction (99), and greater carotid intima-media thickness (cIMT) have also been found in children from ART. At the 5-year follow-up, the team reassessed the vascular function in these children (88). The alterations in FMD of the brachial artery, PWV, and cIMT were not only found to be persistent,

but may also have the potential to translate into arterial hypertension, which has been demonstrated in several studies in humans (11, 15, 88). Furthermore, greater cIMT was confirmed in a smaller cohort (100). In addition to humans, ART mice exhibit signs of endothelial dysfunction and increased stiffness (14, 59, 101), which can even be transmitted to their offspring by male ART mice (14).

Conversely, a recent study in humans showed no differences in early markers of atherosclerosis (cIMT and arterial stiffness) between ART and non-ART groups at ages 22–35 years (102, 103). The study focused on individuals in early adulthood and used noninvasive techniques to identify early markers of subclinical atherosclerosis. However, the researchers did not examine the links between these markers and clinical cardiovascular events. Another study also found no significant difference in vascular function between children, adolescents, and young adults conceived through assisted reproductive technology and their spontaneously conceived peers (104). However, given the limited sample size in this study (66 ART and 86 naturally conceived offspring), larger multi-center studies are necessary to gather clinical evidence.

Collectively, ART may interfere with early development and lead to premature vascular dysfunction in the offspring, potentially due to the variety of *in vitro* manipulations and cultures from gametes to embryos involved in the technology. However, the relationship between these techniques and early atherosclerotic disorders has not been clearly defined and requires further investigation.

3.4 Cardiovascular risk factors in ART populations

3.4.1 Perinatal complications

ART is often associated with adverse pregnancy outcomes, including fetal growth restriction, low birth weight, and preterm birth (PTB) (105), all of which are associated with higher CVD rates in adulthood (106–108). ART is also associated with an increased incidence of preeclampsia in mothers (109–111), which could have a negative effect on systemic and pulmonary vascular function of the offspring (12).

3.4.2 Altered metabolism in ART offspring

Metabolic syndromes in the progression of CVDs, such as obesity, diabetes, dyslipidemia, and impaired glucose metabolism, are known cardiovascular risk factors (112). ART offspring show altered glucose homeostasis and exacerbated obesity in mice and humans (97, 113). In a recent study, ART offspring in childhood were found having similar TG levels, but higher TC (HDLc and LDLc) levels compared to NC; however, these differences were not observed in young adulthood. In contrast, as age increased, those conceived by ART had higher TG and lower HDLc levels than NC, although the differences were small and not statistically significant by age 26 (114). Higher TG levels are known to increase future cardiovascular disease risk, which might suggest an increased risk in ART-conceived offspring (115). Moreover, elevated maternal estrogen levels after ovulation induction have been linked to higher total cholesterol and low-density lipoprotein cholesterol levels in newborns (116). In mice, ICSI or *in vitro* oocyte maturation (IVM) has a significant impact on the hepatic expression and methylation of INSIG-SCAP-SREBP from young to old age (97), and these alterations are involved in cardiometabolic changes (117, 118). Collectively, these metabolic disorders may serve as early indicators of CVD risk (106, 119).

3.4.3 Adverse intrauterine environment

The significance of the intrauterine environment cannot be overstated, as it serves as a mediator of the environment during vital developmental periods. Numerous studies have shown that an inadequate maternal diet (120), stress (121), and hormonal imbalances during pregnancy (122, 123) can affect the developmental programming of future generations. Women who undergo ART may face various challenges, including endocrine issues, advanced maternal age, chronic pelvic inflammation, and insulin resistance (124), all of which could contribute to cardiovascular dysfunction in the offspring. In addition, increased susceptibility to perinatal complications such as low birth weight and PTB during ART pregnancy may be partly due to a compromised intrauterine environment (95).

4 Conclusion and future perspectives

Although many studies have indicated a correlation between ART and an increased risk of CVDs among offspring, there is still conflicting evidence and no clear conclusion has been reached. Epigenetic alterations in ART populations have been reported in multiple studies, but the underlying mechanisms remain unclear. ROS could be one of the culprits for the high ROS production induced by external stimuli in the ART setup, and adding antioxidants to the culture media could mitigate the damage. Dysmethylation of AGTR1 and eNOS are shown to be associated with abnormal blood pressure levels. By applying the ROS inhibitor melatonin, the hypermethylation of eNOS can be effectively prevented. However, considering that ROS can affect numerous cellular processes, alternative mechanisms may contribute to epigenetic alterations. Moreover, considering the multifactorial nature of CVDs, adverse intrauterine environments, perinatal complications, and altered metabolism may play roles in the development of CVDs in ART offspring. Further research with larger, well-defined clinical ART populations and standardized methodologies is required, and more epigenetic experiments are needed to elucidate the potential mechanism of epigenetic inheritance in cardiovascular alterations in ART offspring. Overall, more attention should be paid to the CVD risks in offspring conceived through ART, which could not only contribute to the early diagnosis and prevention of CVD but also improve the safety and precision of ART.

Author contributions

LJ: Writing – review & editing, Funding acquisition. JL: Writing – original draft, Writing – review & editing. YL: Writing – original draft, Writing – review & editing. HH: Funding acquisition, Writing – review & editing.

Conflict of interest

The authors declare that the research was conducted in the absence of any commercial or financial relationships that could be construed as a potential conflict of interest.

Funding

The author(s) declare financial support was received for the research, authorship, and/or publication of this article.

This work is supported by the National Key R&D Program of China (2021YFC2700603, 2022YFC2702504), the National Natural Science Foundation of China (82088102), Collaborative Innovation Program of Shanghai Municipal Health Commission (2020CXJQ01).

Publisher's note

References

1. Sunderam S, Kissin DM, Zhang Y, Jewett A, Boulet SL, Warner L, et al. Assisted reproductive technology surveillance—United States, 2017. *MMWR Surveill Summ*. (2020) 69(9):1–20. doi: 10.15585/mmwr.ss6909a1

2. Yang X, Li Y, Li C, Zhang W. Current overview of pregnancy complications and live-birth outcome of assisted reproductive technology in mainland China. *Fertil Steril*. (2014) 101(2):385–91. doi: 10.1016/j.fertnstert.2013.10.017

3. Faddy MJ, Gosden MD, Gosden RG. A demographic projection of the contribution of assisted reproductive technologies to world population growth. *Reprod Biomed Online*. (2018) 36(4):455–8. doi: 10.1016/j.rbmo.2018.01.006

4. Sanchez-Garrido MA, Garcia-Galiano D, Tena-Sempere M. Early programming of reproductive health and fertility: novel neuroendocrine mechanisms and implications in reproductive medicine. *Hum Reprod Update*. (2022) 28(3):346–75. doi: 10.1093/humupd/dmac005

5. Barker DJ. The fetal origins of coronary heart disease. *Eur Heart J*. (1997) 18 (6):883–4. doi: 10.1093/oxfordjournals.eurheartj.a015368

6. Barker DJ. The origins of the developmental origins theory. *J Intern Med*. (2007) 261(5):412–7. doi: 10.1111/j.1365-2796.2007.01809.x

7. Chen B, Du YR, Zhu H, Sun ML, Wang C, Cheng Y, et al. Maternal inheritance of glucose intolerance via oocyte TET3 insufficiency. *Nature*. (2022) 605(7911):761–6. doi: 10.1038/s41586-022-04756-4

8. Yang G, Wang Y, Zeng Y, Gao GF, Liang X, Zhou M, et al. Rapid health transition in China, 1990–2010: findings from the global burden of disease study 2010. *Lancet*. (2013) 381(9882):1987–2015. doi: 10.1016/s0140-6736(13)61097-1

9. Zhou M, Wang H, Zhu J, Chen W, Wang L, Liu S, et al. Cause-specific mortality for 240 causes in China during 1990-2013: a systematic subnational analysis for the global burden of disease study 2013. *Lancet*. (2016) 387(10015):251–72. doi: 10.1016/s0140-6736(15)00551-6

10. Andersson C, Vasan RS. Epidemiology of cardiovascular disease in young individuals. *Nat Rev Cardiol*. (2018) 15(4):230–40. doi: 10.1038/nrcardio.2017.154

11. Ceelen M, van Weissenbruch MM, Vermeiden JP, van Leeuwen FE, Delemarre-van de Waal HA. Cardiometabolic differences in children born after in vitro fertilization: follow-up study. *J Clin Endocrinol Metab*. (2008) 93(5):1682–8. doi: 10.1210/jc.2007-2432

12. Jayet PY, Rimoldi SF, Stuber T, Salmòn CS, Hutter D, Rexhaj E, et al. Pulmonary and systemic vascular dysfunction in young offspring of mothers with preeclampsia. *Circulation*. (2010) 122(5):488–94. doi: 10.1161/circulationaha.110.941203

13. Scherrer U, Rimoldi SF, Rexhaj E, Stuber T, Duplain H, Garcin S, et al. Systemic and pulmonary vascular dysfunction in children conceived by assisted reproductive technologies. *Circulation*. (2012) 125(15):1890–6. doi: 10.1161/circulationaha.111.071183

14. Rexhaj E, Paoloni-Giacobino A, Rimoldi SF, Fuster DG, Anderegg M, Somm E, et al. Mice generated by in vitro fertilization exhibit vascular dysfunction and shortened life span. *J Clin Invest*. (2013) 123(12):5052–60. doi: 10.1172/JCI68943

15. Valenzuela-Alcaraz B, Crispi F, Bijnens B, Cruz-Lemini M, Creus M, Sitges M, et al. Assisted reproductive technologies are associated with cardiovascular remodeling in utero that persists postnatally. *Circulation*. (2013) 128(13):1442–50. doi: 10.1161/circulationaha.113.002428

16. Wang C, Lv H, Ling X, Li H, Diao F, Dai J, et al. Association of assisted reproductive technology, germline de novo mutations and congenital heart defects in a prospective birth cohort study. *Cell Res*. (2021) 31(8):919–28. doi: 10.1038/s41422-021-00521-w

17. Bi W, Xiao Y, Wang X, Cui L, Song G, Yang Z, et al. The association between assisted reproductive technology and cardiac remodeling in fetuses and early infants: a prospective cohort study. *BMC Med*. (2022) 20(1):104. doi: 10.1186/s12916-022-02303-6

18. Mizrak I, Asserhoj LL, Lund MAV, Kielstrup LR, Greisen G, Clausen TD, et al. Cardiovascular function in 8- to 9-year-old singletons born after ART with frozen and fresh embryo transfer. *Hum Reprod*. (2022) 37(3):600–11. doi: 10.1093/humrep/deab284

19. Chen H, Zhang L, Yue F, Cui C, Li Y, Zhang Q, et al. Effects of assisted reproductive technology on gene expression in heart and spleen tissues of adult offspring mouse. *Front Endocrinol (Lausanne)*. (2023) 14:1035161. doi: 10.3389/fendo.2023.1035161

20. Gullo G, Scaglione M, Lagana AS, Perino A, Andrisani A, Chiantera V, et al. Assisted reproductive techniques and risk of congenital heart diseases in children: a systematic review and meta-analysis. *Reprod Sci*. (2023). 30(10):2896–906. doi: 10.1007/s43032-023-01252-6

21. Sciuk F, Vilsmaier T, Kramer M, Langer M, Kolbinger B, Li P, et al. Left ventricular systolic function in subjects conceived through assisted reproductive technologies. *Front Cardiovasc Med*. (2023) 10:1059713. doi: 10.3389/fcvm.2023.1059713

22. Lopes JS, Ivanova E, Ruiz S, Andrews S, Kelsey G, Coy P. Effect of superovulation treatment on oocyte's DNA methylation. *Int J Mol Sci*. (2022) 23 (24):16158. doi: 10.3390/ijms232416158

23. Zribi N, Feki Chakroun N, El Euch H, Gargouri J, Bahloul A, Ammar Keskes L. Effects of cryopreservation on human sperm deoxyribonucleic acid integrity. *Fertil Steril*. (2010) 93(1):159–66. doi: 10.1016/j.fertnstert.2008.09.038

24. Zhang Z, Mu Y, Ding D, Zou W, Li X, Chen B, et al. Melatonin improves the effect of cryopreservation on human oocytes by suppressing oxidative stress and maintaining the permeability of the oolemma. *J Pineal Res*. (2021) 70(2):e12707. doi: 10.1111/jpi.12707

25. Khodavirdilou R, Pournaghi M, Oghbaei H, Rastgar Rezaei Y, Javid F, Khodavirdilou L, et al. Toxic effect of light on oocyte and pre-implantation embryo: a systematic review. *Arch Toxicol*. (2021) 95(10):3161–9. doi: 10.1007/s00204-021-03139-4

26. Larkindale J, Knight MR. Protection against heat stress-induced oxidative damage in Arabidopsis involves calcium, abscisic acid, ethylene, and salicylic acid. *Plant Physiol*. (2002) 128(2):682–95. doi: 10.1104/pp.010320

27. Will MA, Clark NA, Swain JE. Biological pH buffers in IVF: help or hindrance to success. *J Assist Reprod Genet*. (2011) 28(8):711–24. doi: 10.1007/s10815-011-9582-0

28. Bontekoe S, Mantikou E, van Wely M, Seshadri S, Repping S, Mastenbroek S. Low oxygen concentrations for embryo culture in assisted reproductive technologies. *Cochrane Database Syst Rev*. (2012) (7):Cd008950. doi: 10.1002/14651858.CD008950.pub2

29. Guérin P, El Mouatassim S, Ménézo Y. Oxidative stress and protection against reactive oxygen species in the pre-implantation embryo and its surroundings. *Hum Reprod Update*. (2001) 7(2):175–89. doi: 10.1093/humupd/7.2.175

30. Monk D, Mackay DJG, Eggermann T, Maher ER, Riccio A. Genomic imprinting disorders: lessons on how genome, epigenome and environment interact. *Nat Rev Genet*. (2019) 20(4):235–48. doi: 10.1038/s41576-018-0092-0

31. Bird A. Perceptions of epigenetics. *Nature*. (2007) 447(7143):396–8. doi: 10.1038/nature05913

32. Wang G, Wang B, Yang P. Epigenetics in congenital heart disease. *J Am Heart Assoc*. (2022) 11(7):e025163. doi: 10.1161/JAHA.121.025163

33. Millership SJ, Van de Pette M, Withers DJ. Genomic imprinting and its effects on postnatal growth and adult metabolism. *Cell Mol Life Sci*. (2019) 76(20):4009–21. doi: 10.1007/s00018-019-03197-z

34. Lister R, Pelizzola M, Dowen RH, Hawkins RD, Hon G, Tonti-Filippini J, et al. Human DNA methylomes at base resolution show widespread epigenomic differences. *Nature*. (2009) 462(7271):315–22. doi: 10.1038/nature08514

35. Lee JH, Park SJ, Nakai K. Differential landscape of non-CpG methylation in embryonic stem cells and neurons caused by DNMT3s. *Sci Rep*. (2017) 7(1):11295. doi: 10.1038/s41598-017-11800-1

36. Bird A, Taggart M, Frommer M, Miller OJ, Macleod D. A fraction of the mouse genome that is derived from islands of nonmethylated, CpG-rich DNA. *Cell*. (1985) 40 (1):91–9. doi: 10.1016/0092-8674(85)90312-5

37. Reik W, Dean W, Walter J. Epigenetic reprogramming in mammalian development. *Science*. (2001) 293(5532):1089–93. doi: 10.1126/science.1063443

38. Agarwal A, Maldonado Rosas I, Anagnostopoulou C, Cannarella R, Boitrelle F, Munoz LV, et al. Oxidative stress and assisted reproduction: a comprehensive review of its pathophysiological role and strategies for optimizing embryo culture environment. *Antioxidants (Basel)*. (2022) 11(3):477. doi: 10.3390/antiox11030477

39. Panth N, Paudel KR, Parajuli K. Reactive oxygen Species: a key hallmark of cardiovascular disease. *Adv Med*. (2016) 2016:9152732. doi: 10.1155/2016/9152732

40. Liang J, Wu M, Chen C, Mai M, Huang J, Zhu P. Roles of reactive oxygen species in cardiac differentiation, reprogramming, and regenerative therapies. *Oxid Med Cell Longev*. (2020) 2020:2102841. doi: 10.1155/2020/2102841

41. Campos AC, Molognoni F, Melo FH, Galdieri LC, Carneiro CR, D'Almeida V, et al. Oxidative stress modulates DNA methylation during melanocyte anchorage blockade associated with malignant transformation. *Neoplasia*. (2007) 9 (12):1111–21. doi: 10.1593/neo.07712

42. Ziech D, Franco R, Pappa A, Panayiotidis MI. Reactive oxygen species (ROS)–induced genetic and epigenetic alterations in human carcinogenesis. *Mutat Res*. (2011) 711(1-2):167–73. doi: 10.1016/j.mrfmmm.2011.02.015

43. Wu Q, Ni X. ROS-mediated DNA methylation pattern alterations in carcinogenesis. *Curr Drug Targets*. (2015) 16(1):13–9. doi: 10.2174/1389450116666150113121054

44. Valinluck V, Sowers LC. Endogenous cytosine damage products alter the site selectivity of human DNA maintenance methyltransferase DNMT1. *Cancer Res*. (2007) 67(3):946–50. doi: 10.1158/0008-5472.Can-06-3123

45. Zhao Y, Fan X, Wang Q, Zhen J, Li X, Zhou P, et al. ROS promote hypermethylation of NDRG2 promoters in a DNMTS-dependent manner: contributes to the progression of renal fibrosis. *Redox Biol*. (2023) 62:102674. doi: 10.1016/j.redox.2023.102674

46. Khosravizadeh Z, Khodamoradi K, Rashidi Z, Jahromi M, Shiri E, Salehi E, et al. Sperm cryopreservation and DNA methylation: possible implications for ART success and the health of offspring. *J Assist Reprod Genet*. (2022) 39(8):1815–24. doi: 10.1007/s10815-022-02545-6

47. Barlow DP, Bartolomei MS. Genomic imprinting in mammals. *Cold Spring Harb Perspect Biol*. (2014) 6:2. doi: 10.1101/cshperspect.a018382

48. Saucedo-Cuevas L, Ivanova E, Herta AC, Krueger F, Billooye K, Smitz J, et al. Genome-wide assessment of DNA methylation alterations induced by superovulation, sexual immaturity and in vitro follicle growth in mouse blastocysts. *Clin Epigenetics*. (2023) 15(1):9. doi: 10.1186/s13148-023-01421-z

49. Zhao X, Chang S, Liu X, Wang S, Zhang Y, Lu X, et al. Imprinting aberrations of SNRPN, ZAC1 and INPP5F genes involved in the pathogenesis of congenital heart disease with extracardiac malformations. *J Cell Mol Med*. (2020) 24(17):9898–907. doi: 10.1111/jcmm.15584

50. Whitelaw N, Bhattacharya S, Hoad G, Horgan GW, Hamilton M, Haggarty P. Epigenetic status in the offspring of spontaneous and assisted conception. *Hum Reprod*. (2014) 29(7):1452–8. doi: 10.1093/humrep/deu094

51. Cheng KR, Fu XW, Zhang RN, Jia GX, Hou YP, Zhu SE. Effect of oocyte vitrification on deoxyribonucleic acid methylation of H19, Peg3, and snrpn differentially methylated regions in mouse blastocysts. *Fertil Steril*. (2014) 102 (4):1183–90.e1183. doi: 10.1016/j.fertnstert.2014.06.037

52. Tan K, An L, Miao K, Ren L, Hou Z, Tao L, et al. Impaired imprinted X chromosome inactivation is responsible for the skewed sex ratio following in vitro fertilization. *Proc Natl Acad Sci U S A*. (2016) 113(12):3197–202. doi: 10.1073/pnas.1523538113

53. Wrenzycki C, Lucas-Hahn A, Herrmann D, Lemme E, Korsawe K, Niemann H. In vitro production and nuclear transfer affect dosage compensation of the X-linked gene transcripts G6PD, PGK, and Xist in preimplantation bovine embryos. *Biol Reprod*. (2002) 66(1):127–34. doi: 10.1095/biolreprod66.1.127

54. Torner E, Bussalleu E, Briz MD, Yeste M, Bonet S. Embryo development and sex ratio of in vitro-produced porcine embryos are affected by the energy substrate and hyaluronic acid added to the culture medium. *Reprod Fertil Dev*. (2014) 26 (4):570–7. doi: 10.1071/rd13004

55. Dean JH, Chapman MG, Sullivan EA. The effect on human sex ratio at birth by assisted reproductive technology (ART) procedures–an assessment of babies born following single embryo transfers, Australia and New Zealand, 2002–2006. *Bjog*. (2010) 117(13):1628–34. doi: 10.1111/j.1471-0528.2010.02731.x

56. Maalouf WE, Mincheva MN, Campbell BK, Hardy IC. Effects of assisted reproductive technologies on human sex ratio at birth. *Fertil Steril*. (2014) 101 (5):1321–5. doi: 10.1016/j.fertnstert.2014.01.041

57. Walli-Attaei M, Rosengren A, Rangarajan S, Breet Y, Abdul-Razak S, Sharief WA, et al. Metabolic, behavioural, and psychosocial risk factors and cardiovascular disease in women compared with men in 21 high-income, middle-income, and low-income countries: an analysis of the PURE study. *Lancet*. (2022) 400 (10355):811–21. doi: 10.1016/s0140-6736(22)01441-6

58. Farah C, Michel LYM, Balligand JL. Nitric oxide signalling in cardiovascular health and disease. *Nat Rev Cardiol*. (2018) 15(5):292–316. doi: 10.1038/nrcardio.2017.224

59. Rexhaj E, Pireva A, Paoloni-Giacobino A, Allemann Y, Cerny D, Dessen P, et al. Prevention of vascular dysfunction and arterial hypertension in mice generated by assisted reproductive technologies by addition of melatonin to culture media. *Am J Physiol Heart Circ Physiol*. (2015) 309(7):H1151–56. doi: 10.1152/ajpheart.00621.2014

60. Tamura H, Jozaki M, Tanabe M, Shirafuta Y, Mihara Y, Shinagawa M, et al. Importance of melatonin in assisted reproductive technology and ovarian aging. *Int J Mol Sci*. (2020) 21(3):1135. doi: 10.3390/ijms21031135

61. Truong TT, Soh YM, Gardner DK. Antioxidants improve mouse preimplantation embryo development and viability. *Hum Reprod*. (2016) 31 (7):1445–54. doi: 10.1093/humrep/dew098

62. Truong T, Gardner DK. Antioxidants improve IVF outcome and subsequent embryo development in the mouse. *Hum Reprod*. (2017) 32(12):2404–13. doi: 10.1093/humrep/dex330

63. Truong TT, Gardner DK. Antioxidants increase blastocyst cryosurvival and viability post-vitrification. *Hum Reprod*. (2020) 35(1):12–23. doi: 10.1093/humrep/dez243

64. Rimoldi SF, Sartori C, Rexhaj E, Bailey DM, de Marchi SF, McEneny J, et al. Antioxidants improve vascular function in children conceived by assisted reproductive technologies: a randomized double-blind placebo-controlled trial. *Eur J Prev Cardiol*. (2015) 22(11):1399–407. doi: 10.1177/2047487314535117

65. van Thiel BS, van der Pluijm I, te Riet L, Essers J, Danser AH. The renin-angiotensin system and its involvement in vascular disease. *Eur J Pharmacol*. (2015) 763(Pt A):3–14. doi: 10.1016/j.ejphar.2015.03.090

66. Wang Q, Zhang Y, Le F, Wang N, Zhang F, Luo Y, et al. Alteration in the expression of the renin-angiotensin system in the myocardium of mice conceived by in vitro fertilization. *Biol Reprod*. (2018) 99(6):1276–88. doi: 10.1093/biolre/ioy158

67. Meister TA, Soria R, Dogar A, Messerli FH, Paoloni-Giacobino A, Stenz L, et al. Increased arterial responsiveness to angiotensin II in mice conceived by assisted reproductive technologies. *Int J Mol Sci*. (2022) 23(21):13357. doi: 10.3390/ijms232113357

68. Zhang M, Lu L, Zhang Y, Li X, Fan X, Chen X, et al. Methylation-reprogrammed AGTR1 results in increased vasoconstriction by angiotensin II in human umbilical cord vessel following in vitro fertilization-embryo transfer. *Life Sci*. (2019) 234:116792. doi: 10.1016/j.lfs.2019.116792

69. Jiang Z, Wang Y, Lin J, Xu J, Ding G, Huang H. Genetic and epigenetic risks of assisted reproduction. *Best Pract Res Clin Obstet Gynaecol*. (2017) 44:90–104. doi: 10.1016/j.bpobgyn.2017.07.004

70. Maldonado MB, Penteado JC, Faccio BM, Lopes FL, Arnold DR. Changes in trimethylation profile of lysines 4 and 27 of histone H3 in bovine blastocysts after cryopreservation. *Cryobiology*. (2015) 71(3):481–5. doi: 10.1016/j.cryobiol.2015.09.001

71. Jahangiri M, Shahhoseini M, Movaghar B. H19 and MEST gene expression and histone modification in blastocysts cultured from vitrified and fresh two-cell mouse embryos. *Reprod Biomed Online*. (2014) 29(5):559–66. doi: 10.1016/j.rbmo.2014.07.006

72. Bartel DP. MicroRNAs: genomics, biogenesis, mechanism, and function. *Cell*. (2004) 116(2):281–97. doi: 10.1016/s0092-8674(04)00045-5

73. Chen JF, Mandel EM, Thomson JM, Wu Q, Callis TE, Hammond SM, et al. The role of microRNA-1 and microRNA-133 in skeletal muscle proliferation and differentiation. *Nat Genet*. (2006) 38(2):228–33. doi: 10.1038/ng1725

74. Yang S, Zheng W, Yang C, Zu R, Ran S, Wu H, et al. Integrated analysis of hub genes and MicroRNAs in human placental tissues from in vitro fertilization-embryo transfer. *Front Endocrinol (Lausanne)*. (2021) 12:774997. doi: 10.3389/fendo.2021.774997

75. Tan K, Wang X, Zhang Z, Miao K, Yu Y, An L, et al. Downregulation of miR-199a-5p disrupts the developmental potential of in vitro-fertilized mouse blastocysts. *Biol Reprod*. (2016) 95(3):54. doi: 10.1095/biolreprod.116.141051

76. Wu Y, Ma XJ, Wang HJ, Li WC, Chen L, Ma D, et al. Expression of Cx43-related microRNAs in patients with tetralogy of fallot. *World J Pediatr*. (2014) 10(2):138–44. doi: 10.1007/s12519-013-0434-0

77. Bittel DC, Kibiryeva N, Marshall JA, O'Brien JE. MicroRNA-421 dysregulation is associated with tetralogy of Fallot. *Cells*. (2014) 3(3):713–23. doi: 10.3390/cells3030713

78. Rizzo G, Pietrolucci ME, Mappa I, Bitsadze V, Khizroeva J, Makatsariya A, et al. Fetal cardiac remodeling is affected by the type of embryo transfer in pregnancies conceived by in vitro fertilization: a prospective cohort study. *Fetal Diagn Ther*. (2020) 47(10):772–8. doi: 10.1159/000508987

79. von Arx R, Allemann Y, Sartori C, Rexhaj E, Cerny D, de Marchi SF, et al. Right ventricular dysfunction in children and adolescents conceived by assisted reproductive technologies. *J Appl Physiol (1985)*. (2015) 118(10):1200–6. doi: 10.1152/japplphysiol.00533.2014

80. Cui L, Zhao M, Zhang Z, Zhou W, Lv J, Hu J, et al. Assessment of cardiovascular health of children ages 6–10 years conceived by assisted reproductive technology. *JAMA Netw Open*. (2021) 4(11):e2132602. doi: 10.1001/jamanetworkopen.2021.32602

81. Sciuk F, Vilsmaier T, Kramer M, Langer M, Kolbinger B, Li P, et al. Left ventricular diastolic function in subjects conceived through assisted reproductive technologies. *J Clin Med*. (2022) 11(23):7128. doi: 10.3390/jcm11237128

82. Mitchell SC, Korones SB, Berendes HW. Congenital heart disease in 56,109 births. Incidence and natural history. *Circulation*. (1971) 43(3):323–32. doi: 10.1161/01.cir.43.3.323

83. Wen SW, Miao Q, Taljaard M, Lougheed J, Gaudet L, Davies M, et al. Associations of assisted reproductive technology and twin pregnancy with risk of congenital heart defects. *JAMA Pediatr*. (2020) 174(5):446–54. doi: 10.1001/jamapediatrics.2019.6096

84. Patil AS, Nguyen C, Groff K, Wu J, Elliott J, Gunatilake RP. Severity of congenital heart defects associated with assisted reproductive technologies: case series and review of the literature. *Birth Defects Res*. (2018) 110(8):654–61. doi: 10.1002/bdr2.1228

85. Jwa SC, Jwa J, Kuwahara A, Irahara M, Ishihara O, Saito H. Male subfertility and the risk of major birth defects in children born after in vitro fertilization and intracytoplasmic sperm injection: a retrospective cohort study. *BMC Pregnancy Childbirth*. (2019) 19(1):192. doi: 10.1186/s12884-019-2322-7

86. Zhang L, Zhang W, Xu H, Liu K. Birth defects surveillance after assisted reproductive technology in Beijing: a whole of population-based cohort study. *BMJ Open*. (2021) 11(6):e044385. doi: 10.1136/bmjopen-2020-044385

87. Morimoto Y, Go K, Yamamoto H, Fukasawa Y, Nakai M, Morihana E, et al. Conception by assisted reproductive technology in infants with critical congenital heart disease in Japan. *Reprod Biomed Online*. (2022) 44(1):163–70. doi: 10.1016/j.rbmo.2021.10.005

88. Meister TA, Rimoldi SF, Soria R, von Arx R, Messerli FH, Sartori C, et al. Association of assisted reproductive technologies with arterial hypertension during adolescence. *J Am Coll Cardiol*. (2018) 72(11):1267–74. doi: 10.1016/j.jacc.2018.06.060

89. Forton K, Motoji Y, Pezzuto B, Caravita S, Delbaere A, Naeije R, et al. Decreased pulmonary vascular distensibility in adolescents conceived by in vitro fertilization. *Hum Reprod*. (2019) 34(9):1799–808. doi: 10.1093/humrep/dez113

90. Alipour MR, Pezeshkpour Z, Namayandeh SM, Sarebanhassanabadi M. Pulmonary arterial pressure in at-term in vitro fertilization neonates: a cross-sectional study. *Turk J Obstet Gynecol*. (2020) 17(2):79–83. doi: 10.4274/tjod.galenos.2020.74152

91. Elhakeem A, Taylor AE, Inskip HM, Huang JY, Mansell T, Rodrigues C, et al. Long-term cardiometabolic health in people born after assisted reproductive technology: a multi-cohort analysis. *Eur Heart J*. (2023) 44(16):1464–73. doi: 10.1093/eurheartj/ehac726

92. Nastri CO, Ferriani RA, Rocha IA, Martins WP. Ovarian hyperstimulation syndrome: pathophysiology and prevention. *J Assist Reprod Genet*. (2010) 27(2-3):121–8. doi: 10.1007/s10815-010-9387-6

93. Seggers J, Haadsma ML, La Bastide-Van Gemert S, Heineman MJ, Middelburg KJ, Roseboom TJ, et al. Is ovarian hyperstimulation associated with higher blood pressure in 4-year-old IVF offspring? Part I: multivariable regression analysis. *Hum Reprod*. (2014) 29(3):502–9. doi: 10.1093/humrep/det396

94. Zhu Y, Fu Y, Tang M, Yan H, Zhang F, Hu X, et al. Risk of higher blood pressure in 3–6 years old singleton born from OHSS patients undergone with fresh IVF/ICSI. *Front Endocrinol (Lausanne)*. (2022) 13:817555. doi: 10.3389/fendo.2022.817555

95. Guo XY, Liu XM, Jin L, Wang TT, Ullah K, Sheng JZ, et al. Cardiovascular and metabolic profiles of offspring conceived by assisted reproductive technologies: a systematic review and meta-analysis. *Fertil Steril*. (2017) 107(3):622–31.e625. doi: 10.1016/j.fertnstert.2016.12.007

96. Fernández-Gonzalez R, Moreira PN, Pérez-Crespo M, Sánchez-Martín M, Ramirez MA, Pericuesta E, et al. Long-term effects of mouse intracytoplasmic sperm injection with DNA-fragmented sperm on health and behavior of adult offspring. *Biol Reprod*. (2008) 78(4):761–72. doi: 10.1095/biolreprod.107.065623

97. Le F, Lou HY, Wang QJ, Wang N, Wang LY, Li LJ, et al. Increased hepatic INSIG-SCAP-SREBP expression is associated with cholesterol metabolism disorder in assisted reproductive technology-conceived aged mice. *Reprod Toxicol*. (2019) 84:9–17. doi: 10.1016/j.reprotox.2018.12.003

98. Santos M, Shah AM. Alterations in cardiac structure and function in hypertension. *Curr Hypertens Rep*. (2014) 16(5):428. doi: 10.1007/s11906-014-0428-x

99. Charakida M, Masi S, Lüscher TF, Kastelein JJ, Deanfield JE. Assessment of atherosclerosis: the role of flow-mediated dilatation. *Eur Heart J*. (2010) 31(23):2854–61. doi: 10.1093/eurheartj/ehq340

100. Zhang WY, Selamet Tierney ES, Chen AC, Ling AY, Fleischmann RR, Baker VL. Vascular health of children conceived via in vitro fertilization. *J Pediatr*. (2019) 214:47–53. doi: 10.1016/j.jpeds.2019.07.033

101. Rexhaj E, Bloch J, Jayet PY, Rimoldi SF, Dessen P, Mathieu C, et al. Fetal programming of pulmonary vascular dysfunction in mice: role of epigenetic mechanisms. *Am J Physiol Heart Circ Physiol*. (2011) 301(1):H247–52. doi: 10.1152/ajpheart.01309.2010

102. Halliday J, Lewis S, Kennedy J, Burgner DP, Juonala M, Hammarberg K, et al. Health of adults aged 22–35 years conceived by assisted reproductive technology. *Fertil Steril*. (2019) 112(1):130–9. doi: 10.1016/j.fertnstert.2019.03.001

103. Juonala M, Lewis S, McLachlan R, Hammarberg K, Kennedy J, Saffery R, et al. American heart association ideal cardiovascular health score and subclinical atherosclerosis in 22–35-year-old adults conceived with and without assisted reproductive technologies. *Hum Reprod*. (2020) 35(1):232–9. doi: 10.1093/humrep/dez240

104. Oberhoffer FS, Langer M, Li P, Vilsmaier T, Sciuk F, Kramer M, et al. Vascular function in a cohort of children, adolescents and young adults conceived through assisted reproductive technologies-results from the Munich heARTerY-study. *Transl Pediatr*. (2023) 12(9):1619–33. doi: 10.21037/tp-23-67

105. Pandey S, Shetty A, Hamilton M, Bhattacharya S, Maheshwari A. Obstetric and perinatal outcomes in singleton pregnancies resulting from IVF/ICSI: a systematic review and meta-analysis. *Hum Reprod Update*. (2012) 18(5):485–503. doi: 10.1093/humupd/dms018

106. Mercuro G, Bassareo PP, Flore G, Fanos V, Dentamaro I, Scicchitano P, et al. Prematurity and low weight at birth as new conditions predisposing to an increased cardiovascular risk. *Eur J Prev Cardiol*. (2013) 20(2):357–67. doi: 10.1177/2047487312437058

107. Dodson RB, Miller TA, Powers K, Yang Y, Yu B, Albertine KH, et al. Intrauterine growth restriction influences vascular remodeling and stiffening in the weanling rat more than sex or diet. *Am J Physiol Heart Circ Physiol*. (2017) 312(2):H250–64. doi: 10.1152/ajpheart.00610.2016

108. Bavineni M, Wassenaar TM, Agnihotri K, Ussery DW, Lüscher TF, Mehta JL. Mechanisms linking preterm birth to onset of cardiovascular disease later in adulthood. *Eur Heart J*. (2019) 40(14):1107–12. doi: 10.1093/eurheartj/ehz025

109. Almasi-Hashiani A, Omani-Samani R, Mohammadi M, Amini P, Navid B, Alizadeh A, et al. Assisted reproductive technology and the risk of preeclampsia: an updated systematic review and meta-analysis. *BMC Pregnancy Childbirth*. (2019) 19(1):149. doi: 10.1186/s12884-019-2291-x

110. Chih HJ, Elias FTS, Gaudet L, Velez MP. Assisted reproductive technology and hypertensive disorders of pregnancy: systematic review and meta-analyses. *BMC Pregnancy Childbirth*. (2021) 21(1):449. doi: 10.1186/s12884-021-03938-8

111. Manna C, Lacconi V, Rizzo G, De Lorenzo A, Massimiani M. Placental dysfunction in assisted reproductive pregnancies: perinatal, neonatal and adult life outcomes. *Int J Mol Sci*. (2022) 23(2):659. doi: 10.3390/ijms23020659

112. Silveira Rossi JL, Barbalho SM, Reverete de Araujo R, Bechara MD, Sloan KP, Sloan LA. Metabolic syndrome and cardiovascular diseases: going beyond traditional risk factors. *Diabetes Metab Res Rev*. (2022) 38(3):e3502. doi: 10.1002/dmrr.3502

113. Cerny D, Sartori C, Rimoldi SF, Meister T, Soria R, Bouillet E, et al. Assisted reproductive technologies predispose to insulin resistance and obesity in male mice challenged with a high-fat diet. *Endocrinology*. (2017) 158(5):1152–9. doi: 10.1210/en.2016-1475

114. Bo L, Wei L, Shi L, Luo C, Gao S, Zhou A, et al. Altered local RAS in the liver increased the risk of NAFLD in male mouse offspring produced by in vitro fertilization. *BMC Pregnancy Childbirth*. (2023) 23(1):345. doi: 10.1186/s12884-023-05681-8

115. Holmes MV, Asselbergs FW, Palmer TM, Drenos F, Lanktree MB, Nelson CP, et al. Mendelian randomization of blood lipids for coronary heart disease. *Eur Heart J*. (2015) 36(9):539–50. doi: 10.1093/eurheartj/eht571

116. Meng Y, Lv PP, Ding GL, Yu TT, Liu Y, Shen Y, et al. High maternal serum estradiol levels induce dyslipidemia in human newborns via a hepatic HMGCR estrogen response element. *Sci Rep*. (2015) 5:10086. doi: 10.1038/srep10086

117. Brown MS, Goldstein JL. The SREBP pathway: regulation of cholesterol metabolism by proteolysis of a membrane-bound transcription factor. *Cell*. (1997) 89(3):331–40. doi: 10.1016/s0092-8674(00)80213-5

118. Engelking LJ, Kuriyama H, Hammer RE, Horton JD, Brown MS, Goldstein JL, et al. Overexpression of insig-1 in the livers of transgenic mice inhibits SREBP processing and reduces insulin-stimulated lipogenesis. *J Clin Invest*. (2004) 113(8):1168–75. doi: 10.1172/jci20978

119. Barker DJ, Osmond C, Forsén TJ, Kajantie E, Eriksson JG. Trajectories of growth among children who have coronary events as adults. *N Engl J Med*. (2005) 353(17):1802–9. doi: 10.1056/NEJMoa044160

120. Wang Y, Wang K, Du M, Khandpur N, Rossato SL, Lo CH, et al. Maternal consumption of ultra-processed foods and subsequent risk of offspring overweight or obesity: results from three prospective cohort studies. *Br Med J*. (2022) 379: e071767. doi: 10.1136/bmj-2022-071767

121. Gu J, Guan HB. Maternal psychological stress during pregnancy and risk of congenital heart disease in offspring: a systematic review and meta-analysis. *J Affect Disord*. (2021) 291:32–8. doi: 10.1016/j.jad.2021.05.002

122. Risal S, Pei Y, Lu H, Manti M, Fornes R, Pui HP, et al. Prenatal androgen exposure and transgenerational susceptibility to polycystic ovary syndrome. *Nat Med*. (2019) 25(12):1894–904. doi: 10.1038/s41591-019-0666-1

123. Risal S, Li C, Luo Q, Fornes R, Lu H, Eriksson G, et al. Transgenerational transmission of reproductive and metabolic dysfunction in the male progeny of polycystic ovary syndrome. *Cell Rep Med*. (2023) 4(5):101035. doi: 10.1016/j.xcrm.2023.101035

124. Hart RJ. Physiological aspects of female fertility: role of the environment, modern lifestyle, and genetics. *Physiol Rev*. (2016) 96(3):873–909. doi: 10.1152/physrev.00023.2015

frontiers | Frontiers in Pediatrics

TYPE Original Research
PUBLISHED 07 February 2024
DOI 10.3389/fped.2024.1346006

OPEN ACCESS

EDITED BY
Liqun Sun,
University of Toronto, Canada

REVIEWED BY
Bo Zhang,
Shanghai Jiao Tong University, China
Xikun Han,
Massachusetts Institute of Technology, United States
Wei Lv,
University of Chinese Academy of Sciences, China

*CORRESPONDENCE
Guoying Huang
✉ gyhuang@shmu.edu.cn

RECEIVED 28 November 2023
ACCEPTED 22 January 2024
PUBLISHED 07 February 2024

CITATION
Mu K, Zhang J, Gu Y and Huang G (2024) Development and validation of a nomogram for predicting cardiovascular mortality risk for diffuse large B-cell lymphoma in children, adolescents, and adults.
Front. Pediatr. 12:1346006.
doi: 10.3389/fped.2024.1346006

Development and validation of a nomogram for predicting cardiovascular mortality risk for diffuse large B-cell lymphoma in children, adolescents, and adults

Kai Mu[1,2], Jing Zhang[2], Yan Gu[2] and Guoying Huang[1]*

[1]Pediatric Heart Center, Children's Hospital of Fudan University, Shanghai, China, [2]Department of Pediatric, The First Affiliated Hospital of Shandong First Medical University, Jinan, China

Objective: This study aimed to construct and validate a nomogram for predicting cardiovascular mortality (CVM) for child, adolescent, and adult patients with diffuse large B-cell lymphoma (DLBCL).

Materials and methods: Patients with only one primary tumor of DLBCL first diagnosed between 2000 and 2019 in the SEER database were extracted. We used the cumulative incidence function (CIF) to evaluate the cumulative rate of CVM. The outcome of interest was CVM, which was analyzed using a competing risk model, accounting for death due to other causes. The total database was randomly divided into a training cohort and an internal validation cohort at a ratio of 7:3. Adjustments were for demographics, tumor characteristics, and treatment modalities. Nomograms were constructed according to these risk factors to predict CVM risk at 5, 10, and 15 years. Validation included receiver operating characteristic (ROC) curves, time-dependent ROC, C-index, calibration curves, and decision curve analysis.

Results: One hundred four thousand six hundred six patients following initial diagnosis of DLBCL were included (58.3% male, median age 64 years, range 0–80, White 83.98%). Among them, 5.02% died of CVM, with a median follow-up time of 61 (31–98) months. Nomograms based on the seven risk factors (age at diagnosis, gender, race, tumor grade, Ann Arbor stage, radiation, chemotherapy) with hazard ratios ranging from 0.19–1.17 showed excellent discrimination, and calibration plots demonstrated satisfactory prediction. The 5-, 10-, and 15-year AUC and C-index of CVM in the training set were 0.716 (0.714–0.718), 0.713 (0.711–0.715), 0.706 (0.704–0.708), 0.731, 0.727, and 0.719; the corresponding figures for the validation set were 0.705 (0.688–0.722), 0.704 (0.689–0.718), 0.707 (0.693–0.722), 0.698, 0.698, and 0.699. Decision curve analysis revealed a clinically beneficial net benefit.

Conclusions: We first built the nomogram model for DLBCL patients with satisfactory prediction and excellent discrimination, which might play an essential role in helping physicians enact better treatment strategies at the time of initial diagnosis.

KEYWORDS

pediatric cardiology, cardiovascular mortality, cardio-oncology, diffuse large B-cell lymphoma, nomogram

Introduction

Diffuse large B-cell lymphoma (DLBCL) is the most common subtype of non-Hodgkin lymphoma (NHL) (1), making up roughly 40% of the total NHL population (2, 3). With improvements in treatment methods and increased survival rates, the number of DLBCL survivors is continually growing (2–4). The conventional treatment regimen for DLBCL commonly incorporates drugs like cyclophosphamide, doxorubicin, and rituximab, all of which carry a heightened risk of cardiac damage (1). Therefore, these survivors face an elevated risk of cardiovascular mortality (CVM) (5–7). While numerous previous studies (8–10) have discussed the incidence of cardiovascular events, there is limited literature addressing the CVM risk in DLBCL patients, especially in children and adolescents. To the best of our knowledge, there are no reported studies that have constructed and validated a nomogram for assessing the CVM risk in children, adolescents, and adults with DLBCL.

In child, adolescent, and adult DLBCL survivors, CVM might be related to disease stages, treatment modalities, and genetic factors (6, 7, 11). The challenges in estimating CVM risks have been highlighted in previous studies (5, 7, 12, 13). Previous studies (5, 14) have primarily utilized Cox regression models to investigate the risk of cardiovascular death and specifically focus on the elderly population. Our research distinctively employs a competing risks model for a more nuanced analysis. This approach incorporates the concept of competitive risks, mitigates the impact of death from other causes on the final outcomes, and includes individuals across the entire age spectrum, which facilitates the attainment of more reliable results (15, 16).

This study aims to construct and validate a nomogram to predict the risk of CVM for child, adolescent, and adult DLBCL patients. By better understanding these relationships, we can provide more targeted guidance for the long-term cardiovascular health management of DLBCL survivors, particularly for the younger age demographic, thereby improving their quality of life and survival prospects.

Materials and methods

Data source and study population

As a network of U.S. population-based incident tumor registries, the Surveillance, Epidemiology, and End Results (SEER) program, which is a public registry maintained by the National Cancer Institute, currently encompasses approximately 27.8% of the cancer patient population (17). The SEER collects patient clinical information data, such as demographics, primary tumor site, stage at diagnosis, initial course of treatment, follow-up time, survival, and economic status of residence. We extracted data from patients with only one primary DLBCL between 2000 and 2019 in the SEER database using the SEER*Stat software (version 8.4.2).

We utilized histology codes from the third edition of the International Classification of Diseases for Oncology (ICD-O-3)—codes 9680/3, 9684/3, and 9688/3—to assemble the cohort of interest, including children, adolescents, and adults aged 0–80 years following initial diagnosis of DLBCL. Patients with a diagnosis at autopsy or death certificate and those with incomplete data on certain variables (survival time, cause of death, race, gender) were excluded (Figure 1).

Risk factors

The variables included in this study are based on clinical support (18, 19) and include age at diagnosis (0–18 years, 19–40 years, 41–60 years, 61–80 years), gender, year of diagnosis, tumor grade (no nodal or metastatic disease as local, nodal disease as regional, or any metastatic disease as distant), race (white, black, or other), cause of death, survival time, the Ann Arbor stage (Stage I: Early-stage cancer confined to the organ of origin. Stage II: Local spread, potentially involving nearby lymph nodes. Stage III: More extensive local spread, involving additional lymph nodes. Stage IV: Presence of distant metastasis.), primary site, mean household income (<$60,000, >$60,000), surgery (yes, no), chemotherapy (yes, no/unknown), radiotherapy (yes, no/unknown), and place of residence (rural, urban). Primary site codes were used from SEER*Stat for the "lip, oral, cavity and pharynx" (C0.0–14.9), digestive organs (C15.0–C27.0), "respiratory and intrathoracic organs" (C30.0–C39.9), "bone, joints and articular cartilage" (C40.0–C41.9), hematopoietic (C42.0–C42.9), skin (C44.0–C44.9), nervous system (C47.0–C47.9), peritoneum (C48.0–C48.9), soft tissues (C49.0–C49.9), breast (C50.0–C50.9), female genital organs (C51.0–C57.9), male genital organs (C60.0–C63.9), urinary tract (C64.0–C68.9), "eye, brain and other parts of central nervous system" (C69.0–C72.9), "endocrine system" (C73.0–C76.9), "lymph nodes" (C77.0–C78.0). County median income level was dichotomized into groups based on the SEER-linked county-level data regarding the median household income in the past 12 months using 2019 inflation-adjusted dollars. The initial course of treatment was determined based on whether patients received surgery, chemotherapy, or radiation therapy. Survival time refers to the interval from the diagnosis of cancer to the death of patients due to any cause or the last date of available survival information.

Outcomes

The main outcome of interest was a composite of CVM, defined as any of the following seven causes of death in the SEER database [International Classification of Diseases, 10th Revision (ICD-10) codes]: heart diseases (I00–I09, I11, I13, I20–I51), hypertension without heart disease (I10, I12), cerebrovascular diseases (I60–I69), atherosclerosis (I70), aortic aneurysm and dissection (I71), and other diseases of arteries, arterioles, and capillaries (I72–I78). Competitive risk refers to mortality due to other causes (such as primary diffuse large B-cell lymphoma, infection, and bleeding).

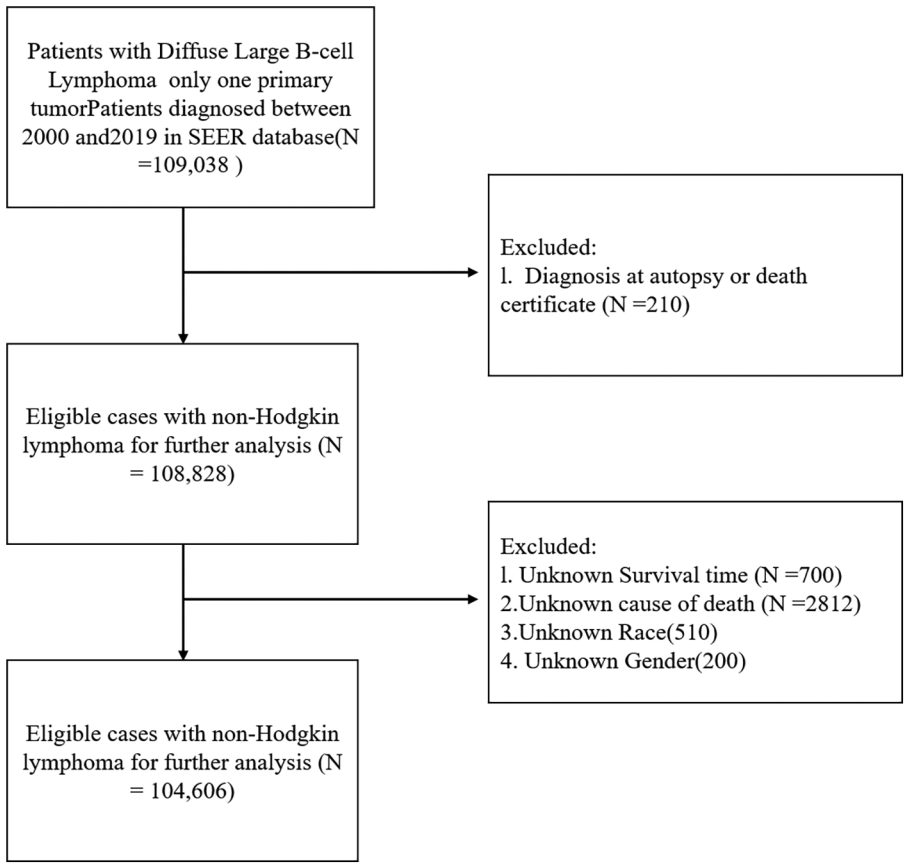

FIGURE 1
Flowchart depicting the enrolment of patients based on inclusion and exclusion criteria.

Statistical analysis

For calculating the sample size required for developing a clinical prediction model, the sample size calculation satisfied both the 15 EPV (events per variable) and pmsampsize rule requirements (20) (T1: estimate the overall outcome proportion with sufficient precision at one or more key time-points in follow-up; T2: target a shrinkage factor of 0.9; T3: target small optimism of 0.05 in the apparent R2Nagelkerke) in the training dataset. The R package "pmsampsize" was used, referring to some statistical parameters from a previous study (5). The minimum sample size calculated by the "pmsampsize" package was 1,450 cases. The sample size of the training dataset satisfies this requirement.

Normally distributed data were expressed as mean ± standard deviation. Non-normally distributed data were expressed as medians with interquartile ranges. Categorical data were presented using counts with percentages and compared using the chi-square test, while when frequencies were below 5, Fisher's exact test was applied.

In the competing risk analyses, we used the cumulative incidence function (CIF) to evaluate the cumulative rate of CVM. Multivariable competing risk survival analyses were performed to identify predictors of CVM. The total database was randomly divided into a training cohort and an internal validation cohort at a ratio of 7:3. The training cohort was used for risk factor analysis and nomogram construction. Factors with p-values < 0.05 in univariate competing risk analysis were added to a multivariate competing risk model to detect indicators of death specifically due to CVM. Based on the results of the competing risk analysis of the training cohort, a nomogram was constructed that incorporated all the independent prognostic factors to predict 5-, 10-, and 15-year CVM risk.

We evaluated the accuracy of the nomogram model by examining the 5-, 10-, and 15-year ROC curves. C-index for 5, 10, and 15 years were calculated to measure the predictive ability and accuracy of the model. The predicting outcomes of the nomogram were evaluated in the respective training and validation cohorts by calibrating curves and the decision curve analysis (DCA). DCA is a critical method for assessing the clinical utility of clinical predictive models and can address the limitations of the ROC curve (21).

Ethical approval of this publicly available information provided by the SEER program was not required by our Institutional Review Board. The manuscript has been prepared in accordance with the guideline of Transparent Reporting of a Multivariable Prediction

Model for Individual Prognosis or Diagnosis (TRIPOD) (22). For detailed information regarding the TRIPOD checklist, please refer to the online supplementary appendix. Statistical analyses were performed using STATA-MP 17.0 (StataCorp, College Station, TX) and R software (version 4.1.2; R Foundation for Statistical Computing, Vienna, Austria). All statistical tests were two-sided, with the significance level set at a p-value of < 0.05.

Results

Patient characteristics

A total of 104,606 DLBCL were included in subsequent analyses. The median age at diagnosis was 64 (53.72) years. The proportion of male patients was 60,953 (58.27%) and the median follow-up time was 61 (31–98) months. The majority of patients were White 87,845 (83.98%) and 56,080 (53.61%) had distant tumor stage. The most common primary site was lymph nodes (64.46%), followed by the digestive system (9.34%) and nervous system (4.67%). A total of 27,713 (26.49%) patients underwent surgery, 82,825 (79.18%) patients received chemotherapy, and only 18,755 (17.93%) patients underwent radiotherapy. Furthermore, 5,254 (5.02%) patients died of CVD, 4,202 (4.02%) died due to heart diseases, 715 (0.68%) due to cerebrovascular diseases, 53 (0.05%) due to aortic aneurysm and dissection, 180 (0.17%) due to hypertension without heart disease, and 38 (0.04%) due to atherosclerosis. The baseline characteristics are detailed in Tables 1, 2.

Univariate and multivariable analyses on the cardiovascular mortality

Risk factor analyses were based on the training set of 73,224 patients. The results of the univariate analysis are summarized in Table 3. In the univariate analysis, factors including age at diagnosis, gender, race, tumor grade, Ann Arbor stage, chemotherapy, and radiation were found to be associated with the CVM risk in child, adolescent, and adult patients with DLBCL.

Risk factor analysis

The multivariate analysis of CVM conducted by competing risk analysis in the training cohort is summarized in Table 4. Multivariate analysis revealed that the following characteristics were associated with risk of CVM: age at diagnosis ([0–18 vs. 61–80] HR: 0.19, 95% CI: 0.15–0.23; [19–40 vs. 61–80] HR: 0.34, 95% CI: 0.32–0.36; [41–60 vs. 61–80] HR: 0.57, 95% CI: 0.55–0.58), gender [(Male vs. Female) HR: 1.17, 95% CI: 1.15–1.21], race [(White vs. Black) HR: 0.73, 95% CI:0.69–0.76], tumor grade ([Localized vs. Distant] HR: 0.62, 95% CI: 0.58–0.65; [Regional vs. Distant] HR: 0.72, 95% CI: 0.68–0.76), Ann Arbor stage ([Stage II vs. Stage I] HR: 0.89, 95% CI: 0.82–0.96; [Stage III vs. Stage I] HR: 0.82, 95% CI: 0.76–0.89; [Stage IV vs. Stage I] HR: 1.05, 95% CI: 0.98–1.11). In terms of treatment, radiation [(Yes vs. No) HR: 0.85, 95% CI: 0.82–0.88] and chemotherapy [(Yes vs. No) HR: 0.56, 95% CI: 0.55–0.57] were associated with CVM in DLBCL patients.

Developing nomograms

The results of the CIF curves of cause of death in DLBCL patients are illustrated in Figure 2 and show that CVM increases with survival time.

In the training cohort, prognostic factors were used to construct the nomogram of CVM for predicting 5-, 10-, and 15-year CVM risk, as presented in Figure 3. In this nomogram, each variable corresponds to a point on the axis of the nomogram, and the corresponding score of the variable was obtained. The sum score of each variable was obtained, the total score corresponded to the point on the risk axis, and the risk value of CVM was obtained.

Internal validation

Internal validation was performed in a cohort of 31,382 patients. Patient baseline characteristics between the two cohorts were well-balanced (Supplementary Table S1). Validation methods demonstrated efficacy and stability. The 5-, 10-, and 15-year ROC curves of CVM and time-dependent ROC curves of the CVM nomogram were displayed (Figures 4, 5). The 5-, 10-, and 15-year AUC of CVM in the training set were 0.716 (0.714–0.718), 0.713 (0.711–0.715), and 0.706 (0.704–0.708), with C-index 0.731, 0.727, and 0.719, respectively; the corroding figures for the validation set were 0.705 (0.688–0.722), 0.704 (0.689–0.718), and 0.707 (0.693–0.722), with C-index 0.698, 0.698, and 0.699, respectively (Table 5). The calibration curves were very close to the diagonal (Supplementary Figure S1) showed high consistencies between the predicted and observed CVM probability in the cohorts. This demonstrates good predictive ability and accuracy of the model. The decision curve analysis for the model is shown in Figure 6. The X-axis indicates the threshold probability for CVM, while the Y-axis indicates the net benefit. The DCA indicated a significantly better net benefit, indicating the effective use of the model in achieving net clinical benefit.

Discussion

Utilizing the SEER database of more than 10,000 patients first diagnosed with DLBCL between the ages of 0 and 80 years, we built the first nomogram to predict the risk of CVM, with excellent results in internal validation. This research reports a 5.02% cumulative occurrence rate of cardiovascular death in diffuse large B-cell lymphoma patients, identifying significant risk factors for predicting CVM, including age at diagnosis, gender, tumor grade, Ann Arbor stage, radiation, and chemotherapy. The

10.3389/fped.2024.1346006

TABLE 1 Clinicopathologic characteristics of patients in different Age groups.

	Levels	Total (*N* = 104,606)	0–18 (*N* = 1,026)	19–40 (*N* = 8,793)	41–60 (*N* = 32,373)	61–80 (*N* = 62,414)
Age at diagnosis		64.00 (53.00, 72.00)	15.00 (11.00, 17.00)	33.00 (28.00, 37.00)	53.00 (48.00, 57.00)	71.00 (66.00, 76.00)
Gender	Female	43,653 (41.73%)	383 (37.3%)	3,396 (38.6%)	12,212 (37.7%)	27,662 (44.3%)
	Male	60,953 (58.27%)	643 (62.7%)	5,397 (61.4%)	20,161 (62.3%)	34,752 (55.7%)
Race	Black	7,765 (7.42%)	142 (13.8%)	1,369 (15.6%)	3,291 (10.2%)	2,963 (4.7%)
	Other	8,996 (8.60%)	96 (9.4%)	897 (10.2%)	2,775 (8.6%)	5,228 (8.4%)
	White	87,845 (83.98%)	788 (76.8%)	6,527 (74.2%)	26,307 (81.3%)	54,223 (86.9%)
Time from diagnosis to therapy		61.00 (31.00–98.00)	91.00 (32.00–162.00)	75.00 (18.00–148.00)	55.00 (13.00–122.00)	28.00 (6.00–78.00)
Tumor grade	Distant	56,080 (53.61%)	422 (41.1%)	3,892 (44.3%)	17,491 (54%)	34,275 (54.9%)
	Localized	25,118 (24.01%)	335 (32.7%)	2,527 (28.7%)	7,615 (23.5%)	14,641 (23.5%)
	Regional	18,277 (17.47%)	225 (21.9%)	2,078 (23.6%)	5,835 (18%)	10,139 (16.2%)
	Unknown	5,131 (4.91%)	44 (4.3%)	296 (3.4%)	1,432 (4.4%)	3,359 (5.4%)
Ann Arbor stage	I	17,605 (16.83%)	226 (22%)	1,732 (19.7%)	5,368 (16.6%)	10,279 (16.5%)
	II	13,034 (12.46%)	158 (15.4%)	1,452 (16.5%)	4,215 (13%)	7,209 (11.6%)
	III	5,724 (5.47%)	53 (5.2%)	318 (3.6%)	1,831 (5.7%)	3,522 (5.6%)
	IV	13,023 (12.45%)	81 (7.9%)	809 (9.2%)	4,095 (12.6%)	8,038 (12.9%)
	Unknown	55,220 (52.79%)	508 (49.5%)	4,482 (51%)	16,864 (52.1%)	33,366 (53.5%)
Primary sit	Bones and joints	1,870 (1.79%)	94 (9.2%)	349 (4%)	503 (1.6%)	924 (1.5%)
	Brain and other nervous system	4,888 (4.67%)	34 (3.3%)	398 (4.5%)	1,514 (4.7%)	2,942 (4.7%)
	breast	768 (0.73%)	3 (0.3%)	55 (0.6%)	245 (0.8%)	465 (0.7%)
	Digestive system	9,765 (9.34%)	99 (9.6%)	658 (7.5%)	3,024 (9.3%)	5,984 (9.6%)
	Endocrine system	1,167 (1.12%)	4 (0.4%)	58 (0.7%)	357 (1.1%)	748 (1.2%)
	Eye and orbit	509 (0.49%)	4 (0.4%)	28 (0.3%)	142 (0.4%)	335 (0.5%)
	Female genital system	393 (0.38%)	1 (0.1%)	88 (1%)	153 (0.5%)	151 (0.2%)
	Hematopoietic	5,147 (4.92%)	13 (1.3%)	166 (1.9%)	1,499 (4.6%)	3,469 (5.6%)
	Lymph nodes	67,434 (64.46%)	606 (59.1%)	5,779 (65.7%)	21,155 (65.3%)	39,894 (63.9%)
	Male genital system	1,215 (1.16%)	4 (0.4%)	48 (0.5%)	289 (0.9%)	874 (1.4%)
	Oral cavity and pharynx	4,292 (4.10%)	71 (6.9%)	390 (4.4%)	1,485 (4.6%)	2,346 (3.8%)
	Peritoneum	372 (0.36%)	3 (0.3%)	20 (0.2%)	94 (0.3%)	255 (0.4%)
	Respiratory system	3,156 (3.02%)	56 (5.5%)	528 (6%)	891 (2.8%)	1,681 (2.7%)
	Skin	1,225 (1.17%)	6 (0.6%)	73 (0.8%)	365 (1.1%)	781 (1.3%)
	Soft tissue including heart	1,414 (1.35%)	13 (1.3%)	100 (1.1%)	407 (1.3%)	894 (1.4%)
	Unknown	414 (0.40%)	6 (0.6%)	19 (0.2%)	114 (0.4%)	275 (0.4%)
	Urinary system	577 (0.55%)	9 (0.9%)	36 (0.4%)	136 (0.4%)	396 (0.6%)
Radiation	None/unknown	85,851 (82.07%)	940 (91.6%)	6,397 (72.8%)	26,029 (80.4%)	52,485 (84.1%)
	Yes	18,755 (17.93%)	86 (8.4%)	2,396 (27.2%)	6,344 (19.6%)	9,929 (15.9%)
Chemotherapy	No/unknown	21,781 (20.82%)	100 (9.7%)	1,166 (13.3%)	5,491 (17%)	15,024 (24.1%)
	Yes	82,825 (79.18%)	926 (90.3%)	7,627 (86.7%)	26,882 (83%)	47,390 (75.9%)
Surgery	No	76,378 (73.01%)	702 (68.4%)	6,358 (72.3%)	23,003 (71.1%)	46,315 (74.2%)
	Unknown	515 (0.49%)	4 (0.4%)	41 (0.5%)	147 (0.5%)	323 (0.5%)
	Yes	27,713 (26.49%)	320 (31.2%)	2,394 (27.2%)	9,223 (28.5%)	15,776 (25.3%)
Year of diagnosis	2000–2004	21,724 (20.77%)	260 (25.3%)	2,389 (27.2%)	7,136 (22%)	11,939 (19.1%)
	2005–2009	24,043 (22.98%)	244 (23.8%)	2,190 (24.9%)	7,993 (24.7%)	13,616 (21.8%)
	2010–2014	27,952 (26.72%)	269 (26.2%)	2,107 (24%)	8,757 (27.1%)	16,819 (26.9%)
	2015–2019	30,887 (29.53%)	253 (24.7%)	2,107 (24%)	8,487 (26.2%)	20,040 (32.1%)
Income	<$60,000	28,306 (27.06%)	759 (74%)	6,711 (76.3%)	24,173 (74.7%)	44,642 (71.5%)
	>$60,000	76,285 (72.93%)	267 (26%)	2,081 (23.7%)	8,196 (25.3%)	17,762 (28.5%)
	Unknown	15 (0.01%)	0 (0%)	1 (0%)	4 (0%)	10 (0%)
Rural/urban	Rural	12,454 (11.91%)	84 (8.2%)	707 (8%)	3,392 (10.5%)	8,271 (13.3%)
	Unknown	91 (0.09%)	2 (0.2%)	7 (0.1%)	31 (0.1%)	51 (0.1%)
	Urban	92,061 (88.01%)	940 (91.6%)	8,079 (91.9%)	28,950 (89.4%)	54,092 (86.7%)

reported AUC exceeds 0.70, indicating good predictive ability. The risk of CVM decreases with earlier diagnosis, as segmented by age groups.

DLBCL is a type of non-Hodgkin's lymphoma, of which complications such as cardiomyopathy and rhythm disturbances are frequently documented in children, adolescents, and adults (3, 12). In most studies (8, 23), the prevalence of cardiovascular disease is described rather than the cardiovascular disease mortality rate. In our current study, we observed a CVM rate of 5.02% among DLBCL patients. This finding is corroborated by

TABLE 2 Categorized results of DLBCL patients who died from cardiovascular diseases.

	Patients died from CV diseases ($N = 5,254$)
Heart diseases	4,202 (79.97%)
Hypertension without heart disease	180 (3.43%)
Cerebrovascular diseases	715 (13.61%)
Aortic aneurysm and dissection	53 (1.01%)
Atherosclerosis	38 (0.72%)
Other diseases of arteries, arterioles, capillaries	66 (1.26%)

TABLE 3 Effect of univariate competing risk result on the cardiovascular mortality.

	HR	(95% CI)	*P*
Age			
0–18 vs. 61–80	0.17	(0.14–0.21)	<0.001
19–40 vs. 61–80	0.32	(0.30–0.34)	<0.001
41–60 vs. 61–80	0.56	(0.54–0.57)	<0.001
Gender			
Male vs. female	1.13	(1.11–1.16)	<0.001
Race			
Other* vs. black	0.85	(0.78–0.89)	<0.001
White vs. black	0.87	(0.83–0.91)	<0.001
Ann Arbor stage			
Stage II vs. stage I	0.94	(0.90–0.99)	<0.001
Stage III vs. stage I	1.30	(1.23–1.38)	<0.001
Stage IV vs. stage I	1.71	(1.64–1.78)	<0.001
Unknown vs. stage I	1.57	(1.52–1.62)	<0.001
Tumor grade			
Localized vs. distant	0.60	(0.59–0.62)	<0.001
Regional vs. distant	0.59	(0.57–0.61)	<0.001
Unknown vs. distant	0.91	(0.87–0.96)	<0.001
Radiation			
Yes vs. no	0.64	(0.62–0.66)	<0.001
Chemotherapy			
Yes vs. no	0.54	(0.53–0.55)	<0.001
Surgery			
Yes vs. no	0.82	(0.80–0.84)	<0.001
Unknown vs. no	1.14	(0.98–1.32)	0.071
Rural/urban			
Urban vs. rural	0.87	(0.84–0.89)	<0.001
Unknown vs. rural	1.11	(0.77–1.58)	0.566

TABLE 4 Multivariate competing risk result on the cardiovascular mortality.

	HR	(95% CI)	*P*
Age			
0–18 vs. 61–80	0.19	(0.15–0.23)	<0.001
19–40 vs. 61–80	0.34	(0.32–0.36)	<0.001
41–60 vs. 61–80	0.57	(0.55–0.58)	<0.001
Gender			
Male vs. female	1.17	(1.15–1.21)	<0.001
Race			
Other vs. black	0.78	(0.73–0.82)	<0.001
White vs. black	0.73	(0.69–0.76)	<0.001
Ann Arbor stage			
Stage II vs. stage I	0.89	(0.82–0.96)	<0.001
Stage III vs. stage I	0.82	(0.76–0.89)	0.005
Stage IV vs. stage I	1.05	(0.98–1.11)	<0.001
Unknown vs. stage I	1.09	(1.04–1.16)	<0.001
Tumor grade			
Localized vs. distant	0.62	(0.58–0.65)	<0.001
Regional vs. distant	0.72	(0.68–0.76)	<0.001
Unknown vs. distant	0.67	(0.64–0.71)	<0.001
Radiation			
Yes vs. no	0.85	(0.82–0.88)	<0.001
Chemotherapy			
Yes vs. no	0.56	(0.55–0.57)	<0.001

the work of Jurczak et al. (24), who reported a 4.59% rate of cardiovascular-related deaths in DLBCL patients undergoing treatment. Additionally, our research demonstrates that for diffuse large B-cell lymphoma patients, an early diagnosis in childhood correlates with a reduced risk of cardiovascular death. A recent study disclosed that among the causes of cardiovascular death, heart-related conditions were the most predominant, accounting for 79.4% of cases, followed by cerebrovascular diseases, at 14.4% (5). These findings are consistent with our own results.

Our findings emphasize that age at diagnosis has a notable correlation with the risk of CVM, in line with previous studies (25–27). This association is particularly pronounced among older individuals, who frequently present with an advanced stage of the disease. Additionally, factors such as limited tolerance to adequate chemotherapy and the presence of pre-existing comorbidities, especially cardiac conditions, exacerbate the risk within this demographic (28). The heightened treatment toxicity observed in elderly patients is further influenced by the diminished reserve capacity of organs susceptible to these toxic effects.

When comparing gender, we observed a higher risk among men than among women. This is consistent with the findings reported in other literature (5, 27, 29–31). This may be attributed to men's metabolism of chemotherapy drugs, which leads to a lower response and survival (32). Race was also identified as a predictor of CVM in our study. This is consistent with the findings of previous studies (27, 30), which reported that black patients had a higher risk of CVM compared to white DLBCL patients. This could be due to disparities in access to healthcare and treatment.

The tumor grade was also identified as a significant predictor of CVM in our study. The findings from the study conducted by Kamel et al. (5) are in alignment with our observations, revealing that patients with a high tumor grade are at an elevated risk of CVM. This could be due to the aggressive nature of high-tumor grade, which often requires intensive treatment that can increase the risk of cardiovascular disease. Simultaneously, in our research, our study revealed that the Ann Arbor stage was correlated with the risk of CVM. This result has also been observed in other research articles (5, 33). Additional clinical research is required to elucidate the predictive roles of tumor grade and Ann Arbor stage in assessing the risk of CVM among DLBCL patients.

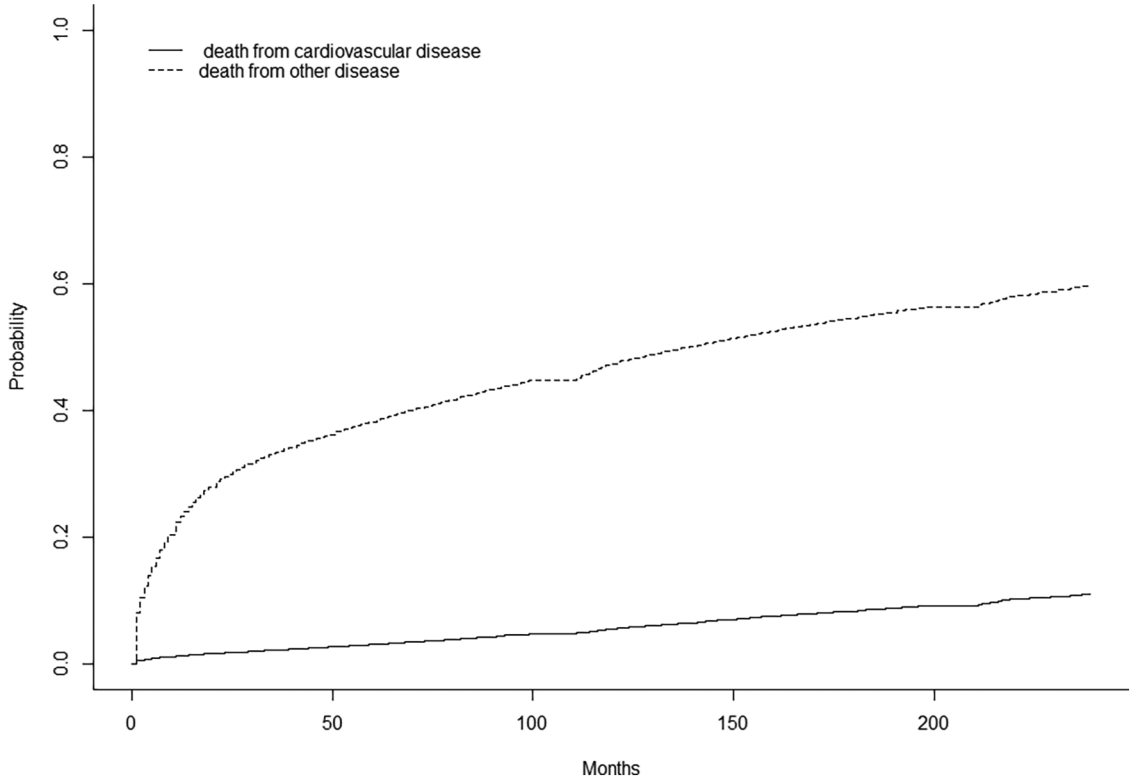

FIGURE 2
Cumulative mortality for all causes of death in DLBCL patients.

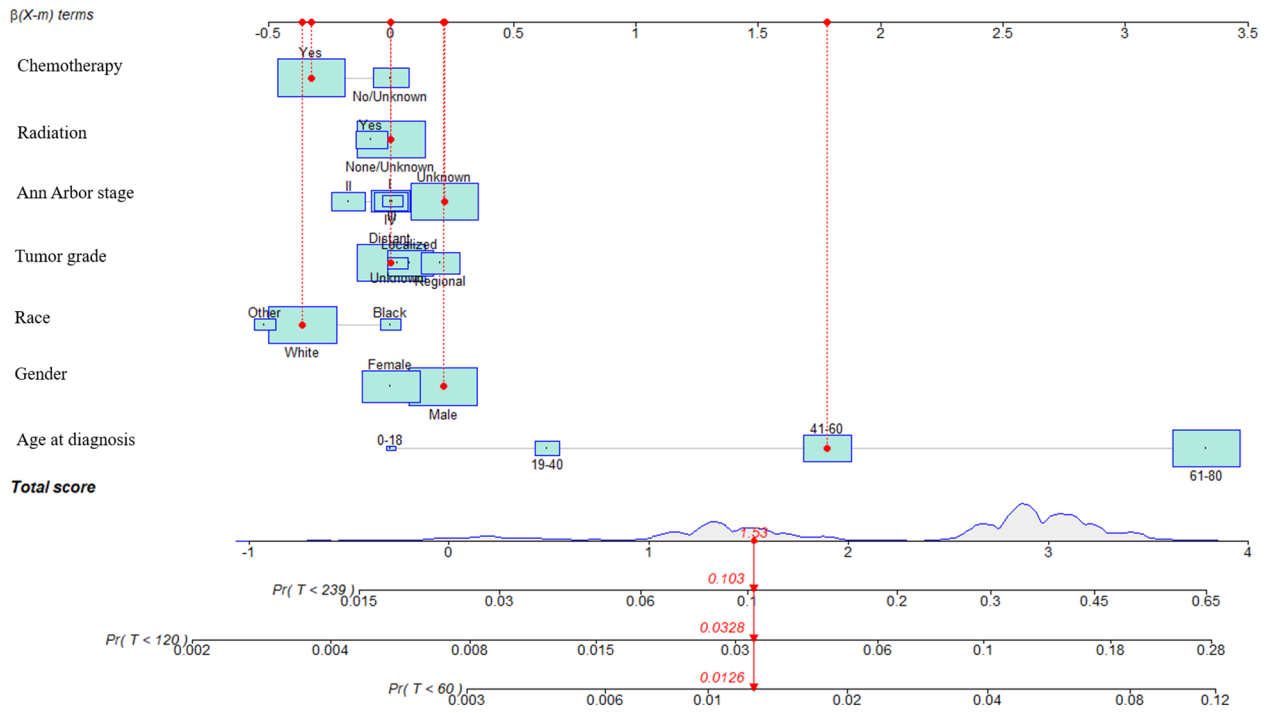

FIGURE 3
Nomograms to predict CVM for patients with DLBCL and risk stratification. In this nomogram, each variable corresponds to a point on the axis of the nomogram, and the corresponding score of the variable was obtained. The sum score of each variable was obtained, the total score corresponded to the point on the risk axis, and the risk value of CVM was obtained.

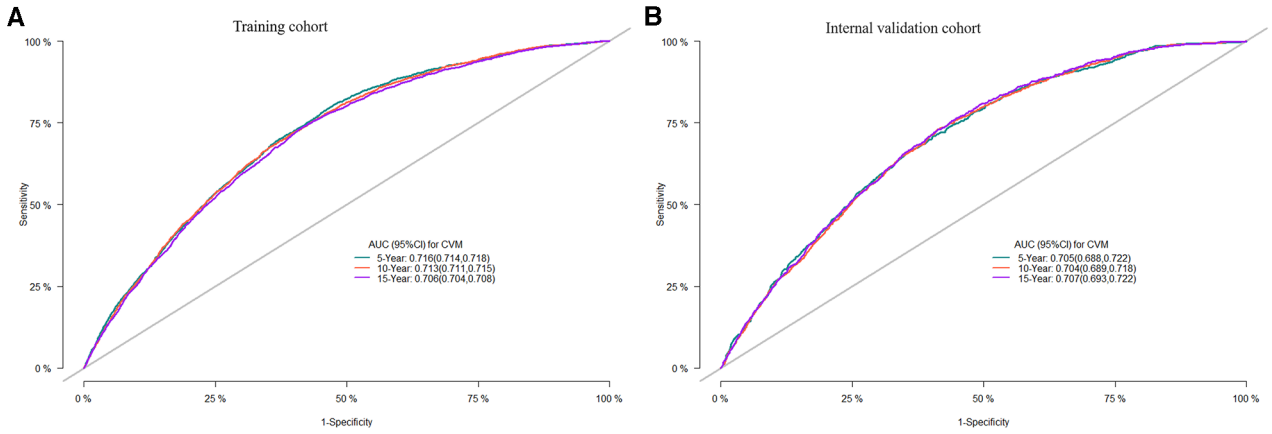

FIGURE 4
ROC curves of the nomogram of DLBCL patients for 5-, 10-, and 15-year CVM rates in the training cohort (A), the internal validation cohort (B); ROC, receiver operating characteristic; AUC, area under the curve.

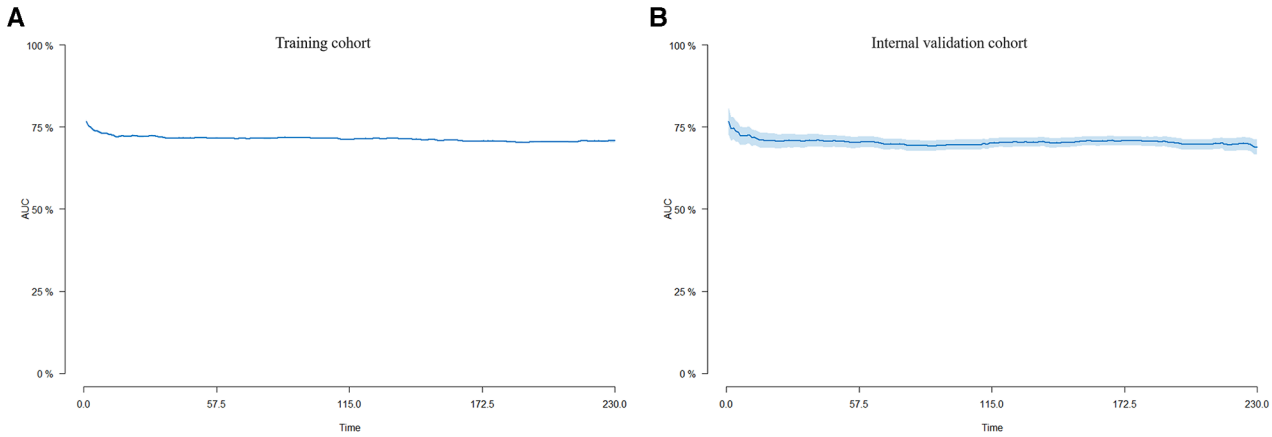

FIGURE 5
Time-dependent AUC curves for the nomogram of CVM in the training cohort (A) and the internal validation cohort (B).

Radiotherapy emerged as the pioneering treatment, offering enduring remission and even a potential cure for DLBCL patients (34, 35). Contrary to traditional understanding, mediastinal or thoracic region radiation can inflict considerable harm on the heart and adjacent vasculature, thereby elevating the risk of ischemic heart disease and valvular irregularities. There is controversy around whether radiotherapy is appropriate for DLBCL patients. Additionally, in our study, both univariate and multivariate competing risk models indicated that patients who underwent radiation therapy had lower cardiovascular disease-related mortality compared to those who did not receive radiation treatment. Our findings are consistent with the studies (35, 36), indicating that the mortality rate is minimized through exposure to radiotherapy compared to patients who did not receive radiation. The latter group showed a higher risk of mortality and a lower survival rate. This may suggest that undergoing radiation therapy is associated with reduced cardiovascular-related mortality rates. Zimmermann et al. (37) indicate that the omission of radiation leads not only to a shorter progression-free survival (PFS) but also to worse overall survival (OS). Radiation should therefore remain standard practice. In the SEER program, a detailed radiotherapy regimen was

TABLE 5 C-index for nomogram model.

Cohort	C-index		
	5-year	10-year	15-year
Training-cohort	0.731	0.727	0.719
Validation cohort	0.698	0.698	0.699

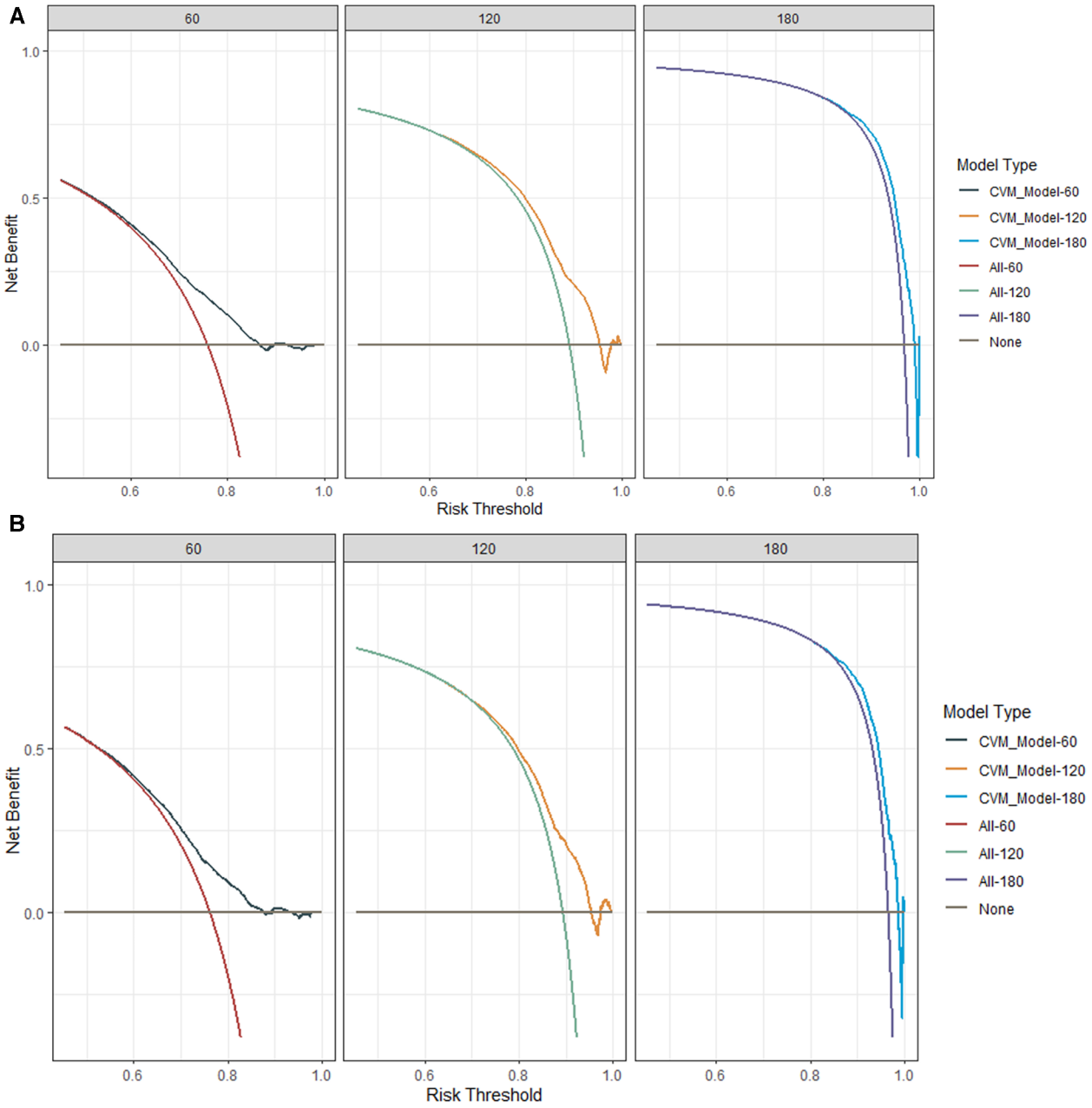

FIGURE 6
The decision-curve analysis (DCA) plots of the nomogram of DLBCL patients for 60-, 120-, and 180-month CVM rates in the training cohort (A) and the internal validation cohort (B).

lacking. As such, additional research is necessary to elucidate the impact of radiotherapy on the risk of CVM in patients diagnosed with DLBCL.

Strengths and limitations

The current study offers several notable advantages that contribute to both its credibility and broader applicability. To begin with, our study has verified the risk factors for CVM in children, adolescents, and adults with DLBL and has constructed the first predictive model for all age groups to predict CVM. However, our study has some limitations. First, the subjects included in our study were patients with initial, solitary occurrences of diffuse large B-cell lymphoma, representing a selective approach. Second, some information associated with CVM that might influence survival was not available, such as doses of radiation, chemotherapy regimens, smoking, alcohol use, transcriptomic or genomic data, and history of cardiovascular diseases. Third, because our study patients were predominantly White, the generalizability of our findings to other populations and ethnicities warrants further investigation.

Conclusions

We first built the nomogram model for DLBCL patients, with satisfactory prediction and excellent discrimination, which might play an essential role in helping physicians enact better treatment strategies at the time of initial diagnosis. Age of diagnosis, gender, race, tumor grade, Ann Arbor stage, radiation, and chemotherapy were predictors for risk of CVM. Clinical variables at diagnosis can identify DLBCL patients at high risk of CVM, for whom preventive interventions should be considered.

Data availability statement

The data set analysis of this study can be found in SEER database. The datasets analyzed in this study are available in the SEER repository and can be obtained from: https://seer.cancer.gov/data/.

Ethics statement

The studies involving humans were approved by Ethics Committee of the First Affiliated Hospital of Shandong First Medical University. The studies were conducted in accordance with the local legislation and institutional requirements. Written informed consent for participation in this study was provided by the participants' legal guardians/next of kin.

Author contributions

KM: Data curation, Formal Analysis, Software, Validation, Visualization, Writing – original draft, Writing – review & editing. JZ: Data curation, Formal Analysis, Investigation, Validation, Writing – original draft. YG: Data curation, Formal Analysis, Writing – original draft. GH: Conceptualization, Formal Analysis, Funding acquisition, Investigation, Software, Validation, Visualization, Writing – original draft, Writing – review & editing.

Funding

The author(s) declare financial support was received for the research, authorship, and/or publication of this article.

This research was supported by the Shandong Provincial Medical Association Clinical Research Funds Qilu Special (YXH2022ZX02181), the Jinan Science and Technology Plan-Clinical Medical Science and Technology Innovation Program (No. 202134003, No. 202225057), Shandong Medical Association Cord Blood Research Program (YXH2020zx005), and the First Affiliated Hospital of Shandong First Medical University National Natural Science Foundation Cultivation Program (QYPY2020NSFC0616).

Conflict of interest

The authors declare that the research was conducted in the absence of any commercial or financial relationships that could be construed as a potential conflict of interest.

Publisher's note

All claims expressed in this article are solely those of the authors and do not necessarily represent those of their affiliated organizations, or those of the publisher, the editors and the reviewers. Any product that may be evaluated in this article, or claim that may be made by its manufacturer, is not guaranteed or endorsed by the publisher.

Supplementary material

The Supplementary Material for this article can be found online at: https://www.frontiersin.org/articles/10.3389/fped.2024.1346006/full#supplementary-material

SUPPLEMENTARY FIGURE 1
Calibration curves of the nomogram of DLBCL patients for 5-, 10-, and 15-year CVM rates in the training cohort (A–C) and the internal validation cohort (D–F).

References

1. Tavakkoli M, Barta SK. 2024 update: advances in the risk stratification and management of large B-cell lymphoma. *Am J Hematol.* (2023) 98 (11):1791–805. doi: 10.1002/ajh.27075

2. Zhang N, Wu J, Wang Q, Liang Y, Li X, Chen G, et al. Global burden of hematologic malignancies and evolution patterns over the past 30 years. *Blood Cancer J.* (2023) 13:82. doi: 10.1038/s41408-023-00853-3

3. Kambhampati S, Herrera AF, Rhee JW. How to treat diffuse large B-cell lymphoma: oncologic and cardiovascular considerations. *JACC CardioOncol.* (2023) 5:281–91. doi: 10.1016/j.jaccao.2023.05.001

4. Lee SF, Vellayappan BA, Wong LC, Chiang CL, Chan SK, Wan EY, et al. Cardiovascular diseases among diffuse large B-cell lymphoma long-term survivors in Asia: a multistate model study. *ESMO Open.* (2022) 7:100363. doi: 10.1016/j.esmoop.2021.100363

5. Kamel MG, El-Qushayri AE, Thach TQ, Huy NT. Cardiovascular mortality trends in non-Hodgkin's lymphoma: a population-based cohort study. *Expert Rev Anticanc.* (2018) 18:91–100. doi: 10.1080/14737140.2018.1409626

6. Ocier K, Abdelaziz S, Kim S, Rowe K, Snyder J, Deshmukh V, et al. Cardiovascular disease risks in younger versus older adult B-cell non-Hodgkin's lymphoma survivors. *Cancer Med.* (2021) 10:4117–26. doi: 10.1002/cam4.3934

7. Zhu C, Shi T, Jiang C, Liu B, Baldassarre LA, Zarich S. Racial and ethnic disparities in all-cause and cardiovascular mortality among cancer patients in the U.S. *JACC CardioOncol.* (2023) 5:55–66. doi: 10.1016/j.jaccao.2022.10.013

8. Upshaw JN, Nelson J, Rodday AM, Kumar AJ, Klein AK, Konstam MA, et al. Association of preexisting heart failure with outcomes in older patients with diffuse large B-cell lymphoma. *Jama Cardiol.* (2023) 8:453–61. doi: 10.1001/jamacardio.2023.0303

9. Barac A. Assessing heart failure vs lymphoma treatment risks and benefits-it takes two to tango. *JAMA Cardiol*. (2023) 8:462–3. doi: 10.1001/jamacardio.2023.0312

10. Maier RH, Plummer C, Kasim AS, Akhter N, Ogundimu E, Maddox J, et al. Preventing cardiotoxicity in patients with breast cancer and lymphoma: protocol for a multicentre randomised controlled trial (PROACT). *Bmj Open*. (2022) 12:e66252. doi: 10.1136/bmjopen-2022-066252

11. Salz T, Zabor EC, Brown PN, Dalton SO, Raghunathan NJ, Matasar MJ, et al. Cardiovascular risk factors, radiation therapy, and myocardial infarction among lymphoma survivors. *Acta Oncol*. (2022) 61:1064–8. doi: 10.1080/0284186X.2022.2107402

12. Moser EC, Noordijk EM, van Leeuwen FE, le Cessie S, Baars JW, Thomas J, et al. Long-term risk of cardiovascular disease after treatment for aggressive non-Hodgkin lymphoma. *Blood*. (2006) 107:2912–9. doi: 10.1182/blood-2005-08-3392

13. Ruiz-Soto R, Sergent G, Gisselbrecht C, Larghero J, Ertault M, Hennequin C, et al. Estimating late adverse events using competing risks after autologous stem-cell transplantation in aggressive non-Hodgkin lymphoma patients. *Cancer Am Cancer Soc*. (2005) 104:2735–42. doi: 10.1002/cncr.21492

14. Zhang Z, Geskus RB, Kattan MW, Zhang H, Liu T. Nomogram for survival analysis in the presence of competing risks. *Ann Transl Med*. (2017) 5:403. doi: 10.21037/atm.2017.07.27

15. Austin PC, Lee DS, Fine JP. Introduction to the analysis of survival data in the presence of competing risks. *Circulation*. (2016) 133:601–9. doi: 10.1161/CIRCULATIONAHA.115.017719

16. Austin PC, Fine JP. Practical recommendations for reporting fine-gray model analyses for competing risk data. *Stat Med*. (2017) 36:4391–400. doi: 10.1002/sim.7501

17. Murphy CC, Tortolero GA, Gerber DE, Pruitt SL. An updated report on the prevalence of prior cancer among persons newly diagnosed with cancer in the surveillance, epidemiology, and end results program. *JAMA Oncol*. (2023) 9:1147–50. doi: 10.1001/jamaoncol.2023.1723

18. Mohan SSR, Ahmad M. Novel technologies must be considered for childhood cancer survivors at risk for cardiomyopathy. *JACC CardioOncol*. (2023) 5:156. doi: 10.1016/j.jaccao.2022.10.012

19. Leong DP, Mukherjee SD. The European society of cardiology cardio-oncology guidelines: evidence base, actionability, and relevance to clinical practice. *JACC CardioOncol*. (2023) 5:137–40. doi: 10.1016/j.jaccao.2022.10.009

20. Riley RD, Ensor J, Snell KIE, Harrell FE, Martin GP, Reitsma JB, et al. Calculating the sample size required for developing a clinical prediction model. *Br Med J*. (2020) 18:368. doi: 10.1136/bmj.m441

21. Fitzgerald M, Saville BR, Lewis RJ. Decision curve analysis. *JAMA*. (2015) 313:409–10. doi: 10.1001/jama.2015.37

22. Debray T, Collins GS, Riley RD, Snell K, Van Calster B, Reitsma JB, et al. Transparent reporting of multivariable prediction models developed or validated using clustered data: TRIPOD-cluster checklist. *Br Med J*. (2023) 380:e71018. doi: 10.1136/bmj-2022-071018

23. Salz T, Zabor EC, de Nully BP, Dalton SO, Raghunathan NJ, Matasar MJ, et al. Preexisting cardiovascular risk and subsequent heart failure among non-Hodgkin lymphoma survivors. *J Clin Oncol*. (2017) 35:3837–43. doi: 10.1200/JCO.2017.72.4211

24. Jurczak W, Szmit S, Sobociński M, Machaczka M, Drozd-Sokołowska J, Joks M, et al. Premature cardiovascular mortality in lymphoma patients treated with (R)-CHOP regimen—a national multicenter study. *Int J Cardiol*. (2013) 168:5212–7. doi: 10.1016/j.ijcard.2013.08.033

25. Rigacci L, Annibali O, Kovalchuk S, Bonifacio E, Pregnolato F, Angrilli F, et al. Nonpeghylated liposomal doxorubicin combination regimen (R-COMP) for the treatment of lymphoma patients with advanced age or cardiac comorbidity. *Hematol Oncol*. (2020) 38:478–86. doi: 10.1002/hon.2764

26. Zinzani PL, Federico M, Oliva S, Pinto A, Rigacci L, Specchia G, et al. The more patients you treat, the more you cure: managing cardiotoxicity in the treatment of aggressive non-Hodgkin lymphoma. *Leuk Lymphoma*. (2015) 56:12–25. doi: 10.3109/10428194.2014.894187

27. Zhao J, Su L, Zhong J. Risk factors for cancer-specific mortality and cardiovascular mortality in patients with diffuse large b-cell lymphoma. *Clin Lymphoma Myeloma Leuk*. (2020) 20:e858–63. doi: 10.1016/j.clml.2020.06.005

28. Volkova M, Russell RR. Anthracycline cardiotoxicity: prevalence, pathogenesis and treatment. *Curr Cardiol Rev*. (2011) 7:214–20. doi: 10.2174/157340311799960645

29. Bai LY, Yang MH, Chiou TJ, Liu JH, Yen CC, Wang WS, et al. Non-Hodgkin lymphoma in elderly patients: experience at Taipei veterans general hospital. *Cancer-Am Cancer Soc*. (2003) 98:1188–95. doi: 10.1002/cncr.11609

30. Crozier JA, Sher T, Yang D, Swaika A, Foran J, Ghosh R, et al. Persistent disparities among patients with T-cell non-Hodgkin lymphomas and B-cell diffuse large cell lymphomas over 40 years: a SEER database review. *Clin Lymphoma Myeloma Leuk*. (2015) 15:578–85. doi: 10.1016/j.clml.2015.06.005

31. Pulte D, Gondos A, Brenner H. Ongoing improvement in outcomes for patients diagnosed as having non-Hodgkin lymphoma from the 1990s to the early 21st century. *Arch Intern Med*. (2008) 168:469–76. doi: 10.1001/archinternmed.2007.125

32. Pfreundschuh M, Müller C, Zeynalova S, Kuhnt E, Wiesen MH, Held G, et al. Suboptimal dosing of rituximab in male and female patients with DLBCL. *Blood*. (2014) 123:640–6. doi: 10.1182/blood-2013-07-517037

33. Diamond A, Ayyappan S, Cao S, Tashtish N, Boughan K, Cooper B, et al. Risk factors for cardiovascular events and mortality in patients diagnosed with diffuse large B-cell lymphoma and treated with anthracyclines. *Hematol Oncol*. (2022) 40:626–36. doi: 10.1002/hon.3034

34. Bush RS, Gospodarowicz M, Sturgeon J, Alison R. Radiation therapy of localized non-Hodgkin's lymphoma. *Cancer Treat Rep*. (1977) 61:1129–36.

35. Choi KH, Lee SJ, Mun SH, Song JH, Choi BO. Consolidative radiotherapy after complete remission following R-CHOP immunochemotherapy in stage III–IV diffuse large B-cell lymphoma patients: a systematic review and meta-analysis. *Cancers (Basel)*. (2023) 15:3940. doi: 10.3390/cancers15153940

36. Miller TP, Dahlberg S, Cassady JR, Adelstein DJ, Spier CM, Grogan TM, et al. Chemotherapy alone compared with chemotherapy plus radiotherapy for localized intermediate- and high-grade non-Hodgkin's lymphoma. *N Engl J Med*. (1998) 339:21–6. doi: 10.1056/NEJM199807023390104

37. Zimmermann M, Oehler C, Mey U, Ghadjar P, Zwahlen DR. Radiotherapy for non-Hodgkin's lymphoma: still standard practice and not an outdated treatment option. *Radiat Oncol*. (2016) 11:110. doi: 10.1186/s13014-016-0690-y

frontiers | Frontiers in Cardiovascular Medicine

TYPE Original Research
PUBLISHED 16 February 2024
DOI 10.3389/fcvm.2024.1340271

OPEN ACCESS

EDITED BY
Laura Muiño Mosquera,
Ghent University Hospital, Belgium

REVIEWED BY
Luc Bruyndonckx,
University of Antwerp, Belgium
Wendy Dewals,
Antwerp University Hospital (UZA), Belgium

*CORRESPONDENCE
Zongjie Weng
✉ wengzongjie1984@fjmu.edu.cn
Caihong Jiang
✉ jch_2008ok@yeah.net

†These authors have contributed equally to this work

RECEIVED 27 November 2023
ACCEPTED 29 January 2024
PUBLISHED 16 February 2024

CITATION
Peng L, Cai Y, Wu J, Ling W, Wu Q, Guo S, Huang B, Jiang C and Weng Z (2024) Prenatal diagnosis and clinical management of cardiac rhabdomyoma: a single-center study. Front. Cardiovasc. Med. 11:1340271. doi: 10.3389/fcvm.2024.1340271

Prenatal diagnosis and clinical management of cardiac rhabdomyoma: a single-center study

Longzhuang Peng†, Youchun Cai†, Jianhang Wu†, Wen Ling, Qiumei Wu, Shan Guo, Biying Huang, Caihong Jiang* and Zongjie Weng*

Department of Medical Ultrasonics, Fujian Maternity and Child Health Hospital, College of Clinical Medicine for Obstetrics & Gynecology and Pediatrics, Fujian Medical University, Fuzhou, China

Objective: The study aims to assess the ultrasonic features of fetal cardiac rhabdomyoma (CR), track the perinatal outcome and postnatal disease progression, investigate the clinical utility of ultrasound, MRI and tuberous sclerosis complex (TSC) gene analysis in CR evaluation, and offer evidence for determing of fetal CR prognosis.

Methods: We conducted a retrospective analysis of prenatal ultrasound-diagnosed fetal CR cases in our hospital from June 2011 to June 2022, tracked the perinatal outcomes, regularly followed live infants to analyze cardiac lesion changes and disease progression, and compared the sensitivities of ultrasound, MRI and their combination in the detecting of intracranial sclerosing nodules.

Results: Our study included 54 fetuses with CR: 32 pregnancies were terminated, 22 were delivered, 35 were diagnosed with TSC, 13 had simple CR without TSC, and in 6 cases, remained unclear whether TSC accompanied the CR due to insufficient evidence. 45 fetuses (83.3%) had multiple lesions, while 9 fetuses (16.7%) presented with a single lesion. Twelve cases had intracardiac complications, all associated with multiple lesions, and these cases exhibited larger maximum tumor diameters than the non-complicated group. Multiple intracardiac lesions were more prevalent in the TSC group than in the simple CR group. However, there was no significant difference in maximum tumor diameter between the two groups. Among 30 fetuses who underwent fetal brain MRI, 23 were eventually diagnosed with TSC, with 11 fetuses showing intracranial sclerosis nodules by ultrasound and 15 by MRI, and the diagnostic consistency was moderate ($k = 0.60$). Twenty-two fetuses were born and followed up for 6–36 months. CR lesions diminished or disappeared in 18 infants (81.8%), while they remained unchanged in 4 infants (18.2%). Ten out of 12 (83.3%) surviving children diagnosed with TSC developed epilepsy, and 7 (58.3%) had neurodevelopmental dysfunction.

Conclusions: The majority of CR cases involve multiple lesions, which are a primary risk factor for TSC. Through prenatal ultrasound examination is crucial for assessing fetal CR prognosis. Although ultrasound combined with MRI can detect intracranial sclerosis nodules in TSC fetuses, its sensitivity is limited. TSC gene sequencing is an essential diagnostic method. Simple CR cases without TSC generally have a favorable prognosis.

KEYWORDS

fetal cardiac rhabdomyoma, tuberous sclerosis complex, ultrasound, genetic testing, prognosis

Introduction

Cardiac rhabdomyoma (CR) is one of the most common primary cardiac tumors, accounting for approximately 60% of the various primary cardiac tumors in children (1, 2). Its incidence in live-born infants ranges from 0.02% to 0.17%, with a prevalence of 0.12% in prenatal fetuses (3, 4). CR is characterized as a benign hamartomatous tumor. In cases where CR lesions do not lead to severe complications, the pregnancy outcome is generally favorable (5). However, complications associated with CR can include arrhythmias, valvular regurgitation, outflow tract obstruction, heart failure, pericardial effusion, fetal edema, and, rarely, stillbirth (3, 6).

CR serves as a significant clinical marker and initial symptom of tuberous sclerosis complex (TSC) (7–9), with a high risk of neurodevelopmental impairment. According to previous studies, the incidence of TSC in fetuses with CR ranges from 50% to 90% (10, 11). Moreover, approximately 90% of infants diagnosed with TSC typically experience infantile seizures, intellectual impairment, or autism (12). TSC is a multilineage-based neurocutaneous syndrome that is an autosomal dominant disorder caused by mutations in the TSC1 and TSC2 genes. While around two-thirds of TSC cases are sporadic, the remaining third have familial origins (8, 13). Cortical and subependymal nodules (SENs) are hallmark brain lesions in TSC and act as sensitive indicators for TSC diagnosis. Studies have shown that nearly all individuals with TSC display pathological changes in the nervous system, with 80%–90% having cortical nodules and/or SENs (14). Notably, there appears to be no significant distinction in pathogenic mutations between TSC1 and TSC2. Furthermore, it has been reported that neuroimaging findings are more sensitive indicators of TSC and correlate with a less favorable prognosis (15). Therefore, the prenatal detection of intracranial lesions is a pivotal component for diagnosing TSC in fetuses exhibiting CR.

Due to the correlation between CR and TSC, diagnosing and assessing CR in pregnant women is crucial. Clinical symptoms of TSC vary widely, and genetic testing for TSC can be costly and not widely recommended (16, 17). Heart and brain abnormalities, especially in the prenatal and early postpartum periods, are often the only signs of TSC (17). Fetal echocardiography is the primary method for detecting cardiac tumors (18). While it's effective for CR, ultrasound's sensitivity in identifying brain lesions in TSC fetuses is unclear. Fetal brain MRI is preferred for diagnosing neurological issues, which complements and confirms the diagnosis of TSC with genetic testing (15). The effectiveness of ultrasound compared to MRI for intracranial nodules remains underexplored. In addition, the connection between TSC and multiple CRs is recognized, but the association with a single CR remains is uncertain (19, 20), making prognostic assessment challenging.

Detecting CR in fetus is essential for assessing short-term perinatal outcomes and long-term prognostic considerations in the context of TSC. Previous studies often focused on prenatal diagnosis or postnatal treatment and prognosis, and rare disease studies require substantial sample size. we analyzed the prenatal and postnatal data of 54 CR fetuses which was diagnosed by prenatal ultrasound. Our goal was to evaluate perinatal risks and prenatal diagnosis of fetuses presenting with CR as the initial symptom, using a multidisciplinary approach. We aimed to determine the clinical value of combining ultrasound and MRI with TSC gene detection for assessing CR fetus prognosis, providing guidance for perinatal management and prognostic evaluation.

Materials and methods

Clinical characterization

We retrospectively analyzed data from 75 fetuses with CR out of 124,589 pregnant women who underwent prenatal ultrasound examinations at Fujian Maternal and Child Health Hospital between June 2011 and June 2022. Our analysis included ultrasonography, brain MRI, genetic testing, pathologic anatomy and medical records of surviving infants. Fetuses with CR underwent systematic ultrasonography were verified through our diagnostic methods. Exclusion criteria comprised cases with cardiac tumor which could not be determined as CR, incomplete clinical data, or a lack of follow-up. After excluding 21 cases due to insufficient diagnostic evidence or incomplete data, the study included 54 cases. The study protocol was reviewed and approved by the Ethics Committee of the Fujian Maternal and Child Health Hospital, with informed consent from all pregnant women.

Fetal ultrasonography

GE Voluson E8 and E10 high-resolution color Doppler ultrasound diagnostic instruments were employed, with a frequency of the transabdominal ultrasound probe of 4∼8 MHz. The conditions of middle and late pregnancy and fetal heart examination were selected, and transvaginal examination was performed to observe the fetal intracranial structure, with a frequency of the cavity probe of 6∼10 MHz. Neonatal echocardiography for live births employed a Phillips EPIQ 7C with 3∼8 MHz phased array probes. All assessments followed International Society of Ultrasound in Obstetrics and Gynecology (ISUOG) guidelines for prenatal ultrasonography (21, 22). Our examinations included the number, location, size, shape, calcification, capsule, liquefaction and pedicle formation of the tumor for diagnosis and differential diagnosis. We also checked for other cardiac malformations and complications, and conducted craniocerebral ultrasound examinations.

Fetal brain MRI

We utilized a GE 1.5 Tesla MR Scanner with gradient field strength and phased line loop channels. The fetal brain scans included SSFSE and FIESTA sequences in standard cross-sections, coronal, and sagittal planes, along with DWI and T 1

fat-pressing sequences in cross-sections. The scanning time for all sequences did not exceed 15 min.

Genetic analysis

For fetuses with CR detected via ultrasound, it is advisable to undergo TSC gene testing. Medical professionals with qualifications in prenatal diagnosis evaluated the need for prenatal testing. Informed consent from pregnant women and their families was obtained for procedures such as amniocentesis, umbilical vein puncture, and the amniotic fluid or umbilical cord blood extraction for karyotype analysis, single-nucleotide polymorphism comparative genomic hybridization or exon sequencing. The diagnosis of TSC was based on the diagnostic criteria of the International Tuberous Sclerosis Conference (23).

Follow-up

In cases of pregnancy termination, anatomical and pathological examination were conducted to verify the diagnosis after obtaining informed consent and signature from patients and their family members. For newborns with cardiac tumors in our hospital, CR was confirmed through repeated clinical follow-up after birth. Children diagnosed with TSC underwent skin and eye examinations, abdominal ultrasonography, assessment of seizures, and brain MRI. Additionally, evaluations were performed for mental and psychomotor development, as well as behavioral and language skills. All children in the study received regular followed up by a pediatrician and an ultrasound physician. Those who declined to participate or could not be reached more than three occasions were considered lost to follow-up.

Statistical analysis

IBM SPSS Statistics 26 and MedCalc 15.2.2 software were used for statistical analysis of the data. The Shapiro–Wilk test was used to test the normality of the measurement data, the t test was used for comparisons between groups, and the Mann–Whitney U test was used for comparisons between groups. The number of cases (%) was used to represent the count data, and the comparison between groups was performed by the χ^2 test or Fisher's exact test. $P < 0.05$ was considered to indicate statistical significance. The kappa test was used for consistency checking. By plotting receiver operating characteristic (ROC) curves, the area under the curve (AUC), sensitivity, specificity, positive predictive value (PPV) and negative predictive value (NPV) were calculated to evaluate the diagnostic efficacy of each diagnostic method.

Results

The study involved 54 pregnant women, with an average age of 28.04 ± 4.01 years (17–39 years) and an average gestational age of 28.91 ± 4.14 weeks (23–40 weeks). Thirty fetuses underwent both ultrasound and brain MRI examinations. Among the 22 fetuses born, 12 were diagnosed with TSC posnatally,8 with TSC1/2 gene mutations, and 4 based on clinical and imaging assessments by pediatric experts. Ten live-born children had simple CR without TSC or TSC gene mutations (TSC gene mutations or TSC-related clinical manifestations during follow-up). Among 32 induced pregnancies, 26 were tested for the TSC gene mutations, with 23 positive and 3 negative results. Autopsy and pathological examination diagnosed 12 cases with CR, including 4 with TSC1/2 gene mutations. In summary, 35 cases were CR with TSC, 13 were CR without TSC (named "simple CR" in this paper), and 6 had confirmed as CR, with TSC status remaining unclear due to insufficient evidence (Figure 1).

Sonographic characterization of fetal CR

54 cases of fetal CR typically displayed round, homogeneous, high/slightly hyperechoic, intramural or intraluminal masses (Figure 2). Most cases (83.3%) had multiple lesions, with an average maximum tumor diameter of 12.26 ± 6.23 mm. Lesions were primarily found in the left ventricle (81.5%) and right ventricle (77.8%), while some appeared in the ventricular septum (42.6%), right atrium (14.8%), and left atrium (1.9%). Around 22.2% of fetuses had intracardiac complications, mainly outflow tract obstruction, arrhythmia, heart failure, pericardial effusion, or severe tricuspid regurgitation (Figure 3). The fetuses with intracardiac complications all had multiple lesions. Five fetuses had outflow tract obstruction because the tumors were located near the upper part of the ventricular septum. The mean maximum CR diameter was significantly larger in the group with intracardiac complications (17.92 ± 8.43 mm) compared to the group without complications (10.64 ± 4.37 mm) with a p-value of 0.000. This highlights the importance of lesion quantity, location, and size in causing fetal cardiac complications.

Comparison of fetal brain ultrasound and MRI

Of the 54 fetuses with CR diagnosed by ultrasound, 30 underwent fetal MRI. On ultrasound, 11 cases displayed intracranial nodules, often appearing as hyperechoic or slightly hyperechoic nodules, typically occurring in multiples (Figure 2). The majority (90.9%) were in the brain parenchyma, and some (27.3%) in the subependymal area. Prenatal brain MRI confirmed 15 cases of intracranial sclerosing nodules, which displayed a high signal on T1 and a low signal on T2 (Figure 2). A substantial portion (40%) was located in the brain parenchyma, while the majority (93.3%) were in the subependymal area. One case showed multiple intracranial lesions on ultrasound but no MRI abnormalities (Figure 4); postnatal MRI later confirmed intracranial nodules. Ultrasound combined with MRI identified 16 fetuses with intracranial sclerosing nodules, with 14 having TSC1/2 gene mutations, and 2 diagnosed with Tuberous Sclerosis

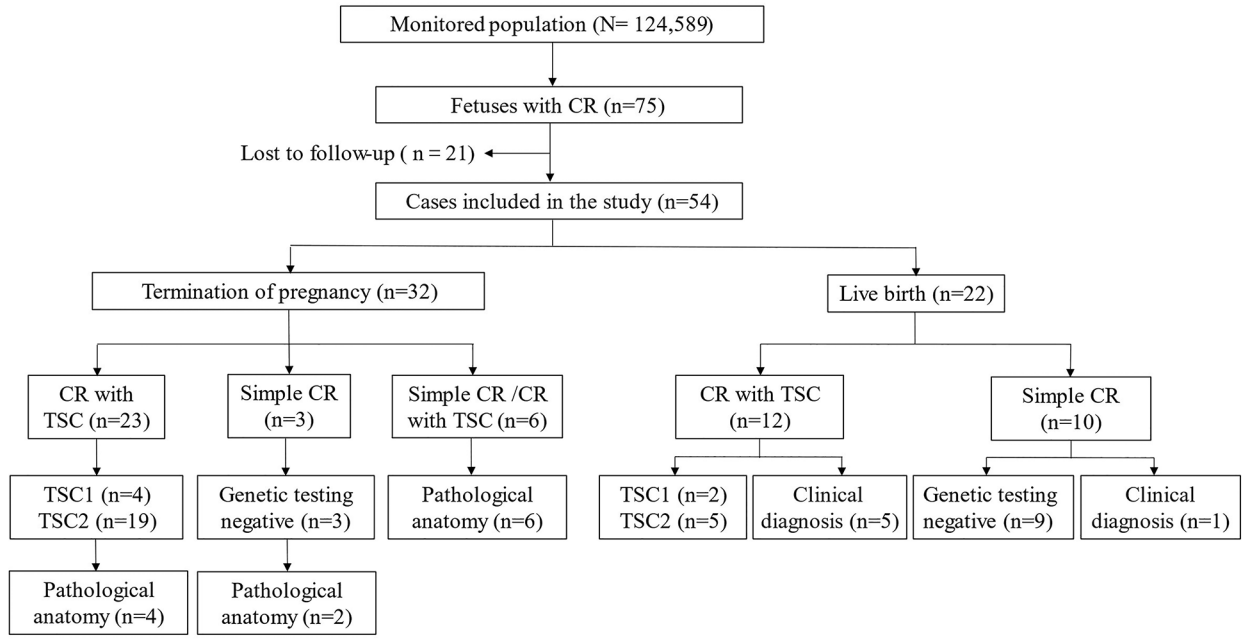

FIGURE 1
Flowchart of this retrospective study.

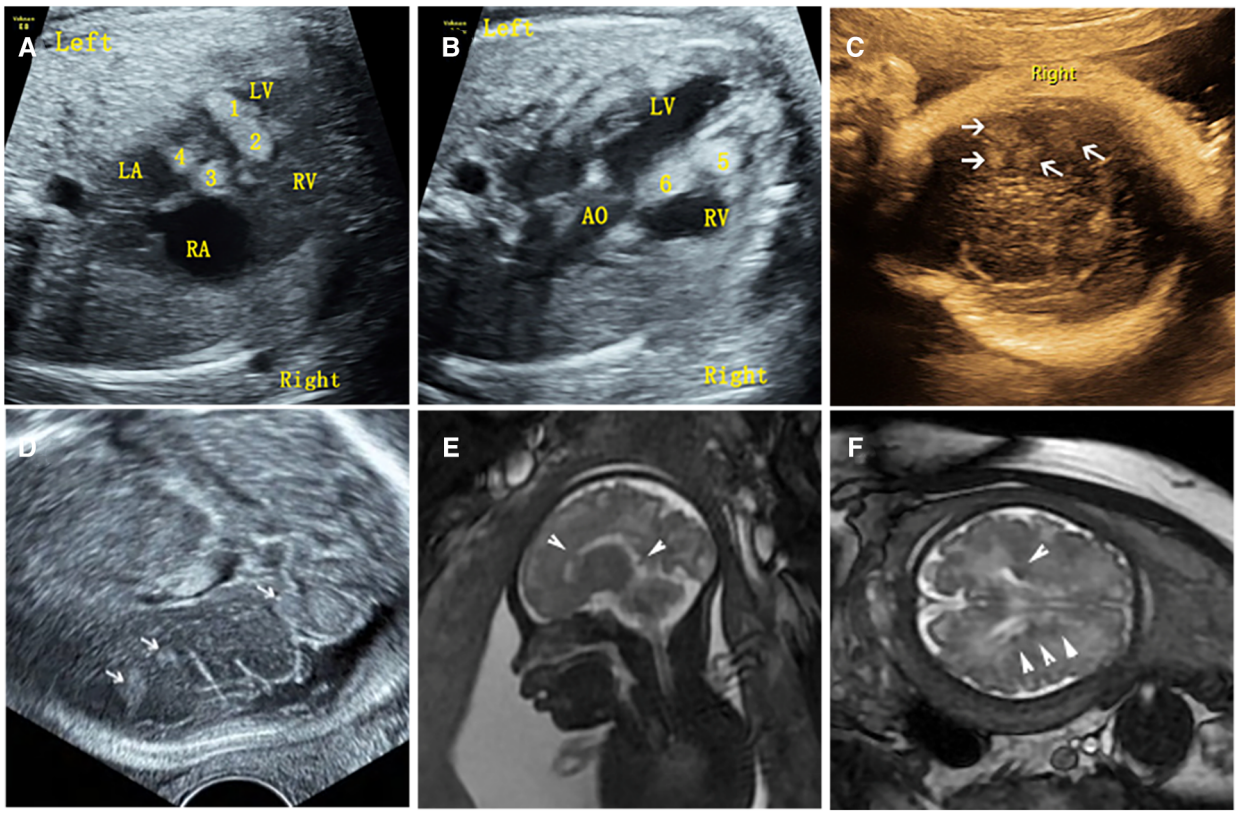

FIGURE 2
Ultrasound and MRI findings of multiple cardiac rhabdomyomas complicated with multiple cranial sclerotic nodules in the fetus (case NO. 51) at 31 weeks of gestation. (**A**) Multiple slightly hyperechoic nodules in the left ventricle of the fetal heart. (**B**) Multiple slightly hyperechoic nodules in the right ventricle of the fetal heart. (**C**) Multiple hyperechoic intracranial nodules of the fetus detected by transvaginal sonography. (**D**) Multiple hyperechoic intracranial nodules of the fetus detected by transabdominal sonography. (**E**) MRI sagittal T2-weighted image with multiple subependymal nodules. (**F**) MRI axial T2-weighted image with multiple subependymal nodules.

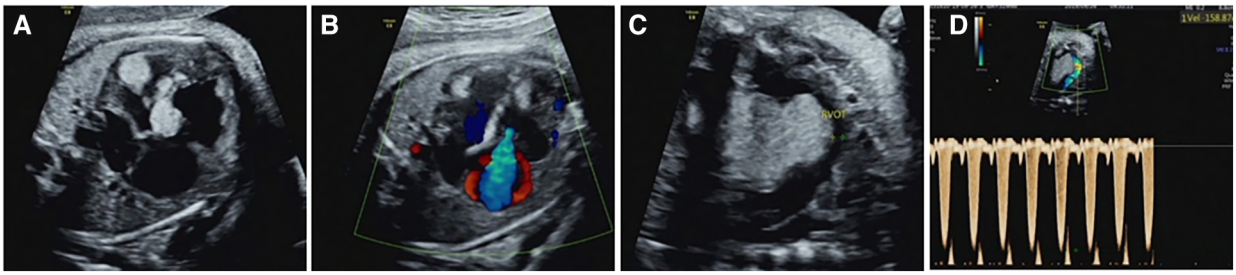

FIGURE 3
Intracardiac complications associated with cardiac rhabdomyoma in the fetus (case NO. 54) at 33 weeks of gestation. (**A**) Heart failure with cardiothoracic ratio enlargement. (**B**) Severe tricuspid regurgitation. (**C**) Rhabdomyoma located in the upper interventricular septum protrudes into the right ventricular outflow tract, resulting in a reduced internal diameter of the right ventricular outflow tract. (**D**) Increased velocity of the right ventricular outflow tract.

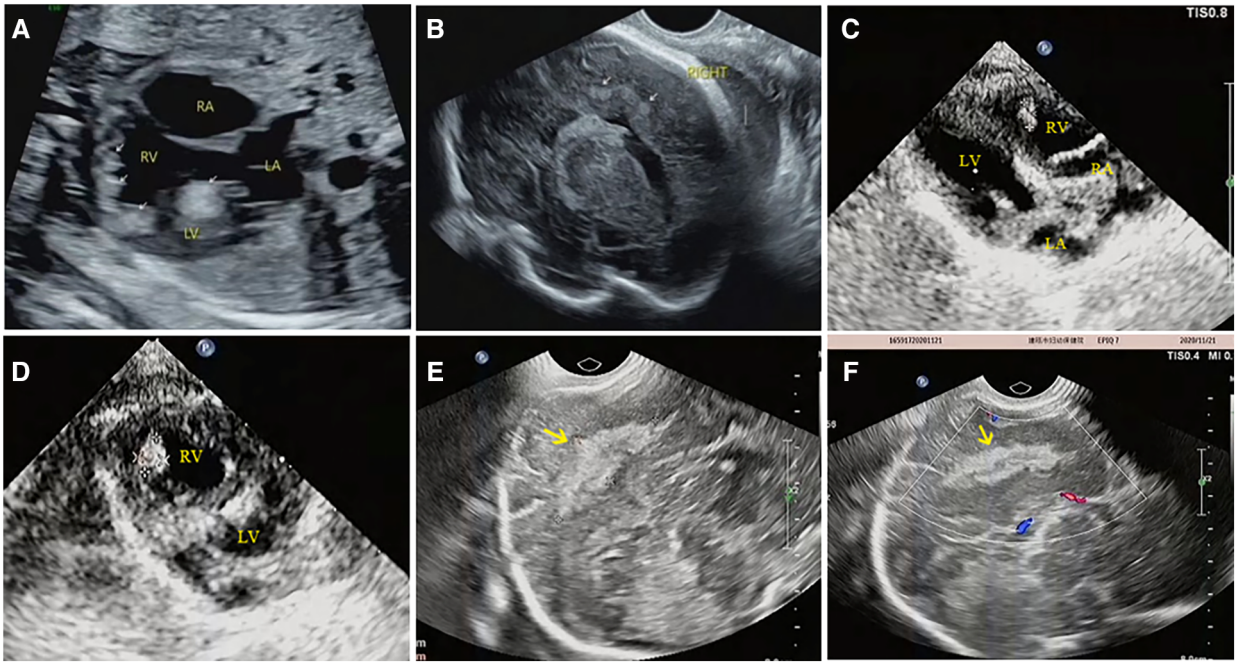

FIGURE 4
Prenatal and postnatal ultrasonography of cardiac rhabdomyoma complicated with cranial sclerotic nodules in case NO. 13. (**A**) Multiple slightly hyperechoic nodules in the ventricle of the fetal heart at 28 weeks of gestation. (**B**) Multiple hyperechoic intracranial nodules of the fetal heart at 28 weeks of gestation; however, no intracranial lesions were detected by MRI at the same time. (**C**,**D**) Multiple slightly hyperechoic nodules in the ventricle of the baby at 1 month after birth. (**E**,**F**) Hyperechoic intracranial nodule of this baby at the same time.

Complex (TSC) postnatally. Among 14 fetuses without prenatal intracranial nodules, 7 had TSC1/2 gene mutations, 6 tested negative for the TSC gene, and 1 did not undergo TSC genetic testing, being diagnosed with simple CR after a 5-year follow-up. Moderate agreement was seen between ultrasound and MRI in diagnosing TSC (K = 0.60). Sensitivity for ultrasound, MRI, and the combination of both in predicting CR with TSC was 47.83, 65.22, and 69.57, respectively (Table 1, Figure 5). The corresponding AUC values were 0.739, 0.826, and 0.848, with MRI demonstrating higher sensitivity in detecting intracranial sclerosing nodules in fetuses with CR. No significant difference in AUC values was observed among the three groups ($P > 0.05$).

Pathological anatomy of CR

Of the 54 fetuses, 32 pregnancies were terminated, none of them with other malformations, and 12 were confirmed to have Cardiac Rhabdomyomas (CR) through anatomical and pathological examination. Pathological analysis showed that these

TABLE 1 Diagnostic performance of ultrasound and MRI in diagnosing TSC.

Diagnostic method	AUC	Sensitivity (%)	Specificity (%)	Positive predictive value (%)	Negative predictive value (%)
US	0.739 (0.547, 0.881)	47.83 (26.8, 69.4)	100 (85.2, 100.0)	76.7 (57.7, 90.1)	36.8 (16.3, 61.6)
MRI	0.826 (0.644, 0.939)	65.22 (42.7, 83.6)	100 (85.2, 100.0)	76.7 (57.7, 90.1)	46.7 (21.3, 73.4)
US&MRI	0.848 (0.670, 0.952)	69.57 (47.1, 86.8)	100 (85.2, 100.0)	76.7 (57.7, 90.1)	50 (23.0, 77.0)

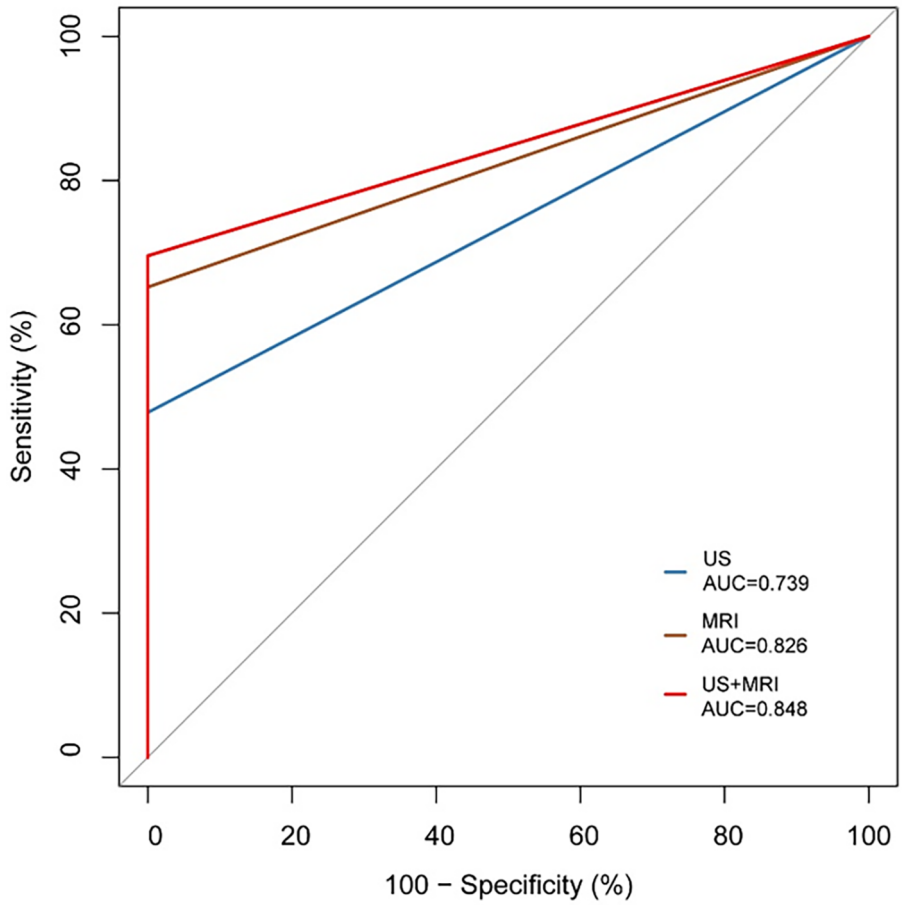

FIGURE 5
Comparison of the ROC of ultrasound and MRI in diagnosing TSC.

cardiac tumors were composed of irregular, swollen cardiomyocytes with vacuolated cytoplasm (Figure 6). In three cases, pathology identified more rhabdomyomas than were initially diagnosed by prenatal ultrasound, with these lesions located within the ventricular wall, often measuring less than 5 mm in diameter. Many of the lesions were only 1–2 mm, making them challenging to detect via ultrasound.

Comparison of heart lesions between the TSC group and simple CR group

Multiple lesions were notably more common in the TSC group (32/35, 91.4%) than in the simple CR group (7/13, 53.8%) with a *p*-value of 0.007, suggesting a higher likelihood of multiple Cardiac Rhabdomyomas (CR) in conjunction with Tuberous Sclerosis Complex (TSC). However, the mean maximum tumor diameter did not significantly differ between the two groups, measuring 11.94 ± 5.64 mm in the TSC group and 11.15 ± 6.00 mm in the simple CR group ($p = 0.672$). Of the 22 live births, 12 were diagnosed with TSC, while 10 were diagnosed with simple CR. These cases were followed up with echocardiography for 3 to 36 months. Among the 22 live births, 27.3% (6/22) experienced tumor disappearance, 54.5% (12/22) saw regression, and 18.2% (4/22) showed no change. In the 12 TSC cases, the rates were 25.0% (3/12), 58.3% (7/12), and 16.7% (2/12), respectively, and in the 10 simple CR cases, the rates were 30.0% (3/10), 50.0% (5/10), and 20.0% (2/10), respectively. No significant difference was observed between the TSC and simple CR groups ($P = 1.000$), shown in Table 2.

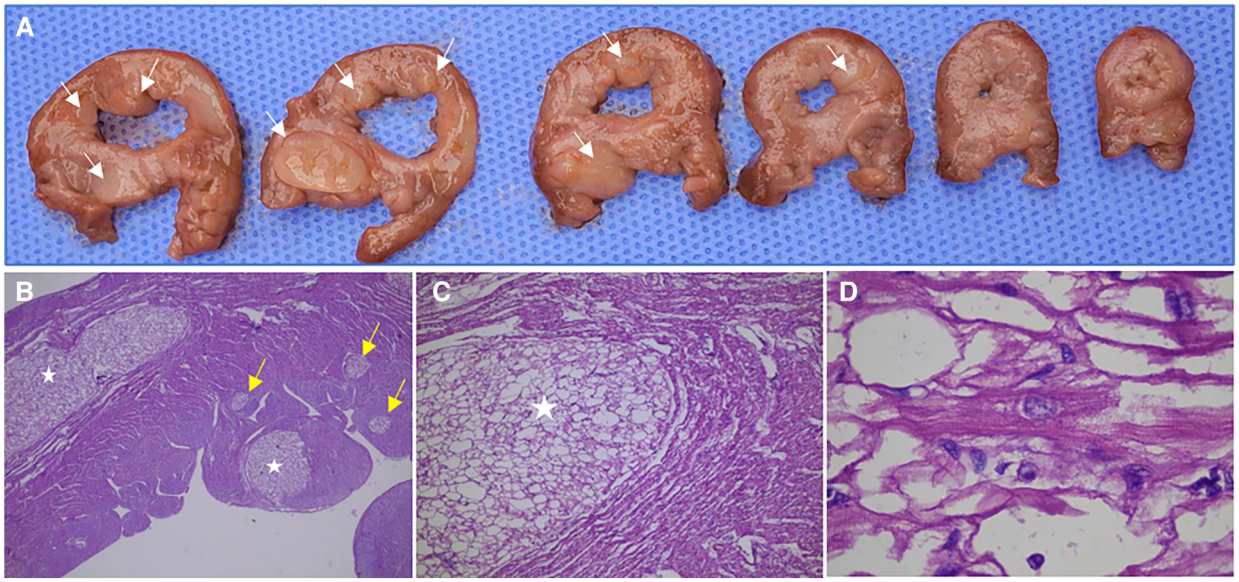

FIGURE 6
Anatomical and pathological specimens of a fetus (case NO. 51) terminated at 31 weeks of gestation. (A) Multiple rhabdomyomas in the left ventricle and interventricular septum were observed in continuous transverse sections. (B) The sections were stained by HE and observed by ×25 magnification, showing multiple intramyocardial rhabdomyomas, some of which were only 1–3 mm in diameter (yellow arrow). (C) The sections were stained by HE and observed by ×50 magnification, showing a rhabdomyoma in the myocardium. (D) The sections were stained by HE and observed by ×250 magnification, showing the cell morphology and arrangement in rhabdomyoma. The cardiac tumors were composed of irregular and swollen cardiomyocytes with vacuolated cytoplasm.

TABLE 2 Comparison of CR by ultrasound between the CR with TSC and simple CR groups.

	CR with TSC	Simple CR	
Number of tumors			
Single	3/35 (8.6%)	6/13 (46.2%)	$P = 0.007$
Multiple	32/35 (91.4%)	7/13 (53.8%)	
Max diameter	11.94 ± 5.64 mm	11.15 ± 6.00 mm	$P = 0.672$
Postnatal change in size			
Progression	0/12 (0%)	0/10 (0%)	$P = 1.000$
No change	2/12 (16.7%)	2/10 (20.0%)	
Decrease	7/12 (58.3%)	5/10 (50.0%)	
Disappear	3/12 (25.0%)	3/10 (30.0%)	

TABLE 3 The clinical manifestations of live-born fetuses with TSC ($N = 12$).

Epilepsy	*n* (%)
Present	10/12 (83.3%)
Absent	2/12 (16.7%)
Neurodevelopmental status	
Severe dysfunction	4/12 (33.3%)
Mild dysfunction	3/12 (25.0%)
Normal	5/12 (41.7%)
Other organs disability	
Skin hypomelanotic macules	9/12 (75.0%)
Eyes retinal hamartomas	3/12 (25.0%)
Eyes retinal pigment degeneration	1/12 (8.3%)
Kidney angiolipomas	1/12 (8.3%)
Kidney multiple renal cysts	2/12 (16.7%)

Survival Status and prognosis of live birth

Out of the 12 surviving patients diagnosed with Tuberous Sclerosis Complex (TSC), 10 (83.3%) experienced epilepsy, 4 (33.3%) had severe neurodevelopmental dysfunction, 3 (25.0%) had mild neurodevelopmental dysfunction, 9 (75.0%) had skin hypomelanotic macules, 3 (25.0%) had eye retinal hamartomas, 1 (8.3%) had eye retinal pigment degeneration, 2 (16.7%) had multiple renal cysts, and 1 (8.3%) had kidney angiolipomas. Clinical manifestations in live-born TSC patients are detailed in Tables 3 and 4. Ten children with simple Cardiac Rhabdomyomas (CR) were monitored for 6 months to 6 years, displaying good growth and development without TSC-related clinical symptoms. Among live births with prenatal intracardiac complications, one patient exhibited antepartum arrhythmias but had an average heart rate during the third trimester and after birth. Two patients had left ventricular outflow tract obstruction, with the number of lesions decreasing and the outflow tract obstruction gradually improving after birth.

Discussion

CR is the most common type of fetal primary cardiac tumor, with an incidence of 60%, followed by fibromas, teratomas, myxomas, and hemangiomas (3). Each tumor type displayed distinct features. Teratomas typically originate in the pericardium, with mixed echoes, cystic structures, and possible

TABLE 4 The outcomes of live-born children with cardiac rhabdomyoma.

Case	TSC	Diagnostic basis	Epilepsy	Other organs disability	Neurodevelopmental status	Family history	CR change after birth
1	No	Genetic	Absent	Absent	Normal	No	6M decrease
2	No	Genetic	Absent	Absent	Normal	No	10M disappear
3	Yes	Genetic	Present	Skin hypomelanotic macules; Eyes retinal pigment degeneration; Kidney multiple renal cysts	Normal	No	12M disappear
4	No	Genetic	Absent	Absent	Normal	No	36M no change
5	Yes	Genetic	Present	Absent	Severe dysfunction	No	36M disappear
6	Yes	Clinical	Present	Skin hypomelanotic macules	Mild dysfunction	No	3M disappear
7	Yes	Clinical	Present	Skin hypomelanotic macules	Severe dysfunction	Yes	12M decrease
8	No	Genetic	Absent	Absent	Normal	No	12M decrease
9	Yes	Clinical	Present	Absent	Severe dysfunction	No	18M decrease
10	Yes	Genetic	Present	Skin hypomelanotic macules	Severe dysfunction	Yes	12M decrease
11	No	Genetic	Absent	Absent	Normal	No	24M decrease
12	No	Genetic	Absent	Absent	Normal	No	12M disappear
13	Yes	Clinical	Present	Skin hypomelanotic macules	Normal	No	24M no change
14	No	Clinical	Absent	Absent	Normal	No	6M decrease
15	No	Genetic	Absent	Absent	Normal	No	3M disappear
16	Yes	Clinical	Present	Skin hypomelanotic macules; Eyes retinal hamartomas; Kidney multiple renal cysts	Normal	No	12M decrease
17	No	Genetic	Absent	Absent	Normal	No	24M decrease
18	Yes	Genetic	Absent	Kidney angiolipomas	Normal	No	9M decrease
19	Yes	Genetic	Absent	Skin hypomelanotic macules; Eyes retinal hamartomas	Normal	No	24M no change
20	Yes	Genetic	Present	Skin hypomelanotic macules; Eyes retinal hamartomas	Mild dysfunction	No	6M decrease
21	No	Genetic	Absent	Absent	Normal	No	36M no change
22	Yes	Genetic	Present	Skin hypomelanotic macules	Mild dysfunction	No	6M decrease

calcifications, often associated with pericardial effusion. Fibromas and hemangiomas are usually solitary, large, and may or may not have calcifications. Myxomas are typically attached to the atria and move with the cardiac cycle. Malignant neoplasms of the fetal heart are rare (15). In the study, to distinguish CR from other cardiac tumors and reduce selection bias, experienced sonographers conducted rigorous fetal echocardiography. In addition, CR diagnoses were supported by family history, clinical symptoms, and genetic tests, and, in some cases, confirmed through multiple prenatal follow-ups, autopsies, or postpartum assessments by pediatricians. For live births, clinical diagnosis of CR is based on confirmation of TSC or tumor shrinkage or disappearance during follow-up, or prenatal and postnatal MRI and ultrasound diagnosis of CR.

It has been reported that the earliest antenatal sonographic detection of cardiac tumors was observed at 15 weeks of gestation, whereas most cases are described after 24 weeks of gestation (10). In this study, the earliest detection was at 23 weeks of gestation, with a median diagnosis at 29 weeks. The delay is often due to mid-term ultrasound screening at around 22 weeks and cases referred from other hospitals after second-trimester ultrasound screenings, resulting in delayed diagnoses. In general, these tumors have a minimal effect on cardiac function, only a few fetuses (15%) exhibited cardiac complications (7). In previous studies, tumor size strongly correlated with fetal mortality (24). In the present study, fetal cardiac complications were observed in 22.2% of cases, always associated with multiple lesions and larger tumor sizes, but there were no cases of fetal death in this study. Multiple lesions were prevalent in 83.3% of fetuses, primarily in the left ventricular wall, right ventricular wall, and interventricular septum, and the number and location of tumors in live infants were consistent with prenatal ultrasound findings, because imaging screening after birth could not detect smaller lesions. Large tumors near the ventricular septum often caused outflow tract obstructions. The results indicated that the number, size and location of the tumor were the main factors leading to intracardiac complications. Moreover, fetal cardiac tumors were sometimes associated with arrhythmias, and the specific type of arrhythmia depended on the tumor's location (25, 26). However, arrhythmias were rare in this study with one case of atrial premature beat without transmitting (presented as bigeminy coupled rhythm, the atrial rate was about 140 beats/min and the ventricular rate was about 70 beats/min) and one case of occasional atrial premature beat, possibly due to the absence of fetal magnetocardiography (FMCG) for accurate electrophysiological assessment of fetal rhythm. The fetus with atrial premature beat without transmitting had a normal postnatal heart rhythm, while the baby with occasional atrial premature beat was terminated.

However, we are more concerned with the relationship between fetal CR and TSC. TSC is a rare autosomal dominant disorder with

an incidence of 1/6,800~1/10,000 live births. It's caused by mutations in the TSC1 or TSC2 genes (27). Detecting intracranial lesions is crucial for diagnosing TSC in fetuses with CRs (28). Although neurological changes are currently difficult to detect in many fetuses with TSC, neuroimaging findings was a much more specific indication of genetic TSC and was proportional to poor prognosis (15). Ultrasound is commonly used for initial imaging, but MRI offers better sensitivity because of MRI provides better contrast between gray and white tissues (29). Previous studies indicated that intracranial nodules of TSC fetuses were rarely detected by ultrasound (11). In our study, intracranial nodules were found in 11 of 35 TSC (31.4%) fetuses by ultrasound with a relatively high detection rate, and combining ultrasound with MRI was the most effective for TSC detection, enhancing the identification of intracranial nodules. Our study highlighted the importance of using both abdominal and transvaginal ultrasound when a fetal heart tumor is identified for accurate diagnosis and prognosis evaluation, this approach improved intracranial nodule detection. And a combination of brain MRI and genetic testing aids in early TSC diagnosis, impacting perinatal management and prognosis.

It is worth mentioning that our study found difference between ultrasound and MRI in detecting fetal intracranial lesions. Previous studies have suggested that subependymal nodules are more easily identified on fetal imaging, however, subcortical lesions are more commonly detected in postnatal brain MRI (10). Our analysis of imaging data found that prenatal ultrasound mostly identifies nodules in the brain parenchyma (90.9%), while prenatal brain MRI primarily detects subependymal nodules (93.3%). For example, ultrasound detected brain parenchyma nodules in case NO. 51, while brain MRI found subependymal nodules (Figure 2). In case NO. 13, prenatal ultrasound identified multiple intracranial nodules, whereas prenatal brain MRI didn't show any abnormalities. However, postpartum ultrasound and neonatal brain MRI revealed intracranial nodules (Figure 4). These phenomena suggested that ultrasound might detect specific fetal brain lesions not visible on MRI, warranting further investigation.

Although both single and multiple CRs were listed as the primary diagnostic criteria for TSC (23), the probability of a diagnosis of TSC varied according to the number of CRs. The presence of multiple CRs is considered a strong predictor of prenatal TSC, with a 95% risk of TSC diagnosis (19, 30). In our study, the TSC group had more multiple intracardiac lesions then simple CR group ($p = 0.007$), aligning with prior research. Notably, the maximum tumor diameter didn't differ significantly between the TSC group and simple CR group ($p = 0.672$). Therefore, multiple CRs has predictive value in the diagnosis of TSC, while the maximum tumor diameter has no significance. In some cases, autopsy revealed more tumors than prenatal ultrasound, which small lesions (1–2 mm) in the ventricular wall went undetected during ultrasound. This underscores the importance of comprehensive scanning to ensure accurate lesion count, particularly in cases of CR with TSC, vital for TSC diagnosis and prognosis assessment.

While TSC is typically an autosomal dominant disorder, most cases result from *de novo* mutations (8, 13). Only 4 fetuses (11.4%) diagnosed with TSC in this study had a family history, family history plays a minor role in TSC diagnosis. Therefore, prenatal diagnosis and prognosis assessment are critical for pregnant individuals and their families. While imaging provides a valuable reference for prenatal TSC diagnosis, genetic sequencing of TSC1/2 exons has been used for a more definitive diagnosis. However, due to the cost and invasiveness of genetic testing, some pregnant individuals opt for termination without genetic testing, so imaging examination is particularly important. In this study, we sought to investigate the efficacy of ultrasound combined with MRI in diagnosing TSC, the result shown that 23 of the 30 fetuses undergoing both prenatal brain MRI and ultrasound were diagnosed with TSC, and 69.6% (16/23) of TSC cases were diagnosed using a combination of ultrasound and MRI, highlighting the sensitivity of this approach. Nevertheless, imaging cannot screen all fetuses with TSC, genetic sequencing remains a recommended method for detecting fetal CR and improving early TSC diagnosis, aiding in perinatal management and prognostic guidance.

Rhabdomyoma cells are glycogen-rich atypical cardiomyocytes, and most of their cytoplasm undergoes vacuolar degeneration and apoptosis after birth so that the tumor will slowly disappear (19). This trend may be influenced by changes in maternal hormone levels and may be related to the pathological basis of CRs. Among 22 live births in the study, CRs of 81.8% (18/22) cases disappeared or shrank after birth, and there was no significant difference in tumor changes between the TSC group and the simple CR group. There were 4 cases with no change in tumor volume, but this may not be the final result because most of the children did not adhere to long-term regular cardiac ultrasonography follow up after birth, the longest follow-up time of echocardiography was only 36 months (3–36 months). In addition, during regular follow-up during pregnancy, we observed that CRs were generally small, slow-growing, and almost unchanged during the third trimester, which was consistent with the self-limited growth pattern of CR. These features are helpful for ultrasound diagnosis of CR.

TSC often involves the central nervous system (CNS), causing epilepsy, cognitive issues, and developmental delays (31–33). Epilepsy is the most prominent neurologic feature in patients with TSC, occurring in 70%–90% of patients and usually occurring within the first year of life (23, 33). In this study, 10 of the 12 surviving TSC-diagnosed children had epilepsy and all occurred within the first year of life, and 4 had developmental delays, and 3 had growth retardation. TSC can also lead to skin issues, retinopathy, and problems with organs such as the kidney and liver (23). In this study, skin hypomelanotic macules were found in 9 cases, retinal hamartoma in 3 cases, retinal pigment degeneration in 1 case, multiple kidney renal cysts in 2 cases, and kidney angiolipomas in 1 case. Skin hypomelanotic macules were very common in children with TSC. The poor prognosis of children with TSC puts tremendous pressure on their families. For children without TSC, a positive prognosis was observed during 6 months to 6 years of follow-up, with no TSC-related symptoms. Patients with simple CR without TSC had better outcomes than those with TSC. Because of the difference in

prognosis between them, prognostic counselling for pregnant women with CR should include not only the prognosis of the tumor itself but also the relationship between CR and TSC and the prognosis of TSC, emphasizing the importance of thorough prenatal imaging evaluation and genetic analysis.

Limitation

Several study limitations warrant consideration. Firstly, there were instances of insufficient pathological data for certain cardiac tumors, and the absence of autopsy information. Secondly, the relatively short follow-up period for echocardiography in some live births may not have fully depicted postnatal changes in cardiac tumors. Lastly, the study did not analyze the prevalence of atrial septal defects (ASD) as comprehensive neuropsychological (NP) tests were not conducted for live births.

Conclusions

The characteristics of CRs in fetuses play a significant role in assessing fetal cardiac complications, particularly with TSC. Multiple CRs are a significant risk factor for TSC, irrespective of their size or location. Detecting small CRs via ultrasound can be challenging, potentially affecting prognosis assessment. Fetal heart enlargement and enhanced myocardial scanning are helpful for prognosis assessment. Ultrasound and MRI can reveal CRs with intracranial nodules and suggest TSC, though their diagnostic accuracy is limited. TSC gene sequencing is essential for a definitive diagnosis. CRs typically regress or shrink after birth, resulting in a good prognosis for children with isolated CRs. However, children with concurrent TSC often face a less favorable prognosis due to conditions like epilepsy and neurological abnormalities.

Data availability statement

The original contributions presented in the study are included in the article/Supplementary Material, further inquiries can be directed to the corresponding authors.

Ethics statement

The studies involving humans were approved by The study protocol was reviewed and approved by the Ethics Committee of the Fujian Maternal and Child Health Hospital, with informed consent from all pregnant women. The studies were conducted in accordance with the local legislation and institutional requirements. The participants provided their written informed consent to participate in this study. Written informed consent was obtained from the individual(s) for the publication of any potentially identifiable images or data included in this article.

Author contributions

LP: Formal Analysis, Methodology, Writing – original draft, Writing – review & editing. YC: Data curation, Formal Analysis, Writing – original draft. JW: Conceptualization, Resources, Writing – review & editing. WL: Data curation, Methodology, Resources, Writing – review & editing. QW: Formal Analysis, Methodology, Resources, Validation, Writing – review & editing. SG: Data curation, Investigation, Resources, Writing – review & editing. BH: Methodology, Writing – review & editing. CJ: Methodology, Resources, Supervision, Writing – review & editing. ZW: Data curation, Funding acquisition, Investigation, Supervision, Writing – original draft.

Funding

The author(s) declare financial support was received for the research, authorship, and/or publication of this article.

This study was supported by Joint Funds for the innovation of science and technology of Fujian province (2020Y9156) and Fujian Natural Science Foundation (2021J01420).

Acknowledgments

The authors thank for the support from Department of Pathology and Department of Obstetrics, Fujian Maternity and Child Health Hospital, College of Clinical Medicine for Obstetrics & Gynecology and Pediatrics, Fujian Medical University, Fuzhou, China. We also thank all the patients and families for their understanding and support.

Conflict of interest

The authors declare that the research was conducted in the absence of any commercial or financial relationships that could be construed as a potential conflict of interest.

Publisher's note

References

1. Padalino MA, Reffo E, Cerutti A, Favero V, Biffanti R, Vida V, et al. Medical and surgical management of primary cardiac tumours in infants and children. *Cardiol Young*. (2013) 24(2):268–74. doi: 10.1017/s104795111300022x

2. Morka A, Kohut J, Radzymińska-Chruściel B, Mroczek T, Gładki M, Weryński P, et al. Echocardiography and newer imaging techniques in diagnosis and long-term follow-up of primary heart tumors in children. *Int J Environ Res Public Health*. (2020) 17(15):5471. doi: 10.3390/ijerph17155471

3. Yuan S-M. Fetal primary cardiac tumors during perinatal period. *Pediatr Neonatol*. (2017) 58(3):205–10. doi: 10.1016/j.pedneo.2016.07.004

4. Isaacs H. Fetal and neonatal cardiac tumors. *Pediatr Cardiol*. (2004) 25(3):252–73. doi: 10.1007/s00246-003-0590-4

5. Yuan S-M. Fetal cardiac tumors: clinical features, management and prognosis. *J Perinat Med*. (2018) 46(2):115–21. doi: 10.1515/jpm-2016-0311

6. Pluym ID, Sklansky M, Wu JY, Afshar Y, Holliman K, Devore GR, et al. Fetal cardiac rhabdomyomas treated with maternal sirolimus. *Prenat Diagn*. (2020) 40 (3):358–64. doi: 10.1002/pd.5613

7. Chen J, Wang J, Sun H, Gu X, Hao X, Fu Y, et al. Fetal cardiac tumor: echocardiography, clinical outcome and genetic analysis in 53 cases. *Ultrasound Obstet Gynecol*. (2019) 54(1):103–9. doi: 10.1002/uog.19108

8. Zhen L, Yang Y-D, He Y, Pan M, Han J, Yang X, et al. Prenatal genetic diagnosis of cardiac rhabdomyoma: a single-center experience. *Eur J Obstetr Gynecol Reprod Biol*. (2020) 249:7–10. doi: 10.1016/j.ejogrb.2020.03.051

9. Słowińska M, Jóźwiak S, Peron A, Borkowska J, Chmielewski D, Sadowski K, et al. Early diagnosis of tuberous sclerosis complex: a race against time. How to make the diagnosis before seizures? *Orphanet J Rare Dis*. (2018) 13(1):25. doi: 10.1186/s13023-018-0764-z

10. Dragoumi P, O'Callaghan F, Zafeiriou DI. Diagnosis of tuberous sclerosis complex in the fetus. *Eur J Paediatr Neurol*. (2018) 22(6):1027–34. doi: 10.1016/j.ejpn.2018.08.005

11. Altmann J, Kiver V, Henrich W, Weichert A. Clinical outcome of prenatally suspected cardiac rhabdomyomas of the fetus. *J Perinat Med*. (2019) 48(1):74–81. doi: 10.1515/jpm-2019-0246

12. Henske EP, Jozwiak S, Kingswood JC, Sampson JR, Thiele EA. Tuberous sclerosis complex. *Nat Rev Dis Primers*. (2016) 2:16035. doi: 10.1038/nrdp.2016.35

13. Curatolo P, Moavero R, Roberto D, Graziola F. Genotype/phenotype correlations in tuberous sclerosis complex. *Semin Pediatr Neurol*. (2015) 22(4):259–73. doi: 10.1016/j.spen.2015.10.002

14. Cotter JA. An update on the central nervous system manifestations of tuberous sclerosis complex. *Acta Neuropathol*. (2020) 139(4):613–24. doi: 10.1007/s00401-019-02003-1

15. Qi Y, Ding H, Huang Y, Zeng Y, Yu L, Liu L, et al. A multidisciplinary approach in prenatal diagnosis of TSC with cardiac rhabdomyoma as the initial symptom. *Front Pediatr*. (2021) 9:628238. doi: 10.3389/fped.2021.628238

16. Rubilar C, Lopez F, Troncoso M, Barrios A, Herrera L. Clinical and genetic study patients with tuberous sclerosis complex. *Rev Chil Pediatr*. (2017) 88(1):41–9. doi: 10.1016/j.rchipe.2016.08.003

17. Goergen SK, Fahey MC. Prenatal MR imaging phenotype of fetuses with tuberous sclerosis: an institutional case series and literature review. *Am J Neuroradiol*. (2022) 43(4):633–8. doi: 10.3174/ajnr.A7455

18. Pavlicek J, Klaskova E, Kapralova S, Prochazka M, Vrtel R, Gruszka T, et al. Fetal heart rhabdomyomatosis: a single-center experience. *J Matern Fetal Neonatal Med*. (2021) 34(5):701–7. doi: 10.1080/14767058.2019.1613365

19. Sciacca P, Giacchi V, Mattia C, Greco F, Smilari P, Betta P, et al. Rhabdomyomas and tuberous sclerosis complex: our experience in 33 cases. *BMC Cardiovasc Disord*. (2014) 14:66. doi: 10.1186/1471-2261-14-66

20. Cavalcante C, Pinto Junior VC, Pompeu RG, Teles A, Bandeira JA, Maia ICL, et al. Perinatal unusual rhabdomyoma location—case report and systematic reviews of the literature. *J Matern Fetal Neonatal Med*. (2019) 34(1):137–51. doi: 10.1080/14767058.2019.1597044

21. Carvalho JS, Allan LD, Chaoui R, Copel JA, DeVore GR, Hecher K, et al. ISUOG practice guidelines (updated): sonographic screening examination of the fetal heart. *Ultrasound Obstet Gynecol*. (2013) 41(3):348–59. doi: 10.1002/uog.12403

22. Salomon LJ, Alfirevic Z, Berghella V, Bilardo C, Hernandez-Andrade E, Johnsen SL, et al. Practice guidelines for performance of the routine mid-trimester fetal ultrasound scan. *Ultrasound Obstet Gynecol*. (2011) 37(1):116–26. doi: 10.1002/uog.8831

23. Northrup H, Krueger DA, Northrup H, Krueger DA, Roberds S, Smith K, et al. Tuberous sclerosis complex diagnostic criteria update: recommendations of the 2012 international tuberous sclerosis complex consensus conference. *Pediatr Neurol*. (2013) 49(4):243–54. doi: 10.1016/j.pediatrneurol.2013.08.001

24. Okmen F, Ekici H, Hortu I, Imamoglu M, Ucar B, Ergenoglu AM, et al. Outcomes of antenatally diagnosed fetal cardiac tumors: a 10-year experience at a single tertiary referral center. *J Matern Fetal Neonatal Med*. (2020) 35(18):3489–94. doi: 10.1080/14767058.2020.1822316

25. Wacker-Gussmann A, Strasburger JF, Cuneo BF, Wiggins DL, Gotteiner NL, Wakai RT. Fetal arrhythmias associated with cardiac rhabdomyomas. *Heart Rhythm*. (2014) 11(4):677–83. doi: 10.1016/j.hrthm.2013.12.018

26. Niewiadomska-Jarosik K, Stańczyk J, Janiak K, Jarosik P, Moll JJ, Zamojska J, et al. Prenatal diagnosis and follow-up of 23 cases of cardiac tumors. *Prenat Diagn*. (2010) 30(9):882–7. doi: 10.1002/pd.2586

27. Wang C-C, Wang C-Y, Lai Y-J, Chang T-Y, Su H-Y. Prenatal diagnosis of tuberous sclerosis complex using fetal ultrasonography and magnetic resonance imaging and genetic testing. *Taiwan J Obstet Gynecol*. (2018) 57(1):163–5. doi: 10.1016/j.tjog.2017.12.029

28. Ebrahimi-Fakhari D, Mann LL, Poryo M, Graf N, von Kries R, Heinrich B, et al. Incidence of tuberous sclerosis and age at first diagnosis: new data and emerging trends from a national, prospective surveillance study. *Orphanet J Rare Dis*. (2018) 13(1):117. doi: 10.1186/s13023-018-0870-y

29. Falip C, Hornoy P, Millischer Bellaïche AE, Merzoug V, Adamsbaum C. Imagerie par résonance magnétique (IRM) fœtale cérébrale: indications, aspects normaux et pathologiques. *Rev Neurol (Paris)*. (2009) 165(11):875–88. doi: 10.1016/j.neurol.2009.01.036

30. Słowińska M, Kotulska-Jóźwiak K, Sadowski K, Szymkiewicz-Dangel J, Bokiniec R, Borszewska-Kornacka M, et al. Multiple cardiac tumours as a biomarker of tuberous sclerosis complex in children below two years of age. *Pediatr Pol*. (2018) 93(2):132–8. doi: 10.5114/polp.2018.76248

31. Uysal SP, Sahin M. Tuberous sclerosis: a review of the past, present, and future. *Turk J Med Sci*. (2020) 50(SI-2):1665–76. doi: 10.3906/sag-2002-133

32. Salussolia CL, Klonowska K, Kwiatkowski DJ, Sahin M. Genetic etiologies, diagnosis, and treatment of tuberous sclerosis complex. *Annu Rev Genomics Hum Genet*. (2019) 20:217–40. doi: 10.1146/annurev-genom-083118-015354

33. Portocarrero LKL, Quental KN, Samorano LP, Oliveira ZNP, Rivitti-Machado M. Tuberous sclerosis complex: review based on new diagnostic criteria. *An Bras Dermatol*. (2018) 93(3):323–31. doi: 10.1590/abd1806-4841.20186972

frontiers | Frontiers in Cardiovascular Medicine

TYPE Original Research
PUBLISHED 06 March 2024
DOI 10.3389/fcvm.2024.1341005

OPEN ACCESS

EDITED BY
Liqun Sun,
University of Toronto, Canada

REVIEWED BY
Fabrizio De Rita,
Newcastle upon Tyne Hospitals NHS Foundation Trust, United Kingdom
Sheng Zhao,
Hubei Maternal and Child Health Hospital, China

*CORRESPONDENCE
Zongjie Weng
✉ wengzongjie1984@fjmu.edu.cn
Qiumei Wu
✉ wqm0620@fjmu.edu.cn

†These authors have contributed equally to this work

RECEIVED 19 November 2023
ACCEPTED 26 February 2024
PUBLISHED 06 March 2024

CITATION
Guo J, Ling W, Dang T, Guo S, Ma H, Huang Q, Zeng L, Weng Z and Wu Q (2024) Prenatal transposition of great arteries diagnosis and management: a Chinese single-center study. Front. Cardiovasc. Med. 11:1341005. doi: 10.3389/fcvm.2024.1341005

Prenatal transposition of great arteries diagnosis and management: a Chinese single-center study

Jie Guo[1†], Wen Ling[1†], Tingting Dang[1†], Shan Guo[1], Hong Ma[2], Qiong Huang[1], Liqin Zeng[1], Zongjie Weng[1*] and Qiumei Wu[1*]

[1]Department of Medical Ultrasonics, Fujian Maternity and Child Health Hospital, College of Clinical Medicine for Obstetrics & Gynecology and Pediatrics, Fujian Medical University, Fuzhou, China, [2]Department of Pathology, Fujian Maternity and Child Health Hospital, College of Clinical Medicine for Obstetrics & Gynecology and Pediatrics, Fujian Medical University, Fuzhou, China

Objective: This study aimed to assess the diagnostic value of prenatal echocardiography for identifying transposition of the great arteries (TGA) during pregnancy and evaluating the associated outcomes.
Methods: We conducted a retrospective analysis of 121 prenatally diagnosed patients with TGA at our hospital between January 2012 and September 2022. This analysis included prenatal ultrasound, prenatal screening, clinical management and follow-up procedures.
Results: Among the 103 fetuses considered in the study, 90 (87.4%) were diagnosed with complete transposition of the great arteries (D-TGA), while 13 (12.6%) exhibited corrected transposition of the great arteries (CC-TGA). Diagnoses were distributed across the trimester, with 8 D-TGA and 2 CC-TGA patients identified in the first trimester, 68 D-TGA patients and 9 CC-TGA patients in the second trimester, and 14 D-TGA and 2 CC-TGA patients referred for diagnosis in the third trimester. Induction of labour was pursued for 76 D-TGA patients (84.4%) and 11 CC-TGA patients (84.6%), and 14 D-TGA patients (15.6%) and 2 CC-TGA patients (15.4%) continued pregnancy until delivery. Among the D-TGA patients, 9 fetuses (10.0%) underwent surgery, two of which were inadvertent fatality, while the remaining seven experienced positive outcomes. Additionally, seven TGA patients received palliative care, leading to four fatalities among D-TGA patients (5.2%), whereas 1 D-TGA patients and 2 CC-TGA patients survived.
Conclusion: This study underscores the feasibility of achieving an accurate prenatal diagnosis of TGA during early pregnancy. The utility of prenatal ultrasound in the development of personalized perinatal plans and the application of multidisciplinary treatment during delivery are conducive.

KEYWORDS

early pregnancy, transposition of the great arteries, prenatal ultrasound, follow-up management, outcome

Introduction

Transposition of the great arteries (TGA) is a common congenital heart condition in which the aorta and pulmonary artery connections are switched (1). TGA account for 5%–7% of patients with congenital heart disease (2). TGA can be categorized into two types. In D-TGA (complete transposition), the atrioventricular connections are preserved, but the

ventricular and arterial connections are switched (3). Children with D-TGA are at risk of early pulmonary hypertension and heart failure, often leading to a high mortality rate if left untreated (4). In CC-TGA (corrected transposition), atrioventricular connections are inconsistent, but haemodynamics can be functionally corrected. Children with CC-TGA generally have a more favourable early prognosis. However, long-term complications may arise, such as severe tricuspid regurgitation, atrioventricular block, and right heart failure, often requiring late-stage surgery (5, 6). The outcome varies depending on the presence of associated abnormalities (7, 8).

Advances in prenatal ultrasound diagnostics have significantly improved the detection rate of TGA in fetuses, increasing from 6% in the 1990s to a range of 38% to 68% in recent years (9, 10). Early pregnancy now allows for the detection of TGA (11). Fetal echocardiography offers a means to enhance postnatal risk assessment for TGA (12, 13). This, in turn, enables a comprehensive approach, combining integrated diagnosis with perinatal management tailored to varying risk levels. While there may be relatively high perioperative mortality, the long-term survival of TGA patients is notably positive (14), with 15-year survival rates reaching as high as 90% (15, 16).

Accurate prenatal diagnosis is pivotal for effective prenatal counselling and provides the foundation for early postnatal intervention and treatment. Experts need to issue detailed prenatal reports to facilitate counselling and enable early intervention and treatment. A comprehensive assessment by ultrasound, obstetrics, and paediatric cardiac surgeons during pregnancy is crucial for integrated perinatal management. However, most related studies have focused primarily on obstetrics and paediatric cardiac surgery (17, 18). Fetal echocardiography has the opportunity to perform more accurate postnatal risk stratification for TGA and provide conditions for the combined integrated diagnosis, treatment and management. Our study aimed to explore the relationships between intracardiac and extracardiac malformations, chromosomal abnormalities, the intrauterine course, and postnatal outcomes. We sought to evaluate the value of ultrasonography for diagnosing TGA in fetuses during early pregnancy. Our goal is to improve the prenatal diagnosis and perinatal management of TGA, ultimately leading to improved pregnancy outcomes.

Materials and methods

Study population

From January 2012 to September 2022, 121 pregnant women were diagnosed with TGA in the Department of Ultrasound Medicine at Fujian Maternity and Child Health Care Hospital. Of these, 103 pregnant women met the inclusion criteria. The average maternal age was 28.79 ± 4.30 years, and the gestational age ranged from 12 to 39 weeks, with an average of 180.12 ± 25.16 days. All pregnant women and their families were informed about the study and provided consent. The study was approved by the Ethics Committee of Fujian Maternity and Child Health Care Hospital (2018-017). Pregnant women who met criteria (1) and (2) or (3) were included in the study: (1) underwent routine prenatal screening with complete measurements; (2) had pathological examinations, such as cardiac micropathological anatomy during early pregnancy, heart topographic anatomy, or cardiovascular casting during mid-pregnancy, were completed; and (3) had fetal echocardiography, prenatal diagnosis and neonatal congenital heart disease screening performed at our hospital. For women who opted for pregnancy termination, informed consent was obtained to verify the local pathological anatomy or vascular cast.

Study protocol

The GE Voluson E8 and E10 ultrasonic diagnostic devices were utilized for prenatal assessments. A convex array probe with a frequency range of 2.0–9.0 MHz was used for transabdominal examinations. In patients suspected of having TGA during early pregnancy, an intracavitary probe with a frequency range of 5.0–8.0 MHz was selected. In the neonatal period, the Phillips IPEIQ 7C device was used, and a phased array probe with a frequency ranging from 3.0 to 8.0 MHz was chosen for the examinations. For perinatal management and the collection of follow-up outcomes, relevant data were gathered from medical records.

Ultrasound examination

Fetal heart exams, including four-section, nine-section, and two-section examinations, were performed during the first, second, and third trimesters, respectively (19, 20). These examinations involved sequential segmental analysis to observe the positions of the atria, ventricles, and great arteries in fetuses with suspected TGA. The primary focus was on assessing the connections between the atria and ventricles, connections between the ventricles and great arteries, the branches and characteristics of the great arteries, the presence of a cross relationship between the great arteries, and the existence of a ventricular septal defect (VSD) and outflow tract stenosis. For fetuses without a VSD, the size and blood flow of the foramen ovale and ductus arteriosus were evaluated. Additionally, the presence of other extracardiac malformations was also observed during these examinations.

Prenatal screening and diagnosis

Prenatal diagnosis is strongly recommended for all fetuses with TGA. This diagnostic process includes noninvasive methods such as noninvasive prenatal genetic testing (NIPT) for screening fetal chromosomal aneuploidy and mid-trimester serological screening (Down's syndrome screening) for additional genetic assessment. In cases where further evaluation was necessary, amniocentesis and umbilical vein puncture were

carried out with informed consent from the pregnant women and their families. Subsequently, G-banded karyotype analysis and single nucleotide polymorphism microarray (SNP array) analysis were performed to evaluate the genetic makeup of the fetuses. These genetic assessments were conducted using fetal tissues or umbilical vein blood, particularly for patients who underwent induced labour.

Multidisciplinary consultation and verification

For women who opted to continue their pregnancy, our center offered a streamlined process that included assistance in diagnosis and treatment. These steps involved regular ultrasound examinations, the creation of personalized pregnancy plans, collaboration among the obstetrics, ultrasound, and paediatrics departments for neonatal care during delivery, and prompt referral to a paediatric cardiac surgeon when necessary. Live-born infants underwent echocardiography and other imaging examinations at our hospital. Periodic echocardiography is recommended for children undergoing surgery, with follow-up intervals of 6 months and every year after surgery. For all live born children, we followed up by telephone communication. Patients who declined access or could not be reached after three attempts were considered lost to follow-up.

Statistical analysis

The data analysis was performed using SPSS Statistics 26 software. Descriptive statistics methods were used to summarize and analyse the relevant data. Quantitative data are expressed as the mean ± standard deviation, while qualitative data are presented in terms of frequencies (n) and percentages (%). A significance level of $P < 0.05$ was used to indicate the statistical significance threshold.

Results

In this study, we assessed 103 fetuses, initially totalling 121 patients with TGA, with 18 patients lost to follow-up. In early pregnancy, D-TGA exhibited characteristic features, including rightward-bent great vessels in the three-vessel-tracheal view, juxtaposed great vessels in the outflow tract oblique view, and consistent atrioventricular connections in the four-chamber view (Figure 1). In the second trimester, the aorta was connected to the right ventricle, and the pulmonary artery was connected to the left ventricle (Figure 2). In early pregnancy, both arteries ran parallel to the aorta anterior to the pulmonary artery congenitally. CC-TGA patients presented with discordant atrioventricular connections (Figure 3). In the second trimester, there were reversed ventricular positions, parallel outflow tracts, pulmonary arteries from the left ventricle, and the aorta from the right ventricle positioned anterior to the pulmonary arteries (Figure 4). The earliest diagnosis occurred at 12 weeks and 3 days of gestation, and 10 mothers (9.7%) were of advanced maternal age. The TGA distribution included 90 D-TGA patients and 13 CC-TGA patients. Diagnoses were made in the first (8 D-TGA, 2 CC-TGA), second (68 D-TGA, 9 CC-TGA), and third trimesters (14 D-TGA, 2 CC-TGA).

Combined intracardiac and extracardiac abnormalities

We observed that 80 (77.7%) TGA patients presented with intracardiac malformations, while 31 (30.0%) exhibited extracardiac abnormalities. Among the D-TGA patients, 56 (62.2%) had ventricular septal defects (VSDs), 19 (21.1%) had pulmonary artery stenosis, and 9 (10.0%) had tricuspid valve abnormalities. Common extracardiac abnormalities in D-TGA included fetal growth restriction in 11 fetuses (12.2%), thickening of the nuchal translucency/nuchal fold (NT/NF) in 5 fetuses (5.5%), and the presence of a single umbilical artery in 3 fetuses (3.3%). In the

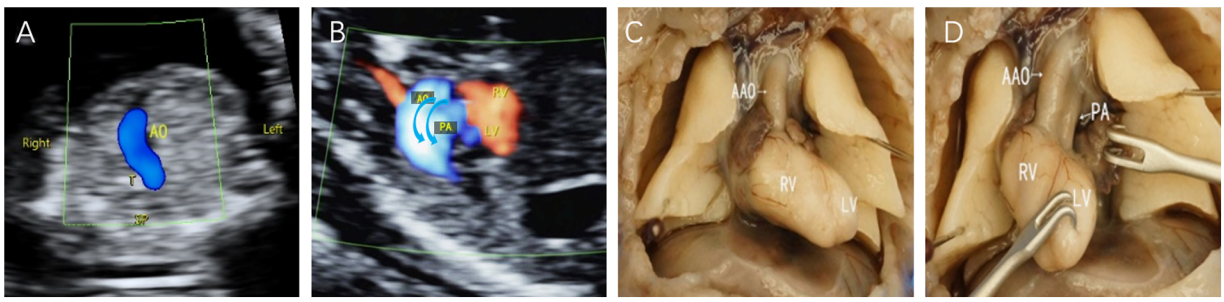

FIGURE 1
Fetal D-TGA patients were assessed via echocardiography at 13 weeks and 2 days. (A) 3VT view showing only one large artery running anteriorly to the right in a "dart-like" pattern. (B) Oblique thoracic view showing the juxtaposition of large vessels. (C,D) Microscopic dissection of the heart: the two large arteries are aligned in parallel, with the aorta located anteriorly to the right of the right ventricle; the pulmonary artery is located posteriorly to the left of the left ventricle.

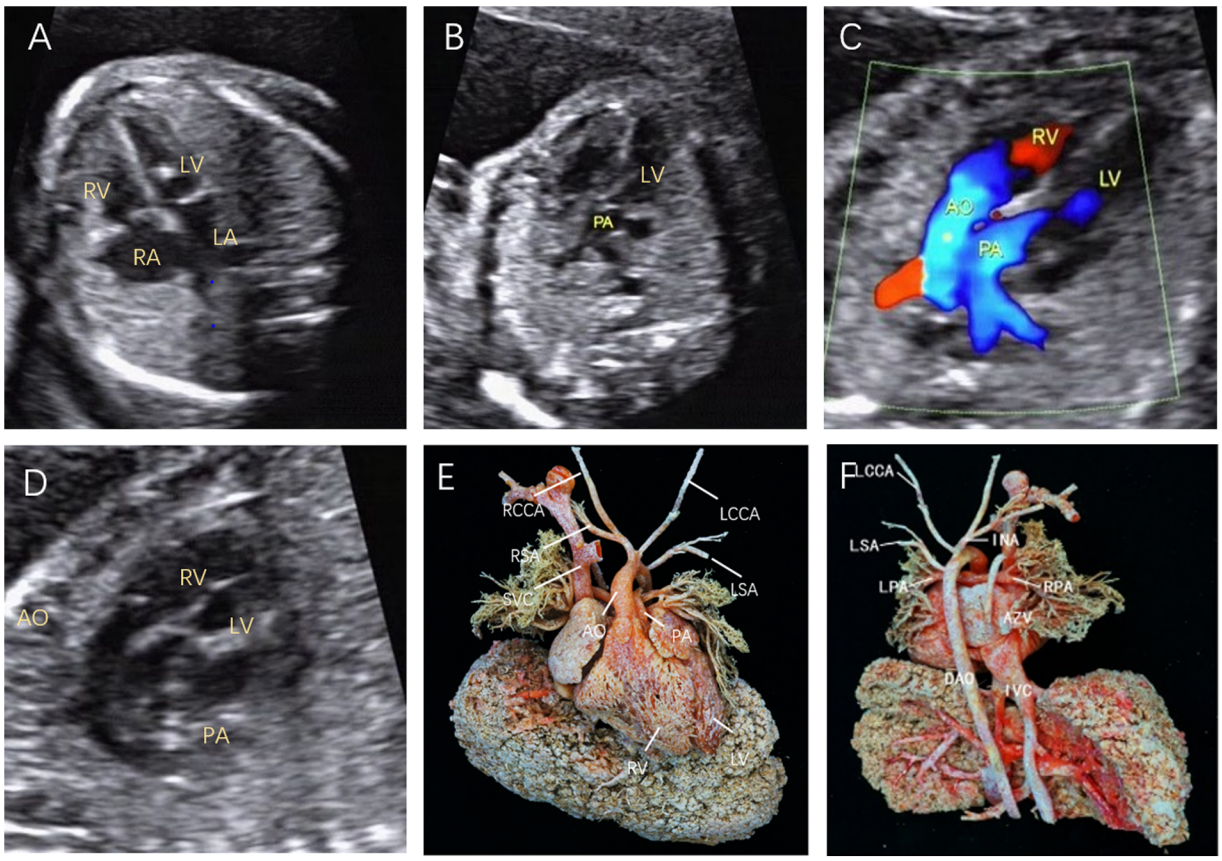

FIGURE 2
Fetal D-TGA was assessed via echocardiography at 23 weeks and 1 day. (**A**) Four-chamber view with consistent atrioventricular connections and strong dotted echogenicity of the left ventricle. (**B**) Five-chamber view showing the pulmonary artery emanating from the left ventricle and bifurcating into the left and right pulmonary arteries a short distance from the beginning of the artery. (**C**) Two large arteries aligned in parallel, with the aorta emanating from the right ventricle and located anteriorly to the pulmonary artery. (**D**) Long-axis view of the great vessels: the aortic arch emanates from the anterior right ventricle, followed by the head and neck vessels, which curl backwards in a 'hockey puck' shape, and the pulmonary artery follows a 'crutch' shape in the long-axis view. (**E**) Anatomical cast: frontal view. F: anatomical cast: dorsal view.

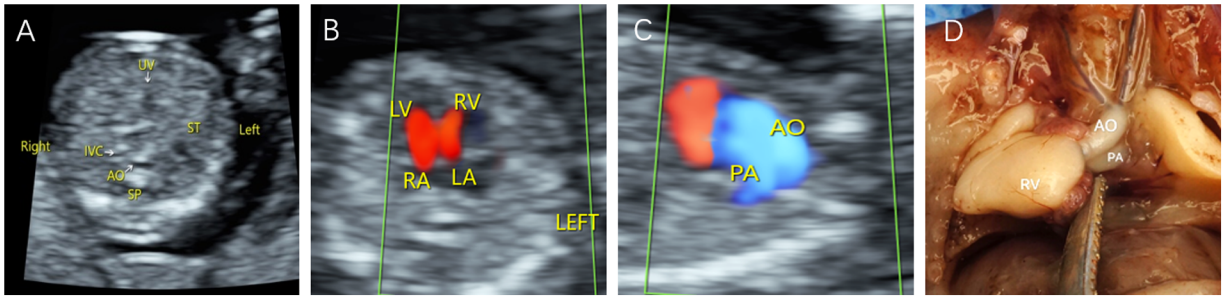

FIGURE 3
Fetal CC-TGA identified by echocardiography at 12 weeks and 6 days. (**A**) The inferior vena cava and descending aorta are located on the right side of the spine, and the gastric vesicle is on the left side. (**B**) The heart is located in the middle of the thoracic cavity with the apices facing right, and inconsistent atrioventricular connections are observed in the four-chamber view. (**C**) The aorta originates from the right ventricle, the pulmonary artery originates from the left ventricle, and the two great arteries are aligned in parallel. (**D**) Microscopic dissection of the heart: CC-TGA of the right heart.

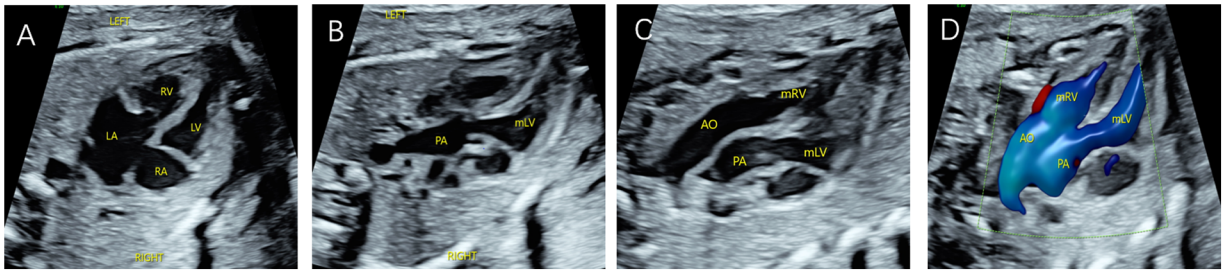

FIGURE 4
Fetal CC-TGA case confirmed by echocardiography at 23 weeks and 4 days. (A) Four-chamber heart view showing inconsistent atrioventricular connections, with the left atrium connected to the morphological right ventricle and the right atrium connected to the morphological left ventricle. (B–D) Right ventricular outflow tract view showing the pulmonary artery arising from the morphological left ventricle and left ventricular outflow tract view showing the aorta arising from the morphological right ventricle, with the aorta located anteriorly to the left of the pulmonary artery.

case of CC-TGA, the most prevalent intracardiac abnormality was VSD in 8 patients (61.5%), with 5 patients (38.5%) exhibiting pulmonary artery stenosis and 2 patients (15.4%) exhibiting tricuspid valve abnormalities, as detailed in Table 1.

Prenatal screening and diagnosis

Prenatal screening: Among the 103 fetuses diagnosed with transposition of the great arteries (TGA), 46 underwent prenatal screening for Down syndrome. This group included 7 high-risk fetuses, 6 fetuses with D-TGA, and 1 fetus with CC-TGA. Additionally, 16 fetuses underwent NIPT, all of which were classified as low risk. Prenatal Diagnosis: Of the 103 TGA-affected fetuses, 40 underwent prenatal diagnosis. Specifically, 32 patients underwent amniocentesis, while in 8 patients, prenatal diagnosis was carried out using umbilical vein blood samples obtained after labour induction. Chromosomal abnormalities were ascertained in 3 fetuses, encompassing 1 instance of standard trisomy 18, 1 case of partial trisomy 5, and 1 case of 21pstk + polymorphism. Subsequently, all three mothers elected to terminate their pregnancies via labour induction during the second trimester. Comprehensive details are available in Table 2.

TABLE 1 TGA combined with malformations.

Combined malformations	D-TGA	CC-TGA	Total number
None	21	2	23
Ventricular septal defect	56	8	64
Pulmonary artery stenosis	19	5	24
Tricuspid valve abnormalities	9	2	11
Right aortic arch	6	1	7
Strongly echogenic ventricular foci	5	0	5
Type II atrioventricular block of degree II	0	1	1
Other intracardiac malformations	8	3	11
Fetal growth restriction	11	0	11
NT/NF thickening	5	0	5
Single umbilical artery	3	0	3
Visceral inversion	1	0	1
Fetal nasal bone dysplasia	1	0	1

Other rare combined intracardiac malformations, such as a slightly narrowed aortic arch, right-sided heart, left subclavian artery vagus, and permanent left superior chamber.

Outcome and prognosis

In the present study, 8 D-TGA patients were identified early in pregnancy. Six patients underwent induction of labour (Figures 1C,D), and two were induced in the second trimester. Additionally, 68 D-TGA patients were diagnosed in the second trimester. Of these, 62 underwent induction (Figures 2E,F), and six were observed until delivery. Fourteen patients with late-stage D-TGA were referred to our hospital. Six mothers underwent induction therapy, seven mothers continued their pregnancies at our hospital, and one delivered elsewhere (Figure 5). Fourteen patients experienced continued pregnancies and delivered full-term without preterm issues. Postnatal echocardiography confirmed D-TGA (Figure 6). Among the 9 children (10.0%) who underwent surgery, two passed away postoperatively. The remaining 7 patients achieved positive outcomes. Four children (5.2%) were discharged without surgery due to conditions such as pulmonary inflammation. One (1.3%) patient had no surgery and maintained a positive prognosis by telephone follow-up, as presented in Table 3.

Two fetuses with CC-TGA were diagnosed in early pregnancy, and both of their mothers chose to induce labour, as presented in Figure 3D. Nine fetuses with CC-TGA were diagnosed in the second trimester; 8 of the fetuses chose to undergo induction of labour, and 1 of the mothers continued pregnancy. Two fetuses with CC-TGA were referred to our hospital in late pregnancy, and after ultrasound confirmation of the diagnosis of CC-TGA in our hospital, the mother of 1 patient chose to induce labour, and the mothers of the other fetuses continued the pregnancy and were delivered at our hospital (Figure 5). Two pregnant women all were monitored until delivery at term without premature delivery. The postnatal echocardiographic findings of fetuses with CC-TGA were consistent with the prenatal findings;

TABLE 2 Prenatal screening and prenatal diagnosis in fetal TGA.

	Specimens	Results	D-TGA	CC-TGA	Total
Down's syndrome	Peripheral blood in pregnant women	High risk	6	1	7
	Peripheral blood in pregnant women	Low risk	36	3	39
NIPT	Peripheral blood in pregnant women	Low risk	14	2	16
Chromosome karyotype	Fetal umbilical vein	No significant abnormalities seen	2	0	2
	Amniotic fluid	No significant abnormalities seen	25	3	28
	Amniotic fluid	21pstk + polymorphism.	1	0	1
	Amniotic fluid	Partial trisomy 5	1	0	1
	Amniotic fluid	Standard trisomy 18	1	0	1
Single nucleotide polymorphism microarray	Fetal umbilical vein	No pathogenic genome found	5	1	6
	Amniotic fluid	No pathogenic genome found	19	1	20

NIPT: noninvasive prenatal genetic testing.

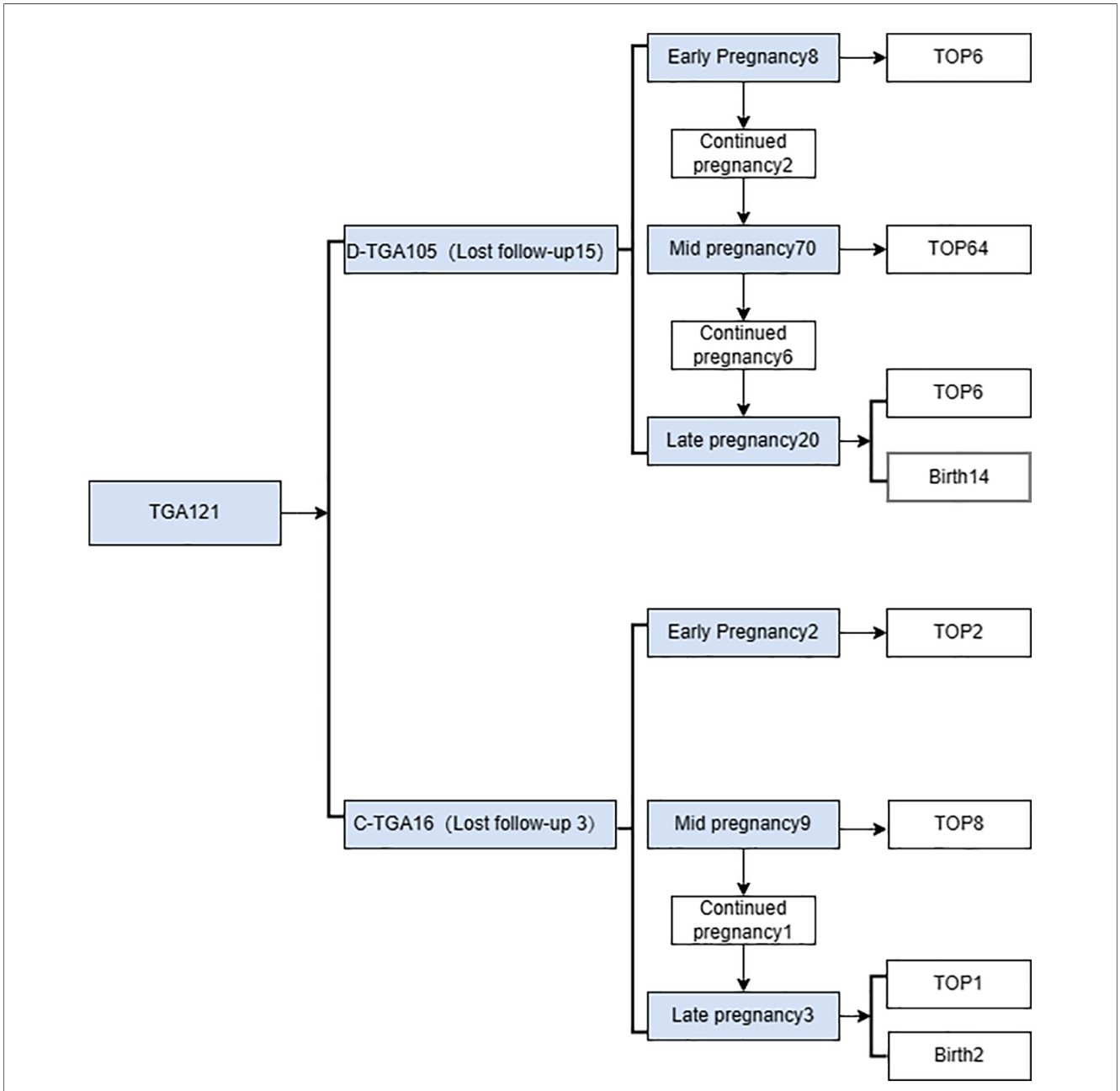

FIGURE 5
Flow chart of the prenatal diagnosis of transposition of the great arteries from pregnancy.

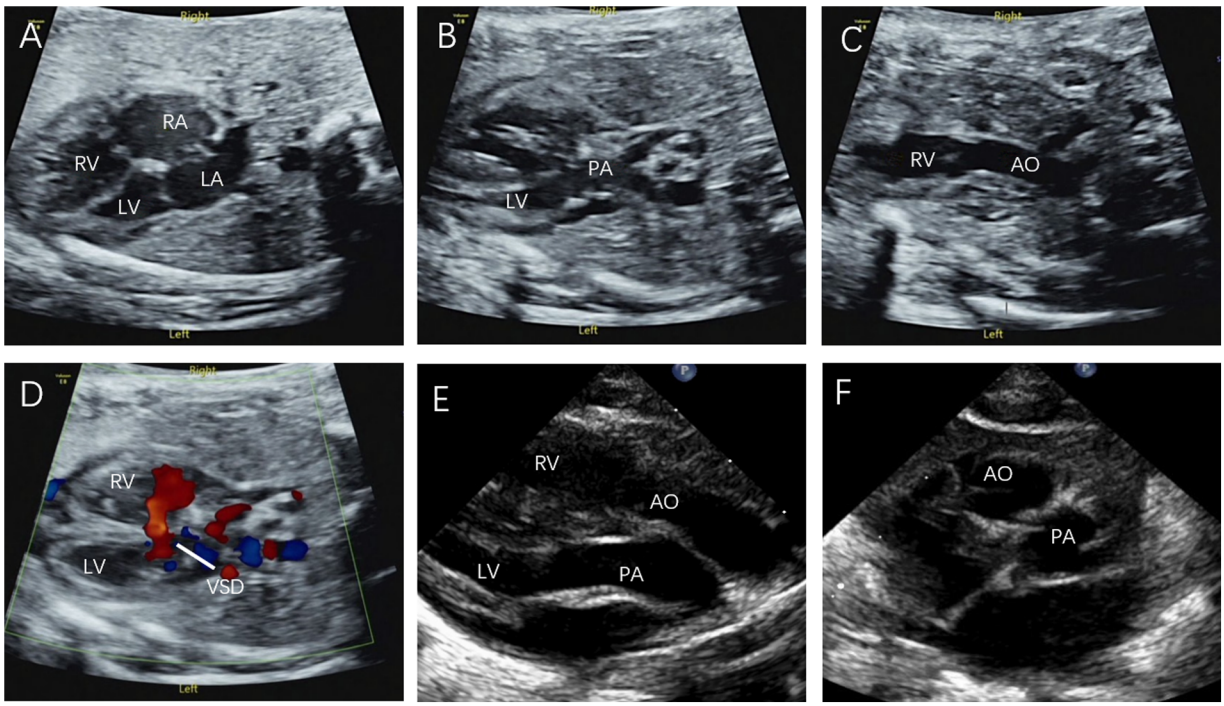

FIGURE 6
Prenatal and postnatal diagnosis of D-TGA. (**A–D**) D-TGA with VSD at 24 w and 6 d gestation. (**E**) Parasternal long-axis view: The two great arteries are aligned in parallel, with the aorta located anteriorly on the right, originating from the right ventricle, and the pulmonary artery located posteriorly on the left, originating from the left ventricle. (**F**) The short axis view of the great arteries: The aorta and pulmonary artery are circumferential and adjacent rather than travelling normally (the longitudinal pulmonary artery surrounds the circular aorta).

surgery was not recommended, and telephone follow-up indicated a good prognosis, as presented in Table 3.

Discussion

TGA is a prevalent congenital heart condition characterized by cyanosis. In recent years, there has been a consistent increase in the rate of prenatal fetal screening, with the detection rate reaching as high as 77% through comprehensive scanning techniques covering the four-chamber heart section, outflow tract section, and three-vessel trachea section (21, 22). Notably, TGA is typically not linked to chromosomal abnormalities or extracardiac malformations (23). The significance of prenatal diagnosis lies in enhancing management strategies. This approach empowers expectant mothers to make well-informed decisions regarding the continuation of their pregnancies and the formulation of delivery plans. Moreover, this approach facilitates the timely implementation of effective treatments after fetal delivery, thereby reducing the occurrence of severe complications and even fetal or neonatal mortality. In this process, prenatal fetal ultrasound screening plays a pivotal role (24).

Most of the cases in the second trimester were TGA suggested by routine prenatal screening at another hospital and referred to our hospital for further definitive diagnosis. Fifteen cases were missed in our hospital in early pregnancy, which may be because the four-chamber view of TGA color Doppler ultrasound was normal, and the oblique view of the great arteries at the base of the heart was mistaken for three-vessel tracheal view blood flow, which was very similar to the "V" -shaped structure. Even in the second trimester, the four-chamber view of D-TGA cases was almost normal, and the outflow view had some limitations in the face of TGA examination, which only showed the initial segment of the outflow tract, without further showing that the aortic arch or the bifurcation of the main pulmonary artery was the section of the left and right pulmonary arteries, so the connection relationship between the ventricles and the large arteries could not be clarified, and TGA was easily missed. In the diagnosis of TGA, the short axis view of the great arteries is one of the important sections observed, and it is also a common section to observe the anatomical site and classification of ventricular septal defects, which can show the relationship between the two great arteries. The basal outflow tract view more clearly shows the relationship between ventricular septal defects and large arteries (away from and riding span). It helps to identify tetralogy of Fallot, transposition of the great arteries, and double outlet right ventricle.

In this study, 90 fetuses with D-TGA and 13 with CC-TGA exhibited intracardiac malformations. Individualized postnatal treatment, with informed consent, was planned for TGA patients with extracardiac abnormalities. One fetus with D-TGA had rare forebrain and facial dysplasia, prompting a second-trimester

10.3389/fcvm.2024.1341005

TABLE 3 TGA prenatal ultrasound diagnosis and postnatal live birth.

Number	Combined intracardiac malformations	Consolidation of other cases	Sex	Weeks of termination of pregnancy	Delivery method	Apgar rating	Birth weight (g)	Surgical situation	Prognosis
1	/	/	Male	39w4d	Forceps assisted	9, 9, 9	3,650	Large artery switch	Good
2	/	/	Male	41w6d	Caesarean section	10, 10, 10	3,880	Large artery switch	Good
3	VSD	Excessive amniotic	Female	41w0d	Spontaneous	10, 10, 10	2,700	Large artery switch + VSD repair	Good
4	VSD	/	Male	40w4d	Spontaneous	10, 10, 10	3,270	Large artery switch + VSD repair	Good
5	/	/	Male	38w5d	Spontaneous	10, 9, 9	3,150	Large artery switch	Good
6	VSD	Bilateral renal collecting system separation	Male	38w5d	Caesarean section	10, 10, 10	3,455	Large artery switch + VSD repair	Good
7	/	/	Male	39w2d	Caesarean section	9, 10, 10	3,200	Large artery switch	Good
8	EIF	/	Male		Caesarean section	9, 9, 9	3,520	Large artery switch	Death
9	VSD	/	Male	39w5d	Caesarean section	9, 9, 9	3,700	Large artery switch + VSD repair	Death
10	VSD, Severe TS, PS	/	Male	40w3d	Spontaneous	10, 10, 10	3,350	Without surgery	General
11	PS, VSD, Small PE	/	Female	37w2d	Caesarean section	10, 9, 9	2,890	Palliative care	Death
12	VSD, PS	HC/AC 0.91%、Excessive amniotic	Male	37w1d	Caesarean section	10, 9, 9	3,400	Palliative care	Death
13	VSD	Excessive amniotic	Male	39w6d	Spontaneous	10, 10, 10	2,680	Palliative care	Death
14	RAA	/	Female	37w4d	Spontaneous	10, 10, 10	2,250	Palliative care	Death
15	PS	/	Male	37w3d	Spontaneous	10, 10, 10	3,400	Surgery is not recommended	General
16	VSD, PA, PLSVC	/	Male	38w6d	Spontaneous	10, 10, 10	3,580	Surgery is not recommended	General

Serial numbers 1-14 are D-TGA fetuses; serial numbers 15-16 are CC-TGA fetuses; VSD, ventricular septal defect; EIF, echogenic intracardiac focus; TS, tricuspid stenosis; PE, pericardial effusion; PS, pulmonary artery stenosis; RAA, right aortic arch; PA, pulmonary artery atresia; PLSVC, persistent left superior vena cava.

induced delivery with consent. Experienced sonographers are recommended to assess cardiac and extracardiac abnormalities for prenatal TGA screening, facilitating multidisciplinary care. Chromosomal abnormalities have rarely been reported in D-TGA patients (25, 26). Prenatal diagnosis, with informed consent, is advisable to exclude these. Moreover, 3 out of 40 D-TGA fetuses (7.5%) had chromosomal abnormalities, which was greater than that in the general population. Only one of the three fetuses had diaphragmatic hernia, and the rest had no other extracardiac abnormalities. CC-TGA patients had a lower incidence of disease (27), with no significant abnormalities detected in the four examined patients. D-TGA has a minimal impact on fetal development due to the open foramen ovale and ductus arteriosus. However, immediate intervention is crucial after birth to prevent severe cyanosis and hypoxemia, which are typically achieved through balloon atrial septostomy (28). An arterial switch operation within the first few weeks of life for newborns with D-TGA leads to a better prognosis (29). Prostaglandin infusion and balloon atrial septostomy are often required for isolated patients to improve oxygenation (14, 28). In congenital CC-TGA patients, where haemodynamics are functionally corrected, the prognosis is generally good (30). However, the outcomes depend on associated cardiac defects, and studies have focused on combining these malformations (7, 31). Early prenatal diagnosis allows for informed consultations and timely interdisciplinary care postdelivery.

In this study, 77 (74.8%) pregnant women were diagnosed in the second trimester and chose to terminate pregnancy 72 (69.9%), possibly because systematic prenatal ultrasonography was routinely performed in the second trimester in China, which included screening for cardiac malformations. Currently, the gestational age at diagnosis of TGA ranges from 12 to 39 weeks, with the earliest diagnosis occurring at 12 weeks and 3 days. Because the fetal heart volume is small in early pregnancy, it is difficult to make a diagnosis of transposition of the great arteries, and for those suspected of TGA in the first trimester, because it is difficult to make a comprehensive evaluation of cardiac structure and function at this time, in addition to the lack of clear gestational age requirements for termination of pregnancy in China, it is often recommended to reexamine after 18 weeks

of gestation. Only eight D-TGA patients and two CC-TGA patients were identified early in pregnancy, leading to recommendations for further genetic examination. Ten fetuses with TGA underwent Down syndrome screening, all of which indicated low risk. Pregnant women were given the choice to continue or terminate the pregnancy. Six cycles of D-TGA and two cycles of CC-TGA were terminated. Specimens from terminated pregnancies were microdissected for verification. For those who continued their pregnancies, the center provided comprehensive support, including regular ultrasound examinations and detailed measurements and observations following fetal echocardiography guidelines. The goal was to ensure accurate and complete diagnosis. In one patient, a D-TGA patient with VSD was diagnosed early and delivered after induced labour during the second trimester. In another D-TGA patient with VSD, dextrocardia, preaxial polydactyly of both hands, and situs invs. were terminated by choice.

Unless in presence of severe extra-cardiac anomalies or diseases associated to TGA, termination is not recommended as the long term outcomes of both operated TGA and operated or not operated CC-TGA are well known (14, 31). In addition, the perinatal management of TGA are extremely well established in order to achieve adequate cardiovascular stability of the newborn. The high induced labour rate of TGA fetuses in our center may be due to our fertility policy. Originally, China advocated that a couple give birth to only one child. Most families wanted their only child to be completely healthy; therefore, if fetal heart abnormalities were found, induction of labour would be selected. However, currently, the three-child policy has been implemented (32), and society has begun to regard fetuses as complete lives and identify fetuses with abnormal hearts as patients with fetal heart disease. With the development of medical technology, many congenital heart diseases are now good treatments, induction of labour is no longer the only solution for congenital heart disease, and the future induction of the labour rate will decrease.

Ultrasound aims to provide scientific and objective medical information for integrated prenatal and postnatal management. When TGA is diagnosed by prenatal and preoperative ultrasound, special attention should be paid to: (1) the continuity of the interventricular septum, intact or only combined with small ventricular septal defect in children are more critical and require early treatment in the neonatal period; (2) aortic valve and pulmonary valve morphology, leaflet number, leaflet opening and closing function; (3) the presence or absence of stenosis under the pulmonary valve, left pulmonary artery and right pulmonary artery development. Postoperative ultrasound should focus on: (1) aortic conditions, almost all cases are associated with aortic root dilatation, resulting in different degrees of aortic regurgitation, the incidence of ascending aortic stenosis is about 5% (33, 34); (2) pulmonary artery conditions, about 10% of patients with progressive supravalvular pulmonary stenosis, pulmonary artery branch stenosis is also one of the common complications (14, 35); (3) VSD with aortic coarctation in children can also be well corrected, but long-term prognosis analysis showed that the risk of arch re-constriction and right ventricular outflow tract obstruction is high (33); (4) postoperative arrhythmia accounts for about 10% (34).

The direction of prenatal diagnosis should align with that of integrated management, including improving the secondary and tertiary prevention systems for birth defects and establishing a multidisciplinary diagnosis and treatment consultation platform to provide effective individualized evaluation and treatment for fetuses with cardiovascular malformations. This approach ensures timely and effective treatment through a streamlined process.

Limitations

This study has several limitations, as it included a small number of patients from a single center, a retrospective study design, a limited number of pregnant women undergoing karyotyping or SNP array examination, and a relatively short follow-up duration. The lesions of the fetal brain and nervous system have not been reported, which would have great clinical significance. Moreover, further research is needed to investigate the mobility, mortality, and quality of life of TGA patients to improve prenatal counselling. Later follow-up should be 1 year, 3 years, 5 years, and cover the heart, development and nervous system status, will be more perfect.

Conclusion

Precise TGA diagnosis can be achieved in early pregnancy through echocardiography. For expectant mothers opting to proceed with their pregnancies, comprehensive prenatal ultrasound monitoring, personalized perinatal management, and multidisciplinary intervention during delivery all play pivotal roles in optimizing outcomes within the TGA population.

Data availability statement

The original contributions presented in the study are included in the article/Supplementary Material, further inquiries can be directed to the corresponding authors.

Ethics statement

The studies involving humans were approved by Ethics Committee of Fujian Maternity and Child Health Care Hospital (2018-017). The studies were conducted in accordance with the local legislation and institutional requirements. The participants provided their written informed consent to participate in this study. Written informed consent was obtained from the individual(s) for the publication of any potentially identifiable images or data included in this article.

Author contributions

JG: Conceptualization, Formal Analysis, Methodology, Resources, Writing – original draft, Writing – review & editing, Data curation, Investigation, Validation, Visualization. WL: Investigation, Software, Writing – original draft, Data curation. TD: Data curation, Project administration, Writing – original draft, Formal Analysis, Validation. SG: Data curation, Methodology, Writing – original draft. HM: Data curation, Formal Analysis, Writing – original draft. QH: Investigation, Methodology, Writing – review & editing. LZ: Formal Analysis, Methodology, Writing – review & editing. ZW: Funding acquisition, Writing – review & editing, Project administration. QW: Data curation, Methodology, Supervision, Writing – review & editing.

Funding

The author(s) declare financial support was received for the research, authorship, and/or publication of this article.

This publication was supported by Joint Funds for the Innovation of Science and Technology, Fujian province (2020Y9156); this publication was also supported by Fujian Natural Science Foundation (2021J01420).

Acknowledgments

The authors thank for the support from Department of Pathology, and Department of Obstetrics, Fujian Maternity and Child Health Hospital, College of Clinical Medicine for Obstetrics & Gynecology and Pediatrics, Fujian Medical University, Fuzhou, China. We also thank all the patients and families for their understanding and support.

Conflict of interest

The authors declare that the research was conducted in the absence of any commercial or financial relationships that could be construed as a potential conflict of interest.

Publisher's note

References

1. Praagh VR. What is congenitally corrected transposition? *N Engl J Med*. (1970) 282(19):1097–8. doi: 10.1056/NEJM197005072821912

2. Ekiz A, Kaya B, Bornaun H, Acar DK, Avci ME, Bestel A, et al. Flecainide as first-line treatment for fetal supraventricular tachycardia. *J Matern Fetal Neonatal Med*. (2018) 31(4):407–12. doi: 10.1080/14767058.2017.1286317

3. Miyoshi T, Maeno Y, Sago H, Inamura N, Yasukochi S, Kawataki M, et al. Antenatal antiarrhythmic treatment for fetal tachyarrhythmias: a study protocol for a prospective multicentre trial. *BMJ open*. (2017) 7(8):e016597. doi: 10.1136/bmjopen-2017-016597

4. Anderson BR, Ciarleglio AJ, Hayes DA, Quaegebeur JM, Vincent JA, Bacha EA. Earlier arterial switch operation improves outcomes and reduces costs for neonates with transposition of the great arteries. *J Am Coll Cardiol*. (2014) 63(5):481–7. doi: 10.1016/j.jacc.2013.08.1645

5. Shin'oka T, Kurosawa H, Imai Y, Aoki M, Ishiyama M, Sakamoto T, et al. Outcomes of definitive surgical repair for congenitally corrected transposition of the great arteries or double outlet right ventricle with discordant atrioventricular connections: risk analyses in 189 patients. *J Thorac Cardiovasc Surg*. (2007) 133 (5):1318–1328.e4. doi: 10.1016/j.jtcvs.2006.11.063

6. Rutledge JM, Nihill MR, Fraser CD, Smith OE, McMahon CJ, Bezold LI. Outcome of 121 patients with congenitally corrected transposition of the great arteries. *Pediatr Cardiol*. (2002) 23(2):137–45. doi: 10.1007/s00246-001-0037-8

7. Day TG, Woodgate T, Knee O, Zidere V, Vigneswaran T, Charakida M, et al. Postnatal outcome following prenatal diagnosis of discordant atrioventricular and ventriculoarterial connections. *Pediatr Cardiol*. (2019) 40(7):1509–15. doi: 10.1007/s00246-019-02176-2

8. Graham TP Jr., Bernard YD, Mellen BG, Celermajer D, Baumgartner H, Cetta F, et al. Long-term outcome in congenitally corrected transposition of the great arteries: a multi-institutional study. *J Am Coll Cardiol*. (2000) 36(1):255–61. doi: 10.1016/S0735-1097(00)00682-3

9. Hautala J, Gissler M, Ritvanen A, Helle E, Pihkala J, Mattila IP, et al. Perinatal and perioperative factors associated with mortality and an increased need for hospital care in infants with transposition of the great arteries: a nationwide 11-year population-based cohort. *Acta Obstet Gynecol Scand*. (2020) 99(12):1728–35. doi: 10.1111/aogs.13953

10. Carvalho JS. Fetal dysrhythmias. *Best Pract Res Clin Obstet Gynaecol*. (2019) 58:28–41. doi: 10.1016/j.bpobgyn.2019.01.002

11. Bravo-Valenzuela NJ, Peixoto AB, Araujo Júnior E, Da Silva Costa F, Meagher S. The reverse boomerang sign: a marker for first-trimester transposition of great arteries. *J Matern Fetal Neonatal Med*. (2019) 32(4):677–80. doi: 10.1080/14767058.2017.1387892

12. Donofrio MT, Skurow-Todd K, Berger JT, McCarter R, Fulgium A, Krishnan A, et al. Risk-stratified postnatal care of newborns with congenital heart disease determined by fetal echocardiography. *J Am Soc Echocardiogr*. (2015) 28 (11):1339–49. doi: 10.1016/j.echo.2015.07.005

13. Donofrio MT, Levy RJ, Schuette JJ, Skurow-Todd K, Sten MB, Stallings C, et al. Specialized delivery room planning for fetuses with critical congenital heart disease. *Am J Cardiol*. (2013) 111(5):737–47. doi: 10.1016/j.amjcard.2012.11.029

14. Santens B, Van De Bruaene A, De Meester P, Gewillig M, Troost E, Claus P, et al. Outcome of arterial switch operation for transposition of the great arteries. A 35-year follow-up study. *Int J Cardiol*. (2020) 316:94–100. doi: 10.1016/j.ijcard.2020.04.072

15. Li YF, Zhou KY, Fang J, Wang C, Hua YM, Mu DZ. Efficacy of prenatal diagnosis of major congenital heart disease on perinatal management and perioperative mortality: a meta-analysis. *World Journal of Pediatrics: WJP*. (2016) 12 (3):298–307. doi: 10.1007/s12519-016-0016-z

16. Escobar-Diaz MC, Freud LR, Bueno A, Brown DW, Friedman KG, Schidlow D, et al. Prenatal diagnosis of transposition of the great arteries over a 20-year period: improved but imperfect. *Ultrasound Obstet Gynecol*. (2015) 45(6):678–82. doi: 10.1002/uog.14751

17. Xie JS, Yin XJ, Yan YN, Pei QY, Yan LH, Zhang L, et al. Integrated management and prognosis analysis of fetus with complete transposition of the great arteries during pregnancy and perinatal period. *Zhonghua fu Chan ke za zhi*. (2020) 55(12):830–6. doi: 10.3760/cma.j.cn112141-20200516-00417

18. Krummholz A, Gottschalk I, Geipel A, Herberg U, Berg C, Gembruch U, et al. Prenatal diagnosis, associated findings and postnatal outcome in fetuses with congenitally corrected transposition of the great arteries. *Arch Gynecol Obstet*. (2021) 303(6):1469–81. doi: 10.1007/s00404-020-05886-8

19. Qiu X, Weng Z, Liu M, Chen X, Wu Q, Ling W, et al. Prenatal diagnosis and pregnancy outcomes of 1492 fetuses with congenital heart disease: role of multidisciplinary-joint consultation in prenatal diagnosis. *Sci Rep*. (2020) 10 (1):7564. doi: 10.1038/s41598-020-64591-3

20. International Society of Ultrasound in Obstetrics and Gynecology, Carvalho JS, Allan LD, Chaoui R, Copel JA, DeVore GR, et al. ISUOG Practice guidelines

(updated): sonographic screening examination of the fetal heart. *Ultrasound Obstet Gynecol*. (2013) 41(3):348–59. doi: 10.1002/uog.12403

21. Ravi P, Mills L, Fruitman D, Savard W, Colen T, Khoo N, et al. Population trends in prenatal detection of transposition of great arteries: impact of obstetric screening ultrasound guidelines. *Ultrasound Obstet Gynecol*. (2018) 51(5):659–64. doi: 10.1002/uog.17496

22. Bertagna F, Rakza T, Vaksmann G, Ramdane-Sebbane N, Devisme L, Storme L, et al. Transposition of the great arteries: factors influencing prenatal diagnosis. *Prenat Diagn*. (2014) 34(6):534–7. doi: 10.1002/pd.4343

23. Lammer EJ, Chak JS, Iovannisci DM, Schultz K, Osoegawa K, Yang W, et al. Chromosomal abnormalities among children born with conotruncal cardiac defects. Birth defects research part A. *Clinical and Molecular Teratology*. (2009) 85(1):30–5. doi: 10.1002/bdra.20541

24. Peake LK, Draper ES, Budd JL, Field D. Outcomes when congenital heart disease is diagnosed antenatally versus postnatally in the UK: a retrospective population-based study. *BMC Pediatr*. (2015) 15:58. doi: 10.1186/s12887-015-0370-3

25. Unolt M, Putotto C, Silvestri LM, Marino D, Scarabotti A, Valerio M, et al. Transposition of great arteries: new insights into the pathogenesis. *Front Pediatr*. (2013) 1:11. doi: 10.3389/fped.2013.00011

26. Škorić-Milosavljević D, Tadros R, Bosada FM, Tessadori F, van Weerd JH, Woudstra OI, et al. Common genetic variants contribute to risk of transposition of the great arteries. *Circ Res*. (2022) 130(2):166–80. doi: 10.1161/CIRCRESAHA.120.317107

27. Paladini D, Volpe P, Marasini M, Russo MG, Vassallo M, Gentile M, et al. Diagnosis, characterization and outcome of congenitally corrected transposition of the great arteries in the fetus: a multicenter series of 30 cases. *Ultrasound Obstet Gynecol*. (2006) 27(3):281–5. doi: 10.1002/uog.2715

28. van Velzen CL, Haak MC, Reijnders G, Rijlaarsdam ME, Bax CJ, Pajkrt E, et al. Prenatal detection of transposition of the great arteries reduces mortality and morbidity. *Ultrasound Obstet Gynecol*. (2015) 45(3):320–5. doi: 10.1002/uog.14689

29. Fuchs IB, Müller H, Abdul-Khaliq H, Harder T, Dudenhausen JW, Henrich W. Immediate and long-term outcomes in children with prenatal diagnosis of selected isolated congenital heart defects. *Ultrasound Obstet Gynecol*. (2007) 29(1):38–43. doi: 10.1002/uog.3900

30. Huhta JC, Maloney JD, Ritter DG, Ilstrup DM, Feldt RH. Complete atrioventricular block in patients with atrioventricular discordance. *Circulation*. (1983) 67(6):1374–7. doi: 10.1161/01.CIR.67.6.1374

31. Vorisek CN, Enzensberger C, Willomeit S, Kurkevych A, Stessig R, Ritgen J, et al. Prenatal diagnosis and outcome of congenital corrected transposition of the great arteries - A multicenter report of 69 cases. *Ultraschall Med*. (2021) 42(3):291–6. doi: 10.1055/a-1069-7698

32. Zhang C, Wei L, Zhu Y, Teng L, Zhang W, Xu J, et al. Fertility intentions among young people in the era of China's three-child policy: a national survey of university students. *BMC Pregnancy Childbirth*. (2022) 22(1):637. doi: 10.1186/s12884-022-04873-y

33. Lachaud M, Dionne A, Brassard M, Charron MA, Birca A, Dehaes M, et al. Cardiac hemodynamics in fetuses with transposition of the great arteries and intact ventricular septum from diagnosis to end of pregnancy: longitudinal follow-up. *Ultrasound Obstet Gynecol*. (2021) 57(2):273–81. doi: 10.1002/uog.21920

34. Kirzner J, Pirmohamed A, Ginns J, Singh HS. Long-term management of the arterial switch patient. *Curr Cardiol Rep*. (2018) 20(8):68. doi: 10.1007/s11886-018-1012-9

35. Wetter J, Belli E, Sinzobahamvya N, Blaschzok HC, Brecher AM, Urban AE. Transposition of the great arteries associated with ventricular septal defect: surgical results and long-term outcome. *Eur J Cardiothorac Surg*. (2001) 20(4):816–23. doi: 10.1016/S1010-7940(01)00912-5

frontiers | Frontiers in Pediatrics

TYPE Case Report
PUBLISHED 08 April 2024
DOI 10.3389/fped.2024.1324585

OPEN ACCESS

EDITED BY
Liqun Sun,
University of Toronto, Canada

REVIEWED BY
Haiyan Yang,
Chongqing General Hospital, China
Felix Sebastian Oberhoffer,
LMU Munich University Hospital, Germany

*CORRESPONDENCE
Jiao Chen
chenjiao@scu.edu.cn

RECEIVED 19 October 2023
ACCEPTED 27 March 2024
PUBLISHED 08 April 2024

CITATION
Zhou J, Liu D and Chen J (2024) Case Report: Rapid and progressive left ventricular endocardial calcification in an infant with Williams syndrome.
Front. Pediatr. 12:1324585.
doi: 10.3389/fped.2024.1324585

Case Report: Rapid and progressive left ventricular endocardial calcification in an infant with Williams syndrome

Jie Zhou[1,2], Dan Liu[1,2] and Jiao Chen[1,2,3]*

[1]Department of Ultrasonic Medicine, West China Second University Hospital of Sichuan University, Chengdu, China, [2]Key Laboratory of Birth Defects and Related Diseases of Women and Children, Ministry of Education, Sichuan University, Chengdu, China, [3]Xizang Autonomous Region Women's and Children's Hospital, West China Second University Hospital of Sichuan University, Lhasa, China

Williams syndrome (WS) is characterized by a range of clinical features, including cardiovascular disease, distinctive facial traits, neurobehavioral disorders, and a condition known as transient infantile hypercalcemia. Among these, endocardial calcification represents a non-specific response to severe, etiologically diverse myocardial injuries. In this report, we document a unique case involving an infant with WS who exhibited rapidly progressive arterial stenosis and left ventricular endocardial calcification, associated with a novel heterozygous deletion. While arterial stenosis is the most frequently observed cardiovascular issue in WS, instances of endocardial calcification during infancy are exceedingly rare and have not previously been reported in the context of WS.

KEYWORDS

Williams syndrome, cardiovascular disease, endocardial calcification, arterial stenosis, infant

1 Introduction

Williams syndrome (WS) is a distinctive multisystem disorder that affects the connective tissues and the cardiovascular and central nervous systems, and it is commonly associated with behavioral, developmental, and cardiovascular abnormalities. WS is caused by a *de novo* deletion of 1.5–1.8 Mb of 26–28 genes located on chromosome 7 at position 7q11.23 (1), with a prevalence rate of 1 in 8,000–20,000 newborns (2, 3). Although cardiovascular defects occur in approximately 80% of patients with WS (4), only 33% of diagnosed cardiovascular defects are detected prenatally, and they tend to be mild, so they are often ignored before birth (5). Structural cardiovascular abnormalities are present in up to 93% of patients with WS and present within the first year of life, with peripheral pulmonary artery stenosis and supravalvular aortic stenosis (SVAS) being the most common (6).

Endocardial calcification is a non-specific reaction to severe etiologically heterogeneous myocardial injuries (7). The etiology of endocardial calcification can be classified into two categories: dystrophic and metastatic, with dystrophic calcification being the main cause. Endocardial calcification may be related to hypoxic-ischemic injury; trauma, such as cardiac surgery; myocarditis (usually fungal or viral); or toxic damage due to alcohol or drugs consumption. Metastatic calcification may be present in patients with hyperparathyroidism, chronic renal failure, oxaluria and aluminum intoxication, dietary calcium and/or vitamin D deficiency, and sarcoidosis (7).

Endocardial calcification is uncommon during infancy. In this report, we present a case of a child with Williams syndrome (WS) who exhibited a typical cardiac structural defect along with rapid and progressive endocardial calcification within the left ventricle (LV).

2 Case presentation

A newborn baby was admitted to the neonatal department due to severe pneumonia, and she was noted to have a murmur. The baby was born to a 28-year-old G1P0 mother after elective induction at 36 + 1 weeks of gestation due to fetal distress. The neonatal birth weight was 2,100 g (p10), and the length was 44 cm (p15). The prenatal examination showed no abnormalities, except for intrauterine growth retardation. The family history was non-contributory, and the mother was not exposed to radiation or toxic substances during pregnancy. An echocardiogram at 15 days (Table 1) revealed mild-to-moderate pulmonary artery stenosis (Vmax = 3.0–3.5 m/s), and extremely mild aortic arch stenosis with a gradient of 20 mmHg with normal LV function (ejection fraction [EF] = 62%, lateral E/e′ [E/e′ Lat] = 7.8).

At 2.5 months of age, the patient was admitted to our hospital due to difficulty with feeding for more than 2 months, which was initially thought to be a result of her severe reflux. The echocardiogram (Table 1) showed moderate-to-severe stenosis of the main pulmonary artery and its branches (Vmax = 3.3–4.2 m/s), a gradient of 55 mmHg across the upper aortic valve, mild aortic arch stenosis with a gradient of 36 mmHg in the setting of LV dysfunction (EF = 35%, E/e′ Lat = 16.2), and increased echo of LV endocardium (Figure 1A). The coronary arteries appeared normal. Computed tomography angiography showed aortic stenosis, pulmonary artery stenosis, and diffusely distributed calcification of the LV endocardium (Figure 1B). The patient's eyelids were swollen, and blood pressure was normal (92/32 mmHg). The electrocardiogram (Figure 2) showed ST-T changes, and LV hypertrophy was suspected. Biochemical examination (Table 2) showed myocardial injury; subclinical hypothyroidism; TORCH complex infection; normal hepatic and renal function; normal calcium (2.65 mmol/L), parathyroid hormone, and vitamin D; and no abnormalities in allergen food groups, respiratory function, and autoantibody tests. WS was highly suspected based on these findings.

Whole-exome sequencing of peripheral blood from the baby and her parents revealed a new pathogenic copy number variation (1.431Mb deletion) in the 7q11.23 region (Chr7: 73303398–74733981), which contains *ELN*, confirming the diagnosis of WS. The baby was given symptomatic treatment, including prednisolone acetate, digoxin as a cardiotonic glycoside, and captopril for diuresis. Echocardiography at the age of 4 months showed improved LV systolic function (EF = 42%, E/e′ Lat = 15.9) with diffusely distributed calcification of the LV endocardium, chordae tendineae, and papillary muscle (Figure 1C). Main pulmonary artery stenosis and SVAS had improved in lesion severity, while peripheral pulmonary artery stenosis and coarctation were unchanged (Table 1).

TABLE 1 The diameter of the affected arteries at different ages in a patient with Williams syndrome measured by echocardiography.

Affected arteries	Corresponding arterial diameter at different months of age(z score)		
	15 day	2.5 month	4 month
Main pulmonary artery	5.0 mm (−3.843)	5.0 mm (−5.591)	7.7 mm (−1.924)
Right pulmonary artery	3.0 mm (−1.091)	3.5 mm (−1.711)	3.6 mm (−1.849)
Left pulmonary artery	3.0 mm (−0.95)	3.0 mm (−3.232)	3.2 mm (−3.084)
Aortic annulus	6.8 mm (0.64)	6.3 mm (−1.332)	8.2 mm (0.903)
Aortic sinuses	7.5 mm (−1.718)	6.6 mm (−4.206)	8.3 mm (−2.315)
Aortic sinotubular junction	6.5 mm (−1.224)	3.9 mm (−6.882)	5.6 mm (−3.638)
Ascending aorta	6.5 mm (−1.224)	6.4 mm (−1.669)	7.1 mm (−1.140)
Transverse aorta	4.2 mm (−3.513)	4.5 mm (−3.998)	4.6 mm (−4.343)
Aortic isthmus	3.5 mm (−3.638)	3.9 mm (−3.787)	4.1 mm (−3.876)

3 Discussion

WS is a rare disease that can affect multiple systems, with cardiovascular defects being the most common cause of death (8).

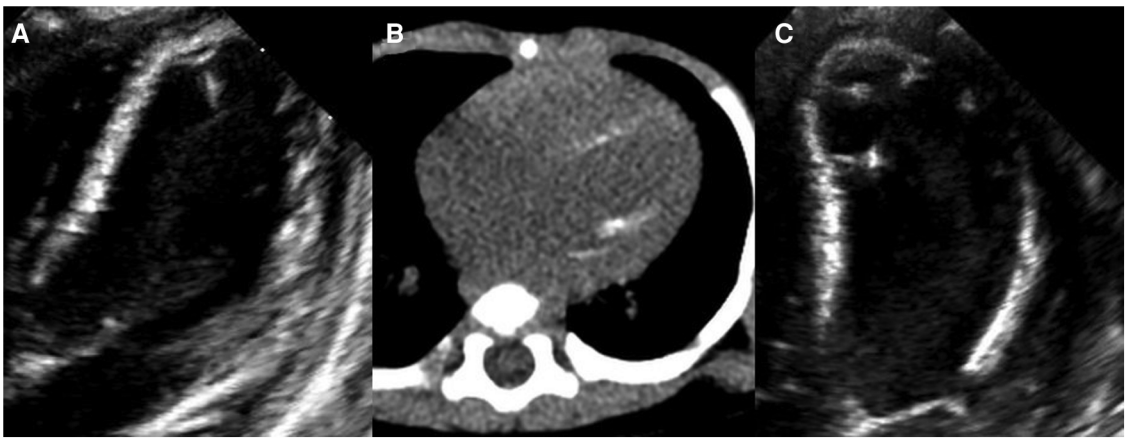

FIGURE 1
Left ventricular (LV) calcification detected by echocardiography and computed tomography angiography (CTA). At 2.5 months of age, (**A**) echocardiography showing increased echo of LV endocardium and (**B**) CTA showing diffusely distributed calcification of the LV endocardium. At 4 months of age, (**C**) echocardiography showing diffusely distributed calcification of the LV endocardium, chordae tendineae, and papillary muscle.

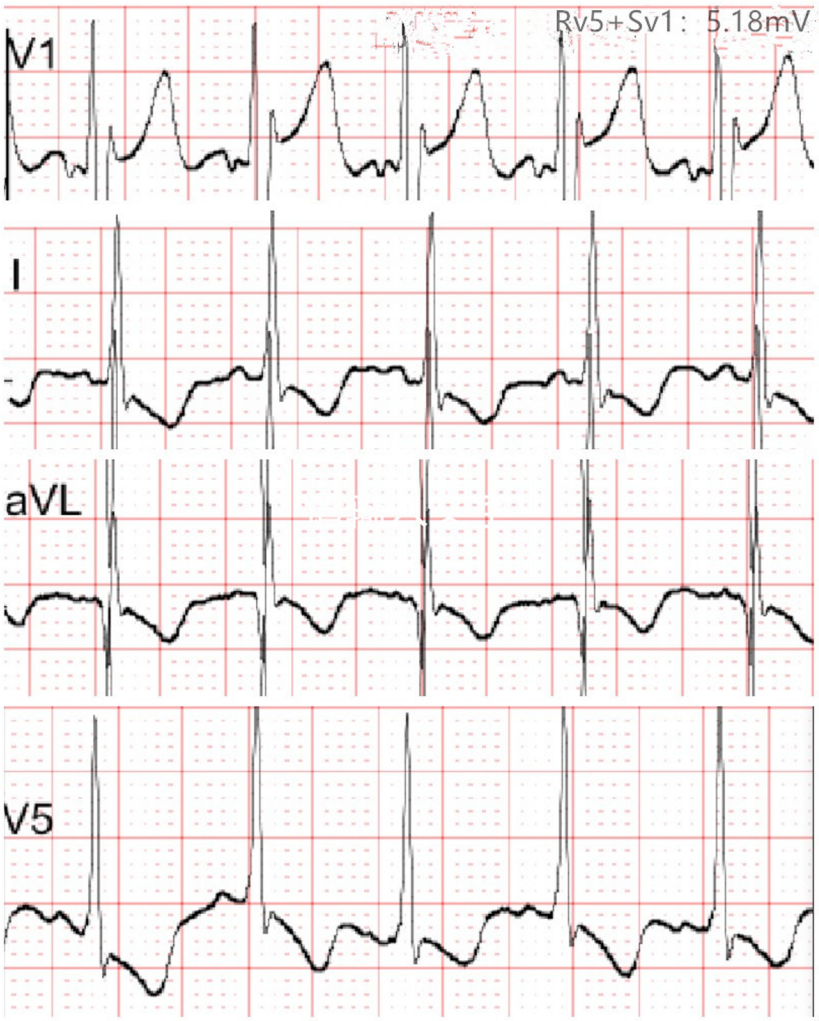

FIGURE 2
Electrocardiogram at 2.5 months of age showing T-wave flattening or inversion in leads I, aVL, and V5, and left ventricular hypertrophy was suspected.

Cardiovascular abnormalities are the direct result of *ELN* deletion (5). In patients with WS, the decrease in arterial elastin content and pathological alignment of elastin fibers lead to smooth muscle overgrowth, multilayer thickening of the media of large arteries, and development of obstructive hyperplastic intimal lesions, leading to vascular diseases in the middle- and large-sized arteries. The most notable stenoses are SVAS and peripheral pulmonary artery stenosis; however, the aortic arch, descending aorta, coronary artery, renal artery, mesenteric artery, and intracranial artery can also be affected (9). Other cardiovascular defects, including tetralogy of Fallot, complete atrioventricular septal defect, total anomalous pulmonary venous return, double-chambered right ventricular, and Ebstein anomaly of the tricuspid valve, have also been reported (10). In the present case, the patient had *ELN* deletion and typical pulmonary artery stenosis, SVAS, and aortic arch stenosis.

Although the typical defect of arterial stenosis and related clinical tests led us to quickly make a diagnosis of WS, which was confirmed by whole-exome sequencing, the etiology of the infant's rapidly progressive endocardial calcification was still unclear. Endocardial calcification is very rare in infancy. At present, only one case of giant cell myocarditis and endomyocardial calcification in a 2.5-month-old infant has been reported, which was triggered by excessive maternal alcohol abuse (11). The patient had poor cardiac function, and electrocardiogram indicated myocardial ischemia. Although the combination of high end-diastolic pressure due to severe SVAS coupled with coronary artery stenosis can result in decreased coronary artery perfusion pressure and myocardial ischemia (12), ultimately resulting in cardiac dysfunction and papillary muscle and endocardial calcification, it often takes a long time to develop. In the present study, echocardiography showed no significant coronary artery stenosis, so the decrease in cardiac function and endocardial calcification could not be explained by SVAS alone. In the present case, calcification of the endocardium progressed rapidly, and biochemical tests excluded calcium deposition, hyperparathyroidism, vitamin D deficiency, renal failure, allergy, and autoantibodies as the cause. The infant's

TABLE 2 Biochemical examination indicators at 2.5 months of age in a patient with Williams syndrome.

Biochemical examination	Results
Myocardial Enzymes	Creatine kinase isoenzyme (CK-MB) 6.04 ug/L[a]
	Phosphocreatine kinase (CK) 115 U/L
	Troponin I (cTnI) 0.259 ug/L[a]
	Myoglobin (Myo) 73.0 ug/L
Brain natriuretic peptide	737.56 pg/ml
Thyroid function	Triiodothyronine (T3) 1.83 nmol/L
	Tetraiodothyronine (T4) 82.60 nmol/L
	Thyroid-stimulating hormone (TSH) 31.558 mIU/L[a]
	Free triiodothyronine (FT3) 5.94 pmol/L
	Free thyroid hormone (FT4) 14.01 pmol/L
The calcium level	2.65 mmol/L
Parathyroid hormone level	15.20 pg/ml
The vitamin D level	41.10 pg/ml
Allergen food groups	Normal
Allergen respiratory function	Normal
Allergen autoantibody tests	Normal
TORCH	Toxoplasma immunoglobin M (Toxo-IgM) < 3.0 AU/ml
	Toxoplasma immunoglobin G (Toxo-IgG) < 3.0 IU/ml
	Cytomegalovirus immunoglobin M (CMV-IgM) < 5.0 U/ml
	Cytomegalovirus immunoglobin G (CMV-IgG) 60.4 U/ml[a]
	Rubella virus immunoglobin M (Ru-IgM) < 10 AU/ml
	Rubella virus immunoglobin G (Ru-IgG) 12.2 IU/ml[a]
	Shingles virus immunoglobin M (HSV-IgM) < 5.0 Index
	Shingles virus immunoglobin G (HSV-IgG) 9.8 Index[a]

[a]Represents abnormal results.

myocardial enzymes were elevated. The TORCH complex examination showed that cytomegalovirus (CMV), rubella virus, and shingles virus immunoglobin G antibodies were positive. The infant had not been vaccinated, indicating that she was previously infected. Dystrophic cardiac calcification is related to CMV infection, and some scholars have found that CMV-infected mice have localized cardiac calcification, mainly in the right ventricle (13). Other animal experiments (14) have shown that mice with *ELN* deletion develop cardiac phenotypes attributed to aortic stenosis, including compromised fractional shortening, cardiac enlargement, necrosis, and calcification in the cardiac chambers. Based on the above literature, although there were no other related clinical symptoms in the present case, myocardial damage caused by CMV infection combined with SVAS seemed to be the most likely cause of the rapid and progressive LV endocardial calcification in the present case, although the possibility of genetic susceptibility caused by delection of new heterozygosity cannot be ruled out.

4 Conclusion

We report a case of progressive arterial stenosis accompanied by endocardial calcification in an infant with Williams syndrome (WS). To our knowledge, endocardial calcification in WS has not been documented before. After ruling out other potential pathogenic causes, we believe that myocardial injury due to Cytomegalovirus (CMV) infection compounded by aortic stenosis is the probable cause. Nonetheless, we cannot overlook the possibility that a genetic predisposition due to a newly identified heterozygous deletion may have played a role.

Data availability statement

The raw data supporting the conclusions of this article will be made available by the authors, without undue reservation.

Ethics statement

The studies involving humans were approved by the ethics committee of West China Second University Hospital of Sichuan University. The studies were conducted in accordance with the local legislation and institutional requirements. Written informed consent for participation in this study was provided by the participants' legal guardians/next of kin.

Author contributions

JZ: Writing – original draft. DL: Writing – review & editing. JC: Writing – review & editing, Funding acquisition.

Funding

The author(s) declare that financial support was received for the research, authorship, and/or publication of this article.

This research was supported by the Fundamental Research Funds for the Central Universities, the National Key R &D Program of China (grant numbers: 2017YFC0211705, 2017YFC0113905), the Key R & D Program of Science and Technology Department of Sichuan Province (grant numbers: 2019YFS0403, 2019YFS0037), and the Popularization and Application Project of the Sichuan Health and Family Planning Commission (grant numbers: 17PJ415).

Acknowledgments

We thank Emily Woodhouse, PhD, from Liwen Bianji (Edanz) (www.liwenbianji.cn) for editing the English text of a draft of this manuscript.

Conflict of interest

The authors declare that the research was conducted in the absence of any commercial or financial relationships that could be construed as a potential conflict of interest.

Publisher's note

References

1. Stanley TL, Leong A, Pober BR. Growth, body composition, and endocrine issues in Williams syndrome. *Curr Opin Endocrinol Diabetes Obes*. (2021) 28(1):64–74. doi: 10.1097/MED.0000000000000588

2. Collins RT 2nd, Kaplan P, Rome JJ. Stenosis of the thoracic aorta in Williams syndrome. *Pediatr Cardiol*. (2010) 31(6):829–33. doi: 10.1007/s00246-010-9713-x

3. Ramírez-Velazco A, Aguayo-Orozco TA, Figuera L, Rivera H, Jave-Suárez L, Aguilar-Lemarroy A, et al. Williams-Beuren syndrome in Mexican patients confirmed by FISH and assessed by aCGH. *J Genet*. (2019) 98(2):34. doi: 10.1155/2015/903175

4. Collins RT, Kaplan P, Somes GW, Rome JJ. Cardiovascular abnormalities, interventions, and long-term outcomes in infantile Williams syndrome. *J Pediatr*. (2010) 156(2):253–8.e1.8. doi: 10.1016/j.jpeds.2009.08.042

5. Szmyd B, Karuga F, Gach A, Moszura T, Kopala M, Respondek-Liberska M. Complex cardiovascular defects in a male infant with Williams syndrome juxtaposed with the results of a preliminary survey illustrating other patients' outcomes. *Kardiol Pol*. (2021) 79(2):188–91. doi: 10.33963/KP.15740

6. Ahrens-Nicklas RC, Reichert SL, Zackai EH, Kaplan PB. Atypical Williams syndrome in an infant with complete atrioventricular canal defect. *Am J Med Genet A*. (2015) 167A(12):3108–12. doi: 10.1002/ajmg.a.37288

7. Nance JW Jr, Crane GM, Halushka MK, Fishman EK, Zimmerman SL. Myocardial calcifications: pathophysiology, etiologies, differential diagnoses, and imaging findings. *J Cardiovasc Comput Tomogr*. (2015) 9(1):58–67. doi: 10.1016/j.jcct.2014.10.004

8. Collins RT. Cardiovascular disease in Williams syndrome. *Curr Opin Pediatr*. (2018) 30(5):609–15. doi: 10.1097/MOP.0000000000000664

9. Abu-Sultaneh S, Gondim MJ, Alexy RD, Mastropietro CW. Sudden cardiac death associated with cardiac catheterization in Williams syndrome: a case report and review of literature. *Cardiol Young*. (2019) 29(4):457–61. doi: 10.1017/S1047951119000295

10. Katt TE, Spicer RL, Yetman AT, Ibrahimiye AN, Hammel JM, Robinson JA. Williams syndrome and neonatal cardiac surgery for congenital single ventricle. *JACC Case Rep*. (2020) 2(11):1716–9. doi: 10.1016/j.jaccas.2020.05.098

11. Krajcovic J, Janik M, Adamicova K, Straka L, Stuller F, Novomesky F. Giant cell myocarditis and endomyocardial calcification in a 2.5-month-old infant triggered by excessive maternal alcohol abuse: case study of an unusual association. *Pediatr Cardiol*. (2013) 34(8):2073–6. doi: 10.1007/s00246-013-0637-0

12. Yuan Y, Zhou R. An infant with suspected missed diagnosis of Williams syndrome failed weaning off CPB after surgical correction of pulmonary stenosis: a case report and literature review. *Perfusion*. (2023) 38(1):203–7. doi: 10.1177/02676591211046876

13. Ritter JT, Tang-Feldman YJ, Lochhead GR, Estrada M, Lochhead S, Yu C, et al. In vivo characterization of cytokine profiles and viral load during murine cytomegalovirus-induced acute myocarditis. *Cardiovasc Pathol*. (2010) 19(2):83–93. doi: 10.1016/j.carpath.2008.12.001

14. Lin CJ, Staiculescu MC, Hawes JZ, Cocciolone AJ, Hunkins BM, Roth RA, et al. Heterogeneous cellular contributions to elastic laminae formation in arterial wall development. *Circ Res*. (2019) 125(11):1006–18. doi: 10.1161/CIRCRESAHA.119.315348

frontiers | Frontiers in Pediatrics

TYPE Original Research
PUBLISHED 25 April 2024
DOI 10.3389/fped.2024.1326804

OPEN ACCESS

EDITED BY
Liqun Sun,
University of Toronto, Canada

REVIEWED BY
Gabriela Corina Zaharie,
University of Medicine and Pharmacy Iuliu Hatieganu, Romania
Nahla Zaghloul,
University of Arizona, United States

*CORRESPONDENCE
Safwat Aly
safwat.aly@cardio.chboston.org

RECEIVED 23 October 2023
ACCEPTED 01 February 2024
PUBLISHED 25 April 2024

CITATION
Aly S, Qattea I, Kattea MO and Aly HZ (2024) Neonatal outcomes in preterm infants with severe congenital heart disease: a national cohort analysis.
Front. Pediatr. 12:1326804.
doi: 10.3389/fped.2024.1326804

Neonatal outcomes in preterm infants with severe congenital heart disease: a national cohort analysis

Safwat Aly[1,2]*, Ibrahim Qattea[3], Mohammad O. Kattea[3] and Hany Z. Aly[4]

[1]Department of Cardiology, Boston Children's Hospital, Boston, MA, United States, [2]Department of Pediatrics, Harvard Medical School, Boston, MA, United States, [3]Department of Pediatrics, Nassau University Medical Center, East Meadow, NY, United States, [4]Department of Neonatology, Cleveland Clinic, Cleveland, OH, United States

Background: Prematurity and congenital heart disease (CHD) are the leading causes of neonatal mortality and morbidity. Limited data are available about the outcomes of premature infants with severe CHD.
Methods: We queried The National Inpatient Database using ICD-10 codes for premature patients (<37 weeks) with severe CHD from 2016 to 2020. Severe CHDs were grouped into three categories: A. left-sided lesions with impaired systemic output, B. Cyanotic CHD, and C. Shunt lesions with pulmonary overcirculation. Patients with isolated atrial or ventricular septal defects and patent ductus arteriosus were excluded. We also excluded patients with chromosomal abnormalities and major congenital anomalies. Patients' demographics, clinical characteristics, and outcomes were evaluated by comparing premature infants with vs. without CHD adjusting for gestational age (GA), birth weight, and gender.
Results: A total of 27710 (1.5%) out of 1,798,245 premature infants had severe CHD. This included 27%, 58%, and 15% in groups A, B, and C respectively. The incidence of severe CHD was highest between 25 and 28 weeks of gestation and decreased significantly with increasing GA up to 36 weeks ($p < 0.001$). Premature infants with severe CHD had a significantly higher incidence of neonatal morbidities including necrotizing enterocolitis (NEC) [OR = 4.88 (4.51–5.27)], interventricular hemorrhage [OR = 6.22 (5.57–6.95)], periventricular leukomalacia [OR = 3.21 (2.84–3.64)] and bronchopulmonary dysplasia [OR = 8.26 (7.50–10.06) compared to preterm infants of similar GA without CHD. Shunt lesions had the highest incidence of NEC (8.5%) compared to 5.3% in cyanotic CHD and 3.7% in left-sided lesions ($p < 0.001$). Mortality was significantly higher in premature infants with CHD compared to control [11.6% vs. 2.5%, $p < 0.001$]. Shunt lesions had significantly higher mortality (11.0%) compared to those with left-sided lesions (8.3%) and cyanotic CHD (6.4%), $p < 0.001$.
Conclusion: Premature infants with severe CHD are at high risk of neonatal morbidity and mortality. Morbidity remains increased across all GA groups and in all CHD categories. This significant risk of adverse outcomes is important to acknowledge when managing this patient population and when counseling their families. Future research is needed to examine the impact of specific rather than categorized congenital heart defects on neonatal outcomes.

KEYWORDS

prematurity, gestational age, congenital heart disease, outcomes, necrotizing enterocolitis

Introduction

Prematurity continues to be the leading cause of neonatal mortality in developed countries (1). The association between gestational age (GA) and neonatal mortality is well known. Gestational age is the major predictor of mortality in extremely preterm infants without congenital anomalies. Even those born at 34–36 weeks of gestation have a higher mortality risk than full-term infants (1, 2). Most of the studies that examined morbidity and mortality in preterm infants excluded congenital heart disease (CHD) to better distinguish the attribute of prematurity on neonatal death (3).

Congenital heart disease is the most common birth defect, affecting ~40,000 infants per year in the United States representing ~0.8% of all births with ~0.2% of them reported to have critical CHD (4, 5). Previous reports demonstrated that CHDs are more frequently encountered in preterm than full-term neonates (6, 7). Having a congenital heart defect raises the risk of premature birth by 2-to-3 fold compared to neonates without CHD (6–8). It is well-known that severe CHDs are associated with higher mortality rates in full-term infants (6–9).

Despite the significant association between prematurity and CHD, less is known about the impact of GA on outcomes in patients with severe CHD. The few studies that examined the outcomes of premature infants with CHD carried significant limitations including relatively small numbers of premature infants, older birth cohorts (before 2005), excluded extreme preterm or moderate/late preterm infants, or did not account for important confounders such as GA, birth weight (BW), and gender (1, 3, 6–9). Moreover, the inclusion of mixed forms of CHDs including minor ones, and the substantial number of patients with non-cardiac anomalies and genetic syndromes might have contributed to the significant variations in the rates of adverse outcomes reported (3, 10, 11).

Therefore, in the current study, we aimed to use the largest national database to (1) Examine the frequency of severe CHD in premature infants born at various GAs, and (2) Quantify the effect of GA on neonatal mortality and major neonatal morbidities in preterm infants with different categories of severe CHD by comparing them to a control group of preterm infants without any CHD.

Methods

Data source

This observational study used deidentified patient data from the National Inpatient Sample (NIS) database during the period from January 1, 2016 to December 31, 2020. This database is part of the Healthcare Cost and Utilization Project (HCUP) and has been used for many previous projects. The NIS database contains ~8 million hospital stays each year and randomly samples 20% of the discharges from the participating hospitals and is weighed to accurately reflect 100% of all US hospital discharges (12). Procedure and diagnostic codes are documented using the International Classification of Diseases. In the current study, we only used International Classification of Disease, Tenth Revisions, and Clinical Modification (ICD10-CM) to identify our patient population.

Patient selection

The study was granted an exempt status from the Institutional Review Board given the use of a deidentified and publicly available database. Patients were included in the study if they were born prematurely (<37 0/7 weeks of gestation) with severe CHD. Severe CHDs were categorized into three main groups based on the underlying physiology: *Category A*: left-sided lesions with impaired systemic output, *Category B*: cyanotic CHD with persistent cyanosis, and *Category C*: Shunt lesions with pulmonary over-circulation and subsequent congestive heart failure. Patients were excluded from the study if they had only a simple or minor CHD including an isolated atrial septal defect, ventricular septal defect, or patent ductus arteriosus. The study excluded patients with genetic or chromosomal abnormalities and/or major congenital anomalies. Patients who were transferred between hospitals were only included at the receiving hospital to avoid duplication. The list of all CHDs included in the study and their respective ICD-10 codes is shown in Supplementary Table S1.

Identification of variables

The NIS database was queried for patients' demographics and clinical characteristics. The main outcomes of interest included in-hospital mortality and major neonatal morbidities. Non-cardiac neonatal morbidities included necrotizing enterocolitis [ICD-10 codes: P77.1, P77.2, and P77.3], severe interventricular hemorrhage (greater than grade II) [P52.2 and P52.0], periventricular leukomalacia (PVL) [P91.2], and bronchopulmonary dysplasia (BPD) [P27.1].

Patient characteristics and outcomes were evaluated by comparing premature infants with severe CHD to a control group of premature infants with matching GA but without any CHD. We also examined the frequency of different procedures (extracorporeal membrane oxygenation support, tracheostomy, and gastrostomy) between the two groups and their association with outcomes.

Statistical analysis

Data were presented using the mean and standard deviation for parametric continuous variables, the median and interquartile range for nonparametric continuous variables, and the frequencies and proportions for categorical variables. To examine the occurrence of CHD and its association with outcomes of interest, we classified premature infants based on GA into the following categories; extremely premature [≤27 6/7 weeks], very

premature [28 0/7 to 31 6/7 weeks], moderate preterm [32 0/7 to 33 6/7 weeks], late preterm [34 0/7 to 36 6/7 weeks]. Premature infants with severe CHD were compared to those without any CHD using the Mann–Whitney *U*-test for continuous characteristics and chi-square tests for categorical characteristics. Both cases and controls were matched for GA, gender, and BW. Patients with CHD were further grouped into three main categories (left-sided CHD, cyanotic CHD, and shunt lesions with pulmonary overcirculation). The odds ratios (OR) of developing the different neonatal outcomes of interest in the different CHD categories in comparison to controls were evaluated using chi-square tests. $P < 0.05$ was considered significant. Data analysis was performed using SAS version 9.4 (SAS Institute Inc., Cary, NC).

Results

Between 2016 and 2020, there were 1,827,044 preterm births in the NIS database. This included 27,710 (1.5%) with severe CHD. Premature infants with severe CHD were classified based on the underlying cardiovascular physiology into three main groups including; −26% left-sided lesions with impaired systemic output (*category A*), −62% with sustained cyanosis (*category B*), and −12% with shunt lesions and pulmonary overcirculation (*category C*).

There was no significant difference in the distribution of the three different categories of CHD in preterm infants when compared to full-term infants born with similar CHDs during the study period. Figure 1 illustrates the flow chart for the study population.

The incidence of severe CHD in premature birth (premature patients with severe CHD/all preterm births in the same year) varied from 1.39% to 1.65% per year. The association between prematurity and incidence of severe CHD was more frequent in males (54%) and whites (41%). Low median household income was associated with a higher frequency of having a premature infant with severe CHD. Regional differences existed in the association of prematurity and CHD. Demographics of premature infants with vs. without severe CHD are demonstrated in Table 1.

A total of 3.2% of extremely premature infants (≤27 weeks) had severe CHD compared to 2.3% in very preterm, 1.5% in moderate preterm, and 1.1% in late preterm infants ($p < 0.01$). The numbers and frequencies of the different categories of severe CHD in preterm infants according to their GA category are demonstrated in Figure 2.

Premature birth of infants with severe CHD was more likely to occur in pregnancies complicated by maternal hypertension [3.9% vs. 0.6%, $p < 0.001$, OR of 3.19 (2.99–3.41)]. Preexisting diabetes and gestational diabetes were associated with a higher frequency of severe CHD in preterm infants [10.1% vs. 1.2%, $p < 0.001$, OR of 7.86 (7.54–8.19) and 5.8% vs. 2.0%, $p < 0.001$, OR of 3.02 (2.87–3.18), respectively], Tables 2, 3.

The frequency of being born before 25 weeks of gestation with severe CHD was much less compared to the other gestational weeks till the 34th week. The highest frequency of premature birth associated with severe CHD occurred in premature infants born after 25 weeks and before 28 weeks of gestation. After the 28th weeks of gestation, there was a steady decrease in the incidence of severe CHD in premature infants until reaching the 36th week of gestation. Figure 2 and Supplementary Figure S1.

In-hospital mortality was significantly higher in premature infants with CHD compared to those without CHD [11.6% vs. 2.5%, $p < 0.001$]. Shunt lesions with pulmonary over-circulation had significantly higher mortality (11.0%) compared to left-sided lesions (8.3%) and cyanotic CHD (6.4%), $p < 0.001$. There was no statistically significant difference in the trends of mortality within each CHD category over the study period. Trends of in-hospital mortality in premature infants with the different categories of CHD compared to controls are shown in Figure 3.

Major neonatal morbidities were more frequent in premature infants with CHD compared to controls. Necrotizing enterocolitis was more common in premature infants with CHD [3.92% vs. 0.95%, $P < 0.001$, 4.88 (4.51–5.27)]. Extremely preterm infants (born ≤27 weeks) with severe CHD were associated with the highest frequency of having NEC (−11%) compared to −4% for those born between 28 and 32 weeks of gestation and −2% for late preterm infants with CHD. Shunt lesions were associated with the highest incidence of NEC in preterm infants occurring in 8.5% compared to 5.3% in the cyanotic CHD group and 3.7% in left-sided CHD Figure 4A.

Similarly, bronchopulmonary dysplasia rates were significantly higher in premature infants with CHD compared to those without CHD [18.7% vs. 2.3%, $p < 0.001$, OR = 18.3 (14.5–20.1)]. The frequency of developing BPD was significantly higher in patients with cyanotic CHD and left-sided CHD (12.6% and 11.8%, respectively) compared to 6.2% in those with shunt lesions ($p < 0.001$) Figure 4B.

Premature infants with CHD had a higher frequency of having severe neonatal brain injury (defined as having IVH grades III or IV (1.7% vs. 0.4%, $p < 0.001$, 6.2 (5.6–6.9) or PVL [1.4% vs. 0.4%, $p < 0.001$, 3.2 (2.8–3.6)]. Figures 4C,D. Cyanotic CHD had a significantly higher incidence of severe IVH (4.7%) compared to left-sided lesions (3.8%) and shunt lesions (3.6%), $p < 0.001$ Figure 4 illustrates the frequency of the different neonatal morbidities associated with the different categories of severe CHD in relation to the degree of prematurity.

Premature infants with CHD had a higher frequency of sepsis (2.3% vs. 0.3%, $p < 0.001$) and acute renal failure (5.8% vs. 0.5%, $p < 0.001$) compared to those without CHD. Premature infants with CHD received more non-cardiac procedures compared to controls including tracheostomy and gastrostomy tubes Table 4.

Premature infants with CHD had higher odds of having the composite outcome (mortality and major neonatal morbidity) compared to those without CHD after adjusting for GA, BW, and gender (27.3% % vs. 6.6%, $p < 0.001$). Extremely preterm infants without CHD had a higher frequency of developing the composite outcome compared to those with similar GA but without CHD (47.6% vs. 35.9%, $p < 0.001$). Similarly, very preterm, and moderate preterm had a higher frequency of developing the composite outcome compared to those with

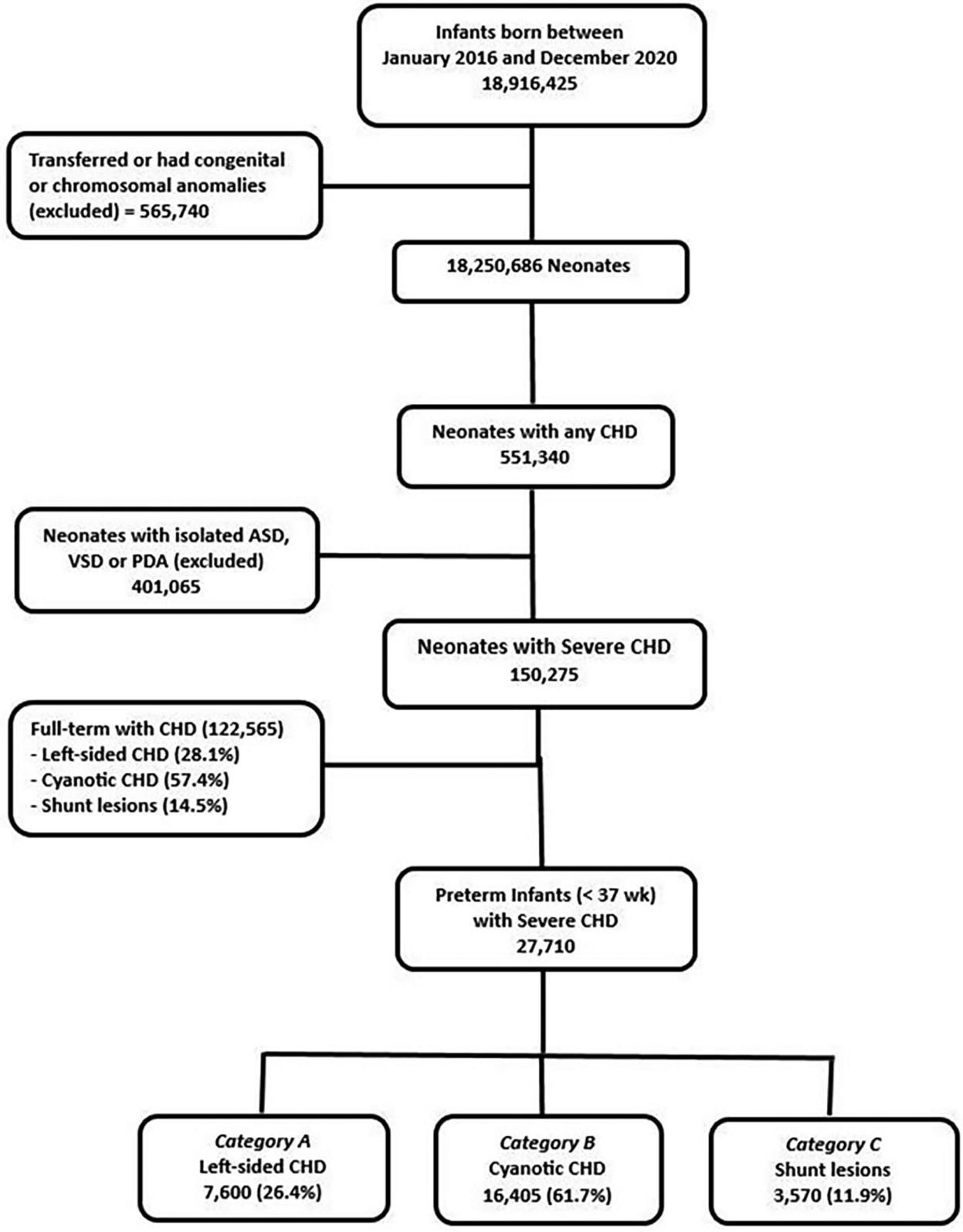

FIGURE 1
Flow chart for the patient population.

10.3389/fped.2024.1326804

TABLE 1 Demographics and distribution of the study population.

		Preterm infants with severe CHD		Preterm infants without severe CHD		*P*-value
Indicator of sex	Male	15,025	54.2%	960,340	53.4%	
	Female	12,685	45.8%	837,905	46.6%	<0.001
Race (uniform)	White	11,395	41.1%	776,560	43.2%	<0.001
	Black	5,110	18.4%	333,740	18.6%	
	Others	11,205	40.4%	689,035	38.3%	
Primary expected payer (uniform)	Medicare/Medicaid	15,320	55.3%	927,380	51.6%	<0.001
	Private insurance	10,565	38.1%	740,725	41.2%	
	Others	1,825	6.6%	131,230	7.3%	
Calendar year	2016	5,335	19.3%	358,380	19.9%	<0.001
	2017	5,125	18.5%	361,335	20.1%	
	2018	5,620	20.3%	361,865	20.1%	
	2019	5,730	20.7%	366,545	20.4%	
	2020	5,900	21.3%	351,210	19.5%	
Median household income national quartile for patient ZIP Code	0–25th percentile	9,290	33.5%	562,315	31.3%	<0.001
	26th–50th percentile	7,310	26.4%	454,390	25.3%	
	51st–75th percentile	5,975	21.6%	419,545	23.3%	
	76th–100th percentile	4,860	17.5%	345,755	19.2%	
Location/teaching status of the hospital	Rural	155	0.6%	61,330	3.4%	<0.001
	Urban nonteaching	1,360	4.9%	183,055	10.2%	
	Urban teaching	14,570	52.6%	837,485	46.6%	
Region of hospital	Northeast	2,110	7.6%	158,395	8.8%	<0.001
	Midwest	3,490	12.6%	239,510	13.3%	
	South	7,015	25.3%	450,180	25.0%	
	West	3,470	12.5%	233,785	13.0%	
Control/ownership of hospital	Government, nonfederal	2,270	8.2%	128,090	7.1%	<0.001
	Private, non-profit	12,220	44.1%	817,030	45.4%	
	Private, invest-own	1,595	5.8%	136,750	7.6%	

similar GA but without CHD (25.2% vs. 18.6%, $p < 0.001$ and 12.0% vs. 5.1%, $p < 0.001$, respectively). The occurrence of composite outcomes continued to be significantly higher in late preterm infants compared to controls (9.6% vs. 4.2%, $p < 0.001$). Figure 5 illustrates the differences in developing the composite outcome between the two groups (cases vs. controls) in relation to their GA.

Discussion

In the current study, we used the largest national multicenter database to examine the interactions between prematurity and severe CHD over a five-year period. We included 27,710 premature infants with severe CHD and compared them to a control group of premature infants without CHD. The main findings in our study include: (a) premature infants are at higher risk of having severe CHD compared to full-term infants during the study period (1.5% vs. 0.5%, $P < 0.001$ respectively). (b) Severe CHD in premature infants increases the risk of developing non-cardiac prematurity-related complications including NEC, BPD, and severe brain injury. (c) Shunt lesions with pulmonary over-circulation were associated with the highest mortality rates while cyanotic CHDs were associated with the most favorable outcome. (d) Advanced GA was not associated with a significant decline in developing the composite outcome (mortality and major neonatal morbidities) in preterm infants with severe CHD in contrast to those of similar GA but without CHD.

Prematurity and CHD

The incidence of all CHD in full-term infants is known to be ~1% (4–6). However, the true occurrence of CHD especially the severe forms in premature infants is unknown. In the current national analysis of a 5-year period, the incidence of severe CHD in premature infants ranged from 1.39% to 1.65% per year. While full-term infants during the same period had severe CHD ranges of 0.43%–0.49%. This is in agreement with previous reports of high frequency of CHD in preterm infants (6, 7). In an international cohort study, not including the USA, the estimated incidence of severe CHD in premature infants was reported to be ~0.8% (3). Despite the international and multicenter nature of the former report, it only included ~600 patients with severe CHD. Locally, in a population-based study from the state of California between 2005 and 2012, ~0.5% of premature patients included had a critical CHD (13). Our study likely offers more reliable estimates given the enormous patient sample and the wide range of regions included across the United States. Fetal distress occurring secondary to severe CHD might trigger preterm birth in these patients.

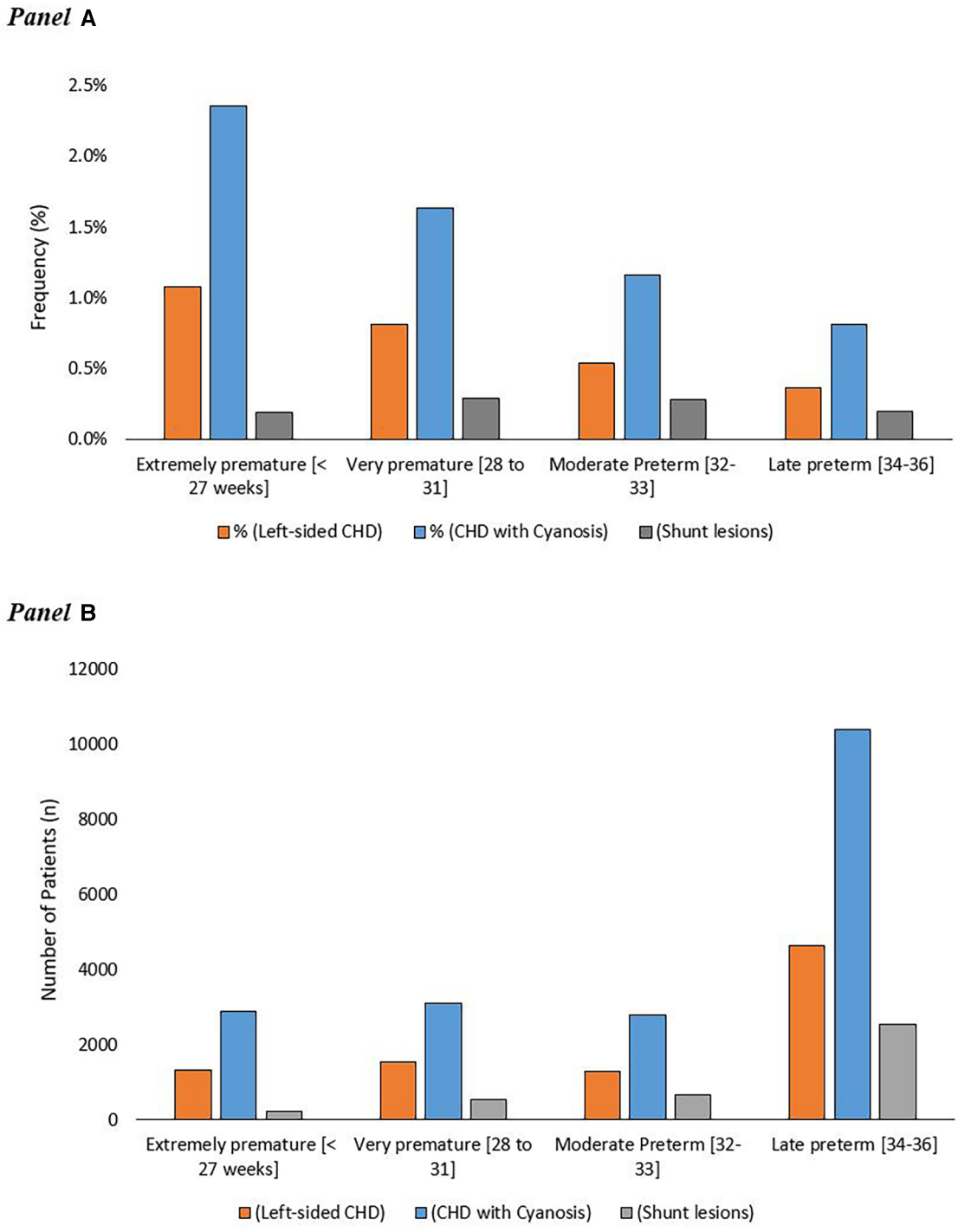

FIGURE 2
Frequency of different categories of severe congenital heart disease in premature infants in relation to gestational ages (A) the absolute number of premature patients with different categories of severe CHD in relation to their gestational age (B).

Demographic Variations. The association between CHD and prematurity was more frequent in males and in the White population. Previous studies reported controversial results regarding the demographic distribution of CHD with preterm birth. In the state of Florida, Nembhard et al. reported higher odds of preterm birth associated with CHD in Black infants compared to the White while the Hispanic population had no increased risk (14).

Desai et al. examined the Kids' Inpatient Database and reported a higher frequency of CHD in the White population (52%) compared to 15% in Black and 19.5% in the Hispanics (15).

Regional variations existed in the association between prematurity and severe CHD. The Northeast had the lowest incidence of CHD in premature infants. This might be, in

10.3389/fped.2024.1326804

TABLE 2 Clinical outcomes of study population: *cases* (preterm infants with severe CHD) versus *controls* (preterm infants without any CHD).

		Preterm with severe CHD		Preterm without severe CHD		*P*-value
Maternal factors						
Maternal hypertension	No	26,640	96.1%	18,780,255	99.4%	
	Yes	1,070	3.9%	114,510	0.6%	<0.001
Gestational diabetes	No	26,110	94.2%	18,510,576	98.0%	
	Yes	1,600	5.8%	384,190	2.0%	<0.001
Preexisting diabetes	No	24,915	89.9%	18,659,036	98.8%	
	Yes	2,795	10.1%	235,730	1.2%	<0.001
NIS	No	27,325	98.6%	18,748,466	99.2%	
	Yes	385	1.4%	146,300	0.8%	<0.001
CS	No	16,860	60.8%	13,398,563	70.9%	
	Yes	10,850	39.2%	5,496,202	29.1%	<0.001
Neonatal morbidities						
Necrotizing enterocolitis	No	26,625	96.08%	1,782,189	99.05%	
	Yes	1,085	3.92%	17,145	0.95%	<0.001
Severe IVH	No	27,250	98.30%	1,819,939	99.60%	
	Yes	460	1.70%	6,805	0.40%	<0.001
Periventricular leukomalacia	No	27,320	98.60%	1,819,589	99.60%	
	Yes	390	1.40%	7,155	0.40%	<0.001
Bronchopulmonary dysplasia	No	25,295	91.30%	1,785,014	97.70%	
	Yes	2,415	8.70%	41,730	2.30%	<0.001
Arrhythmia	No	26,885	97.02%	1,795,889	99.81%	
	Yes	825	2.98%	3,445	0.19%	<0.001
Pulmonary hypertension	No	27,415	98.94%	1,798,079	99.93%	
	Yes	295	1.06%	1,255	0.07%	<0.001
Sepsis	No	27,070	97.69%	1,792,644	99.63%	
	Yes	640	2.31%	6,690	0.37%	<0.001
Acute renal failure	No	26,085	94.14%	1,789,069	99.43%	
	Yes	1,625	5.86%	10,265	0.57%	<0.001
Pleural effusion	No	27,530	99.35%	1,798,829	99.97%	
	Yes	180	0.65%	505	0.03%	<0.001
Pneumothorax	No	27,595	99.58%	1,798,274	99.94%	
	Yes	115	0.42%	1,060	0.06%	<0.001
Cardiac arrest	No	27,635	99.73%	1,799,119	99.99%	
	Yes	75	0.27%	215	0.01%	<0.001
ECMO	No	27,360	98.74%	1,798,899	99.98%	
	Yes	350	1.26%	435	0.02%	<0.001
Tracheostomy	No	27,630	99.71%	1,799,009	99.98%	
	Yes	80	0.29%	325	0.02%	<0.001
Gastrostomy	No	27,665	99.84%	1,799,164	99.99%	
	Yes	45	0.16%	170	0.01%	<0.001
Catheterization	No	27,635	99.73%	1,799,329	99.99%	
	Yes	75	0.27%	15	0.01%	<0.001
Died during hospitalization	No	24,480	88.30%	1,779,409	97.40%	
	Yes	3,210	11.60%	46,290	2.50%	<0.001
Length of stay for alive		42 (26–81)		17 (9–22)		
Length of stay for died		25 (18–32)		9 (6–17)		<0.001

Both cases and controls were matched for GA, gender, and birth weight.

part, related to the highly diverse nature of the population in this region where dissimilar genes might have played a role in lessening such association. On the other side, the South had the highest incidence of severe CHD in premature infants. The relative unavailability of antenatal screening for CHD and probably the lack of an opportunity to terminate pregnancy might have contributed to higher rates of CHD in preterm infants (16).

In our study, lower socioeconomic status was associated with a higher incidence of severe CHD in premature infants. While the impact of social determinants of health on short and long-term outcomes after the surgical repair of CHD is well-documented, the role of these factors in the development of congenital heart defects is largely unknown, especially in premature infants. However, exposure to toxic environmental agents and environmental pollutants has been linked to

TABLE 3 The odds ratio for the association of maternal characteristics, neonatal comorbidities, and need for interventions in preterm infants with severe CHD.

	P-value	Odds-ratio (confidence interval)
Maternal hypertension	<0.001	3.19 (2.99–3.41)
Gestational diabetes	<0.001	3.02 (2.87–3.18)
Preexisting diabetes	<0.001	7.86 (7.54–8.19)
Cesarean section	<0.001	1.41 (1.37–1.44)
Neonatal abstinence syndrome	<0.001	1.7 (1.53–1.89)
Necrotizing enterocolitis	<0.001	4.88 (4.51–5.27)
Severe interventricular hemorrhage	<0.001	6.22 (5.57–6.95)
Periventricular leukomalacia	<0.001	3.21 (2.84–3.64)
Bronchopulmonary dysplasia	<0.001	18.26 (14.50–20.06)
Arrhythmia	<0.001	9.69 (8.86–10.61)
Pulmonary hypertension	<0.001	5.62 (4.83–6.54)
Heart failure	<0.001	5.91 (4.98–7.03)
Sepsis	<0.001	2.76 (2.49–3.06)
Acute kidney injury	<0.001	6.66 (6.19–7.16)
Pleural effusion	<0.001	4.84 (3.96–5.9)
Pneumothorax	<0.001	2.99 (2.35–3.8)
Cardiac arrest	<0.001	1.57 (1.15–2.16)
Extracorporeal membrane oxygenation	<0.001	1.98 (1.71–2.3)
Gastrostomy	<0.001	8.49 (5.6–12.87)
Gastrostomy	<0.001	8.49 (5.6–12.87)
Tracheostomy	<0.001	3.06 (2.33–4.02)

prematurity, low BW, and the occurrence of congenital anomalies in multiple previous studies. Exposure to these factors might also contribute to the higher risk of CHD in premature infants (17, 18).

Mortality

In our study, 11.6% of premature infants with severe CHD died before discharge from the hospital. Significant variations exist in the previous reports of mortality in preterm infants with CHD (19–21). A study of all CHD (including minor or simple CHD) reported the lowest mortality rates (22). While the highest mortality rate of −45% was reported in very low BW infants (<1,500 g, GA 22–29 weeks) (11). Steurer et al. reported a 12.6% in- hospital mortality of infants with critical CHD but this cohort included patients with gestational ages between 22 and 42 weeks (13). An international study reported a mortality rate of 18.6% in preterm infants with severe CHD compared to 8.9% in preterm infants without CHD (3). The high mortality rates even in the control group, compared to −2% in the United States, might reflect not only the variations in CHD outcomes but also the neonatal intensive care of preterm infants in general. Moreover, the inconsistencies in definitions, inclusion criteria, and denominators in these studies might explain the variations in outcomes between studies.

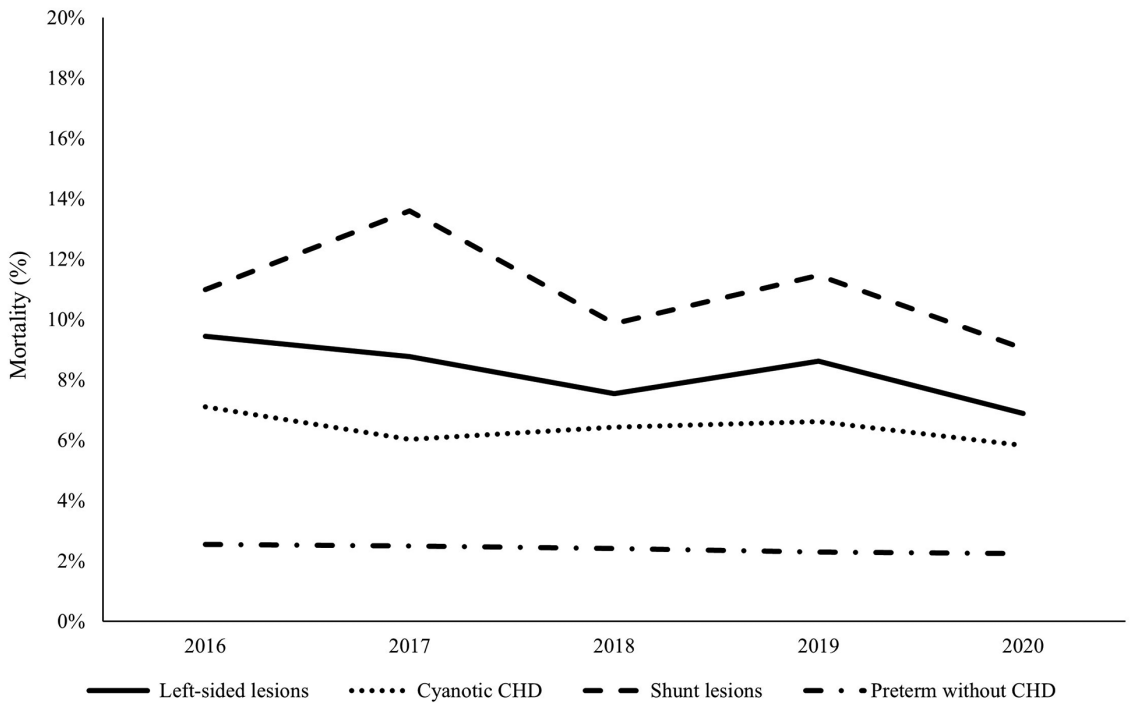

FIGURE 3
Mortality trends in premature infants with congenital heart disease versus controls during the study period (2016–2020). The dashed line represents shunt lesions, the solid line represents left-sided lesions, the dotted line represents cyanotic CHDs, and the dashed-dotted line represents the control group (preterm infants without CHD). Shunt lesions were associated with the highest mortality rates while cyanotic CHDs were associated with the lowest mortality. There was no significant improvement in survival of preterm infants with CHD during the study period.

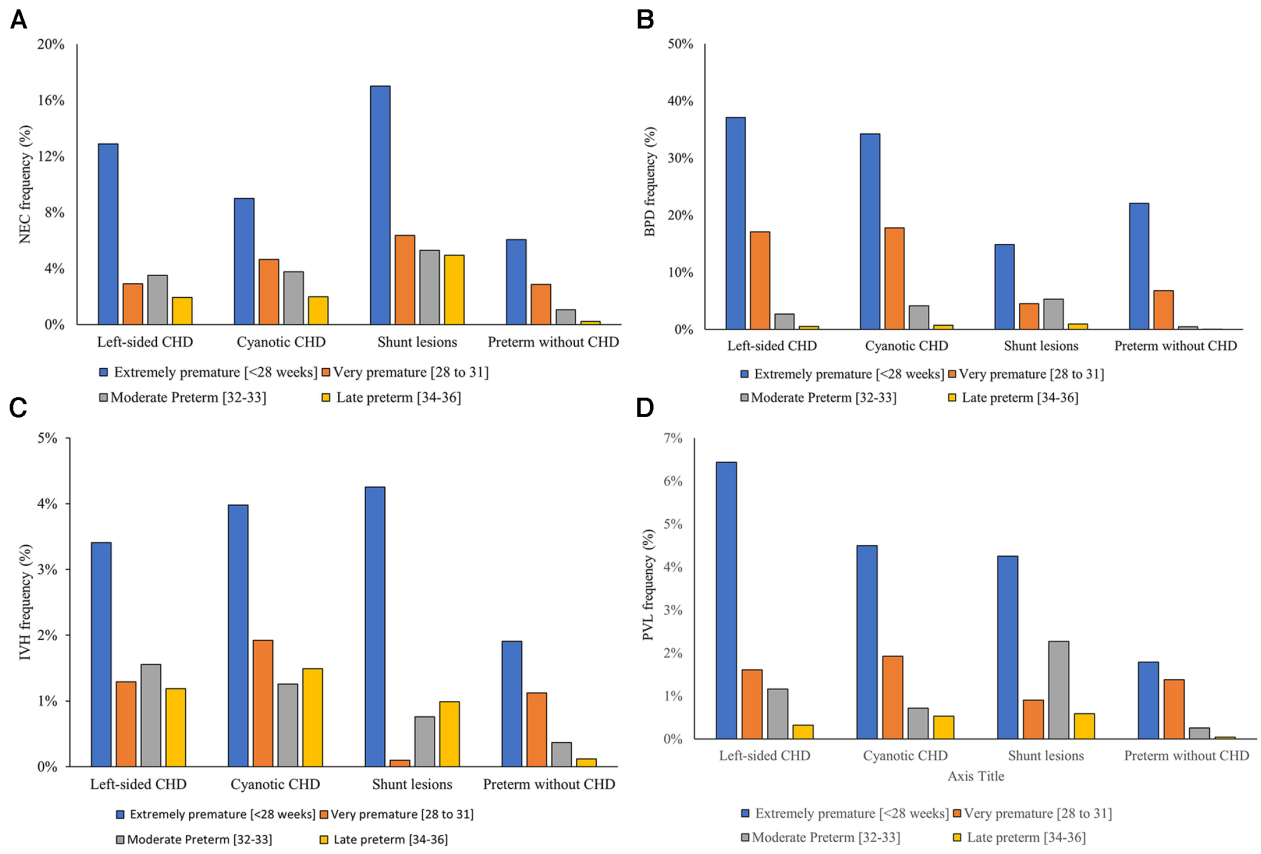

FIGURE 4
Gestational age-specific major neonatal morbidity rates in infants with versus without severe congenital heart disease. (A) Necrotizing enterocolitis, (B) bronchopulmonary dysplasia, (C) interventricular hemorrhage, (D) periventricular leukomalacia.

Necrotizing enterocolitis

The association between NEC and CHD in full-term infants is known (23, 24). It is also known that preterm infants have inherent risk factors for developing NEC (25, 26). However, outcome data about the intersection between prematurity and CHD on the development of NEC is controversial. A report of ~600 premature infants with severe CHD did not find an association between NEC and CHD (3). Another study of ~200 premature infants with BW <2,500 grams showed a 1.7-fold increase in the risk of NEC compared to all patients admitted to NICU with mixed GAs without adjusting for important variables such as GA and BW (27). Others who studied individual CHDs found a higher risk of NEC in simple CHD as isolated ASD and VSD (28) and an independent association between hypoplastic left heart syndrome or truncus arteriosus and NEC (24). In the current analysis, Preterm infants with severe CHD had a ~4-fold increase in the risk of NEC after controlling for GA, BW, and gender. The systemic inflammatory response that occurs in the presence of pulmonary overcirculation and congestive heart failure might elucidate the high risk of NEC in this CHD category. Meanwhile, the impaired systemic output and the subsequent episodic or chronic mesenteric under-perfusion might explain the significant risk of NEC in patients with left-sided obstructive lesions.

Interventricular hemorrhage

Previous studies reported a wide range of incidence of IVH in infants with CHD ranging from 2 to 24% (13, 29–31). However, these studies were limited to single institutions, small sample sizes, or mostly included full-term infants. The impact of GA on the development of severe IVH in preterm infants with CHD has not been fully examined. Preterm infant literature demonstrated an inverse relationship between the presence and severity of IVH and GA (29, 32). However, this association has not been described in preterm infants with severe CHD. Preterm infants with CHD were reported to experience a wide extent and mostly mild forms of IVH [all the above]. Others reported a lower risk of IVH in preterm infants with CHD compared to controls (9). In the current analysis, the presence of severe CHD in premature infants was associated with a 6-fold increase in the risk of developing severe IVH. Extremely premature infants (<28 weeks) were associated with the highest risk of severe IVH regardless of the category of CHD. It was

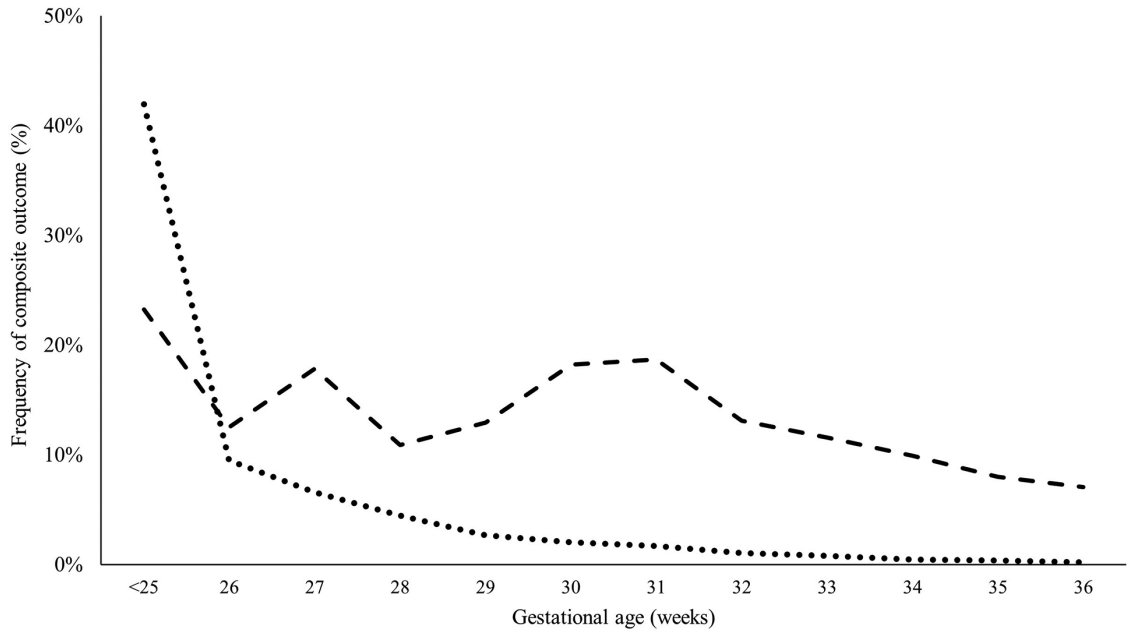

FIGURE 5
Probability of having composite outcome (mortality or severe morbidity) in infants with significant CHD versus controls based on gestational age. Adjusted for birth weight, sex, and multiple gestation.

also noticeable that this risk did not significantly decline with increasing GA. Even late preterm infants (34–36 weeks of gestation) had a significantly higher incidence of severe IVH across all categories of severe CHD compared to controls.

Periventricular leukomalacia

Full-term infants with severe CHD are at high risk of brain injury and impaired brain maturity. This hit to the brain is "doubled" in premature infants according to previous reports (33, 34). Our study showed a 3-fold increase in the risk of PVL in premature infants with severe CHD in comparison to those without CHD after adjusting for GA, BW, and gender. The combination of brain immaturity, impairment of cerebral blood flow, and low cerebral oxygen saturation might contribute to the high risk of white matter injury and subsequent PVL in premature infants with CHD (34, 35).

Bronchopulmonary dysplasia

It is not surprising and consistent with previous studies that the incidence of BPD (defined as oxygen dependency at 36 weeks of postmenstrual age) was significantly higher in preterm infants with CHD (3, 36). This high risk might reflect the pathophysiology of the underlying CHD as in cyanotic CHD with an increased need for supplemental oxygen or mechanical ventilation rather than a true BPD.

While shunt lesions with excessive left to right shunt lead to increased pulmonary blood flow, left-sided lesions with impaired forward blood flow might be associated with pulmonary venous hypertension, pulmonary edema, and subsequently impaired lung tissue development and change respiratory mechanics necessitating prolonged mechanical ventilation and oxygen supplementation.

Strengths and limitations

The current study offers the most contemporary estimation of outcomes in preterm infants (from 22 to 36^{+6} weeks' gestation) with severe CHD based on their gestation ages. We used the NIS which is the largest multicenter database for morbidity and mortality of preterm infants in the USA. To minimize coding errors, we intentionally avoided including ICD-9 codes which were available before 2016. This might have limited our ability to examine the outcomes of premature infants with severe CHD over a longer period. We opted to use ICD-10 codes which provide more detailed information related to cardiac diagnoses. Patients were well-matched with non-CHD premature infants for GA, BW, and gender, which are all known risk factors for poor outcomes in preterm infants.

The study has limitations. We limited our outcomes to the initial hospital stay. This restricted our ability to examine mortality and other comorbidities beyond discharge from the hospital. The current study did not include the specific details of surgical repair which might be institutionally different across the United States. The impact of this limitation on the provided estimations of outcomes in premature infants might be minimal given most patients with severe CHD do not undergo surgical repair or palliation until they reach a reasonable weight and corrected GA.

Conclusion

Premature infants with severe CHD are at high risk of neonatal morbidity and mortality. Morbidity remains increased across all GA groups and in all CHD categories. This significant risk of adverse outcomes is important to acknowledge when managing this patient population and when counseling their families. Future research is needed to examine the impact of specific rather than categorized CHD on neonatal outcomes.

Data availability statement

The original contributions presented in the study are included in the article/**Supplementary Material**, further inquiries can be directed to the corresponding author.

Ethics statement

Ethical approval was not required for the study involving humans in accordance with the local legislation and institutional requirements. Written informed consent to participate in this study was not required from the participants or the participants' legal guardians/next of kin in accordance with the national legislation and the institutional requirements.

Author contributions

SA: Conceptualization, Investigation, Methodology, Writing – original draft, Writing – review & editing. IQ: Formal Analysis, Investigation, Software, Writing – review & editing, Methodology. MK: Methodology, Writing – review & editing, Investigation. HA: Conceptualization, Methodology, Supervision, Validation, Writing – review & editing.

Funding

The author(s) declare that no financial support was received for the research, authorship, and/or publication of this article.

Conflict of interest

The authors declare that the research was conducted in the absence of any commercial or financial relationships that could be construed as a potential conflict of interest.

Publisher's note

Supplementary material

The Supplementary Material for this article can be found online at: https://www.frontiersin.org/articles/10.3389/fped.2024.1326804/full#supplementary-material

SUPPLEMENTARY FIGURE S1
Frequency of different categories of CHD in premature infants based on gestational age in weeks.

SUPPLEMENTARY TABLE S1
List of CHDs included in the study with the associated ICD-10 codes.

References

1. Liu L, Oza S, Hogan D, Perin J, Rudan I, Lawn JE, et al. Global, regional, and national causes of child mortality in 2000–13, with projections to inform post-2015 priorities: an updated systematic analysis. *Lancet*. (2015) 385:430–40. doi: 10.1016/S0140-6736(14)61698-6

2. Helenius K, Sjörs G, Shah PS, Modi N, Reichman B, Morisaki N, et al. International network for evaluating outcomes (iNeo) of neonates. Survival in very preterm infants: an international comparison of 10 national neonatal networks. *Pediatrics*. (2017) 140(6):e20171264. doi: 10.1542/peds.2017-1264

3. Norman M, Håkansson S, Kusuda S, Vento M, Lehtonen L, Reichman B, et al. International network for evaluation of outcomes in neonates (iNeo) investigators* †. neonatal outcomes in very preterm infants with severe congenital heart defects: an international cohort study. *J Am Heart Assoc*. (2020) 9(5):e015369. doi: 10.1161/JAHA.119.015369

4. Hoffman JIE, Kaplan S. The incidence of congenital heart disease. *J Am Coll Cardiol*. (2002) 39:1890–900. doi: 10.1016/S0735-1097(02)01886-7

5. Reller MD, Strickland MJ, Riehle-Colarusso T, Mahle WT, Correa A. Prevalence of congenital heart defects in metropolitan Atlanta, 1998–2005. *J Pediatr*. (2008) 153:807–13. doi: 10.1016/j.jpeds.2008.05.059

6. Tanner K, Sabrine N, Wren C. Cardiovascular malformations among preterm infants. *Pediatrics*. (2005) 16:e833–8. doi: 10.1542/peds.2005-0397

7. Matthiesen NB, Østergaard JR, Hjortdal VE, Henriksen TB. Congenital heart defects and the risk of spontaneous preterm birth. *J Pediatr*. (2021) 229:168–74.e5. doi: 10.1016/j.jpeds.2020.09.059

8. Laas E, Lelong N, Thieulin AC, Houyel L, Bonnet D, Ancel PY, et al. Preterm birth and congenital heart defects: a population-based study. *Pediatrics*. (2012) 130:e829–37. doi: 10.1542/peds.2011-3279

9. Dumitrascu Biris I, Mintoft A, Harris C, Rawn Z, Jheeta JS, Pushparajah K, et al. Mortality and morbidity in preterm infants with congenital heart disease. *Acta Paediatr*. (2022) 111(1):151–6. doi: 10.1111/apa.16155

10. Anderson AW, Smith PB, Corey KM, Hill KD, Zimmerman KO, Clark RH, et al. Clinical outcomes in very low BW infants with major congenital heart defects. *Early Hum Dev*. (2014) 90:791–5. doi: 10.1016/j.earlhumdev.2014.09.006

11. Archer JM, Yeager SB, Kenny MJ, Soll RF, Horbar JD. Distribution of and mortality from serious congenital heart disease in very low BW infants. *Pediatrics*. (2011) 127:293–9. doi: 10.1542/peds.2010-0418

12. Agency for Healthcare Research and Quality. Overview of the National (Nationwide) Inpatient Sample (NIS). Available online at: https://www.hcup-us.ahrq.gov/nisoverview.jsp (Accessed February 15, 2024).

13. Steurer MA, Baer RJ, Keller RL, Oltman S, Chambers CD, Norton ME, et al. Gestational age and outcomes in critical congenital heart disease. *Pediatrics*. (2017) 140(4):e20170999. doi: 10.1542/peds.2017-0999

14. Nembhard WN, Salemi JL, Hauser KW, Kornosky JL. Are there ethnic disparities in risk of preterm birth among infants born with congenital heart defects? *Birth Defects Res A Clin Mol Teratol*. (2007) 79:754–64. doi: 10.1002/bdra.20411

15. Desai J, Aggarwal S, Lipshultz S, Agarwal P, Yigazu P, Patel R, et al. Surgical interventions in infants born preterm with congenital heart defects: an analysis of the Kids' inpatient database. *J Pediatr*. (2017) 191:103–9.e4. doi: 10.1016/j.jpeds.2017.07.015

16. Nelson JS, Strassle PD. Regional differences in right versus left congenital heart disease diagnoses in neonates in the United States. *Birth Defects Res*. (2018) 110(4):325–35. doi: 10.1002/bdr2.1140

17. Peyvandi S, Baer RJ, Chambers CD, Norton ME, Rajagopal S, Ryckman KK, et al. Environmental and socioeconomic factors influence the live-born incidence of congenital heart disease: a population-based study in California. *J Am Heart Assoc*. (2020) 9(8):e015255. doi: 10.1161/JAHA.119.015255

18. Enders C, Pearson D, Harley K, Ebisu K. Exposure to coarse particulate matter during gestation and term low birthweight in California: variation in exposure and risk across region and socioeconomic subgroup. *Sci Total Environ*. (2019) 653:1435–44. doi: 10.1016/j.scitotenv.2018.10.323

19. GBD 2017 Congenital Heart Disease Collaborators. Global, regional, and national burden of congenital heart disease, 1990–2017: a systematic analysis for the global burden of disease study 2017. *Lancet Child Adolesc Health*. (2020) 4(3):185–200. doi: 10.1016/S2352-4642(19)30402-X

20. Oster ME, Lee KA, Honein MA, Riehle-Colarusso T, Shin M, Correa A. Temporal trends in survival among infants with critical congenital heart defects. *Pediatrics*. (2013) 131:e1502–8. doi: 10.1542/peds.2012-3435

21. Polito A, Piga S, Cogo PE, Corchia C, Carnielli V, Da Fre M, et al. Increased morbidity and mortality in very preterm/VLBW infants with congenital heart disease. *Intensive Care Med*. (2013) 39:1104–12. doi: 10.1007/s00134-013-2887-y

22. Best KE, Tennant PWG, Rankin J. Survival, by BW and gestational age, in individuals with congenital heart disease: a population-based study. *J Am Heart Assoc*. (2017) 6(7):e005213. doi: 10.1161/JAHA.116.005213

23. Giannone PJ, Luce WA, Nankervis CA, Hoffman TM, Wold LE. Necrotizing enterocolitis in neonates with congenital heart disease. *Life Sci*. (2008) 82(7–8):341–7. doi: 10.1016/j.lfs.2007.09.036

24. McElhinney DB, Hedrick HL, Bush DM, Pereira GR, Stafford PW, Gaynor JW, et al. Necrotizing enterocolitis in neonates with congenital heart disease: risk factors and outcomes. *Pediatrics*. (2000) 106(5):1080–7. doi: 10.1542/peds.106.5.1080

25. Kelleher ST, McMahon CJ, James A. Necrotizing enterocolitis in children with congenital heart disease: a literature review. *Pediatr Cardiol*. (2021) 42(8):1688–99. doi: 10.1007/s00246-021-02691-1

26. Carlo WF, Kimball TR, Michelfelder EC, Border WL. Persistent diastolic flow reversal in abdominal aortic Doppler-flow profiles is associated with an increased risk of necrotizing enterocolitis in term infants with congenital heart disease. *Pediatrics*. (2007) 119(2):330–5. doi: 10.1542/peds.2006-2640

27. Cheung PY, Hajihosseini M, Dinu IA, Switzer H, Joffe AR, Bond GY, et al. Outcomes of preterm infants with congenital heart defects after early surgery: defining risk factors at different time points during hospitalization. *Front Pediatr*. (2021) 28(8):616659. doi: 10.3389/fped.2020.616659

28. Bain J, Benjamin DK Jr, Hornik CP, Benjamin DK, Clark R, Smith PB. Risk of necrotizing enterocolitis in very-low-birth-weight infants with isolated atrial and ventricular septal defects. *J Perinatol*. (2014) 34:319–21. doi: 10.1038/jp.2013.174

29. Stoll BJ, Hansen NI, Bell EF, Shankaran S, Laptook AR, Walsh MC, et al. Neonatal outcomes of extremely preterm infants from the NICHD neonatal research network. *Pediatrics*. (2010) 126(3):443–56. doi: 10.1542/peds.2009-2959

30. Costello JM, Polito A, Brown DW, McElrath TF, Graham DA, Thiagarajan RR, et al. Birth before 39 weeks' gestation is associated with worse outcomes in neonates with heart disease. *Pediatrics*. (2010) 26(2):277–84. doi: 10.1542/peds.2009-3640

31. Pappas A, Shankaran S, Hansen NI, Bell EF, Stoll BJ, Laptook AR, et al. Outcome of extremely preterm infants (<1,000 g) with congenital heart defects from the national institute of child health and human development neonatal research network. *Pediatr Cardiol*. (2012) 33(8):1415–26. doi: 10.1007/s00246-012-0375-8

32. Ortinau CM, Anadkat JS, Smyser CD, Eghtesady P. Intraventricular hemorrhage in moderate to severe congenital heart disease. *Pediatr Crit Care Med*. (2018) 19(1):56–63. doi: 10.1097/PCC.0000000000001374

33. Katz JA, Levy PT, Butler SC, Sadhwani A, Lakshminrusimha S, Morton SU, et al. Preterm congenital heart disease and neurodevelopment: the importance of looking beyond the initial hospitalization. *J Perinatol*. (2023) 43(7):958–62. doi: 10.1038/s41372-023-01687-4

34. Levy PT, Thomas AR, Wethall A, Perez D, Steurer M, Ball MK. Rethinking congenital heart disease in preterm neonates. *Neoreviews*. (2022) 23(6):e373–87. doi: 10.1542/neo.23-6-e373

35. Gaynor JW, Stopp C, Wypij D, Andropoulos DB, Atallah J, Atz AM, et al. Neurodevelopmental outcomes after cardiac surgery in infancy. *Pediatrics*. (2015) 135(5):816–25. doi: 10.1542/peds.2014-3825

36. Kumar KR, Clark DA, Kim EM, Perry JD, Wright K, Thomas SA, et al. Association of atrial septal defects and bronchopulmonary dysplasia in premature infants. *J Pediatr*. (2018) 202:56–62.e2. doi: 10.1016/j.jpeds.2018.07.024

frontiers | Frontiers in Pediatrics

TYPE Case Report
PUBLISHED 01 May 2024
DOI 10.3389/fped.2024.1251274

OPEN ACCESS

EDITED BY
Liqun Sun,
University of Toronto, Canada

REVIEWED BY
Nathalie Jeanne M. Bravo-valenzuela,
Federal University of Rio de Janeiro, Brazil
Rongzhou Wu,
Wenzhou Medical University, China

*CORRESPONDENCE
Silin Pan
✉ silinpan@126.com

RECEIVED 01 July 2023
ACCEPTED 11 April 2024
PUBLISHED 01 May 2024

CITATION
Luo G, Liu A, Sun H, Wang K and Pan S (2024) A case report of pulmonary atresia with intact ventricular septum: an extraordinary finding of subsystemic right ventricle.
Front. Pediatr. 12:1251274.
doi: 10.3389/fped.2024.1251274

A case report of pulmonary atresia with intact ventricular septum: an extraordinary finding of subsystemic right ventricle

Gang Luo, Ai Liu, Hongxiao Sun, Kuiliang Wang and Silin Pan*

Heart Center, Women and Children's Hospital, Qingdao University, Qingdao, China

Background: Massive tricuspid regurgitation (TR) is the most common feature of pulmonary atresia with intact ventricular septum (PA/IVS), and mild or absent TR is observed in severe right ventricular (RV) dysplasia or RV-to-coronary fistulous connections, resulting in non-biventricular (BV) outcomes postnatally.
Case summary: We report a case of fetal severe pulmonary stenosis with IVS diagnosed at 26 weeks of gestation. The severity of RV hypoplasia did not worsen or reach indications for intrauterine intervention, while the jet velocity of TR decreased significantly during pregnancy. The fetus was definitely diagnosed with PA/IVS with mild RV dysplasia after birth. Unusually, the fetus did not experience severe TR and myocardial sinusoids, the TR jet velocity was maintained at 2.0 m/s, and the coronary artery was almost normal. The incapable RV cannot pump blood into pulmonary circulation after RV decompression from valvular perforation and balloon dilation. It may be an extraordinary finding of subsystemic RV.
Conclusion: PA/IVS is a heterogeneous disease with various degrees of RV dysplasia. Mild or no baseline TR is a reliable indicator with non-BV outcomes for fetal PA/IVS, even with acceptable dysplasia RV structures.

KEYWORDS

pulmonary atresia with intact ventricular septum, tricuspid regurgitation, echocardiography, fetus, case report

1 Introduction

Severe pulmonary stenosis or atresia with intact ventricular septum (PA/IVS) is a rare form of complex congenital heart disease characterized by hypoplasia of the right ventricle (RV) and the tricuspid valve (TV). As a heterogeneous disease, there are various associated factors with postoperative results in PA/IVS, including RV size and morphology, TV size and function, and the right ventricle-dependent coronary circulation (RVDCC). It remains challenging to determine the appropriate surgical approach for patients with moderate developmental indicators, unlike those with severe or mild dysplasia. There is no exact regulation for the development of pathological modification in fetal PA/IVS. Currently, the evaluation of RV function in fetal PA/IVS remains challenging. With the conviction that good structure can result in improved function, structural markers, such as the TV size and the ratio of the left and right ventricles on fetal echocardiography, may provide useful intrauterine indications to the postpartum outcome of PA/IVS (1).

Tricuspid regurgitation (TR) can be readily identified during a regular obstetric ultrasound, making it a good indicator of RV function during pregnancy. A multicenter study indicates that fetuses with mild or no baseline TR may not be able

to achieve biventricular (BV) outcomes due to the presence of severe RV dysplasia or RVDCC (2). Only by opening the pulmonary valve can the "true capacity" of RV to pump blood to the pulmonary artery be truly revealed, though the results may not always meet expectations, as found in clinical research (3). We observed a fetus diagnosed with severe pulmonary stenosis with IVS at 26 weeks of gestation whose TR jet velocity decreased during gestation in a manner that was not expected based on the cardiac structural assessment, an extraordinary type of deterioration in RV function, and a postnatal outcome that did not achieve BV repair.

2 Methods and results

2.1 Case presentation

A 36-year-old woman underwent a routine prenatal examination at 26 weeks of pregnancy at the Women and Children's Hospital, Qingdao University. Fetal echocardiography indicated severe pulmonary stenosis with IVS and moderate TR with a jet velocity of 4.7 m/s (Figure 1A). Four weeks later, the woman (at 30 weeks of pregnancy) underwent fetal echocardiography; the results showed a TR jet velocity of 2.56 m/s, pulmonary stenosis, and reversed flow in the ductus arteriosus. The predictors of non-BV outcome related to the degree of RV development with no RV sinusoids are shown in Table 1. The fetus had not reached the point of necessitating intrauterine invasive procedures in accordance with the standards put forth by Gómez-Montes et al. in 2011 (4). Fetal echocardiography was repeated every 2–3 weeks and the relevant indicators are detailed in Table 1. All indicators can be summarized by the following characteristics: the severity of RV hypoplasia did not worsen and failed to meet the indicators for an intrauterine intervention; and the degree and velocity of TR decreased significantly.

A female infant was delivered at 38 weeks with a birth weight of 3,100 g, heart rate of 128 beats/min, respiratory rate of 45 breaths/min, and percutaneous arterial oxygen saturation (SPO_2) of 93%. A bedside echocardiogram was immediately conducted on the infant, which showed the small RV cavity (Figure 1B); the foramen ovale measured 6.4 mm and the pulmonary valve annulus measured 7.6 mm. There was no obvious blood flow through the valve during systole. The patent ductus arteriosus (PDA) measured 4.3 mm and supplied the pulmonary circulation (Figure 1B). The tricuspid valvular annulus was 10 mm with a TV-Z score of −1.13, with a slight amount of blood flow in diastole and mild regurgitation in systole, and no severe abnormalities observed (Figure 1B). The morphology and structure of the aorta (AO) and pulmonary artery (PA) were normal. The female infant was definitely diagnosed as PA/IVS.

On her first day of life, the SPO_2 of the infant decreased to 85%, and the echocardiography showed that the PDA tended to close. The prostaglandin E1 (1–3 ng kg^{-1} min^{-1}) was administered and SPO_2 was maintained to 92% of the total. The following problems were evaluated repeatedly before the operation: no severe TV malformation (Ebstein's anomaly); the TR jet velocity was maintained at 2.0 m/s; no myocardial sinusoids; and the coronary artery was normal. Radiofrequency-assisted perforation is a feasible valvotomy option in catheterization laboratories with proper equipment; cost limitations and a considerable success rate are essential in developing countries, explaining the decision to opt for balloon catheter dilation. In addition, the possibility of ductus-dependent pulmonary blood supply is low after percutaneous balloon pulmonary valvuloplasty.

2.2 Cardiac catheterization

On the infant's 20th day of life, she underwent a catheterization intervention. The right ventriculography confirmed pulmonary atresia and the presence of three parts of RV (the inflow, outflow, and trabecula) (Figure 1C). The aortogram showed that the ductus arteriosus was measured approximately 4.5 mm, and the origin and course of the coronary artery were normal. Cardiac catheterization manometry has shown that the RV was 67/10(14) mmHg, AO was 59/25(39) mmHg and PA was 35/22 (28) mmHg.

A 4F goose neck snare was manipulated from AO through PDA and kept opening against the pulmonary valve. The soft end of the available coronary wire (Conquest Pro 8–20 wire) was gently manipulated and advanced along the catheter, keeping both the wire and the catheter close to the membranous valve. The wire was required to be pushed very gently to perforate the valve. Once the wire perforated the membrane, the guidewire was manipulated into the PA, the snare grabbed the guidewire, further advancing carefully through the PDA into the descending aorta, and was then exteriorized through the femoral arterial sheath, creating an arteriovenous wire loop and achieving stable position (Figure 1C). A coronary balloon measuring 1.25 mm × 15 mm was maneuvered over the wire to perform the first dilatation. The balloon size was gradually increased from 2.5 mm to the maximum of 8 mm (Figure 1C). At the end of the procedure, the results of the cardiac catheter manometry were as follows: RV 53/13(32) mmHg; AO 52/21(32) mmHg; and PA 34/20(27) mmHg.

After the intervention, the infant was given a continuous dose of prostaglandin E1, and her SPO_2 was 92%. The oxygen saturation was significantly reduced when the dose of prostaglandin E1 was downregulated. Multiple echocardiography showed no antegrade blood flow across the pulmonary valve (Figure 1D), which was considered to be RV insufficiency, and the pulmonary circulation was dependent on the PDA. After 7 days of intervention, the infant's SPO_2 level dropped drastically to below 60%, and an echocardiography indicated that the PDA was closed; an increased dose of prostaglandin E1 was not effective.

A Blalock–Taussig shunt or Glenn's surgery was proposed as the default course of action in emergency scenarios, while the ultimate surgical technique was based on the RV function. The families were unwilling to accept the potential negative long-term outlook and the failure of BV circulation and chose to end the treatment with regret.

10.3389/fped.2024.1251274

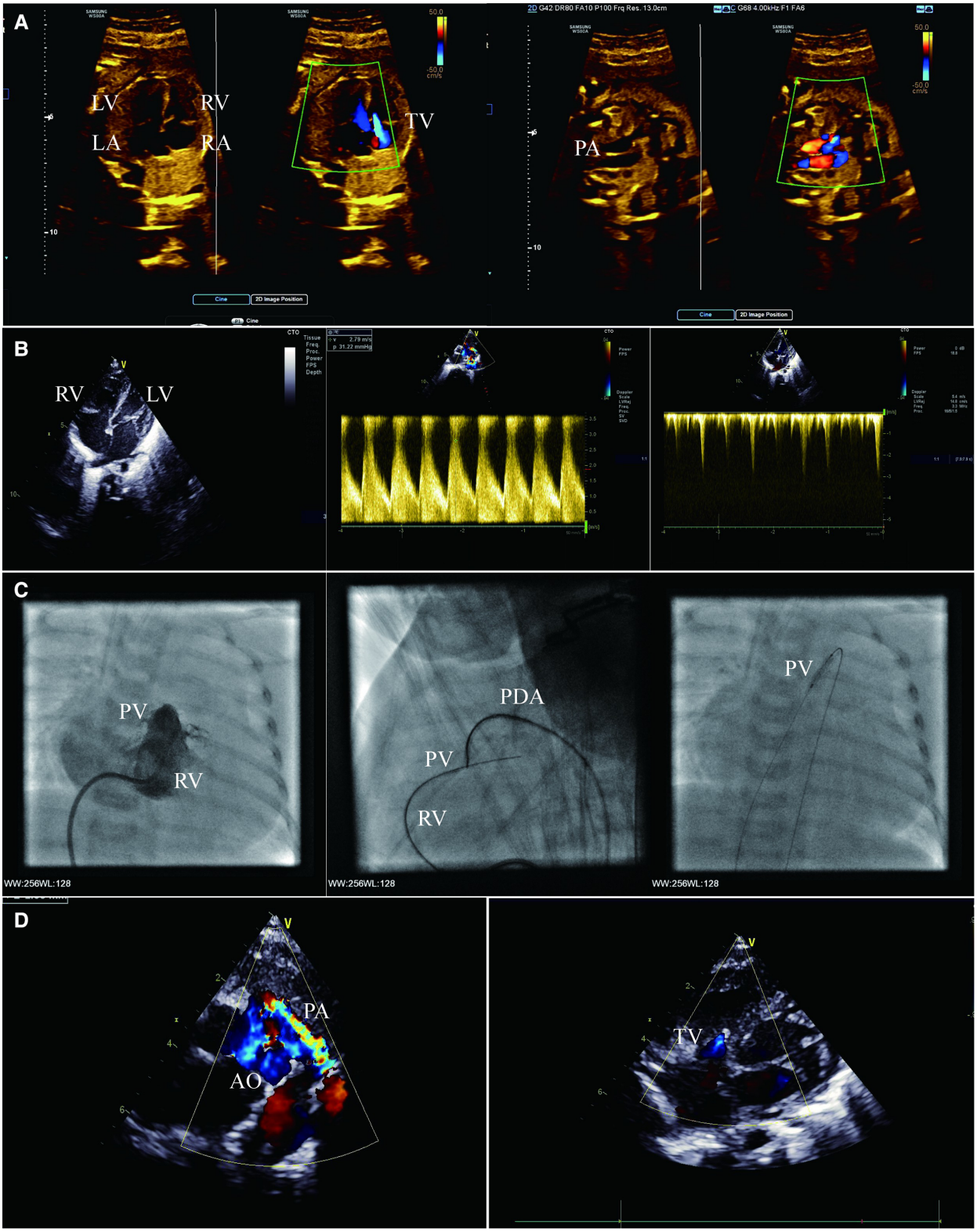

FIGURE 1
(**A**) Fetal echocardiogram apical four-chamber view (left) and right ventricular outflow tract view (right) showing severe pulmonary stenosis and massive tricuspid regurgitation. (**B**) Transthoracic echocardiogram apical four-chamber view (left and right) and short-axis view (middle) showing mild hypoplasia of RV, pulmonary atresia and patent ductus arteriosus, no serious abnormality of TV, and mild tricuspid regurgitation. (**C**) Right ventriculography (left) showing mild hypoplasia of RV and pulmonary valvular atresia. Lateral right ventriculography (middle) showing guide wire creating an arteriovenous wire loop. Anterior chest fluoroscopy (right) showing percutaneous balloon pulmonary valvuloplasty. (**D**) Transthoracic echocardiogram short-axis view (left) and apical four-chamber view (right) showing ductus arteriosus supply pulmonary blood flow, no antegrade blood flow across the pulmonary valve, and mild tricuspid regurgitation. LA, left atrium; LV, left ventricle; PV, pulmonary valve.

10.3389/fped.2024.1251274

TABLE 1 Fetal echocardiography data during pregnancy.

Gestational age (weeks)	Pulmonary valve orifice flow velocity (m/s)	Tricuspid regurgitant jet velocity (m/s)	RV/LV	TV/MV	PV/AV	TVI/CC	TV-Z score
26	2.13	4.70	—	—	—	—	—
30	1.90	2.56	0.76	0.88	0.96	0.43	−0.67
32	2.71	1.66	0.78	0.82	0.90	0.39	−0.88
34	3.10	1.58	0.80	0.75	0.92	0.40	−1.30
37	2.70	1.56	0.82	0.72	0.94	0.38	−1.24

—, no data; RV/LV, right ventricle/left ventricle long-axis ratio; TV/MV, tricuspid/mitral annulus ratio; PV/AV, pulmonary valve/aortic valve annulus ratio; TVI/CC, tricuspid valve inflow duration/cardiac cycle ratio.

3 Discussion

The pathophysiological characteristics of severe pulmonary valve stenosis with a tendency toward atresia are similar to those of PA/IVS. We presented a fetal case with severe pulmonary valve stenosis and RV of moderate dysplasia in size and morphology. As the pregnancy progressed, there was a considerable drop in the velocity of fetal TR. After birth, the morphology and size of RV and TV were examined to assess mild to moderate RV dysplasia, although TR velocity was at a low level. There were no myocardial sinusoids and severe TV malformation after repeated evaluations. However, cardiac catheterizations indicated the low RV pressure before and after decompression (approximately 60 mmHg), and RV function was severely deteriorating. The ejection functions could not be supported by the RV, and the flow of blood in the pulmonary circulatory system was dependent on PDA. This may be the first report of a case of fetal severe pulmonary valve stenosis with RV dysfunction when the RV is appropriately dysplastic.

Anomalous RV morphology in cases of PA/IVS is often irregular and singular, which raises the debate on how to assess the severity of RV development. The most effective compromise between sensitivity and specificity predicting a non-BV management pathway are TV/mitral valve ratio ≤0.83, pulmonary valve/aortic valve ratio ≤0.75, tricuspid inflow duration/cardiac cycle length ≤36.5%, and RV/left ventricle length ratio ≤0.64. If three out of four markers are present, this predicts a non-BV outcome with a sensitivity of 100% and specificity of 92% (it is 100% if the four requirements are met) (4). Unfortunately, there are cases where fetal RV decompression is performed, but the patients fail to achieve BV circulation, and an even greater proportion of cases where multiple reoperations are necessary after RV decompression.

Obstruction of the antegrade flow of the RV of PA/IVS causes a high-pressure state in the RV cavity, which is often accompanied by severe TR (5). With the amount of blood entering the RV cavity before decompression being equal to the TV regurgitation volume, TR may aid in guiding prenatal counseling regarding postnatal outcome in PA/IVS (4). In addition, as TR is easily identified by fetal color Doppler during routine obstetric sonography, these patients might come to notice the practitioner more often. Yu et al. diagnosed PA by an expected finding in severe TR in the first trimester prenatal screening (6). Fetal studies have implied that the outcomes after decompression of RV in infants with PA/IVS are associated with the degree of the TR (7). The absence or presence of mild baseline TR is a contributing factor to not reaching the desired BV circulation outcome (8). Lacobelli et al. demonstrated that the absence of TR in fetal PA/IVS correlated to single ventricle circulation postnatally in addition to ventriculocoronary connections (9). Abnormal coronary circulation was associated with severity of TV and RV dysplasia in both fetal and neonatal patients with PA/IVS. In cases of small RV cavity and severe dysplasia, a higher pressure increases the probability of RV-to-coronary flow with fistulous connections. Once the fistulous connections are formed, the pressure in the RV cavity decreases and TR is naturally reduced. Conversely, the absence of TR is highly predictive of fistulous connections in fetuses affected by PA/IVS and is even more reliable at predicting such connections than direct visualization (10). However, in this case, although TR decreased, the formation of a fistula did not occur, and the structure of the RV was moderate. Therefore, the anatomy of this case is difficult to explain due to the above reasons.

Two prototypes of PA/IVS have been presented: type I, which is more frequent, has pulmonary valvular atresia, dysplasia of the TV with the small annulus, sub-developed RV with hypoplastic cavity and hypertrophy, atrial septal defect, and PDA; type II, which is less common, is associated with more severe dysplasia of the TV and enlargement of the RV, right atrium (RA), and right atrioventricular junction, and a notable thinning of the RV wall (11). Choi et al. described a case of fetal PA/IVS with moderate RV dysplasia and enlarged RA. The heart exhibited a dysplastic thickened TV with the leaflet directly attached to the papillary muscle without chords. This is different from types I and II, which is classified as a separate type (type III) (12). Because the specimen is a fetal heart, the RV may not be given adequate time to develop a hypertrophic wall, necessitating further sample collection to ascertain the type III hypothesis.

4 Conclusion

PA/IVS is a heterogeneous disease with various degrees of RV dysplasia. Mild or no baseline TR is a reliable indicator with non-BV outcomes for fetuses with PA/IVS, even with the acceptable dysplasia RV structures.

Data availability statement

The original contributions presented in the study are included in the article/Supplementary Material, further inquiries can be directed to the corresponding author.

Ethics statement

The study was approved by the ethical committees of Qingdao Women and Children's Hospital (No. QFELL-KY-2019-64). Written informed consent was obtained from the patient's guardian/next of kin for the publication of this case report.

Author contributions

SP conceptualized and designed the study, coordinated and supervised data collection, and critically reviewed and revised the manuscript for important intellectual content. GL and HS collected data, carried out the initial analyses, drafted the initial manuscript, and critically reviewed and revised the manuscript. AL and KW collected data, carried out the initial analyses, and critically reviewed and revised the manuscript. All authors agree to be accountable for the content of the work. All authors contributed to the article and approved the submitted version.

Funding

This work was supported by the National Natural Science Foundation of China (Nos. 82271725).

Conflict of interest

The authors declare that the research was conducted in the absence of any commercial or financial relationships that could be construed as a potential conflict of interest.

Publisher's note

All claims expressed in this article are solely those of the authors and do not necessarily represent those of their affiliated organizations, or those of the publisher, the editors and the reviewers. Any product that may be evaluated in this article, or claim that may be made by its manufacturer, is not guaranteed or endorsed by the publisher.

References

1. Hogan WJ, Grinenco S, Armstrong A, Devlieger R, Dangel J, Ferrer Q, et al. Fetal cardiac intervention for pulmonary atresia with intact ventricular septum: international fetal cardiac intervention registry. *Fetal Diagn Ther*. (2020) 7:1–9. doi: 10.1159/000508045

2. Maskatia SA, Petit CJ, Travers CD, Goldberg DJ, Rogers LS, Glatz AC, et al. Echocardiographic parameters associated with biventricular circulation and right ventricular growth following right ventricular decompression in patients with pulmonary atresia and intact ventricular septum: results from a multicenter study. *Congenit Heart Dis*. (2018) 13:892–902. doi: 10.1111/chd.12671

3. Luo G, Zhang B, Wang D, Pan S, Sun Y, Wang S. Fetal pulmonary valvuloplasty for pulmonary atresia with intact ventricular septum: a single-center clinical experience. *Chin Med J (Engl)*. (2023) 136:740–2. doi: 10.1097/CM9.0000000000002268

4. Gómez-Montes E, Herraiz I, Mendoza A, Albert L, Hernández-García JM, Galindo A. Pulmonary atresia/critical stenosis with intact ventricular septum: prediction of outcome in the second trimester of pregnancy. *Prenat Diagn*. (2011) 31:372–9. doi: 10.1002/pd.2698

5. Peterson RE, Levi DS, Williams RJ, Lai WW, Sklansky MS, Drant S. Echocardiographic predictors of outcome in fetuses with pulmonary atresia with intact ventricular septum. *J Am Soc Echocardiogr*. (2006) 19:1393–400. doi: 10.1016/j.echo.2006.05.021

6. Yu D, Sui L, Zhang N. Performance of first-trimester fetal echocardiography in diagnosing fetal heart defects: meta-analysis and systematic review. *J Ultrasound Med*. (2020) 39:471–80. doi: 10.1002/jum.15123

7. Petit CJ, Glatz AC, Qureshi AM, Sachdeva R, Maskatia SA, Justino H, et al. Outcomes after decompression of the right ventricle in infants with pulmonary atresia with intact ventricular septum are associated with degree of tricuspid regurgitation: results from the congenital catheterization research collaborative. *Circ Cardiovasc Interv*. (2017) 10:e004428. doi: 10.1161/CIRCINTERVENTIONS.116.004428

8. Cordisco A, Lozza V, Filice ME, Chiappa E. First trimester prenatal diagnosis of a severe tricuspid valve regurgitation and pulmonary valve atresia. *Echocardiography*. (2021) 38:2119–21. doi: 10.1111/echo.15242

9. Lacobelli R, Pasquini L, Toscano A, Raimondi F, Michielon G, Tozzi AE, et al. Role of tricuspid regurgitation in fetal echocardiographic diagnosis of pulmonary atresia with intact ventricular septum. *Ultrasound Obstet Gynecol*. (2008) 32:31–5. doi: 10.1002/uog.5356

10. Wolter A, Markert N, Wolter JS, Kurkevych A, Degenhardt J, Ritgen J, et al. Natural history of pulmonary atresia with intact ventricular septum (PAIVS) and critical pulmonary stenosis (CPS) and prediction of outcome. *Arch Gynecol Obstet*. (2021) 304:81–90. doi: 10.1007/s00404-020-05929-0

11. Liu L, Wang H, Cui C, Li Y, Liu Y, Wang Y, et al. Prenatal echocardiographic classification and prognostic evaluation strategy in fetal pulmonary atresia with intact ventricular septum. *Medicine (Baltimore)*. (2019) 98:e17492. doi: 10.1097/MD.0000000000017492

12. Choi YH, Seo JW, Choi JY, Yun YS, Kim SH, Lee HJ. Morphology of tricuspid valve in pulmonary atresia with intact ventricular septum. *Pediatr Cardiol*. (1998) 19:381–9. doi: 10.1007/s002469900333

Frontiers in
Cardiovascular Medicine

Innovations and improvements in cardiovascular treatment and practice

Focuses on research that challenges the status quo of cardiovascular care, or facilitates the translation of advances into new therapies and diagnostic tools.

Discover the latest Research Topics

See more →

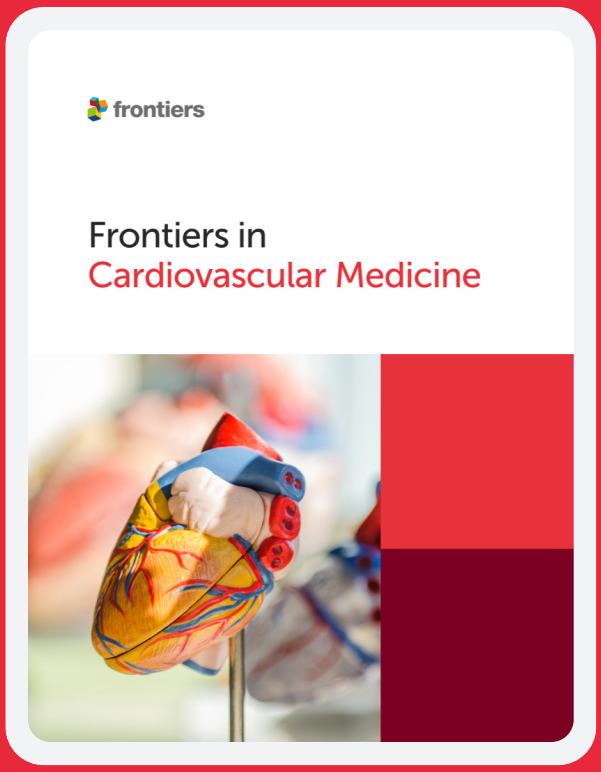

Frontiers

Avenue du Tribunal-Fédéral 34
1005 Lausanne, Switzerland
frontiersin.org

Contact us

+41 (0)21 510 17 00
frontiersin.org/about/contact